Caracterización estructural y funcional de la forma nitrada de la peroxirredoxina 2

Lía M. Randall Carlevaro

Directores:
Dra. Ana Denicola
Dr. Javier Santos

Gracias

En especial a mamá y papá por todo el amor y el apoyo constante. Por siempre creer en mí, por acompañarme y hacerme sentir siempre abrazada.

A mis hermanos por los mejores abrazos del mundo.

A Guz por el apoyo incondicional y la paciencia.

A Guille y Emma por siempre ser la luz.

Al Tata. A las abuelas.

A la Negrita por la ayuda interminable con el diseño gráfico. A Nati por las horas de niñera para poder terminar los experimentos.

A los compañeros del lab por ser el mejor grupo para aprender y en especial a las Rubias por siempre estar.

A Javi por todo lo aprendido.

A Ana por todo y más.

ÍNDICE

RESUMEN

Las peroxirredoxinas son enzimas ubicuas y ampliamente conservadas que catalizan la reducción de peróxidos mediante un mecanismo que depende de una cisteína reactiva (cisteína peroxidática, C_P). Las peroxirredoxinas de 2 cisteínas típicas (2-Cys Prx típicas), entre las que se encuentra la peroxirredoxina 2 (Prx2), forman un disulfuro intermolecular con la cisteína resolutiva (C_R) de la subunidad adyacente, cuyo reductor por excelencia es el sistema tiorredoxina/tiorredoxina reductasa/NADPH. Las 2-Cys Prx típicas en general se organizan como dímeros o decámeros, cuyo equilibrio acompaña el ciclo catalítico de estas enzimas y regula su interacción con otras proteínas intracelulares. Por ser tan abundantes y su reacción con H_2O_2 tan rápida, se postulan como primera línea de oxidación en la señalización por H_2O_2. La C_P en sulfénico puede reaccionar con una segunda molécula oxidante y sobreoxidarse a ácido cisteinsulfínico o incluso sulfónico, modificación que debe ser reducida por sulfirredoxina a expensas de ATP y glutatión para recuperar la actividad peroxidasa de la enzima, por lo que se entiende a la sobreoxidación como un mecanismo modulador de esta enzima.

En trabajos recientes, nuestro grupo reportó la nitración de Prx2 por exposición a peroxinitrito, un potente agente oxidante que se forma *in vivo*, producto de la reacción controlada por difusión entre óxido nítrico y superóxido. Nuestro trabajo se centra en la caracterización fisicoquímica de la forma nitrada de la Prx2 y en cómo afecta esta modificación postraduccional su organización estructural y su funcionalidad como peroxidasa y a la vez sensora de peróxido, lo que tiene un alto impacto en señalización redox y el desarrollo de patologías asociadas con estrés oxidativo. Los resultados obtenidos asocian la nitración de Prx2 por peroxinitrito con una ganancia de actividad peroxidasa y una menor sensibilidad a sobreoxidarse por H_2O_2 de la enzima. Nuestros resultados implican a la Y193 -perteneciente al motivo YF conservado en Prx sensibles a sobreoxidación- como residuo fundamental en esta modulación de la actividad de Prx2, cuya nitración favorece el cambio conformacional necesario para que se forme el disulfuro en el sitio activo de la enzima, protegiéndola así de inactivarse y aumentando su actividad peroxidasa. El extremo C-terminal (que contiene el motivo YF) aparece nuevamente como un punto estructural sensible que modula la velocidad de cierre del disulfuro y por ende, el rol de Prx2 en las vías de señalización redox.

ÍNDICE DE ABREVIATURAS

AhpC	alquilhidroperóxido reductasa C
ASK1	quinasa reguladora de la señal de la apoptosis 1
BCK	creatinin cinasa cerebral humana (BCK, monómero, CKBB, dímero)
CD	dicroísmo circular
C_P	cisteína peroxidática
C_R	cisteína resolutiva
CRMP2	collapsin response mediator protein 2
*Ec*TR	tiorredoxina reductasa de *E. coli*
*Ec*Trx	tiorredoxina 1 de *E. coli*
ERp46	proteína del retículo endoplásmico 46
FF	*fully folded*, completamente plegada
GAPDH	gliceraldehído-3-fosfato deshidrogenasa
GPx	glutatión peroxidasa
GSH	glutatión
GSNO	nitrosoglutatión
H_2O_2	peróxido de hidrógeno
HRP	peroxidasa de rábano picante
LU	*locally unfolded*, localmente desplegada
MMTS	S-metil metanotiosulfonato
NO_2Y	nitrotirosina
NOX	NADPH oxidasa
ONOOH	peroxinitrito
PARP	poli(ADP ribosa) polimerasa
Prx	peroxirredoxina
PTM	modificación postraduccional
PTP1B	proteína tirosin fosfatasa 1B
RNS	especies reactivas del nitrógeno
ROS	especies reactivas del oxígeno
SEC	cromatografía de exclusión molecular
SH	tiol
SNO	S-nitrosotiol
SOH	ácido sulfénico
SO_2H	ácido sulfínico
Srx	sulfirredoxina
STAT3	signal transducer and activator of transcription 3

1. INTRODUCCIÓN

Existe consenso sobre el origen de la vida en un ambiente reductor (1). Es recién unos 2.1-2.4 billones de años atrás con la actividad de un grupo de bacterias fotosintéticas, las cianobacterias, que aumentan los niveles de oxígeno en la atmósfera como producto secundario de la reducción del CO_2 (2). Esta fotosíntesis oxigénica evolucionó y permitió a estos microorganismos expandirse y colonizar la Tierra (3,4), adaptando su metabolismo para permitir la síntesis de moléculas orgánicas compuestas como reserva energética a largo plazo, favoreciendo que la vida se mantuviera en esa atmósfera oxigenada y pudieran evolucionar organismos multicelulares (5-7).

Frente a la aparición de la atmósfera aeróbica, los organismos desarrollaron distintas estrategias entre los que se encuentran los procesos generadores de energía mediante la respiración, a su vez generando sistemas de protección a la presencia de oxígeno y sus derivados (8). Las estrategias antioxidantes desarrolladas en los sitios de producción de oxígeno hicieron posible la protección de los componentes celulares frente a moléculas oxidantes altamente reactivas producidas (especies reactivas del oxígeno o ROS, por sus siglas en inglés) (Figura 1). Independientemente de la estrategia evolutiva, la exposición a las ROS era inevitable (9-11), y algunas de estas especies oxidantes tienen la capacidad de reaccionar de manera inespecífica con componentes de las células pudiendo causar daño irreversible -por ejemplo a lípidos, proteínas, metales, clorofilas o centros ferrosulfurados. Es así que fueron apareciendo sistemas antioxidantes -tanto enzimáticos como no enzimáticos- para protegerse de estas especies reactivas y mecanismos celulares de respuesta a estos estímulos, abriendo así la puerta para su uso en vías de señalización y regulación (8).
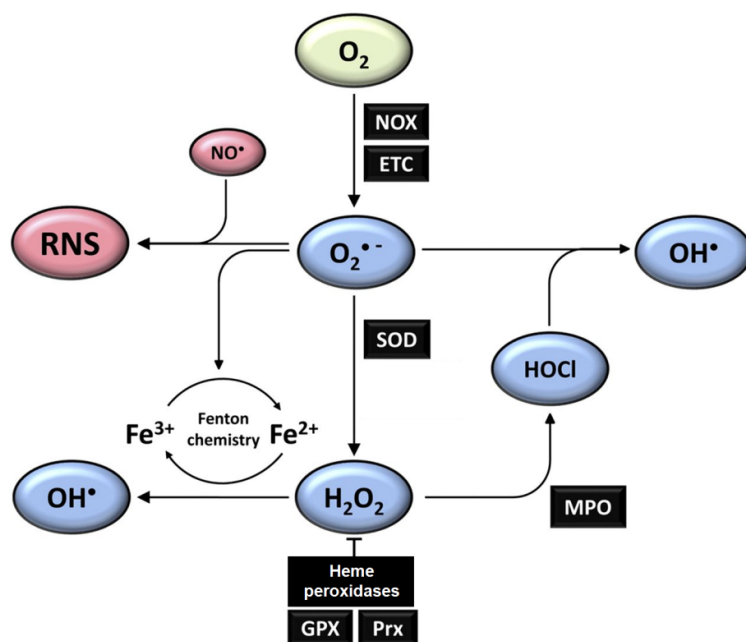
Figura 1. Vías fisiológicas de formación y descomposición de especies reactivas del oxígeno y del nitrógeno. La reducción por un electrón del oxígeno molecular resulta en la formación de superóxido ($O_2^{\bullet-}$), lo que puede ocurrir como producto de la actividad de NADPH oxidasas (NOX), y también como producto secundario de la fosforilación oxidativa en la cadena de transporte electrónico de la membrana mitocondrial (ETC). El superóxido puede actuar como reductor o como oxidante, y es una molécula clave en numerosas reacciones fisiológicas subsecuentes. La mayoría del superóxido generado *in vivo* es convertido en peróxido de hidrógeno (H_2O_2) por la acción de las superóxido dismutasas (citosólica, mitocondrial y extracelular). Los niveles de H_2O_2 están a su vez regulados por varios mecanismos que incluyen la acción de enzimas como la catalasa, las glutatión peroxidasas (GPx) y las peroxirredoxinas (Prx), y de sistemas no enzimáticos como el glutatión (GSH). El H_2O_2 puede ser sustrato de las mieloperoxidasas (MPO) durante una respuesta inmune generándose ácido hipocloroso (HOCl). A su vez, en presencia de cationes metálicos libres como Fe^{2+} ó Cu^+, el H_2O_2 puede formar radical hidroxilo ($OH^{\bullet}$) mediante mecanismo tipo Fenton. Cuando superóxido y óxido nítrico ($^{\bullet}NO$) se producen en un mismo compartimento, pueden formar peroxinitrito y a partir de ahí otras especies reactivas del nitrógeno (RNS). En verde se representa el oxígeno molecular, en azul las ROS derivadas del O_2 y en rojo el óxido nítrico y las demás RNS derivadas. Figura editada de (12).

Este trabajo se centra en la caracterización estructural y funcional de la peroxirredoxina 2 humana (Prx2), una proteína que reduce peróxidos protegiendo a la célula de posible daño oxidativo, y protagonista de vías de señalización celular dependientes de peróxido. En esta introducción primero se describirán las especies oxidantes -más concretamente peróxidos- que son sustrato de esta enzima, para luego pasar a describir a las peroxirredoxinas (Prx) en general y a la Prx2 en particular.

1.1. Peróxidos y sistemas de reducción de peróxidos intracelulares

1.1.1. Peróxido de hidrógeno (H_2O_2)

El peróxido de hidrógeno (H_2O_2) pertenece al grupo de las llamadas ROS y es producido como producto secundario de la respiración a nivel mitocondrial y como producto final de numerosas reacciones metabólicas, oxidasas u oxidorreductasas. A esto se suma que diversos estímulos (como pueden ser factores de crecimiento, citocinas, insulina) pueden activar el ensamblaje de distintas subunidades de la NADPH oxidasa (Nox) de la membrana, o inducir la expresión de los genes Nox, resultando en la producción de superóxido ($O_2^{\bullet-}$). La mayoría del H_2O_2 en las células se forma a partir de la reacción de dismutación del $O_2^{\bullet-}$ (en la que una molécula de $O_2^{\bullet-}$ se oxida y otra se reduce, generando como productos H_2O_2 y O_2) (Figura 1), por lo que las fuentes de $O_2^{\bullet-}$ son consideradas también fuentes de H_2O_2 (10,13). La dismutación del $O_2^{\bullet-}$ se da espontáneamente a una velocidad relativamente alta ($\approx 10^5$ $M^{-1}s^{-1}$ a pH 7.0), y puede además ser catalizada por las enzimas superóxido dismutasas (SOD) que la aceleran hasta 10^9 $M^{-1}s^{-1}$, convirtiéndolo en un proceso casi controlado por difusión (14). Las superóxido reductasas (SOR) catalizan la reducción directa del $O_2^{\bullet-}$ formando como producto H_2O_2 (14). En las células de mamíferos, las NADPH oxidasas (NOX) y las cadenas transportadoras de electrones de las mitocondrias son consideradas las principales fuentes de $O_2^{\bullet-}$, pero además existen otros sistemas capaces de generar $O_2^{\bullet-}$, como la xantina oxidasa y el sistema enzimático del citocromo P450, entre otros (15).

El H_2O_2 es un oxidante fuerte, $E^{\circ\prime}$ (H_2O_2, H_2O) = 1.32 V a pH 7.0 (16) pero las barreras cinéticas hacen que sea reactivo sólo con tiol, selenol, hemo (que son la base de su rol en señalización redox), o con metales de transición (que dan lugar a la formación de radical hidroxilo vía mecanismo Fenton, altamente reactivo y oxidante) (17).

Los oxidantes biológicos como el H_2O_2 han sido largamente reconocidos como los principales responsables de las modificaciones oxidativas de macromoléculas causando disfunción celular como última consecuencia del estrés oxidativo. También cumple un rol fisiológico en la activación de células del sistema inmune contra la infección por patógenos.

Más recientemente se ha acumulado evidencia que indica que la producción de bajos niveles de H_2O_2 tiene un efecto fisiológico, participando en procesos de señalización redox y regulando eventos celulares mayores como la proliferación, crecimiento, migración, apoptosis y supervivencia (18-21).

El H_2O_2 es una molécula pequeña y polar, y como tal, difunde libremente en compartimientos acuosos. Por ser una molécula pequeña y sin carga puede difundir a través de membranas biológicas, como lo hace el agua (22,23). El coeficiente de permeabilidad de las membranas celulares al H_2O_2 varía entre 10^{-3} y 2×10^{-4} cm s^{-1} y depende de la composición de la misma (24). Más recientemente se reportó que su pasaje a través de membranas biológicas puede ser facilitado por la presencia de acuaporinas (25). La difusión intracelular también se ve limitada por el *crowding* molecular y se estima que el coeficiente de difusión efectivo de moléculas pequeñas puede ser reducido hasta en un 60% por este efecto (26). Esta capacidad de difundir rápidamente del H_2O_2 implica que cuando la fuente de producción de este oxidante es extracelular, el mismo difundirá aleatoriamente en distintas direcciones y una porción menor del peróxido producido entrará a las células pudiendo oxidar componentes intracelulares, dependiendo del volumen extracelular y de la composición de las membranas celulares (27).

A pesar de estar ampliamente aceptado hoy en día que a niveles fisiológicos el H_2O_2 actúa como molécula señalizadora, los mecanismos moleculares por los que ejerce esta función aún se encuentran bajo intensa investigación (27). La manera en que el H_2O_2 participa en procesos de señalización intracelular necesita entenderse a nivel mecanístico. A diferencia de otros segundos mensajeros (*i.e.*, cAMP), el H_2O_2 es una molécula tan sencilla químicamente que su reconocimiento molecular representa un desafío. De hecho, no se conoce ninguna proteína capaz de unir H_2O_2 de forma reversible. Sin embargo, la señal se transmite mediante la oxidación de residuos de cisteína de proteínas blanco y el efecto que esta modificación química pueda tener río abajo en la vía (27-29).

1.1.2. Peroxinitrito (ONOO⁻/ONOOH)

Desde que se reportó la participación del peroxinitrito[1] en procesos fisiopatológicos hace casi 30 años (30-32), se han hecho importantes avances en cuanto a sus vías de formación, mecanismos de reacción, detoxificación y acción celular (33-35). Actualmente se sabe que participa en el desarrollo de numerosas enfermedades (36), incluyendo patologías neurodegenerativas (37), cardiovasculares (38,39), diabetes (40,41) y desórdenes inmunológicos e inflamatorios (42-44). La comprensión de los mecanismos por los cuales el peroxinitrito ejerce sus efectos citopatológicos puede aportar en el desarrollo racional de tratamientos para estas patologías (36).

La principal ruta de formación del peroxinitrito en sistemas biológicos es la reacción de terminación entre los radicales superóxido ($O_2^{\bullet-}$) y óxido nítrico ($^\bullet NO$) (Figura 1), con una constante de velocidad controlada por difusión de 10^9-10^{10} M^{-1} s^{-1} (45-47), por lo tanto suficientemente rápida como para competirle a la reacción de dismutación del superóxido catalizada por la SOD. Dada la naturaleza aniónica del $O_2^{\bullet-}$ a pH fisiológico (pK_a $HO_2^\bullet$ = 4.8), y por ende su limitada capacidad de difusión a través de membranas, y el tamaño pequeño del $^\bullet NO$, molécula neutra y lipofílica que puede fácilmente difundir a través de membranas biológicas, se desprende que la formación biológica de peroxinitrito se dará en compartimientos donde se produce superóxido (36).

El ácido peroxinitroso puede atravesar membranas biológicas por difusión pasiva, mientras la forma desprotonada (pK_a = 6.5–6.8) (45,47,48) -que predomina a pH fisiológico- utiliza canales aniónicos, por lo que su permeación se ve limitada por el número de canales disponibles en la membrana celular (49,50).

Tanto el peroxinitrito anión como el ácido peroxinitroso son oxidantes fuertes que reaccionan directamente con diferentes macromoléculas. Una propiedad importante del ácido peroxinitroso es que decae por homólisis de su enlace peroxo (k = 0.9 s^{-1}, pH 7.4, 37°C), dando como productos los radicales hidroxilo ($^\bullet OH$) y dióxido de nitrógeno ($^\bullet NO_2$) con un 30% de rendimiento (45,51). Ambos radicales participan en reacciones secundarias que pueden llevar a la oxidación/nitración de distintos blancos (Figura 2) (36,52).

---

[1] El término peroxinitrito refiere a la mezcla de anión peroxinitrito (ONOO⁻) y ácido peroxinitroso (ONOOH); la nomenclatura recomendada por IUPAC es oxoperoxinitrato e hidrógeno peroxonitrato respectivamente.
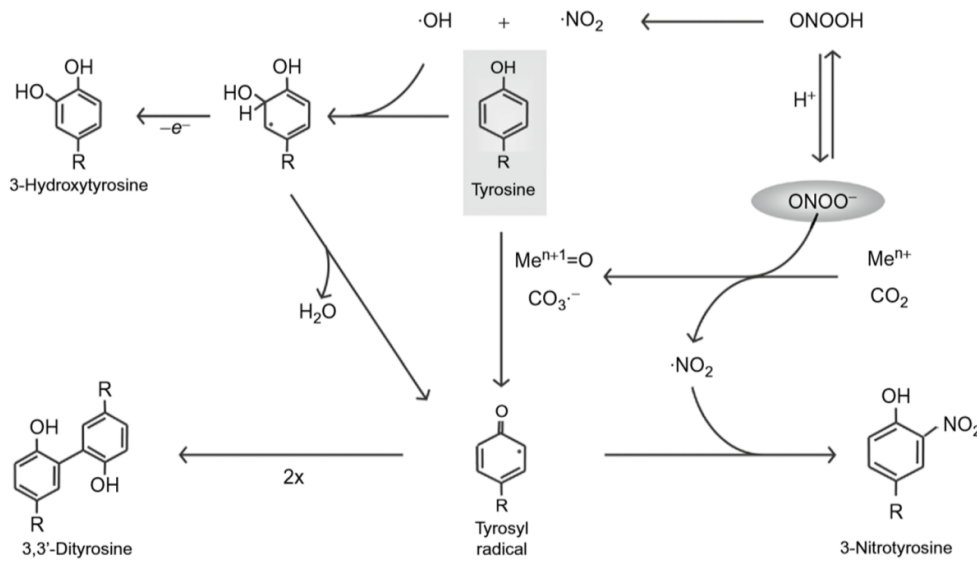
Figura 2. Mecanismos de modificación de proteínas por peroxinitrito. El peroxinitrito anión ($ONOO^-$) en equilibrio con su ácido conjugado (ácido peroxinitroso, ONOOH) puede reaccionar con centros metálicos (Me^{n+}) o dióxido de carbono (CO_2) para dar las especies altamente oxidantes complejo oxo-metálico ($Me^{n+1} = O$) y radical carbonato ($CO_3^{\cdot-}$), respectivamente, junto con radical dióxido de nitrógeno ($^{\cdot}NO_2$). $Me^{n+1} = O$ y $CO_3^{\cdot-}$ pueden a su vez oxidar una tirosina a radical tirosilo que puede entonces combinarse con $^{\cdot}NO_2$ para dar el aminoácido postraduccionalmente modificado 3-nitrotirosina. Dos radicales tirosilo pueden también recombinar para dar 3-3'-ditirosina. Por otro lado, en ausencia de blancos, el ácido peroxinitroso homoliza parcialmente (30%) para dar $^{\cdot}OH$ y $^{\cdot}NO_2$. El radical hidroxilo reacciona con tirosinas generando un aducto intermediario que puede deshidratarse para dar radical tirosilo u oxidarse a 3-hidroxitirosina. Figura tomada de (36).

1.1.3. Sistemas de reducción de peróxidos

1.1.3.1. Sistemas no enzimáticos

Las reacciones de H_2O_2 y peroxinitrito con distintos blancos intracelulares han sido ampliamente caracterizadas. El H_2O_2 reacciona fundamentalmente con tioles en reacciones que se describen más adelante, mientras que el peroxinitrito tiene diversidad de vías de oxidación de blancos celulares (Figura 2). Entre éstos, los tioles de bajo peso molecular y proteicos, centros metálicos y dióxido de carbono (CO_2) constituyen los principales blancos para el peroxinitrito *in vivo* (33,36). Los mecanismos por los que ocurre esta oxidación varían dependiendo de cada blanco (36). El peroxinitrito reacciona rápidamente con centros metálicos de proteínas, particularmente con hierro hemo y no-hemo, cobre y manganeso, con constantes de reacción entre ~10^4 a 10^7 $M^{-1}s^{-1}$, y los mecanismos dependerán de la proteína

14

conteniendo el centro metálico. Para las hemoproteínas, el peroxinitrito reacciona como oxidante de un electrón para dar $^{\bullet}NO_2$ mientras que al participar de un proceso de dos electrones se genera nitrito (NO_2^-) además del centro metálico oxidado (Figura 3). A su vez, algunos complejos metálicos pueden catalizar la isomerización de peroxinitrito a nitrato (NO_3^-) (53).

Por otro lado, la interacción del peroxinitrito con proteínas especializadas en su descomposición catalítica resulta en detoxificación de peroxinitrito sin una modificación neta de la proteína involucrada, ya sea porque la proteína cataliza la isomerización del peroxinitrito (54), o como resultado de la rápida re-reducción de la proteína oxidada por otros componentes celulares (55).
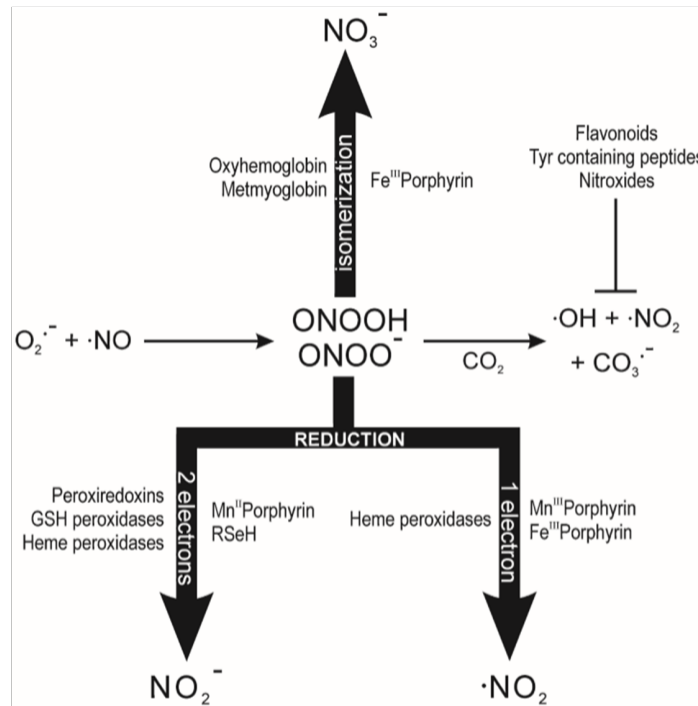
Figura 3. Principales vías de detoxificación del peroxinitrito. La detoxificación de peroxinitrito puede ocurrir por isomerización a nitrato o por reducción. La isomerización a nitrato es catalizada por algunas hemoproteínas, como la oxihemoglobina y la metamioglobina, y por Fe^{III} porfirinas sintéticas. La reducción puede involucrar procesos de 1 ó 2 electrones. Enzimas tales como las peroxirredoxinas, glutatión peroxidasa, y algunas hemoperoxidasas catalizan la reducción por 2 electrones del peroxinitrito a nitrito, y esta reacción es también catalizada por algunas Mn^{II} porfirinas y por selenoles sintéticos. La reducción por 1 electrón que da lugar a dióxido de nitrógeno es catalizada por algunas hemoperoxidasas o por Mn^{III} y Fe^{III} porfirinas sintéticas. Otros compuestos, como los flavonoides y péptidos que contengan tirosinas pueden proteger contra el daño oxidativo por peroxinitrito reaccionando con sus radicales derivados. Varios de los compuestos nombrados pueden también reaccionar con los radicales precursores del peroxinitrito, evitando su formación. Figura tomada de (55).

El caso específico de la reducción de peroxinitrito por tioles ha sido ampliamente estudiado desde una perspectiva cinética (56-58). Los tioles son blancos preferenciales de las especies reactivas, y las constantes de segundo orden de la reacción de cisteína libre, glutatión (GSH), homocisteína y el tiol de la albúmina humana (Cys34) con peroxinitrito son cercanas a 10^3 M^{-1} s^{-1} a pH 7.4 y 37 °C, cerca de tres órdenes de magnitud mayores que la reacción correspondiente con H_2O_2 (56-58). Por ejemplo, el H_2O_2 reacciona con el glutatión reducido (GSH) con una k = 0.87 M^{-1} s^{-1} a pH 7.4 y 37 °C, que toma particular relevancia por su alta concentración intracelular en el orden milimolar (27,59).

La reactividad de los tioles es un tema complejo que involucra una diversidad de funciones como pueden ser catalítica, estructural, reguladora, como quelante de metales, o ninguna de las anteriores (60). La base de las reacciones de tioles en bioquímica involucra el ataque nucleofílico del tiolato sobre un electrófilo. Esto significa que, al estudiar la reactividad de un tiol, dependiendo de su pK_a y del pH de trabajo, sólo una fracción estará disponible como tiolato, y por ende solamente parte de la reactividad es detectable a dicho pH. En este sentido, en la literatura suele compararse la reactividad de distintos tioles de bajo peso molecular a un mismo pH (58,61-63), pero esto puede llevar a la errónea conclusión general de que los tioles más ácidos son en general más reactivos (64). Se definen entonces las constantes cinéticas independientes del pH (k_{RS^-}), correspondientes a la reacción general expresada en la Ecuación 1, que son mejores predictores de la reactividad independientemente de las condiciones experimentales empleadas para determinar las constantes de reacción.

$$RS^- + \text{reactivo} \rightarrow \text{Productos} \qquad \text{Ecuación 1}$$

El valor numérico de k_{RS^-} se obtiene dividiendo la constante cinética aparente a un pH dado (k^{pH}_{app}) por la fracción de tiolato disponible a ese mismo pH de la siguiente manera:

$$k_{RS^-} = k^{pH}_{app} \left(\frac{K^{RSH}_a + [H^+]}{K^{RSH}_a} \right) \qquad \text{Ecuación 2}$$

Donde K^{RSH}_a es la constante de ionización del tiol. De hecho, k_{RS^-} puede ser extrapolado determinando k^{pH}_{app} experimentalmente en un rango de pH cercano al valor del pK_a y ajustando los resultados a la Ecuación 2. (28)

1.1.3.2. Sistemas enzimáticos

Por muchos años considerado tóxico, con el tiempo el H_2O_2 ha pasado a ser visto como protagonista de numerosos procesos fisiológicos. En un principio la reducción de H_2O_2 se asociaba a la presencia de un grupo prostético hemo y a la acción de la catalasa (65,66). La catalasa es una hemoperoxidasa que se encuentra en todos los organismos, y en humanos se expresa en todos los órganos, midiéndose los mayores niveles de actividad en el hígado, riñones y eritrocitos, y su localización subcelular es principalmente en peroxisomas (67). Con un número de recambio extraordinariamente elevado ($\sim 2 \times 10^6$ s^{-1} (68)), su principal función reportada es catalizar la dismutación de H_2O_2 para dar oxígeno molecular y agua ($2H_2O_2 \rightarrow 2H_2O + O_2$), para lo que utiliza hemo como cofactor (69). Se ha reportado que la catalasa puede además reducir peroxinitrito (70,71).

Años después se describieron las primeras glutatión peroxidasas, selenoproteínas reductoras de peróxido (72-74). En mamíferos, y en particular en humanos, varios miembros de esta familia tienen selenocisteína en su sitio activo, lo que les confiere una extraordinaria reactividad con H_2O_2 ($k > 10^7$ $M^{-1} s^{-1}$), mientras que otras GPx poseen un residuo de cisteína en su sitio activo (75). Interesantemente, se ha descrito también que reducen peroxinitrito (76,77). La SeCys oxidada de las GPx 1-4 es reducida por GSH, mientras que las que contienen Cys en su sitio activo prefieren reaccionar con Trx u otras proteínas (75,78).

Más recientemente se han descripto las peroxirredoxinas (Prx), enzimas que reducen H_2O_2 a expensas de cisteínas, sin necesidad de grupo prostético ni de selenocisteína, y que tienen una extraordinaria reactividad con peróxidos (79,80). Varias peroxirredoxinas poseen además actividad peroxinitrito reductasa con constantes de reacción del orden de $10^5 - 10^7$ $M^{-1} s^{-1}$ (81-95) y podrían por lo tanto proteger la célula contra el estrés nitroxidativo mediado por peroxinitrito (96-98). Las Prx serán abordadas en mayor profundidad a continuación.

1.2. Peroxirredoxinas: ciclo catalítico, clasificación y estructura cuaternaria

1.2.1. Generalidades

Las peroxirredoxinas (Prx) son enzimas que reducen H_2O_2, hidroperóxidos orgánicos y peroxinitrito mediante un mecanismo dependiente de cisteínas y sin la necesidad de cofactores. Ampliamente distribuidas en el árbol evolutivo, se expresan en todos los tipos celulares del cuerpo humano en cantidades relativamente importantes (15 - 410 µM) (99-102).

Estas enzimas han sido principalmente descritas como peroxidasas, aunque se les atribuyen otras funciones, como la actividad chaperona o "foldasa" en algunas Prx (103,104), y han sido asociadas a numerosos procesos fisiológicos y fisiopatológicos, entre ellos el desarrollo de procesos tumorales (29).

1.2.2. Mecanismo catalítico de Prx

El mecanismo catalítico de las Prx depende de la presencia de una cisteína llamada cisteína peroxidática (C_P), absolutamente conservada. Este residuo se encuentra formando parte de un sitio activo altamente conservado, con una Pro y una Arg absolutamente conservados y una Thr solamente sustituida por Ser en un bajo porcentaje de variantes de Prx (Figura 4).

Estos residuos se organizan de manera tal de favorecer la activación de la molécula de peróxido unida y catalizar la escisión del enlace O-O, a su vez promoviendo el ataque del tiolato de la C_P sobre el hidroxilo terminal del sustrato (Figura 4B) (28,105). Es así que el motivo Pxxx(T/S)xxC, en conjunto con la Arg próxima espacialmente pero proveniente de una región alejada en la secuencia aminoacídica, son una característica esencial del sitio activo de las Prx (106). A su vez, las Prx tienen un plegamiento que consiste en 7 láminas beta rodeadas por 5 hélices alfa (Figura 5A) que es también muy conservado, a pesar de las diferencias que puedan existir tanto en su secuencia como en mecanismo catalítico. A este plegado se lo denomina de tipo tiorredoxina por sus similitudes estructurales (Figura 5B).
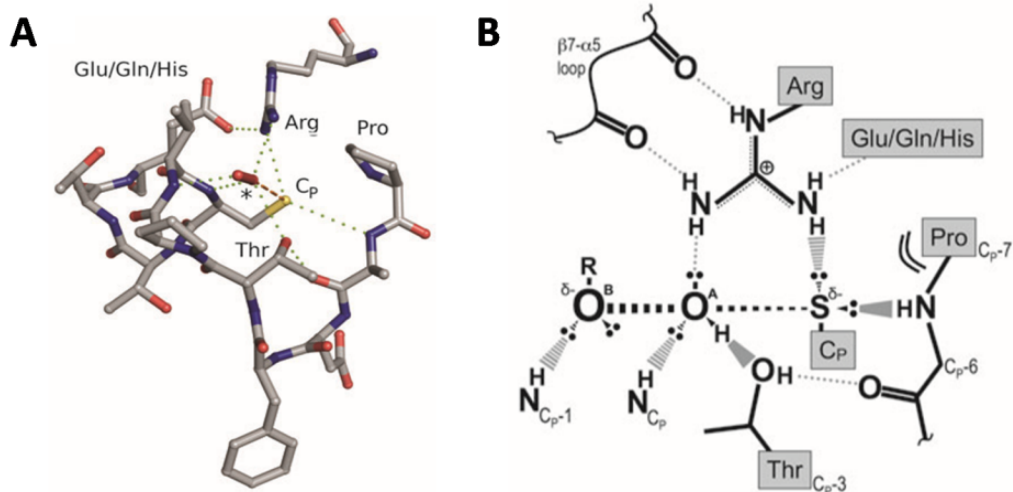
Figura 4. (A) Representación del sitio activo conservado de Prx. Los residuos conservados C_P, Arg y Pro y la Thr están marcados, así como el residuo Glu/Gln/His no tan conservado pero que colabora en orientar la Arg correctamente. Las líneas punteadas representan la red de enlaces de hidrógeno que favorece la unión y activación del peróxido y de la C_P para la catálisis. **(B)** Representación de la conformación del sitio activo en el estado de transición. Las interacciones estabilizadoras entre los átomos clave de la cadena principal y los cuatro residuos conservados, y con el H_2O_2 sustrato, están indicadas. En el estado de transición, un enlace se forma entre el átomo de S de la C_P y el O^A del H_2O_2, y un enlace se está rompiendo entre los átomos O^A y O^B del peróxido. La geometría del sitio activo es ideal para estabilizar la mayor distancia entre los átomos O^A y O^B a medida que se rompe el enlace. Figura editada de (107).
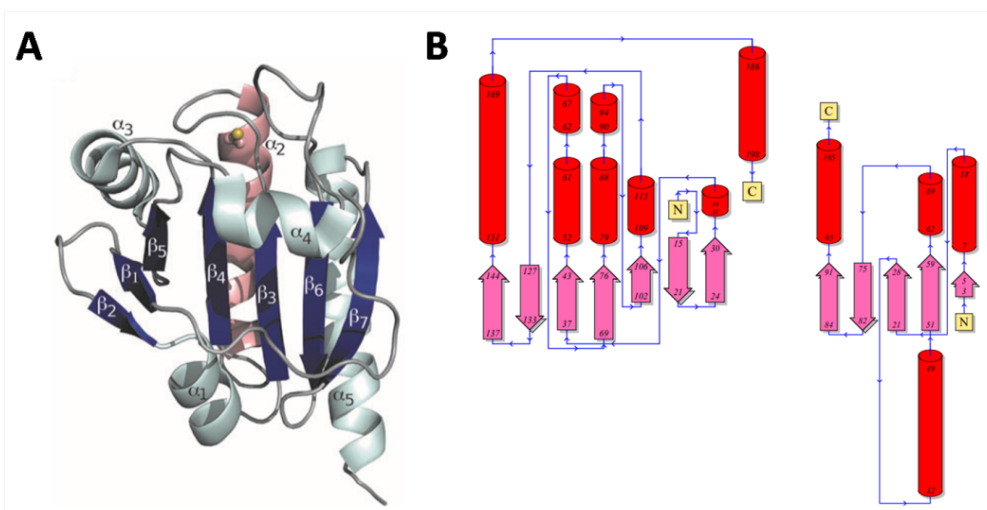
Figura 5. Elementos comunes de estructura secundaria de Prx. **(A)** Estructura representativa de una Prx monomérica en la que se muestran las α-hélices (celeste claro y rosa) y las hojas β (azul oscuro) comunes a todas las Prx conocidas. La C_P (en la que el átomo se azufre está amarillo) se localiza en la primera vuelta de la hélice α_2 (rosa). La estructura representada es la de una Prx monomérica de la subfamilia de las BCP. **(B)** Esquema de la topología de Prx2 (izquierda) y Trx (derecha). La Figura del panel A fue editada de (107). La Figura del panel B fue creada usando PDBsum y los PDB 1QMV y 1AUC para la Prx2 humana (izquierda) y la Trx1 humana (derecha), respectivamente.

Como se esquematiza en la Figura 6, la reacción del peróxido con el tiolato de la C_P reducida es el primer paso de la oxidación de las Prx. Una vez formado el ácido cisteinsulfénico, el ciclo catalítico continúa con la formación de un enlace disulfuro intermolecular con la llamada cisteína resolutiva (C_R) en el caso de las Prx de 2 cisteínas (2-Cys Prx) típicas, o intramolecular en el caso de las 2-Cys Prx atípicas ya que reacciona con C_R de la misma subunidad. En mamíferos, estos disulfuros son luego reducidos por sistemas como el de la Trx/TR que utiliza NADPH (108). En las Prx de 1 cisteína (1-Cys Prx), el disulfuro se forma con el tiol de otra proteína o un tiol de bajo peso molecular como por ejemplo con glutatión reducido, GSH.
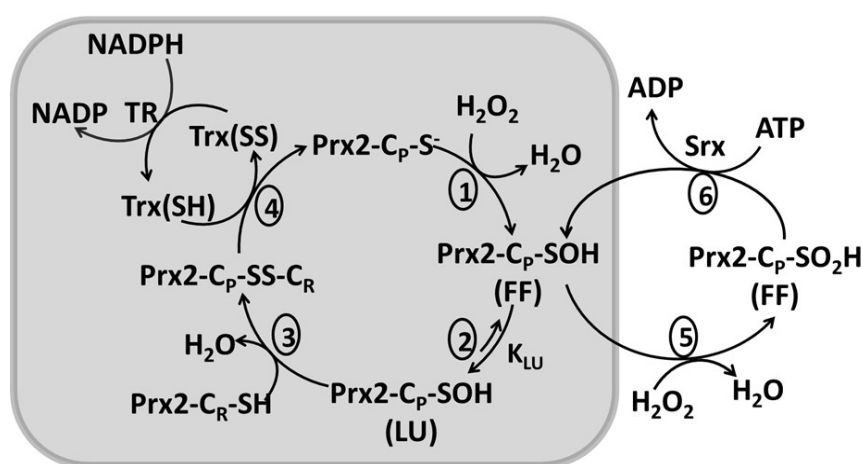
Figura 6. Ciclo catalítico de Prx2. 1, reacción de una molécula de H_2O_2 con el tiolato de la C_P para formar ácido cisteinsulfénico. 2, transición de la forma FF a la conformación LU. 3, reacción del ácido cisteinsulfénico de la C_P con la C_R. 4, reducción del enlace disulfuro de Prx2. 5, sobreoxidación de la C_P a ácido cisteinsulfínico. 6, reducción del ácido cisteinsulfínico por sulfirredoxina (Srx)/ATP. La proteína está representada como un único sitio activo dentro de un dímero funcional. Figura tomada de (109).

Luego de la formación del ácido sulfénico de la C_P, se ve favorecido un cambio conformacional en el sitio activo que favorece el pasaje de un estado "completamente plegado" (FF por "fully folded") a uno "localmente desplegado" (LU por "locally unfolded") (paso 2 en la Figura 6). La velocidad a la que ocurre este cambio conformacional y la reacción de resolución afectan el tiempo en que el sulfénico permanece en FF, lo que ha sido vinculado a la facilidad con que ese sulfénico reacciona con una segunda molécula de peróxido para dar ácido cisteinsulfínico, incapaz de formar el disulfuro necesario para continuar el ciclo catalítico (paso 5 en la Figura 6). Esta reacción, denominada sobreoxidación (o hiperoxidación), ocurre con distinta facilidad entre las Prx, encontrándose Prx más sensibles y otras menos.

En particular, las Prx de 2-Cys típicas eucariotas son notoriamente más sensibles a esta forma de inactivación, y esta variabilidad en la susceptibilidad a sobreoxidarse por sustrato se ha visto vinculada a diversos motivos estructurales que afectan el equilibrio entre las formas FF y LU de la proteína, entre los que se destacan los motivos YF y GGLG (Figura 7) (110). Se ha descrito que la presencia de estos motivos en la secuencia favorece la sobreoxidación de C_P, enlenteciendo el cambio conformacional necesario para que se forme el disulfuro y favoreciendo así la permanencia del sulfénico en la conformación FF disponible para reaccionar con un segundo peróxido (107,111,112).
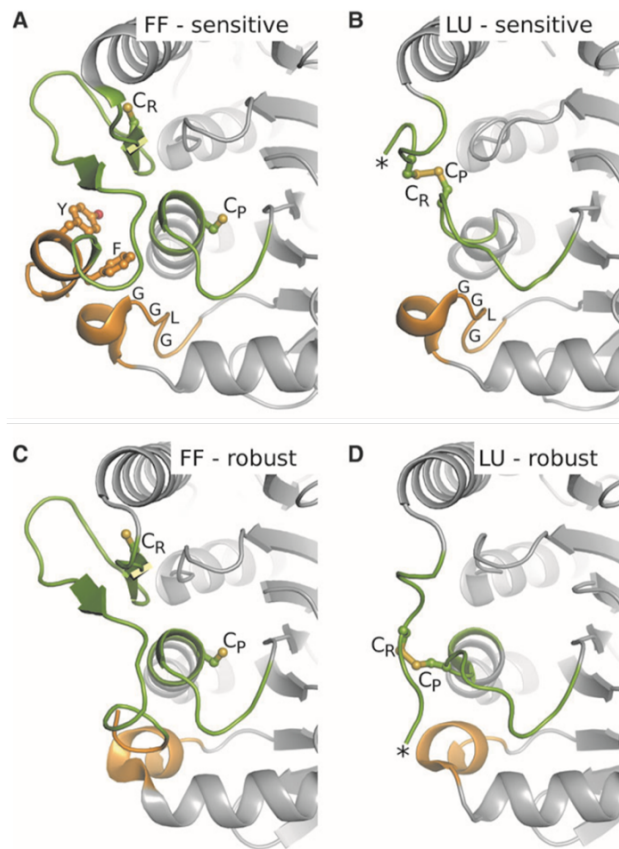
Figura 7. Motivos estructurales implicados en la sensibilidad a sobreoxidarse de las Prx. **(A, B, C, D)** Representación del sitio activo de una Prx sensible (*Rn*Prx1) y una robusta (*St*AhpC), ambas pertenecientes a la subfamilia Prx1. Los paneles **A** y **C** muestran las proteínas en la conformación FF y los paneles **B** y **D** en la conformación LU. Los motivos YF y GGLG están presentes en las enzimas sensibles pero ausentes en las robustas. En las conformaciones LU no se ve el extremo C-terminal debido a que no se ha logrado resolver en esta conformación por cristalografía, por lo que se indica el segmento truncado con un asterisco. Figura tomada de (107).

Comprender este equilibrio entre las formas FF y LU de las Prx eucariotas implica entender que las proteínas son dinámicas por naturaleza, que tienen movilidad interna y que los movimientos ocurren en un amplio rango de escalas temporales que van desde los pico y nanosegundos hasta los micro y milisegundos, o incluso ciertos procesos transcurren en el rango de los segundos (113). Lo que se observa en una estructura cristalográfica, en un modelo obtenido por RMN o en un espectro de dicroísmo circular, son representaciones promedio del conjunto de microestados

conformacionales que existe en el cristal o en solución (114). La actividad biológica de las proteínas está determinada no sólo por su estructura, la secuencia primaria de aminoácidos, su habilidad para plegarse, sino también por la particular dinámica de dicha estructura. No entendemos a las proteínas como estructuras rígidas e imperturbables, sino por el contrario, como un conjunto dinámico de conformaciones. La dinámica estructural proteica presenta restricciones impuestas tanto por la topología de la proteína -el recorrido de la cadena polipeptídica en el espacio- como por las estabilidades locales. Además, la estabilidad conformacional global impone un marco termodinámico, también definido por las condiciones fisicoquímicas del entorno (composición química del medio, temperatura, pH). Las proteínas responden a perturbaciones redistribuyendo las movilidades y las fluctuaciones que producen los estados conformacionales (113). En este contexto, el balance entre dinámica y consolidación de interacciones nativas impacta en la estabilidad conformacional a través de posibles compensaciones entálpicas y entrópicas del estado nativo (115).

El estado nativo, a diferencia de las conformaciones desplegadas, por lo general, presenta baja entropía conformacional. Aun así, consiste de múltiples subestados que se interconvierten rápidamente (114). Estos subestados pueden presentar energías muy similares, pero sus conformaciones locales pueden ser muy diferentes como resultado del movimiento de algún elemento de estructura secundaria, cambio en la conformación de un loop, o reorientaciones de cadenas laterales (115).

Ciertos subestados pueden presentar energías significativamente mayores que los subestados basales, determinando una baja proporción de los primeros con respecto a los segundos en solución. A estos subestados poco representados (o poco poblados) se los suele llamar subestados o estados "excitados" (114). La energía de estos subestados puede modularse mediante procesos de unión de ligandos, interacción con otras proteínas o modificaciones postraduccionales (113). La población de cada subestado está determinada por su energía libre relativa, en tanto que la tasa de interconversión está determinada por las barreras de energía entre los subestados. El ensamble de subestados también puede variar con la condición de trabajo (temperatura, presión, pH, fuerza iónica, interacción con ligando, concentración de proteína y estado de oligomerización) (115).
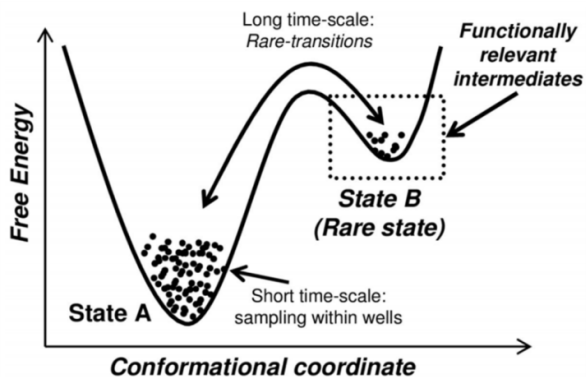
Figura 8. Las transiciones conformacionales permiten a la proteína transitar distintos sub-estados de energía. En el caso hipotético en el que una enzima se encuentre en dos posibles sub-estados A y B, el sub-estado A es de menor energía y está más poblado que el sub-estado B. El sub-estado B contiene conformaciones que son funcionalmente relevantes; por ende, las transiciones entre las conformaciones que permitan poblar el sub-estado B a más largo plazo (y su velocidad) afectarán la función proteica. Figura tomada de (113).

La facilidad con que la cadena polipeptídica se aparta del estado basal no es pareja a lo largo de toda la secuencia (116), y el estado biológicamente activo suele no coincidir con el de menor energía (114) (Figura 8), motivo por el que la función proteica depende de breves excursiones a conformaciones levemente más energéticas, posibles debido a la flexibilidad conformacional asociada al estado nativo (114,115).

1.2.3. Reactividad de Prx con peróxidos

Como se describió anteriormente, las Prx reducen peróxidos por un mecanismo dependiente de cisteínas. La constante de reacción aparente a pH 7.4 es mayor para los tioles con menor pK_a, lo que se debe a una mayor concentración de la especie desprotonada a ese pH, por ser el tiolato la especie reactiva. Si se grafica la constante de reacción independiente del pH (reactividad intrínseca de los tiolatos) (Figura 9) se observa la tendencia inversa (117,118).

Esta relación se cumple para los tioles de bajo peso molecular y muchas cisteínas proteicas. Sin embargo, como se observa en la Figura 9, algunos tioles proteicos denominados "tioles proteicos rápidos" -entre ellos la C_P de algunas Prx- no siguen dicha correlación en el gráfico de Brønsted, indicando que existen otros factores proteicos determinando su reactividad (118).
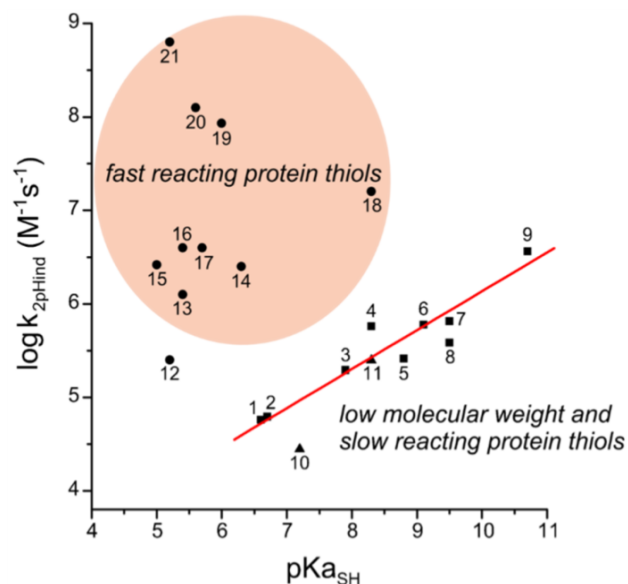
Figura 9. Cinética de reducción de peroxinitrito por tioles. La reactividad intrínseca de distintos tiolatos (k_2 independiente de pH), calculada a partir de constantes cinéticas previamente reportadas, fueron graficadas en función del pK_a del tiol (pK_{SH}). Los tioles de bajo peso molecular (cuadrados, 1-9) muestran una correlación de Bronsted positiva, como indica la recta, en la que se cumple que los tioles con mayor pK_a son mejores nucleófilos. Algunos tioles proteicos (triángulos, 10 y 11) reaccionan con peroxinitrito según lo esperado dado el pK_a de su tiol. Otros tioles proteicos (círculos, 12-21), reaccionan mucho más rápido de lo esperado, indicando que existen otros factores proteicos determinantes de su reactividad. 1. cisteína etil éster, 2. cisteína metil éster, 3. penicilamina, 4. cisteína, 5. glutatión, 6. mercapto-etil guanidina, 7. homocisteína, 8. N-acetil cisteína, 9. ácido dihidrolipoico, 10. triparredoxina de Trypanosoma brucei, 11. seroalbúmina humana, 12. arilamina N-acetiltransferasa humana 1, 13. DJ1, 14. TSA2, 15. AhpC de Mycobacterium tuberculosis, 16. creatin cinasa, 17. TSA1, 18. GAPDH, 19. Prx2 de glóbulos rojos humanos, 20. PTP1B, 21. Prx5 humana. Figura tomada de (119).

De hecho, varios de estos tioles altamente reactivos tienen una estructura que estabiliza al tiolato (28,119), lo que sería contradictorio con una alta reactividad considerando lo discutido anteriormente. La forma de explicar la alta reactividad de las Prx con sus sustratos, y en particular la alta reactividad de Prx2 con H_2O_2 y peroxinitrito, involucra el aumento de la nucleofilicidad del tiolato de la C_P mediante la formación de enlaces de hidrógeno con cadenas laterales de residuos aminoacídicos del sitio activo, favoreciendo así la desprotonación de esta cisteína, junto con la estabilización del grupo saliente (Figura 10) (28,107,118,120).
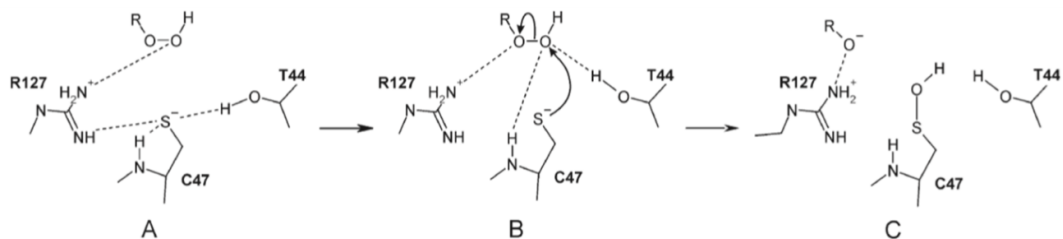
Figura 10. (A) Encuentro difusional del peróxido con el sitio activo de la Prx. **(B)** Desplazamiento de los enlaces de hidrógeno del tiolato al sustrato aumentando la nucleofilicidad del tiolato y promoviendo el ataque de éste sobre el oxígeno distal. **(C)** Clivaje del enlace peroxo del sustrato y estabilización del anión saliente por el residuo de arginina. Figura tomada de (28).

1.2.4. Clasificación de Prx

Las Prx pueden ser clasificadas según su mecanismo catalítico en Prx 1-Cys, 2-Cys típicas y 2-Cys atípicas (Figura 11). Esta clasificación ha permitido discutir diferencias y similitudes desde el punto de vista mecanístico. En este sentido, también pueden distinguirse las Prx "sensibles" de las "robustas" según la facilidad con que se sobreoxidan por el peróxido sustrato. En este sentido, existen por ejemplo Prx de 2-Cys típicas sensibles (*Hs*Prx2) y robustas (*St*AhpC).

Una clasificación más reciente se basa en el estudio comparativo y evolutivo de las secuencias que codifican para Prx, organizándolas en 6 subfamilias: Prx1/AhpC (abreviada como Prx1), Prx5, Prx6, Tpx, BCP/PrxQ y AhpE, que varían en estado oligomérico e interfaces, así como en la localización de la C_R (121). En general, las enzimas de la subfamilia Prx1 –típicamente organizadas como decámeros (pentámeros de dímeros)– son las que más se expresan, llegando a representar hasta el 0.1–1% de las proteínas solubles intracelulares (122), y coinciden con las llamadas Prx de 2-Cys típicas (120). Sin embargo, no todas las subfamilias coinciden con una de las categorías de la clasificación mecanística nombradas anteriormente.

Como se describe en (108), en mamíferos las enzimas de la subfamilia Prx1 se localizan en citosol y núcleo (Prx1 y Prx2), mitocondria (Prx3) y retículo endoplásmico (Prx4). Además, estos organismos expresan Prx de dos de las demás subfamilias: Prx5 (localizada en peroxisomas, mitocondria y citosol) y Prx6, citosólica (123). No parece haber miembros de la subfamilia PrxQ en mamíferos, ni Prx5 en archaea, y las subfamilias Tpx y AhpE están prácticamente restringidas a bacterias (121).
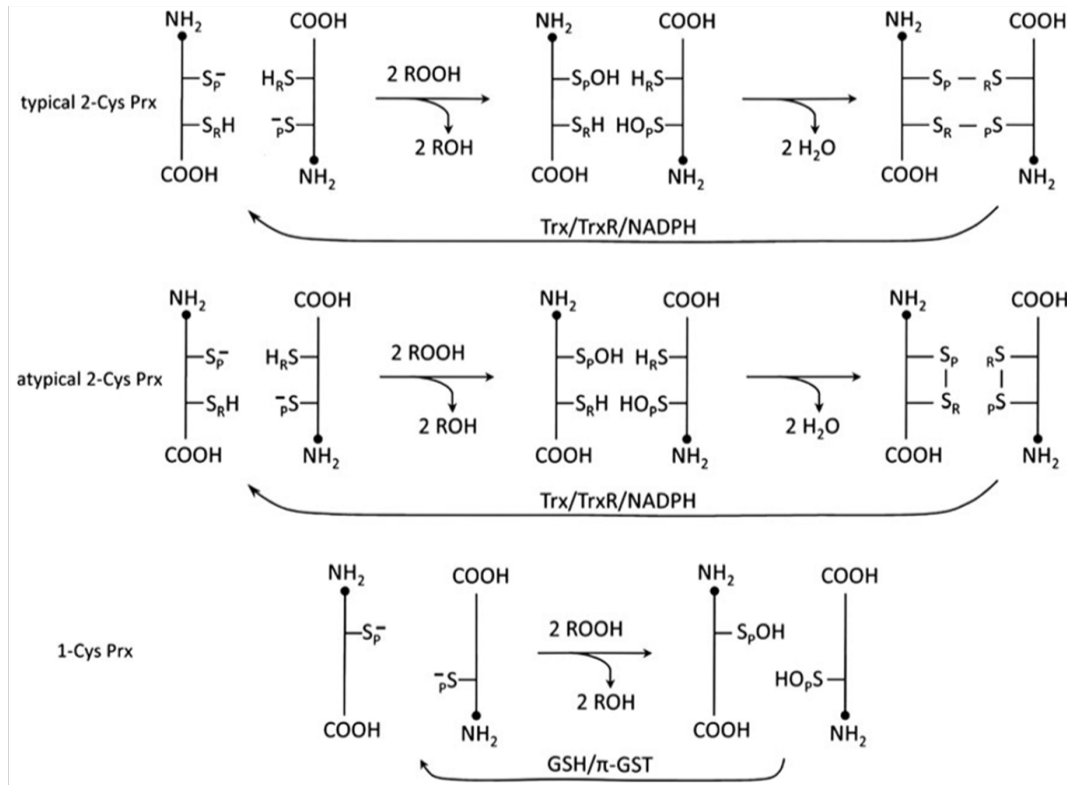
Figura 11. Mecanismo catalítico de las Prx. Todas las distintas subfamilias de Prx están representadas como dímeros. Las Prx de 2-Cys típicas forman dos enlaces disulfuro intermoleculares entre el sulfénico de la C_P (CysSOH) y la cisteína resolutiva del monómero adyacente. Las Prx de 2-Cys atípicas forman un disulfuro intramolecular por monómero, a pesar de que existe un dímero antiparalelo al igual que en las Prx de 2-Cys típicas. Las Prx de 1-Cys no forman un disulfuro ya que no tienen un residuo de Cys cercano disponible. Necesitan que participe el glutatión con la isoforma π de la glutatión transferasa en la etapa de resolución de la C_P (π-GST). Figura tomada de (124).

1.2.5. Estado oligomérico de Prx

La mayoría de las Prx existen en solución formando oligómeros; solamente algunos miembros de la subfamilia PrxQ han sido descritos como monómeros estables y activos (108). Los dímeros en los que se organizan las Prx pueden formarse mediante dos interfaces de interacción: en la interface de tipo A (por "ancestral") las subunidades interaccionan por sus extremos (subfamilias Tpx, Prx5 y los miembros diméricos de PrxQ). Los dímeros de Prx pertenecientes a las subfamilias Prx1, Prx6 y AhpE se forman por interacción entre las hojas β de dos subunidades de manera antiparalela, generando una hoja β extendida (interface de tipo B) (Figuras 12A y 12B). En el caso de las proteínas de las subfamilias Prx1 y Prx6, el extremo C-terminal, que es relativamente más largo, estabiliza estos dímeros cabeza-cola. A su vez, en las Prx

de 2-Cys típicas (miembros de la subfamilia Prx1), este C-terminal flexible contiene la C_R.
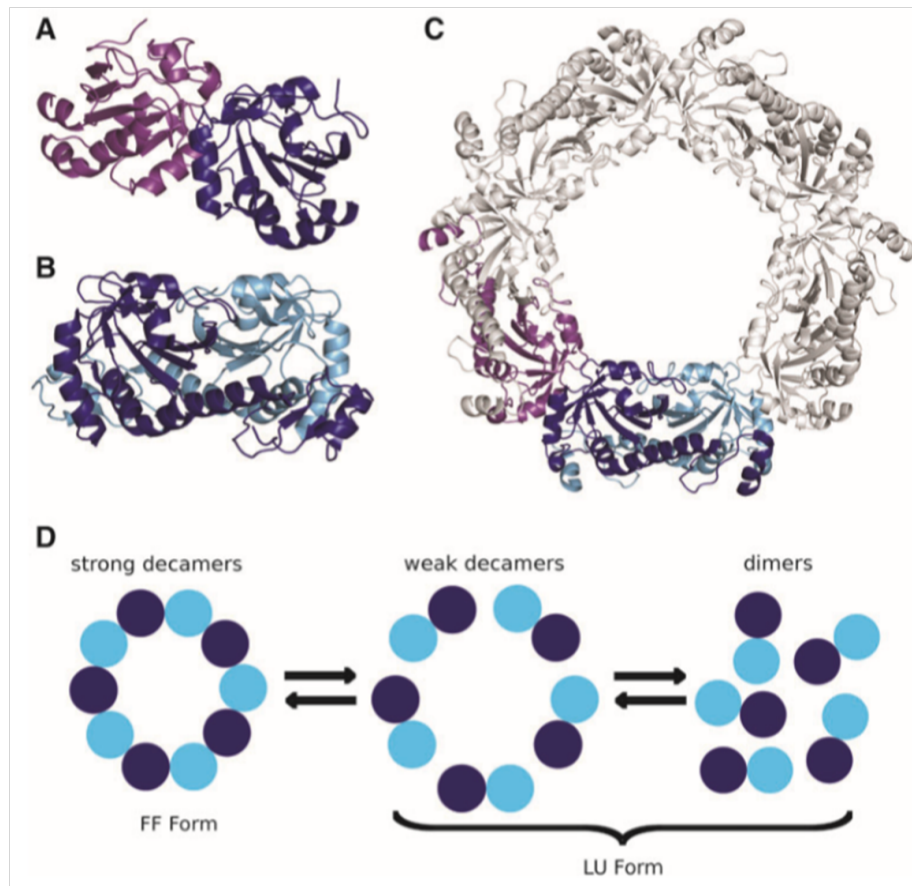
Figura 12. Estructura cuaternaria de Prx. **(A)** Dímero con interface de tipo A. **(B)** Dímero formado por interface de tipo B. **(C)** Decámero de Prx2 formado por dímeros interactuando entre sí por interfaces de tipo A. **(D)** El estado oligomérico de Prx2 es redox-dependiente, con las formas reducida y sobreoxidada favoreciendo la interacción entre dímeros (forma FF) y el disulfuro favoreciendo la conformación LU, desestabilizando el decámero. Figura tomada de (107).

Los dímeros formados por interfaces de tipo B pueden asociarse mediante interfaces de tipo A para formar complejos toroidales (Figura 12C). En general se organizan en pentámeros de dímeros ((α_2)$_5$) pero se han descrito también octámeros y dodecámeros ((α_2)$_6$) (107). Estos toroides pueden además, bajo ciertas condiciones, formar estructuras de mayor complejidad ya sea como agregados esféricos o como polímeros lineales por apilamiento de los toroides, que han sido vinculados a sobreoxidación de la C_P y actividad chaperona (103,125-129).

Una propiedad de la Prx2 humana así como de muchas de las Prx decaméricas es que residuos ubicados cerca del loop C-terminal participan de la

estabilización de la interface tipo A entre dímeros, por lo que el estado de oxidación de su C_P y el cambio a una conformación LU determina la fuerza de la interacción de dicha interface, debilitándola (Figura 12D) (107,126,130,131). Existen numerosos estudios biofísicos usando tanto cromatografía de exclusión molecular (SEC, por sus siglas en inglés) como ultracentrifugación analítica que demuestran este efecto (131-133). Esto ocurre debido a que la oxidación a disulfuro de las cisteínas del sitio activo debilita la interacción de tipo A, dando lugar a un decámero más relajado, que en Prx2 puede verse como estados intermedios (82), mientras que en otras Prx puede verse totalmente disociado a dímeros (84).

Numerosos estudios han identificado modificaciones postraduccionales, mutaciones y cambios en el pH o fuerza iónica que promueven la formación de oligómeros de alto peso molecular de Prx, aumentando así su actividad chaperona (134-137).

1.3. Prx humanas

Como se mencionó anteriormente, en mamíferos existen seis Prx (Prx1 - Prx6), que mecanísticamente se subdividen en Prx de 2-Cys típicas (Prx1 - Prx4), Prx de 2-Cys atípicas (Prx5) y Prx de 1-Cys (Prx6). A su vez, estas enzimas tienen distinta localización subcelular, encontrándose Prx1 y Prx2 en citosol y núcleo, Prx3 en mitocondria, Prx4 en retículo endoplásmico, Prx5 en peroxisomas, mitocondria y citosol y Prx6 en citosol (123).

En particular, una interrogante en el área ha sido la expresión de Prx1 y Prx2, ambas Prx de 2-Cys típicas, citosólicas, con más de 95% de similitud de secuencia y 77% de identidad de secuencia (Figura 13), pero con funciones biológicas diferenciadas (84). Las diferencias en actividad peroxidasa y chaperona, propiedades de oligomerización, sensibilidad a sobreoxidarse, sensibilidad a otras modificaciones postraduccionales e interacción diferencial con blancos intracelulares han sido y siguen siendo hoy objeto de estudio de varios grupos de investigación (84,100,131,132). Sin embargo, cada vez hay mayor consenso en que no son proteínas "duplicadas" y que cumplen funciones complementarias y no redundantes. La relevancia de estas dos peroxirredoxinas en la homeostasis celular y su rol diferencial se evidencian en los ratones *knock out* de ambas proteínas. La falta de Prx1 genera ratones que desarrollan tumores malignos y mueren prematuramente (138), mientras que la carencia de Prx2 da lugar a anemia hemolítica y esplenomegalia (139).

El rol de cada una en la señalización redox aún no se comprende totalmente, y se siguen describiendo interacciones con proteínas que participan de distintos procesos en las células y que son específicas de cada una de ellas. A su vez, se han visto diferencias en su susceptibilidad a sufrir distintas PTM tanto *in vitro* como *in vivo*. En particular, a pesar de un primer reporte en el que Prx1 aparecía como más sensible a sobreoxidación que Prx2 (132), los reportes posteriores coinciden en que Prx2 es la más sensible de las dos (84,112,140,141) y se han identificado incluso motivos en la secuencia de estas proteínas que explican estas diferencias (112).

```
Prx1   1   - - - - - - - - - -  - - - - - - - - - -  - - - - - - - - - -  - - - - - - - - - -  - - - M S S G N - -    5
Prx2   1   - - - - - - - - - -  - - - - - - - - - -  - - - - - - - - - -  - - - - - - - - - -  - - - M A S G N - -    5
Prx3   1   M A A A V G R L L R  A S V A R H V S A I  P W G I S A T A A L  R P A A C G R T S L  T N L L C S G S S Q   50

Prx1   5   - - - - - - - - - -  - - A K I G H P A P  N F K A T A V M P D  G Q F K D I S L S D  Y K G K Y V V F F F   43
Prx2   5   - - - - - - - - - -  - - A R I G K P A P  D F K A T A V V - D  G A F K E V K L S D  Y K G K Y V V L F F   42
Prx3  51   A K L F S T S S S C  H A P A V T Q H A P  Y F K G T A V V - N  G E F K D L S L D D  F K G K Y L V L F F   99

Prx1  44   Y P L D F T F V C P  T E I I A F S D R A  E E F K K L N C Q V  I G A S V D S H F C  H L A W V N T P K K   93
Prx2  43   Y P L D F T F V C P  T E I I A F S N R A  E D F R K L G C E V  L G V S V D S Q F T  H L A W I N T P R K   92
Prx3 100   Y P L D F T F V C P  T E I V A F S D K A  N E F H D V N C E V  V A V S V D S H F S  H L A W I N T P R K  149
                              ★

Prx1  94   Q G G L G P M N I P  L V S D P K R T I A  Q D Y G V L K A D E  G I S F R G L F I I  D D K G I L R Q I T  143
Prx2  93   E G G L G P L N I P  L L A D V T R R L S  E D Y G V L K T D E  G I A Y R G L F I I  D G K G V L R Q I T  142
Prx3 150   N G G L G H M N I A  L L S D L T K Q I S  R D Y G V L L E G S  G L A L R G L F I I  D P N G V I K H L S  199

Prx1 144   V N D L P V G R S V  D E T L R L V Q A F  Q F T D H G E V C  P A G W K P G S D T  I K P D V Q K S K E  193
Prx2 143   V N D L P V G R S V  D E A L R L V Q A F  Q Y T D E H G E V C  P A G W K P G S D T  I K P N V D D S K E  192
Prx3 200   V N D L P V G R S V  E E T L R L V K A F  Q Y V E T H G E V C  P A N W T P D S P T  I K P S P A A S K E  249
                                                                  ★

Prx1 194   Y F S K Q K -   199
Prx2 193   Y F S K H N -   198
Prx3 250   Y F Q K V N Q   256
           ★
```

Figura 13. Alineamiento de las secuencias de las proteínas humanas Prx1, Prx2 y Prx3. En negro se muestran los residuos que son idénticos y en gris los que son similares. La estrella roja señala la C_P, la naranja la C_R y la verde el motivo YF del extremo C-terminal de estas Prx. El alineamiento se realizó utilizando el programa Bioedit.

En la búsqueda de entender la sensibilidad diferencial de Prx eucariotas catalogadas como "sensibles" en relación a las demás Prx, aparece la observación de que Prx3, Prx mitocondrial de la misma subfamilia, a pesar de ser sensible a sobreoxidarse por H_2O_2, es notoriamente más robusta que Prx1 y Prx2 (111,140). Las diferencias en la sensibilidad a sobreoxidarse entre estas Prx sensibles también se han vinculado a diferencias en la secuencia del extremo C-terminal de Prx3 en relación a Prx1 y Prx2 (111). Por otra parte, la resistencia de Prx3 a sobreoxidarse es

consistente con su habilidad para mantenerse activa en un ambiente altamente oxidante como lo es la mitocondria (111).

1.4. Prx2

La Prx2, objeto de estudio de esta tesis, es una peroxirredoxina de 2-Cys típica perteneciente a la subfamilia Prx1/AhpC. Por lo tanto, se organiza como dímeros estabilizados mediante una interface de tipo B, que a su vez se asocian por interfaces de tipo A formando decámeros. Este equilibrio entre estados oligoméricos es dependiente del estado redox de la C_P de la proteína, y ha sido reportado que la sobreoxidación de la C_P puede inducir al apilamiento de estos decámeros toroidales, formando estructuras que han sido descritas *in vivo* (128).

Previamente conocida como tiorredoxina peroxidasa B (TPx-B), natural killer enhancing factor-B (NKEF-B), peroxidasa asociada a tiorredoxina, calpromotina, torina y la proteína banda 8 (142), la Prx2 tiene 198 aminoácidos y un peso molecular de ~22 kDa. La concentración intracelular en los glóbulos rojos de esta enzima es de 240-410 µM, y es por ende la tercera proteína más abundante en el citosol del eritrocito luego de la hemoglobina y la anhidrasa carbónica (101,102). Además de encontrarse a altas concentraciones en los glóbulos rojos, se expresa en todos los tejidos del cuerpo humano a concentraciones en el rango micromolar.

Los ratones *knock-out* en Prx2 son en apariencia sanos y fértiles, pero desarrollan anemia hemolítica asociada a la formación de cuerpos de Heinz y esplenomegalia (139). A su vez, los autores detectaron mayor daño oxidativo en los eritrocitos y en particular a nivel de sus proteínas de membrana. Por otra parte, un estudio más reciente demuestra que los ratones que carecen de Prx2 tienen menor activación de las vías de señalización vinculadas a plasticidad sináptica, en particular en el hipocampo. Los autores proponen que la Prx2 es esencial para preservar la integridad funcional de estas neuronas frente al daño oxidativo asociado a envejecimiento (143).

Esta Prx, altamente sensible a sobreoxidarse por su sustrato peróxido, cataliza la reducción del H_2O_2 con una constante de velocidad de segundo orden de 1 x 10^8 M^{-1} s^{-1} y del peroxinitrito con una constante de segundo orden de 1.4 x 10^7 M^{-1} s^{-1} a pH 7.4 (82). Además, el peroxinitrito como sustrato de las Prx es capaz de sobreoxidar su C_P, al igual que el H_2O_2, pero además puede nitrar residuos de tirosina durante la catálisis (82). La alta reactividad de Prx2 así como su alta concentración intracelular la ubican como primera línea de contacto con el peróxido de

hidrógeno y el peroxinitrito en la célula. Asimismo, varias modificaciones postraduccionales han sido reportadas para esta enzima, tanto *in vitro* como *in vivo*, que afectan su actividad peroxidasa y su estructura, pudiendo así afectar su función intracelular.

Todas estas características hacen interesante su estudio para así poder seguir profundizando en la comprensión de los mecanismos moleculares de señalización redox mediados por H_2O_2.

1.5. Modificaciones postraduccionales (PTM) en Prx2

Varias modificaciones postraduccionales ocurren en Prx2, tanto en residuos catalíticos (C_P, C_R) como en residuos no catalíticos (Tyr, Trp, Lys). Estas modificaciones son capaces de alterar la actividad de la enzima, su estructura cuaternaria, y su interacción con otras proteínas, modulando así su función. A continuación se describen las PTM sintetizadas en la Figura 14.
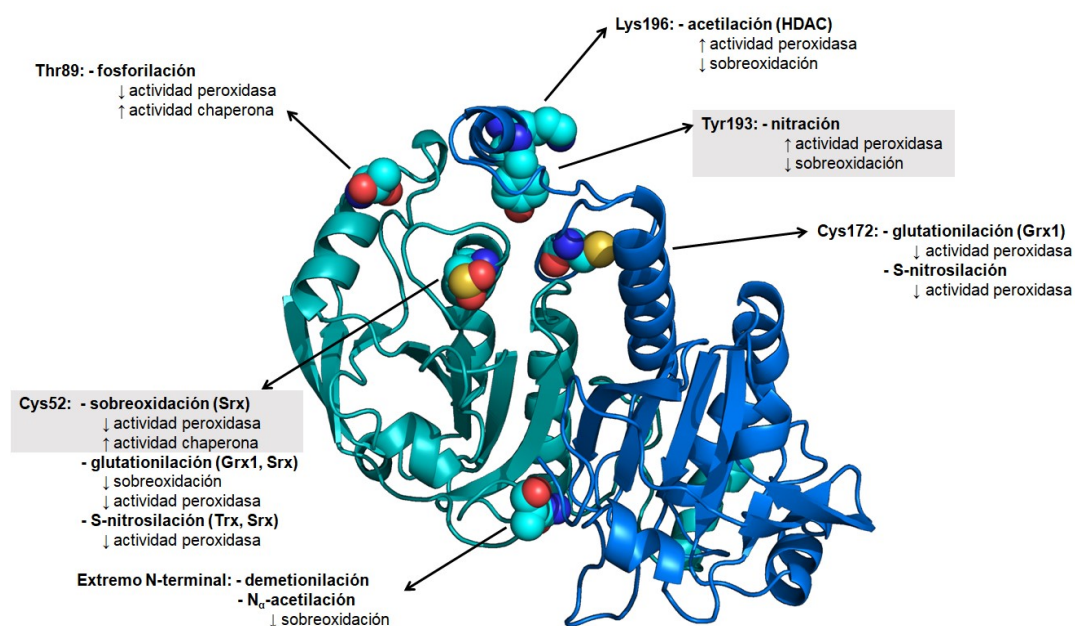
Figura 14. Modificaciones postraduccionales de Prx2. Representación de un dímero de Prx2 en el que se señalan las PTM descritas en distintos aminoácidos catalíticos y no catalíticos de las cadenas A (celeste) y B (azul), así como sus efectos en la actividad de la enzima. Entre paréntesis se indican las enzimas responsables de la reversibilidad de algunas de las PTM. Además, se señala la nitración de la tirosina 193, objeto de estudio de esta tesis.

1.5.1. PTM en residuos catalíticos

1.5.1.1. Sobreoxidación

Como se describió más arriba, la sobreoxidación de Prx2 es resultado de una competencia entre el cambio conformacional que debe ocurrir para permitir que se forme el disulfuro intermolecular en el sitio activo, y la reacción de una segunda molécula de H_2O_2 con el sulfénico de la C_P en la conformación LU (Figuras 6 y 15). Ha sido recientemente demostrado que, para Prx2, esta segunda reacción para dar ácido cisteinsulfínico es unas 1000 veces más lenta que la primera (144). La cisteína peroxidática sobreoxidada puede además reaccionar nuevamente con peróxido para dar ácido cisteinsulfónico (C_P-SO_3H) (145).
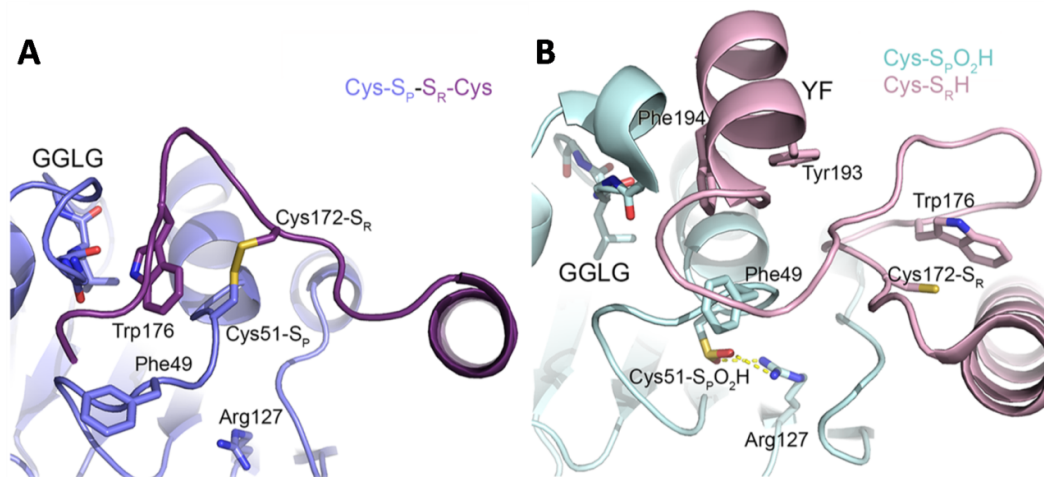
Figura 15. Cambios conformacionales en el sitio activo de la Prx2 humana. **(A)** Estructura del sitio activo de la Prx2 oxidada a disulfuro, Prx2-$S_P$$S_R$. En esta conformación LU, el extremo C-terminal está presente como un giro que posiciona al Trp176 (subunidad violeta) de manera que se ubica en una hendidura generada por el enlace disulfuro y el motivo GGLG (subunidad azul). Este residuo se encuentra a 20 Å de su posición en la estructura Prx2-SO_2H, como se ve en el panel B. **(B)** Estructura del sitio activo de la Prx2 sobreoxidada (cadenas A-B). En esta conformación FF, el ácido cisteinsulfínico de la C_P (Cys51-$S_P$$O_2H$) (celeste) establece una interacción electrostática con la Arg127. El extremo C-terminal de la subunidad adyacente (rosa) ubica a la C_R (Cys172-S_R) a unos 14 Å del la C_P (Cys51-S_P). El motivo YF (residuos 193-194) está presente en una hélice que se empaqueta contra el motivo GGLG. Figura editada de (112).

La sobreoxidación de Prx2 favorece la forma decamérica de la enzima, así como la formación de apilamientos de los toroides llegando incluso a formar agregados filamentosos vinculados a la detención del ciclo celular (129).

Es importante resaltar que a pesar de ser relativamente fácil sobreoxidar Prx sensibles *in vitro*, *in vivo* no es tan evidente su sobreoxidación. Esto puede deberse a que el paso dependiente de Trx/TR/NADPH sea relativamente lento, generando un stock de Prx2 en disulfuro, protegida de la reacción con peróxido. Esto parece ocurrir especialmente para Prx2 en glóbulos rojos humanos (146,147). Sin embargo, en algunas condiciones se ha identificado la Prx2 sobreoxidada *in vivo*, en particular en glóbulos rojos humanos se observó una variación circadiana de la cantidad de Prx2 sobreoxidada (148) y la aparición matutina de Prx2 sobreoxidada en pacientes con apnea obstructiva del sueño (149).

Se han encontrado evidencias apoyando varios posibles roles biológicos para esta modificación postraduccional, entre los cuales se encuentran el rol original como inactivador de Prx permitiendo así la acumulación local de H_2O_2 (hipótesis de la compuerta o "*floodgate hypothesis*"), el de un agente 'triage' capaz de conservar poder redox bajo condiciones de alto estrés oxidativo (150), el de proteína chaperona o como señal de alarma y detención del ciclo celular, estos últimos vinculados a la formación de estructuras de alto peso molecular favorecidas por sobreoxidación de la C_P (103,129). Estos cuatro posibles roles para esta modificación (Figura 16) no son excluyentes y aún no se conoce si existen como tales, así como también es posible que existan otras formas aún no conocidas en las que la sobreoxidación modifique el devenir de las Prx y el peróxido en la célula. Es interesante mencionar que los primeros dos roles mencionados hacen referencia a la pérdida de función de la enzima al sobreoxidarse, mientras los últimos dos dependen de una ganancia de función asociada a esta PTM.
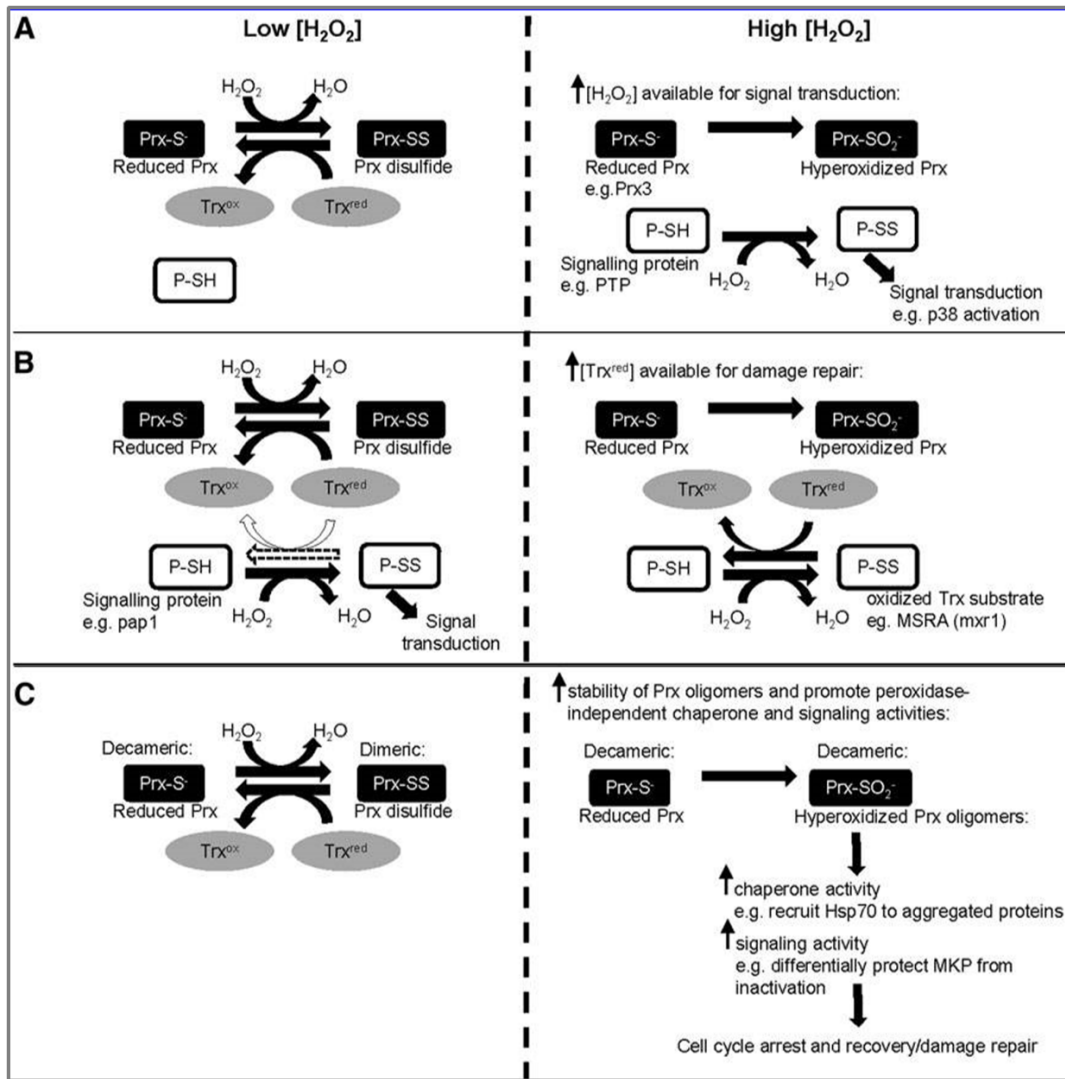
Figura 16. Roles propuestos para la sobreoxidación de Prx. Se ha propuesto que la sobreoxidación **(A)** permite señalización de otras proteínas por H_2O_2, **(B)** permite conservar a la Trx reducida para que pueda reducir otras proteínas oxidadas a disulfuro, y **(C)** promueve actividades alternativas de las Prx como ser la actividad chaperona u otras. Figura editada de (136).

En un principio considerada una modificación irreversible, en el año 2003 se describe la sulfirredoxina (Srx), proteína capaz de catalizar la reducción del ácido cisteinsulfínico de la C_P a sulfénico (151). Esta reacción, dependiente de ATP y Mg^{2+} y de una enzima cuyos niveles de expresión aumentan en respuesta a estrés oxidativo, ubicó a la sobreoxidación como un mecanismo modulador de la actividad de Prx y por ende de las vías de señalización redox intracelulares.

1.5.1.2. Glutationilación de Cys

La glutationilación y deglutationilación de proteínas son procesos mediados por señales redox generadas en respuesta a la activación de receptores de superficie de membrana. En el caso de las Prx, la glutationilación puede incluso actuar como un mecanismo protector de la C_P evitando que se sobreoxide a ácido cisteinsulfínico, debido a la acción de la glutarredoxina y la sulfirredoxina, que catalizan la deglutationilación de las cisteínas de Prx. Varias Prx han sido reportadas glutationiladas tanto *in vitro* como *in vivo*, y esta modificación postraduccional se ha visto involucrada en varios procesos fisiológicos como ser crecimiento, progresión del ciclo celular, activación de la transcripción, funciones del citoesqueleto, y metabolismo (152). Dada la concentración intracelular del glutatión del orden milimolar, la glutationilación de proteínas constituye un mecanismo de regulación celular mayor (152). En particular, la C_P de Prx2 forma disulfuros mixtos estables con GSH reducibles por glutarredoxina 1 (Grx1) (153).

1.5.1.3. Nitrosilación

La actividad biológica del óxido nítrico se explica principalmente por su interacción con centros metálicos o mediante modificaciones postraduccionales de proteínas, como la S-nitrosilación y la nitración de tirosinas, las cuales pueden regular la función de las proteínas blanco (154). Estas PTM dependientes de NO se han visto involucradas en mecanismos de señalización celular tanto en condiciones fisiológicas como fisiopatológicas (155,156).

En particular, la S-nitrosilación consiste en la adición de un nitrosonio (NO^+) al azufre del tiolato de una cisteína, formándose un S-nitrosotiol (SNO). Cabe destacar que no hay reacción directa entre NO y cisteína, sino que es necesario un primer paso de oxidación por un electrón. La modificación de cisteínas por S-nitrosilación puede afectar la función de gran variedad de proteínas (157,158). El S-nitrosoglutatión (GSNO), formado por la S-nitrosilación del glutatión, es el mayor SNO de bajo peso molecular, y se considera un reservorio intracelular de NO (159-161). De hecho, el GSNO puede mediar reacciones de transnitrosilación en las que se genera un nuevo SNO por transferencia del grupo NO a otra cisteína (157). Por otra parte, la S-nitrosilación es reversible ya que la Trx puede reducir específicamente nitrosotioles (162,163), además de los mecanismos no enzimáticos capaces de descomponer los nitrosotioles como el ascorbato o el glutatión. Existe también la S-nitrosoglutatión

reductasa, que descompone el GSNO y controla así indirectamente los niveles de NO (15,155,164).

Algunas Prx han sido encontradas nitrosiladas en plantas y animales. En particular, la Prx2 puede sufrir S-nitrosilación por óxido nítrico tanto sobre su C_P como sobre su C_R, inhibiendo su actividad peroxidasa (165). Estos autores también encontraron niveles elevados de Prx2 nitrosilada en cerebros de pacientes con enfermedad de Alzheimer, por lo que esta modificación podría tener un rol en la fisiopatología de esta enfermedad.

A esto se agrega el hecho de que la sulfirredoxina, descrita previamente por su rol en la reducción de la C_P sobreoxidada de vuelta a sulfénico, puede denitrosilar la C_P de Prx2, pudiendo ser ésta una función adicional de la sulfirredoxina *in vivo* (166,167). Recientemente, un estudio identifica numerosas proteínas adicionales reducibles por Srx (168), replanteando el rol fisiológico de esta proteína, inicialmente propuesta como reductor específico de la cisteína peroxidática sobreoxidada de las Prx de 2-Cys típicas.

1.5.2. PTM en residuos no-catalíticos

1.5.2.1. Fosforilación

Prx2 puede ser fosforilada en su Thr89 por Cdk5/p35 (169). Esta modificación lleva a una inhibición de la actividad peroxidasa de la enzima, e induce un cambio conformacional que lleva a un cambio en la función de la enzima, de peroxidasa a chaperona. Además, la fosforilación de Prx2 por Cdk5 vía p35 conduce a muerte neuronal tanto en un modelo celular como en un modelo de ratones con Enfermedad de Parkinson, demostrando la actividad citoprotectora de Prx2 en estas células (169). En el mismo estudio, los autores reportan un aumento de la Prx2 fosforilada en neuronas de pacientes con Parkinson en comparación con los pacientes control.

1.5.2.2. Acetilación de Lys

La acetilación de una lisina C-terminal en Prx2 (Lys196) da lugar a una enzima más activa como peroxidasa, y menos sensible a sobreoxidarse por H_2O_2 (170). Asimismo, la presencia de una proteína tipo HDAC con actividad desacetilasa de Prx2 sugiere un posible rol fisiológico de esta modificación (170).

1.5.2.3. Modificaciones del extremo N-terminal

En Prx2, ocurre primero una demetionilación en el extremo N-terminal, y luego la acetilación N_α-terminal. Esta modificación en Prx2 lleva a cambios estructurales significativos y protege a la Prx2 de inactivación oxidativa por sobreoxidación sin alterar su actividad peroxidasa (171).

1.5.2.4. Nitración de Tyr

La nitración de tirosinas consiste en la adición de NO_2 a uno de los dos carbonos orto equivalentes del anillo aromático de la tirosina, formando 3-nitrotirosina a través de un mecanismo radicalar (Figura 2) (52,172,173). En sistemas biológicos, las fuentes principales del agente nitrante NO_2 son la ruptura homolítica de peroxinitrito, la oxidación de nitrito por H_2O_2 y hemoperoxidasas, así como la autooxidación del NO (reacción catalizada en membranas) (172,174). Esta modificación convierte a la tirosina en un residuo cargado dado que causa un cambio importante en el pK_a del fenol (de 10 a 7.5 en general) (175,176), pudiendo resultar en una ganancia, pérdida o cambio de función de la proteína blanco (177,178). En algunos casos la nitración de tirosinas conduce a la agregación (179,180) o favorece su degradación por el proteosoma (179,181,182).

Aunque la nitración de tirosinas ha sido históricamente considerada irreversible y un marcador de estrés oxidativo, existen reportes de reversibilidad de la nitración de proteínas independiente de degradación proteica, llegando incluso a describirse una posible actividad denitrasa capaz de reducir la 3-nitrotirosina de vuelta a tirosina en mamíferos (183-188), lo que podría sugerir un rol para esta modificación en los procesos de señalización celular mediados por NO, como discuten algunos autores (155,189).

Más recientemente, se ha demostrado que las proteínas modificadas por peroxinitrito son inmunogénicas y están implicadas en el desarrollo de patologías inflamatorias, lo que ha llevado a utilizar la 3-nitrotirosina como marcador de estrés nitroxidativo en sangre (190). A su vez, la nitración de proteínas se ve incrementada en pacientes con enfermedad de Alzheimer (98,191-195), enfermedad de Parkinson (196), esclerosis lateral amiotrófica (197,198) y en modelos de daño cerebral traumático (199) e isquemia–reperfusión (200-202). En particular, la Prx2 humana fue identificada nitrada en cerebros de pacientes con Alzheimer temprano (203). Existen a la fecha varios reportes adicionales de Prx nitradas tanto *in vitro* como en modelos biológicos. En particular, Prx1, Prx2 y Prx3 resultan nitradas luego de tratarlas con

peroxinitrito *in vitro* (82-84). La PrxII E de *Arabidopsis thaliana* se encontró selectivamente nitrada en plantas en condiciones de estrés oxidativo inducido (204) y la Prx1 humana se detectó nitrada luego de tratar células Jurkat con peroxinitrito, identificándose nitrada la Y194 de esta proteína, perteneciente al motivo YF previamente descrito (205). Por otra parte, se identificó Prx3 nitrada en modelos de Diabetes Mellitus tanto *in vitro* como *in vivo* (175).

Es importante notar que la detección de proteínas nitradas *in vivo* presenta un desafío, tanto en relación al bajo número de tirosinas nitradas (que en células u órganos dañados podría ser tan bajo como el 0.00001– 0.001% de todas las tirosinas presentes (177), por lo que puede ser necesario enriquecer la muestra en estudio antes de analizarla (205)), como por limitaciones de las técnicas de detección empleadas (206,207). Como se mencionó anteriormente, la nitración puede además disminuir la estabilidad o la vida media de las proteínas modificadas *in vivo* (179,182) pudiendo limitar su identificación a partir de muestras de pacientes.

En particular, esta tesis se centra en la caracterización *in vitro* de la forma nitrada de Prx2 humana y en el estudio de los efectos de esta modificación postraduccional en residuos no catalíticos de esta enzima sobre su estructura y su función.

1.6. Interacciones con otras proteínas

Cada vez más interactores son reportados para las Prx, describiéndose su participación en vías de señalización tan diversas como las vinculadas con efectos citoprotectores en diversos tipos de cáncer o el desarrollo de patologías neurodegenerativas (29). Entre los interactores intracelulares de la Prx2 se encuentran proteínas redox, como la Trx, reductora del disulfuro intermolecular de la proteína, y la sulfirredoxina, reductora del ácido cisteinsulfínico de la C_P.

La Trx ha sido ampliamente planteada como mediador central de múltiples vías de señalización dependientes de H_2O_2 (29,136,208). A pesar de ser una interacción fundamental del ciclo catalítico de las Prx, aún se desconocen los detalles de la manera en la que interaccionan estas proteínas entre sí. Existen resultados que indican que la interacción entre estas proteínas se ve favorecida en el dímero en relación al decámero (133), pero poco más se conoce al respecto.

La sulfirredoxina, en cambio, fue cristalizada asociada al dímero de Prx1 humana, y se plantea que la asociación con Prx2 iría en el mismo sentido (209). En este trabajo los autores construyen un modelo de cristal de Prx1 decamérica usando

como base la estructura de Prx2 humana sobreoxidada (PDB 1QMV). En este modelo se ve cómo quedan los sitios activos de Prx1 orientados hacia la periferia del decámero, y cómo la Srx envuelve a la Prx decamérica "como un cinturón" (Figura 17) (209). Como se observa en la figura, para que se dé esta interacción entre la Prx sobreoxidada y la Srx, el extremo C-terminal de la Prx conteniendo al motivo YF asociado a sobreoxidación de estas enzimas -que en la forma sobreoxidada se encuentra empaquetado sobre el sitio activo de la enzima- debe modificar su conformación, abriéndose y dándole lugar a la Srx para interaccionar. El abrazo que observan entre la Prx1 y la Srx se da mediante interacciones de los residuos 172-186 de Prx1 -entre los que se encuentra la C_R- y un surco hidrofóbico altamente conservado de la Srx, como se observa en la estructura obtenida. A su vez, el motivo GGLG previamente asociado a la sensibilidad de estas Prx a sobreoxidarse, participa en la reparación por Srx facilitando la unión del ATP durante la catálisis (209).
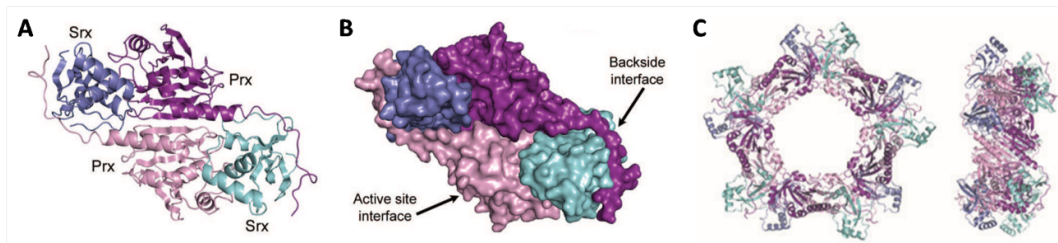
Figura 17. Complejo entre la Prx1 y la Srx humanas. **(A)** Representación del dímero de Prx1 unido a Srx. Los dos monómeros de Prx1 se muestran en violeta/rosado y los de Srx en celeste y azul. **(B)** Representación de la superficie del complejo Srx-Prx1 en que se señalan la interface del sitio activo y la del "backside". **(C)** Vista frontal y lateral del modelo del complejo toroidal Srx-Prx1 conteniendo 10 monómeros de Prx (violetas y rosados) y 10 de Srx (celestes y azules). Las figuras A y B fueron tomadas de (209) y C fue tomada de (125).

Actualmente se conocen otros sustratos de la Srx y se sabe también que puede denitrosilar la C_P de Prx2 (166). Recientemente, un estudio identifica numerosas proteínas adicionales reducibles por Srx (168), siendo la interacción con Prx2 tan sólo un eslabón más en la intrincada red de interacciones intracelulares de esta proteína.

La Prx2 se ha encontrado asociada a varias proteínas vinculadas a la circulación sanguínea, en particular se describió que la Prx2 era reclutada por el receptor de membrana para el factor de crecimiento derivado de plaquetas (PDGFR) post-estimulación por dicho factor de crecimiento (PDGF) (210). Por otra parte, se reportó su interacción con proteínas integrales de membrana o membranas celulares mediante su región C-terminal (211,212). En el eritrocito se reportó su interacción con

la hemoglobina y la catalasa, entre otras proteínas (213-215) y en relación a su interacción con la proteína Banda 8 se planteó su participación en el proceso de eritroptosis, fenómeno similar a la apoptosis que ocurre en los eritrocitos (216).

En 2015, Sobotta y colaboradores demostraron por primera vez la interacción en células de mamífero entre Prx2 y un factor de transcripción, STAT3, mediante un enlace disulfuro intermolecular, reafirmando la idea de que la señal redox tiene que pasar necesariamente por las Prx (o Gpx) antes de llegar a la proteína blanco (217). La Prx2 actúa como un receptor primario de H_2O_2 ultrasensible, transmitiendo específicamente los equivalentes de oxidación al factor de transcripción redox regulado STAT3. En particular, la Prx2 cataliza la formación de oligómeros de STAT3 unidos por enlaces disulfuro, los cuales comprometen su actividad transcripcional. Demuestran incluso que la actividad de STAT3 depende fuertemente de los niveles de expresión de Prx2.

A pesar de que aún se desconoce el rol exacto de Prx2 en las vías de señalización intracelular, el reporte de la interacción con STAT3 por enlace disulfuro viene a consolidar la teoría del *redox relay* para la señalización por H_2O_2. Existen además otros reportes de interacción de Prx2 con proteínas de distinta naturaleza, vínculos que evidencian la diversidad de procesos celulares en los que participa Prx2. Pace y colaboradores reportaron la interacción de Prx2 sobreoxidada con ERp46, una proteína disulfuro isomerasa, mediante una interacción no-covalente estable disociada por la reducción de los enlaces disulfuros de ERp46 o por disrupción del decámero de Prx2 (218). Más recientemente, el mismo grupo reportó la interacción redox-dependiente de Prx2 con CRMP2 (collapsin response mediator protein 2), proteína humana expresada ubicuamente que regula el ensamblaje y desensamblaje de los microtúbulos (219,220), función importante en el desarrollo y mantenimiento de las extensiones neuríticas (221) y la migración de linfocitos (222).

Otros autores reportaron la interacción de Prx2 con la creatinin quinasa cerebral humana (BCK, monómero, CKBB, dímero), una quinasa cuya actividad se ha visto gradualmente reducida en cerebros afectados por patologías neurodegenerativas (223). Se ha propuesto también a Prx2 como promotora de tumores en cáncer colorrectal por su interacción con una poli(ADP ribosa) polimerasa (PARP) (224). Por otra parte, recientemente se describió que la oxidación dependiente de H_2O_2 de DJ-1, una de las proteínas redox-sensibles más abundantes en corazón, vinculada a la aparición temprana de Parkinson, es mediada por Prx2 por formación de un disulfuro mixto entre estas proteínas (225), vinculándola así a esta patología neurodegenerativa.
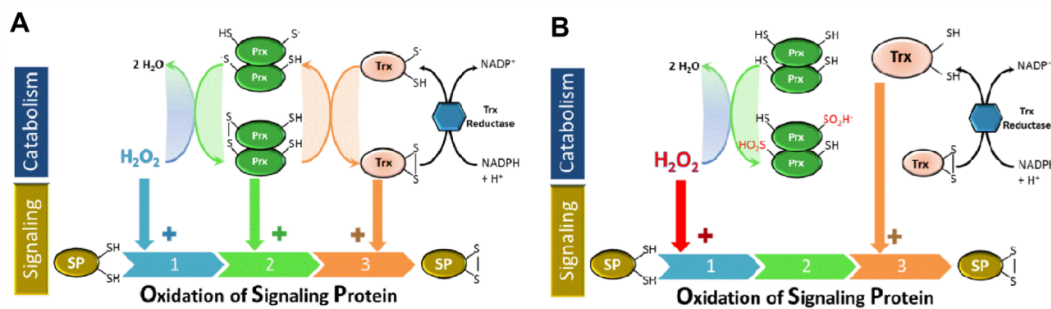
1.7. Prx y señalización por H_2O_2

Las Prx reaccionan con H_2O_2 con constantes de segundo orden importantes (10^3 - 10^8 M^{-1} s^{-1}) (82,84,86,87,92,94,226-230), y en particular Prx2 reacciona con una constante de 10^8 M^{-1} s^{-1} (82), por lo que estas proteínas -dada su alta concentración- constituyen la primera línea intracelular de reacción con peróxidos, es decir la primera línea en las vías de señalización redox mediadas por H_2O_2 (27,28,231,232). De hecho, se estima que en células humanas más del 99% del peróxido citosólico y del 90% del peróxido mitocondrial reacciona con Prx y no con otras enzimas o tioles de bajo peso molecular (Figura 18) (233,234).
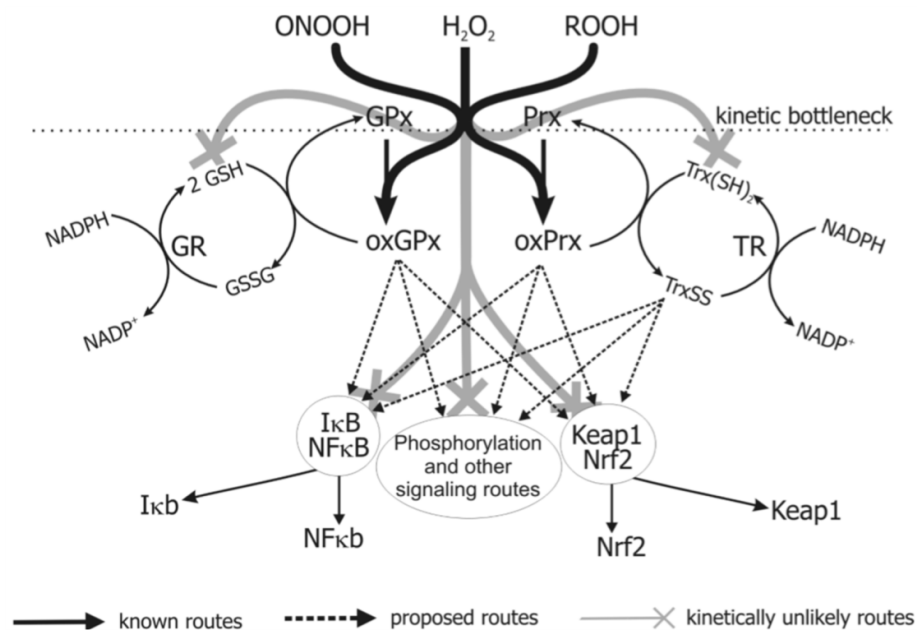
Figura 18. Vías de señalización mediadas por H_2O_2. Las glutatión peroxidasas (GPx) y peroxirredoxinas (Prx) son blancos cinéticamente favorecidos para la oxidación por peróxido de hidrógeno de tal manera que previenen prácticamente cualquier otra reacción tiol-H_2O_2. Estas enzimas son reducidas en su función antioxidante mediante vías que terminan en la oxidación de NADPH. La interacción entre hidroperóxidos y moléculas efectoras como los factores de transcripción NFκB y Nrf2 se da indirectamente vía reacciones redox entre proteínas que involucran a las GPx, Prx, Trx y posiblemente otros intermediarios en secuencias de reacciones cinéticamente favorecidas. Figura tomada de (28).

Como se discute en (29), tres mecanismos no excluyentes han sido planteados para las Prx como mediadoras de la señalización por H_2O_2 (Figura 19): 1) regulando la concentración intracelular de peróxido, el cual podría reaccionar directamente con proteínas blanco en ciertas condiciones (inactivación por sobreoxidación, ver apartado

1.5.1.1), 2) siendo el primer blanco de oxidación por H_2O_2 y luego transmitiendo la señal al oxidar otras proteínas redox (por ejemplo un factor de transcripción o una fosfatasa) y 3) siendo el primer blanco de oxidación por H_2O_2 para luego ser reducidas por Trx, que a su vez pasa a cumplir el rol de transmisor de la señal oxidando otros blancos intracelulares. Se plantea que las Prx participen en regular el estado de oxidación de Trx, más que la concentración de H_2O_2 intracelular (235). En la literatura existen evidencias apoyando la participación de las Prx en todos estos mecanismos de transmisión de señal, variando la vía según el sistema biológico en estudio (organismo unicelular, línea celular en cultivo, bacteria, etc.) (29).


Figura 19. Mecanismos de señalización por H_2O_2. En el panel **(A)** se muestran los tres mecanismos presentados: **(1)** oxidación directa de la proteína señalizadora (SP) por H_2O_2; **(2)** la oxidación de SP está mediada por una peroxirredoxina (Prx); **(3)** la oxidación de la SP está mediada por una tiorredoxina (Trx). En **(B)** se muestra la sobreoxidación de una Prx, llevando a la potencial acumulación de H_2O_2 y oxidación directa de SP, a la vez que acumula Trx reducida para reducir otras proteínas oxidadas a disulfuro. Figura tomada de (29).

Cualquier modificación postraduccional que afecte la actividad peroxidasa de Prx o su estructura oligomérica e interacción con otras proteínas puede modular su participación en vías de señalización redox (Figura 20). La sobreoxidación, por ejemplo, aparece como un mecanismo modulador de la concentración de Prx reducida seleccionado en eucariotas. Aunque reversible por Srx, existen diversos mecanismos de regulación transcripcional, postranscripcional y postraduccional que aseguran que los niveles de Srx se mantengan bajos y restringidos a determinados compartimientos subcelulares (151,236-239). La sensibilidad de las Prx eucariotas a sobreoxidarse, así como la expresión y localización de Srx fuertemente regulada, sugieren que existen ventajas evolutivas para la sobreoxidación de Prx en respuesta al aumento de los niveles intracelulares de H_2O_2 (136). Según la hipótesis de la compuerta ya mencionada (104,110), cuando los niveles de H_2O_2 aumentan lo suficiente, las Prx se sobreoxidan permitiendo a otros blancos celulares cercanos a la fuente de H_2O_2

oxidarse directamente. Otros autores plantean a la sobreoxidación como moduladora de los niveles de Trx reducida (150) (Figura 19), es decir que al inactivarse la Prx, la tiorredoxina reducida queda disponible para reducir a otros blancos.

Cabe destacar que el mecanismo de transmisión de señal por cascada tiol-disulfuro observado en levaduras (236,240-242) también se demostró como viable en mamíferos, (18,217) luego denominado "*redox relay pathway*" (217) donde la Prx oxidada a sulfénico forma disulfuro con proteína redox señalizadora, en vez de reaccionar con H_2O_2 y sobreoxidarse (Figura 20).
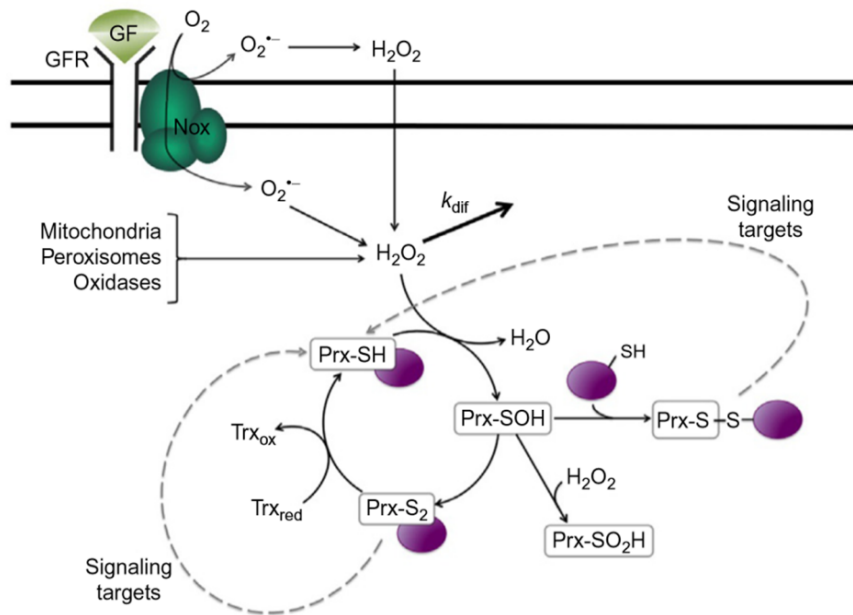
Figura 20. H_2O_2 y 2-Cys Prx en vías de señalización redox. La unión de ligandos, como pueden ser los factores de crecimiento (GF), a sus receptores (GFR) estimula el ensamblaje de las NADPH oxidasas (Nox), fuente de superóxido extra e intracelular que dismuta formando H_2O_2. El H_2O_2 intracelular es también generado en mitocondrias y peroxisomas y por oxidasas citosólicas. El destino de este H_2O_2 es difundir y/o reaccionar con sus blancos intracelulares preferenciales, las Prx, iniciando su ciclo catalítico. La cisteína peroxidática (C_P) oxidada a ácido cisteinsulfénico puede reaccionar con la C_R, cerrando el ciclo catalítico, o con una segunda molécula de peróxido, sobreoxidándose, o alternativamente con el tiol de otra proteína reducida generando disulfuros mixtos. Las interacciones proteína–proteína pueden ocurrir entre distintas formas redox de las Prx y otras proteínas señalizadoras (cículos violetas), amplificando así la respuesta hacia efectores río abajo. Figura tomada de (27).

Además de la sobreoxidación, pueden ocurrir otras modificaciones postraduccionales de las Prx que modulen su actividad, como la glutationilación de la C_P de Prx1 y Prx2 humanas, que inhiben reversiblemente su actividad enzimática,

pero a su vez protegen a la C_P de la hiperoxidación hasta ser reducidas por la glutarredoxina 1 (Grx 1) (153) o la Srx (243).

Considerando al H_2O_2 como mensajero de la señal redox, sabiendo las concentraciones intracelulares de los principales blancos moleculares del H_2O_2 y las constantes catalíticas determinadas, se puede calcular la velocidad relativa de reacción del H_2O_2 con estos blancos (27):

velocidad relativa = constante de velocidad x concentración del blanco

Por otra parte, la reacción con un blanco molecular puede verse como una competencia con la difusión del H_2O_2. La Figura 21 integra estos conceptos y muestra cómo la reacción directa de H_2O_2 con fosfatasas como PTP1B es altamente improbable.
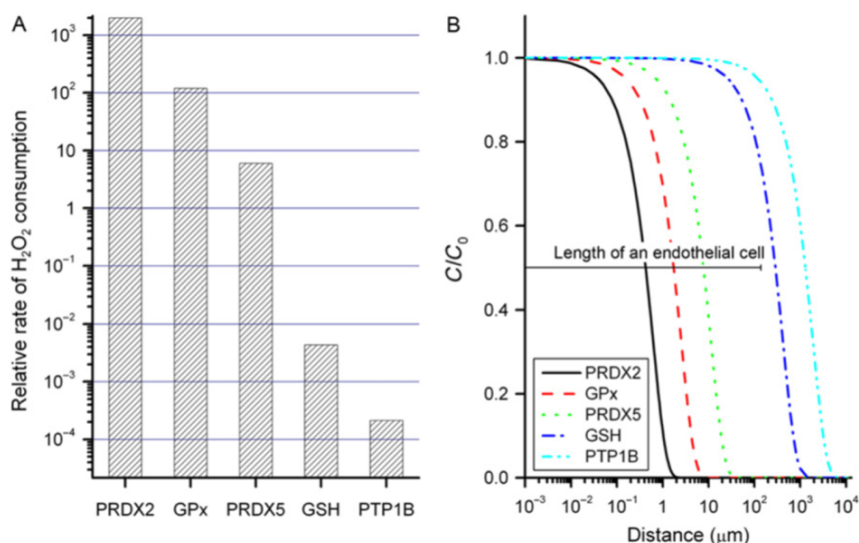
Figura 21. (A) Los blancos moleculares de H_2O_2 favorecidos cinéticamente representan barreras que le impiden reaccionar con posibles proteínas señalizadoras, como PTP1B. No solo enzimas como la Prx2 (la cual puede ser inhibida o inactivada) representan vías de consumo de peróxido, sino que existen también blancos no enzimáticos como el GSH. **(B)** La presencia de cada molécula blanco permite ir generando un gradiente de H_2O_2 asumiendo formación localizada del oxidante- El largo y profundidad del gradiente depende de la competencia entre la velocidad de reacción y de difusión, por lo que 20 μM Prx2 generarían un gradiente de 1 μm donde la mitad del H_2O_2 es consumida. En cambio, el gradiente generado por 5 μM PTP1B es de varios milímetros de ancho. En otras palabras, no se observarán cambios en la concentración intracelular de H_2O_2 intracelular que dependan de blancos moleculares lentos y escasos como PTP1B. Figura tomada de (27).

Sin embargo, existen múltiples reportes que apoyan esta hipótesis (244). Este mecanismo de transducción de señal ha sido demostrado en particular en estudios en

bacteria (29). En levaduras, las peroxidasas de cisteínas son la primera línea de reacción con H_2O_2, como demostraron muy elegantemente Fomenko y colaboradores al generar una cepa mutante de *Saccharomyces cerevisiae* sin peroxidasas, la cual, a pesar de ser viable, no respondía al estímulo por H_2O_2 (245). En este caso, la oxidación de las Prx ya sea a sulfénico o disulfuro, es necesaria para luego transmitir esos equivalentes de oxidación a proteínas reguladoras mediante interacción específicas proteína-proteína y reacciones de intercambio tiol-disulfuro (Figura 22) (29,246). En particular, ha sido reportado que la Prx2 humana transmite directamente sus equivalentes de reducción al mediador celular STAT3 en el contexto de señalización por citoquinas en células HEK293T (217).
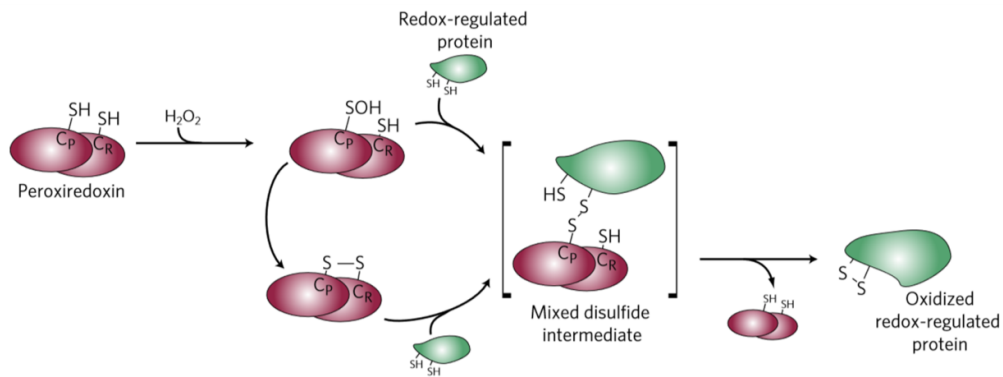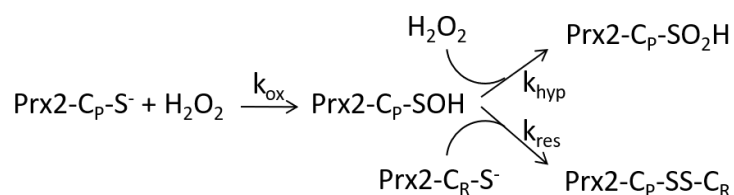

Figura 22. Posibles vías de oxidación de tioles proteicos mediados por Prx. La cisteína peroxidática (C_P) reacciona con H_2O_2 para formar ácido cisteinsulfénico (-SOH), que puede reaccionar directamente con un tiol en la proteína blanco (vía de arriba en el esquema) o con la cisteína resolutiva (C_R) formando el disulfuro intermolecular (vía inferior en el esquema). Este disulfuro puede luego ser transferido a la proteína blanco mediante reacciones de intercambio tiol-disulfuro. En ambos casos, un intermediario disulfuro existe por breve período de tiempo (paréntesis rectos en el esquema) y se reorganiza para dar lugar a la proteína blanco oxidada. Figura tomada de (217).

Es probable que coexistan varios mecanismos de señalización por H_2O_2 donde las Prx participen de diferente manera. Dada su compleja interrelación entre estado redox y estado oligomérico, sumado a la expresión de múltiples Prx, así como la diversidad de procesos celulares en los que participan, cualquier modificación postraduccional que afecte su estructura, su actividad o interacción con otras proteínas podrá afectar el camino que esta señal seguirá en la célula. El camino a seguir dependerá de las constantes catalíticas de reacción de las distintas proteínas con el peróxido, del pH del compartimiento intracelular en que se encuentren, y de las concentraciones de proteína señalizadora, oxidante, Prx y sistema reductor, entre otros (29).

1.8. Cinética de oxidación de cisteína peroxidática por peróxidos

La caracterización cinética de las distintas reacciones que intervienen en la regulación y control del estado redox de las Prx permite completar piezas clave del rompecabezas que implica la elucidación del rol que juegan estas enzimas *in vivo*, y en particular en la señalización redox. Como se comentó anteriormente, el ciclo catalítico de las Prx de 2-Cys típicas comienza con la oxidación de la C_P por el peróxido. Esta reacción es muy rápida a pH fisiológico, lo que en un principio limitó la capacidad de determinar las constantes cinéticas de reacción de distintas Prx con peróxidos (k_{ox} en Esquema 1). Sin embargo, se han puesto a punto varias metodologías para la determinación de esta constante para distintas Prx con numerosos peróxidos. En los últimos años se ha profundizado también en la caracterización cinética de la sobreoxidación de la C_P (reacción del sulfénico con una segunda molécula de peróxido, k_{hyp}) y de la resolución para formar el disulfuro (k_{res}).

$$Prx2\text{-}C_P\text{-}S^- + H_2O_2 \xrightarrow{k_{ox}} Prx2\text{-}C_P\text{-}SOH$$

$$H_2O_2 \quad \xrightarrow{k_{hyp}} \quad Prx2\text{-}C_P\text{-}SO_2H$$

$$Prx2\text{-}C_R\text{-}S^- \quad \xrightarrow{k_{res}} \quad Prx2\text{-}C_P\text{-}SS\text{-}C_R$$

Esquema 1. Reacciones de oxidación de C_P.

1.8.1. Métodos indirectos: competencia

Los ensayos de competencia entre una reacción previamente caracterizada y la que se busca analizar pueden utilizarse para determinar las constantes cinéticas de interés (247). Este método es particularmente útil si la reacción conocida puede ser monitoreada por cambio de una propiedad física (por ej. por cambios en la absorbancia o en la emisión de fluorescencia), de manera de poder seguir el avance de la reacción de manera directa y con alta sensibilidad.

El esquema general de una competencia química simple es el siguiente:

$$A_1 + B \rightarrow P_1 \qquad k_1 \qquad \text{reacción 1}$$
$$A_2 + B \rightarrow P_2 \qquad k_2 \qquad \text{reacción 2}$$
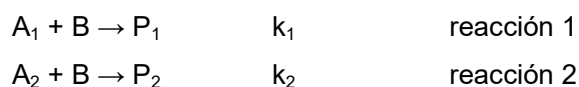
En donde A_1 y A_2 compiten por el sustrato B con constantes cinéticas k_1 y k_2, respectivamente. Conociendo una de las constantes cinéticas, así como la concentración inicial de los reactivos y la concentración final de al menos un producto, se puede obtener la constante de velocidad de segundo orden para la reacción deseada (247).

Cuando A_1 y A_2 son utilizados en exceso en relación a B y las reacciones 1 y 2 están en condiciones de pseudo-primer orden, siguiendo la concentración de uno de los productos se puede utilizar la siguiente ecuación:

$$k_1 \frac{[A_1]_0 \, F}{(1-F)} = k_2 \, [A_2]_0 \qquad \text{Ecuación 3}$$

Donde F es la fracción de inhibición de la formación de P1 en presencia de una $[A_2]_0$ dada. El término de la izquierda en la Ecuación 3 puede graficarse en función de $[A_2]_0$ y obtener k_2 a partir de la pendiente de la recta obtenida.

Cuando no se puede utilizar un exceso de ambos sustratos, la Ecuación 3 ya no es aplicable y debe utilizarse la siguiente relación:

$$\frac{k_1}{k_2} = \frac{\ln \left([A_1]_0/([A_1]_0 - [P_1]_\infty)\right)}{\ln \left([A_2]_0/([A_2]_0 - [P_2]_\infty)\right)} \qquad \text{Ecuación 4}$$

Para Prx2, se ha utilizado esta metodología para determinar la constante de reacción de segundo orden de Prx2 con H_2O_2 y con peroxinitrito, utilizando constantes de reacción conocidas de estos peróxidos con HRP y con $Mn^{III}TE\text{-}2\text{-}PyP$, respectivamente. Es así que se determinaron constantes de reacción de Prx2 con H_2O_2 y peroxinitrito, obteniéndose valores de constantes de segundo orden de $1.0 \times 10^8 \, M^{-1} s^{-1}$ y $1.4 \times 10^7 \, M^{-1} s^{-1}$ a 25°C y pH 7.4, respectivamente (82).

1.8.2. Métodos directos

1.8.2.1. Seguimiento del consumo de peroxinitrito por absorbancia

Dada la absorbancia del peroxinitrito anión a 302 nm, puede seguirse la cinética de descomposición del mismo en presencia o ausencia de enzima utilizando un espectrofotómetro acoplado a un equipo de flujo detenido (56). A 310 nm, existen menos interferencias, lo que permite obtener datos con menos error asociado, y el ácido peroxinitroso tiene un coeficiente de absortividad molar de 1600 $M^{-1}cm^{-1}$ (248). La dificultad de implementación de la técnica en estudios de cinética pre-estacionaria,

son las asociadas a tener que trabajar con concentraciones de proteína diez veces en exceso, por lo tanto un decaimiento rápido del peroxinitrito que ocurre en gran parte antes del tiempo de mezclado del equipo (2 ms), por lo que es más útil en experimentos de velocidad inicial (247).

1.8.2.2. Ensayo acoplado

La velocidad del consumo de H_2O_2 por Prx puede seguirse utilizando el ensayo acoplado (Prx/Trx/TR/NADPH) y siguiendo el consumo de NADPH a 340 nm, siempre y cuando ésta dependa únicamente de Prx. A partir del gráfico v_0 en función de $[H_2O_2]$ a concentraciones saturantes de Trx, se puede determinar k_{cat} y K_m para el sustrato peróxido, de donde se determina la constante bimolecular de reacción con peróxido (k_{cat}/K_m). Las Prx presentan un muy bajo valor de K_m aparente para H_2O_2, por lo que se alcanza fácilmente la saturación. Por lo tanto, el método tiene mucho error para seguir la reacción de oxidación de C_P por H_2O_2.
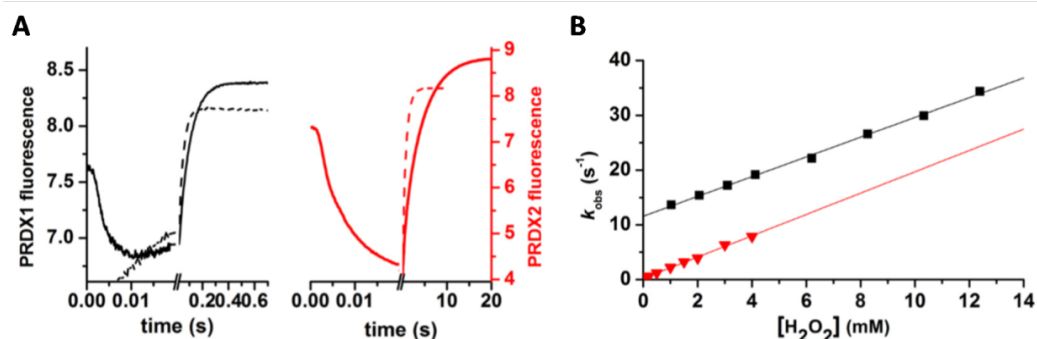
1.8.2.3. Cambios en la fluorescencia intrínseca de Prx

Otra manera de determinar constantes de reacción de C_P con peróxido es siguiendo el cambio en la fluorescencia intrínseca de la proteína en un equipo de flujo detenido. Varios autores han empleado ya este método para determinar constantes de reacción de Prx de distintas subfamilias con diversos peróxidos (83,84,86,94,141,230,249,250). En particular, cuando se sigue la emisión de fluorescencia a 340 nm en el tiempo al mezclar Prx2 reducida con H_2O_2, se obtienen corridas bifásicas con un primer descenso rápido de la fluorescencia (> 0.1 s) para luego registrar un aumento de la señal más lento (algunos segundos) (Figura 23A) (84,141).

Del ajuste a una curva del tipo exponencial simple de la fase rápida se obtiene una constante observada (k_{fast}), que al ser graficada en función de la concentración de peróxido permite calcular k_{ox} a partir de la pendiente. Esta técnica ha sido empleada para determinar las constantes de reacción de distintas Prx de 2-Cys típicas con diferentes sustratos (84,86,141,249,250). Una vez formado, el sulfénico de la C_P en FF puede reaccionar con una segunda molécula de peróxido (con una constante de sobreoxidación k_{hyp}), o bien la proteína puede adoptar una conformación LU y reaccionar con la C_R para formar el enlace disulfuro intermolecular (con una constante cinética asociada k_{res}). Estos dos posibles destinos para ese sulfénico implican una competencia entre esa segunda molécula de peróxido y la formación del disulfuro (lo

que incluye el cambio conformacional a LU y la reacción propiamente dicha entre C_P y C_R).

Figura 23. Estudio de la cinética de oxidación de Prx2 por H_2O_2. **(A)** Curso temporal de los cambios en fluorescencia intrínseca de 0.25 µM Prx1 (negro) o Prx2 (rojo) reducidas luego de oxidarlas con 1.25 ó 1.5 µM H_2O_2, respectivamente (línea entera) y 1 mM H_2O_2 en ambos casos (línea punteada) en un equipo de flujo detenido. Estos experimentos fueron realizados a pH 7.4 y los trazos presentados son el promedio de 15 corridas. **(B)** La fase lenta se ajustó a una exponencial simple y se graficó la constante de primer orden obtenida en función de la concentración de peróxido para la Prx1 (negro) y la Prx2 (rojo). Figura tomada de (84).

La fase más lenta de las corridas de fluorescencia intrínseca de Prx2 en el tiempo a concentraciones crecientes de H_2O_2 puede ajustarse a una exponencial simple, obteniéndose valores que dependen linealmente de la concentración de H_2O_2. A partir del ajuste de k_{slow} *vs* $[H_2O_2]$ a una recta se pueden obtener la constante de cierre del disulfuro, independiente de H_2O_2 (k_{res}, ordenada en el origen), y la constante de sobreoxidación dependiente de $[H_2O_2]$ (k_{hyp}, pendiente de la recta) (Figura 23B) (83,84,141). Es así que se han determinado k_{res} y k_{hyp} para varias Prx, obteniéndose valores de 0.2 s^{-1} y 1.97 x 10^7 M^{-1} s^{-1}, respectivamente, para Prx2 a pH 7.4 (84).

1.8.3. Cuantificación de la sensibilidad a sobreoxidarse de las Prx: cálculo de $C_{hyp}1\%$

1.8.3.1. Determinación de $C_{hyp}1\%$ utilizando el ensayo acoplado

En los últimos años varios autores han intentado cuantificar la sensibilidad a sobreoxidarse de las distintas Prx para facilitar su comparación y clasificación entre robustas y sensibles (111,144,249). Recientemente, Nelson et al. definieron la $C_{hyp}1\%$ como la concentración de H_2O_2 a la cual se inactiva el 1% de las moléculas de Prx, y describieron un método para determinarla (249). Los autores utilizan el ensayo

acoplado para medir la actividad de la Prx a distintas concentraciones de H_2O_2. Es a partir de ajustes de estas corridas que reportan el $C_{hyp}1\%$ para varias Prx, valores que explicarían adecuadamente las diferencias reportadas en su sensibilidad a inactivarse por peróxido. Esta metodología tiene la desventaja de que a concentraciones muy altas de H_2O_2, es posible oxidar directamente al sistema reductor de la Prx (TR/Trx/NADPH), para lo que es necesario ser cuidadosos con los controles. En este sentido, se hace difícil el estudio de las Prx más robustas, en las que es necesario subir mucho la concentración del oxidante para poder ver inactivación.

1.8.3.2. Determinación directa de $C_{hyp}1\%$ a partir de las constantes cinéticas

En presencia de suficiente peróxido, el ácido cisteinsulfénico de la C_P puede ya sea reaccionar con una segunda molécula del sustrato para dar ácido cisteinsulfínico (k_{hyp}), o reaccionar con la cisteína resolutiva del monómero adyacente para formar el disulfuro (k_{res}). Esta competencia entre el peróxido y la C_R por la C_P-SOH puede seguirse por cambios en la fluorescencia intrínseca de la Prx2 en un equipo con stopped-flow, como se describió anteriormente. Considerando entonces una cinética simple de competencia (251) y utilizando las constantes obtenidas por cambios en la fluorescencia intrínseca (sección 1.5.2.2), se puede llegar a estimar la fracción de enzima sobreoxidada, f_{inact} como:

$$f_{inact} \approx k_{hyp} [H_2O_2] / k_{res} \qquad \text{Ecuación 5}$$

Es así como puede definirse el *direct* $C_{hyp}1\%$ como la concentración de H_2O_2 necesaria para inactivar al 1% de la Prx luego del agregado de H_2O_2 en condiciones no-catalíticas (en ausencia de reductor que recupere la enzima luego de formado el sulfénico de la C_P). En ese caso $f_{inact} = 0.01$, y entonces

$$\textit{direct } C_{hyp}1\% = 0.01 \times k_{res} / k_{hyp} \qquad \text{Ecuación 6}$$

Cabe notar que para las Prx de 2-Cys típicas, como la Prx2, la reacción de formación del disulfuro ocurre dentro del dímero funcional y por ende es considerada de orden 1 a pesar de ser estrictamente intermolecular (144,250).

El valor de $C_{hyp}1\%$ obtenido por cualquiera de las dos formas es un indicador de la sensibilidad a sobreoxidarse de las Prx, permitiendo comparar las distintas isoformas de una manera cuantitativa. Estos intentos por cuantificar la sensibilidad de las distintas Prx reflejan la necesidad de entender en base a datos numéricos el rol

diferencial de las distintas Prx en la fisiología celular. Esto permite además evaluar el rol de distintas PTM en la función de las Prx, y eventualmente generar modelos teóricos que pudieran predecir el destino tanto de los peróxidos como de las Prx en la célula, tomando en cuenta todos los parámetros conocidos hasta el momento.

2. OBJETIVOS

2.1. Objetivo general

Caracterización de la forma nitrada de la Prx2 *in vitro* y comprensión de los mecanismos por los que esta modificación afecta la estructura y funcionalidad de la enzima.

2.2. Objetivos específicos

1. Evaluación del efecto del tratamiento con peroxinitrito en la actividad y estructura de la Prx2 purificada de glóbulo rojo humano y recombinante.

2. Obtención de las formas nitradas de Prx2 por nitración co-traduccional.

3. Estudio del rol de Y193 en la función de Prx2, mediante la obtención de mutantes específicos en dicho residuo.

4. Caracterización estructural, *in silico* y funcional de la enzima *wild-type* y cada una de las variantes nitradas, así como de las mutantes tratadas con peroxinitrito.

5. Evaluación de los efectos del tratamiento con peroxinitrito en Prx1 y Prx3 en comparación con Prx2, en particular en lo que respecta a modificaciones en su susceptibilidad a sobreoxidación y en su actividad peroxidasa.

3. RESULTADOS Y DISCUSIÓN

3.1. Efectos del tratamiento con peroxinitrito en la función peroxidasa de Prx2

3.1.1. Resumen

Las peroxirredoxinas son peroxidasas muy eficientes que tienen un mecanismo dependiente de tioles y que son claves en la señalización redox mediada por H_2O_2. Cualquier cambio estructural que pueda afectar su estado de oxidación, estructura oligomérica, y/o interacciones con otras proteínas, podría tener un impacto en las cascadas de señalización redox. Varias modificaciones postraduccionales han sido reportadas como moduladoras de la actividad de Prx. Entre estas, la sobreoxidación de la cisteína peroxidática a ácido cisteinsulfínico inactiva la enzima y ha sido propuesta como un mecanismo de acumulación de H_2O_2 (hipótesis de la compuerta). La nitración de Prx ha sido reportada tanto *in vitro* como *in vivo* y en particular, se ha encontrado a la Prx2 nitrada en cerebros de pacientes con Alzheimer. En este trabajo caracterizamos la nitración de tirosinas en Prx2, una modificación postraduccional en residuos no-catalíticos que aumenta su actividad peroxidasa y su resistencia a sobreoxidarse. Estudios de espectrometría de masa revelaron que el tratamiento de Prx2 previamente oxidada a disulfuro con un exceso de peroxinitrito da lugar a una enzima mayoritariamente nitrada en un único sitio o en dos. La tirosina 193, que pertenece al motivo YF del extremo C-terminal de la proteína, asociado con la sensibilidad a inactivarse de las Prx eucariotas, fue encontrada nitrada y probablemente sea responsable del efecto protector de la C_P luego del tratamiento con peroxinitrito. Análisis cinéticos sugieren que la nitración de la tirosina 193 facilita la formación del disulfuro intermolecular, transformando una Prx sensible en una robusta. De esta manera, la nitración de tirosinas aparece como otro mecanismo modulador de estas enzimas en el complejo entramado de la señalización redox.

3.1.2. Principales resultados obtenidos

- El tratamiento con peroxinitrito de la Prx2 purificada de glóbulos rojos humanos dio lugar a una proteína nitrada en tirosinas, mayoritariamente con un único residuo modificado por monómero, no observándose más de dos residuos nitrados por monómero.

- La Prx2 nitrada tiene mayor actividad peroxidasa y mayor resistencia a la sobreoxidación por H_2O_2.

- Se identificaron 3 tirosinas nitradas por espectrometría de masa, entre las cuales se encuentra la tirosina 193, perteneciente al motivo YF del extremo C-terminal de la proteína, vinculado a las diferencias en la sensibilidad a sobreoxidarse de las Prx eucariotas.

3.1.3. Artículo publicado en Journal of Biological Chemistry

Nitration Transforms a Sensitive Peroxiredoxin 2 into a More Active and Robust Peroxidase*

Lía M. Randall[‡§1], **Bruno Manta**[‡¶1,2], **Martín Hugo**[§‖2], **Magdalena Gil**[**‡‡], **Carlos Batthyàny**[§‖**], **Madia Trujillo**[§‖], **Leslie B. Poole**[§§], **and Ana Denicola**[‡§3]

From the ‡Laboratorio de Fisicoquímica Biológica, Instituto de Química Biológica, Facultad de Ciencias, Universidad de la República, 11400 Montevideo, Uruguay, the §Center for Free Radical and Biomedical Research, Facultad de Medicina, Universidad de la República, Montevideo 11100, Uruguay, the ¶Laboratorio de Biología Redox de Tripanosomas, Institut Pasteur de Montevideo, 11400 Montevideo, Uruguay, the ‖Departamento de Bioquímica, Facultad de Medicina, Universidad de la República, 11100 Montevideo, Uruguay, the **Unidad de Bioquímica y Proteómica Analíticas, Institut Pasteur de Montevideo, 11400 Montevideo, Uruguay, the ‡‡Unidad de Bioquímica y Proteómica Analíticas, Instituto de Investigaciones Biológicas Clemente Estable, Ministerio de Educación y Cultura, 11600 Montevideo, Uruguay, and the §§Department of Biochemistry, Wake Forest School of Medicine, Winston-Salem, North Carolina 27157

Background: Peroxiredoxin 2 (Prx2) reduces peroxides through a cysteine-dependent mechanism and is susceptible to overoxidation of its reactive cysteine during catalysis.
Results: Nitration rendered a more active peroxidase, less sensitive to overoxidation.
Conclusion: Nitration of Prx2 favors disulfide bond formation over overoxidation.
Significance: Understanding the mechanisms by which post-translational modifications modify Prx2 functionality *in vitro* is crucial to evaluate potential *in vivo* consequences for redox signaling.

Peroxiredoxins (Prx) are efficient thiol-dependent peroxidases and key players in the mechanism of H_2O_2-induced redox signaling. Any structural change that could affect their redox state, oligomeric structure, and/or interaction with other proteins could have a significant impact on the cascade of signaling events. Several post-translational modifications have been reported to modulate Prx activity. One of these, overoxidation of the peroxidatic cysteine to the sulfinic derivative, inactivates the enzyme and has been proposed as a mechanism of H_2O_2 accumulation in redox signaling (the floodgate hypothesis). Nitration of Prx has been reported *in vitro* as well as *in vivo*; in particular, nitrated Prx2 was identified in brains of Alzheimer disease patients. In this work we characterize Prx2 tyrosine nitration, a post-translational modification on a noncatalytic residue that increases its peroxidase activity and its resistance to overoxidation. Mass spectrometry analysis revealed that treatment of disulfide-oxidized Prx2 with excess peroxynitrite renders mainly mononitrated and dinitrated species. Tyrosine 193 of the YF motif at the C terminus, associated with the susceptibility toward overoxidation of eukaryotic Prx, was identified as nitrated and is most likely responsible for the protection of the peroxidatic cysteine against oxidative inactivation. Kinetic analyses suggest that tyrosine nitration facilitates the intermolecular disulfide formation, transforming a sensitive Prx into a robust one. Thus, tyrosine nitration appears as another mechanism to modulate these enzymes in the complex network of redox signaling.

Peroxiredoxins (Prx,[4] EC 1.11.1.15) are a group of enzymes that efficiently reduce peroxides based on a critical cysteine residue (peroxidatic cysteine, C_P). The first step in catalysis is the reaction of C_P with H_2O_2 to form a sulfenic acid derivative (C_P-SOH) which, in 2-cysteine Prx (2-Cys Prx), reacts with another cysteine residue (the resolving cysteine, C_R) to form a disulfide that is then reduced by the thioredoxin/thioredoxin reductase/NADPH system (Fig. 1) (1–4). In typical 2-Cys Prx or Prx1 subfamily (Prx 1–4 in mammals (5)), the reaction occurs between the C_P-SOH of one subunit with the C_R-SH of another subunit; thus, each homodimer contains two active sites (3). In addition, for the intermolecular disulfide to be formed, a conformational change is needed to approach the C_P-SOH from one subunit toward the C_R from the other subunit. This rearrangement involves the transition from the so-called fully folded (FF) form, in which the C_P and the C_R are approximately 14 Å apart, to a locally unfolded (LU) conformation (Fig. 1) (2, 7, 8).The sulfenic acid intermediate can react with the C_R-SH forming a disulfide, or with a second molecule of H_2O_2 to form sulfinic acid (overoxidation), inactivating the peroxidase activ-

---

[4] The abbreviations used are: Prx, peroxiredoxin(s); C_P, peroxidatic cysteine; C_R, resolving cysteine; C_P-SOH, cysteine sulfenic acid; C_P-SO_2H, cysteine sulfinic acid; DTDP, 4′,4′-dithiodipyridine; DTNB, 5′,5′-dithio-bis(2-nitrobenzoic acid); DTPA, diethylenetriaminepentaacetic acid; ESI, electrospray ionization; FF, fully folded; LU, locally unfolded; NEM, N-ethylmaleimide; Prx2, peroxiredoxin 2; PTM, post-translational modification; QTOF, quadrupole time-of-flight; ROA, reverse-order addition; TR, thioredoxin reductase; Trx, thioredoxin.
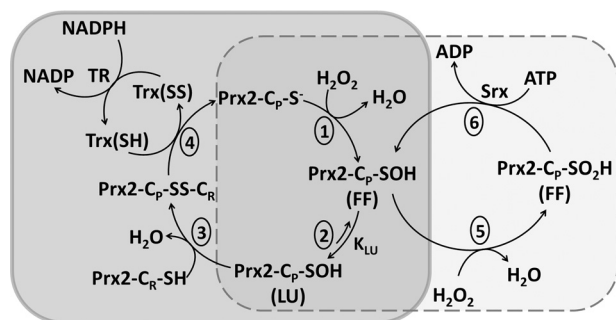
FIGURE 1. **Catalytic cycle of eukaryotic typical 2-Cys Prx.** *1*, reaction of a molecule of peroxide with the C_P thiolate to form cysteine sulfenic acid. *2*, transition from the FF to the LU conformation. *3*, reaction of C_P sulfenic acid with C_R. *4*, reduction of disulfide Prx. *5*, overoxidation of C_P to sulfinic acid. *6*, reduction of cysteine sulfinic acid by sulfiredoxin (*Srx*). The protein is represented as one of two active sites within a functional dimer.

ity. The oxidation of cysteine to cysteine sulfinic acid (C_P-SO_2H) is an irreversible post-translational modification (PTM) for most proteins other than 2-Cys Prx, where the specific enzymatic reduction of C_P-SO_2H by sulfiredoxin in an ATP-dependent mechanism was demonstrated (9, 10).

Prx are ubiquitous and highly expressed proteins, and their extraordinary reactivity and specificity for hydroperoxides make them ideal sensors of endogenous H_2O_2 and probably the first step in H_2O_2-induced signaling pathways (11–15). PTM of Prx that could affect their activity, redox state, oligomeric structure, or interaction with other proteins will undoubtedly affect redox signaling by H_2O_2, and it has been hypothesized that Prx inactivation via overoxidation is a way to accumulate H_2O_2 to allow oxidation of other redox proteins (the floodgate hypothesis) (2). The presence of sulfiredoxin as an enzyme that specifically reduces typical 2-Cys Prx cysteine sulfinic acid supports the biological relevance of their peroxidase activity and the signaling role of their oxidative inactivation (16).

Prx2, the most abundant peroxidase in mammalian erythrocytes (17, 18), is capable of reducing hydroperoxides as well as peroxynitrite,[5] a potent oxidant formed *in vivo* by the diffusion-controlled reaction between superoxide and nitric oxide. Our group recently demonstrated that erythrocyte Prx2 not only is susceptible to overoxidation by peroxynitrite, but it can also get nitrated during catalysis (19). Moreover, nitrated Prx2 was detected in brains of patients with early Alzheimer disease (20).

Protein tyrosine nitration is a common PTM occurring under conditions of nitroxidative stress, which alters the structure and function of the modified protein. The biological mechanism of tyrosine oxidation begins with the formation of the tyrosyl radical followed by addition of nitrogen dioxide yielding 3-nitrotyrosine, and one of the major pathways of protein nitration *in vivo* involves the reaction of radicals derived from peroxynitrite homolysis (21–25).

We herein report the effects of Prx2 modification by peroxynitrite treatment, focusing on tyrosine nitration, which increases its peroxidase activity along with resistance to overoxidation by H_2O_2. We hypothesize that nitration of tyrosine 193 from the YF motif at the C terminus, close to the active site,

favors transition from the FF to the LU conformation, promoting disulfide formation and inhibiting C_P overoxidation.

EXPERIMENTAL PROCEDURES

Chemicals—Dithiothreitol (DTT), DTNB, and reduced nicotinamide adenine dinucleotide phosphate (NADPH) were purchased from AppliChem (Germany). DTDP was purchased from ACROS Organics, Fisher Scientific. Hydrogen peroxide (H_2O_2) and DTPA were purchased from Sigma. Peroxynitrite was synthesized as in Ref. 26. All other reagents were of analytical grade and used as received.

Purification of Proteins—Human Prx2 was purified from human erythrocytes according to Ref. 19. Recombinant human thioredoxin (hTrx1), *Escherichia coli* thioredoxin 1 (*Ec*Trx1), and recombinant *E. coli* thioredoxin reductase (*Ec*TR) were produced and purified as reported in Refs. 19 and 27. *Ecchinococcus granulosus* (*Eg*TR) was kindly provided by Dr. G. Salinas (28).

Peroxide and Protein Quantification—The concentration of H_2O_2 stock solutions was measured at 240 nm ($\epsilon_{240} = 43.6$ M^{-1} cm^{-1}). Peroxynitrite concentration was determined at 302 nm ($\epsilon_{302} = 1670$ M^{-1} cm^{-1}) as in Ref. 26. Protein concentration was measured by absorption at 280 nm in the assay buffer, using the corresponding ϵ determined for the oxidized proteins according to Ref. 29: ϵ_{280}(Prx2) = 19,380 M^{-1} cm^{-1}, ϵ_{280}(hTrx) = 7100 M^{-1} cm^{-1}, ϵ_{280}(*Ec*Trx) = 14,060 M^{-1} cm^{-1}, and ϵ_{280}(*Ec*TR) = 19,160 M^{-1} cm^{-1}. Concentration of active *Eg*TR was estimated according to FAD and selenium content (28).

Thiol Quantification—The thiol concentration of the reduced proteins was measured according to Ref. 30 with minor modifications. Briefly, the protein was reduced with DTT (>10-fold molar excess for 30 min) and the remnant reductant removed by buffer exchange with a HiTrap coupled to a FPLC with online UV detection equilibrated in 50 mM potassium phosphate buffer, pH 7.4, with 0.1 mM DTPA and 150 mM NaCl. An excess of DTDP was added to the protein sample in the assay buffer, and absorption was measured at 324 nm ($\epsilon_{324} = 21,400$ M^{-1} cm^{-1}).

Prx2 Thiol Reduction and Oxidation—For reduction of purified Prx2, the enzyme was reduced with 1 mM DTT for 30 min at room temperature immediately before the experiment, and the mixture was passed twice through a Bio-Spin column (Bio-Rad) preequilibrated with the assay buffer. Thiol concentration was determined just after elution from the column, and controlled oxidation to its disulfide form was achieved with the addition of 0.6 eq of H_2O_2.

Nitration of Prx2 by Peroxynitrite—To prevent overoxidation of C_P, treatment with peroxynitrite was performed on the disulfide-oxidized enzyme. The corresponding molar excess of peroxynitrite was added in a unique bolus or a flux-like addition. Previously decomposed peroxynitrite in the assay buffer (reverse-order addition (ROA)) was used as a control of peroxynitrite-derived products reaction with Prx2. Tyrosine nitration of Prx2 was confirmed by Western blot analysis using specific antibodies. Briefly, samples were prepared for 15% SDS-PAGE under reducing (Figs. 2*B* and 4*C*) or nonreducing conditions (Fig. 3) without heating and transferred to a PVDF membrane. The membrane was incubated with anti-nitroty-

---

[5] The term peroxynitrite is used to refer to the sum of peroxynitrite anion ($ONOO^-$) and peroxynitrous acid (ONOOH) unless specified.
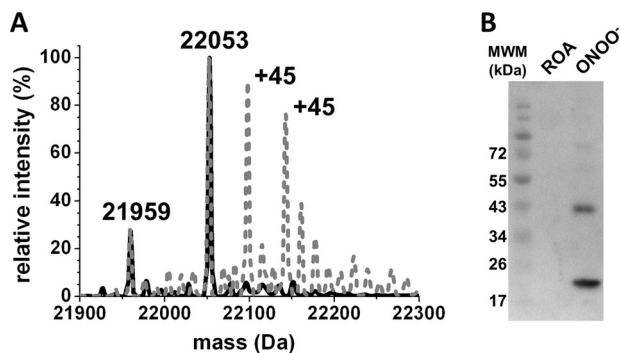
FIGURE 2. **Analysis of Prx2 nitration after peroxynitrite treatment.** *A*, QTOF-ESI MS analysis. Disulfide-oxidized Prx2 was treated with a 5-fold excess peroxynitrite, then reduced with 5 mM DTT for 15 min at room temperature, followed by addition of 20 mM NEM to block the reduced thiols. The remaining DTT and NEM were removed by gel filtration, and samples in 30 mM ammonium bicarbonate buffer were analyzed by QTOF-ESI MS. Control Prx2 is shown in *black* (shown as 100%), and the *gray dotted line* shows the peroxynitrite-treated enzyme. *B*, Western blot analysis. Disulfide Prx2 was treated with a 5-fold excess peroxynitrite (ONOO⁻) or ROA. 2.4 μg of control or peroxynitrite-treated Prx2 was resolved on 15% SDS-PAGE under reducing conditions and analyzed by Western blot using α-NO$_2$Y antibodies.
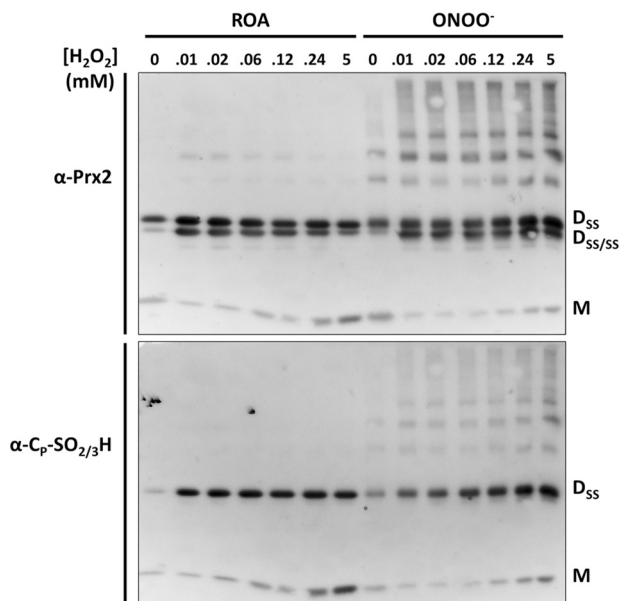
FIGURE 3. **Differential overoxidation of control and peroxynitrite-treated Prx2.** After treatment with the ROA control or a 5-fold excess of peroxynitrite (ONOO⁻), Prx2 was treated with DTT for reduction of its thiols, and residual DTT was removed. 5 μM Prx2 was incubated with 0, 0.01, 0.02, 0.06, 0.12, 0.24, or 5 mM H$_2$O$_2$ in 50 mM phosphate buffer, pH 7.4. After 5 min, 30 mM NEM was added to alkylate the remaining thiols. Samples were prepared for SDS-PAGE under nonreducing conditions, analyzed by Western blotting using α-Prx2 antibody and α-C$_P$-SO$_{2/3}$H after mild stripping. One μg of protein was loaded on each *lane* (D_{ss}, dimer with one C$_P$ disulfide-oxidized; $D_{ss/ssSS/SS}$, dimer with both C$_P$ disulfide-oxidized; *M*, monomer).

rosine antibodies (α-NO$_2$Y (31)) in a 1/1000 dilution and with goat anti-rabbit IRDye® 800 CW (LI-COR Biosciences) secondary antibody (1/20,000).

Overoxidation of Prx2 by H$_2$O$_2$—To study the effect of nitration on the susceptibility of Prx2 to overoxidation, it was necessary to start with a reduced nonoveroxidized but yet nitrated form of Prx2. Disulfide-oxidized Prx2 was treated with peroxynitrite for nitration as described above, then reduced, and after removal of residual DTT the enzyme was treated with H$_2$O$_2$. Samples were resolved in 15% SDS-PAGE under nonre-

ducing conditions, transferred to a PVDF membrane, and blotted with specific α-Prx2-C$_P$-SO$_{2/3}$H antibodies (AbFrontier). For control, rabbit polyclonal antibodies against Prx2 were used (α-Prx2; AbFrontier).

Mild Stripping of Western Blot Membranes—Membranes were incubated for 10-min in mild stripping buffer (1.5% glycine, 0.1% SDS, pH 2.2) twice, followed by two 10-min incubations in PBS and two 5-min incubations in TBS-Tween 0.1%. Blockage was performed for 2 h or overnight in 5% milk in TBS-Tween 0.1%.

NADPH-linked Peroxidase Activity—NADPH consumption was followed spectrophotometrically at 340 nm in a Cary 50 spectrophotometer (Varian). Prx2 was mixed with 120 μM NADPH, 0.4 μM *Eg*TR, 8 μM hTrx1 in the described buffer, and the reaction was started with the addition of H$_2$O$_2$. An Applied Photophysics RX2000 Rapid Kinetics Spectrophotometer Accessory was used for stopped-flow experiments.

Thioredoxin-linked Peroxidase Activity—The catalytic H$_2$O$_2$ decomposition by Prx2 was followed through the intrinsic fluorescence (λ_{exc} = 280 nm, λ_{em} = 340 nm) of reduced *Ec*Trx1 (10 μM) in a coupled assay with Prx2 (50 nM) and H$_2$O$_2$ (7 μM) in a thermostatted Cary Eclipse spectrofluorometer (Varian). Fluorescence changes were calibrated using a known concentration of reduced and oxidized *Ec*Trx1.

MS Analysis of Prx2 Tryptic Digestion—For analysis of proteins obtained from acrylamide gels, selected bands were manually cut and in-gel digested with trypsin (sequence grade; Promega) as described (32). Peptides were extracted from gels using aqueous 60% acetonitrile containing 0.1% TFA and concentrated by vacuum drying. Mass spectra of peptides mixtures were acquired in a linear ion trap mass spectrometer (LTQ Velos, Thermo) coupled on-line with a nano-liquid chromatography system (easy-nLC; Proxeon-Thermo). Peptides were separated in a reversed-phase column (EASY-column™ C18, 75 μm × 10 cm, inner diameter) equipped with a trap column (EASY-column C18, 100 μm × 2 cm, inner diameter) with solvent A (0.1% formic acid in H$_2$O) and solvent B (0.1% formic acid in acetonitrile), and eluted using a linear gradient from 0 to 45% B in 70 min at 300 nl/min. Electrospray voltage was 1.6 kV, capillary temperature was 270 °C. Peptides detected in the positive ion mode using a mass range of 300–2000.

Proteins were identified by database searching of measured peptide *m/z* values using the MASCOT search engine (Matrix Science) and Sequest (Thermo) software, based on the following search parameters: monoisotopic mass tolerance, 1.5 Da; fragment mass tolerance, 0.8 Da; partial methionine oxidation, cysteine carbamidomethylation, tyrosine nitration, and three missed tryptic cleavages allowed. Protein mass and taxonomy were unrestricted. Significant scores ($p < 0.05$) were used as criteria for positive peptide identification.

Whole Protein Mass Spectrometry Analysis of Peroxynitrite-treated Prx2—Control and peroxynitrite-treated Prx2 were reduced, and 20 mM NEM was added to alkylate thiols. Remaining DTT and NEM were removed using Bio-Gel P6 Gel® (Bio-Rad) columns and 30 mM ammonium bicarbonate buffer for elution. Samples were diluted from 4 to 40 μl with methanol: H$_2$O 1:1 2% formic acid, and 2–3 μl were analyzed using a Waters Q-Tof API US operated in "V" mode using a Triversa

Nanomate sprayer from Advion. Sprayer voltage ~ 1.8 kV; Q-T of cone voltage 45 V; source temperature 80 °C; nitrogen desolvation temperature 200 °C. Data were acquired from 600–1900 m/z in positive ion continuum mode; scan time 2.4 s; interscan delay 0.1 s. Max Ent data were produced for 10,000–50,000 Da.

RESULTS

Treatment of Prx2 with Peroxynitrite Yields a Nitrated Enzyme—Disulfide-oxidized Prx2 was treated with a 5-fold excess of peroxynitrite or its decomposition products, as a control designated ROA. Nitration of Prx2 was confirmed by immunoblotting and mass spectrometry analyses (Fig. 2). For QTOF-ESI mass spectrometry analysis, disulfide-oxidized Prx2 was reduced with DTT and alkylated with NEM. A main peak of m/z 22,053 was obtained for control Prx2, which corresponds to the Prx monomer (21,803 Da) with both C_P and C_R alkylated with NEM (125 Da) (Fig. 2A). When treated with a 5-fold excess of peroxynitrite, mainly mononitrated (m/z 22,053 ± 45) and dinitrated (m/z 22,053 ± (2 × 45)) species were detected, confirming that nitration is the main modification after peroxynitrite treatment of disulfide Prx2. The minor species detected in both experiments (m/z 21,959) corresponds to the monomer of Prx2 with one Cys NEM-alkylated and the other one overoxidized, suggesting initial oxidation of Prx2 with H_2O_2 to obtain the disulfide form rendered a minor portion of overoxidized protein (Fig. 2A). Western blot analysis using antibodies against nitrotyrosine residues confirmed tyrosine nitration after the peroxynitrite treatment (Fig. 2B). Some nonreducible dimers were observed, suggesting the presence of di-tyrosine dimers, characteristic of peroxynitrite treatment of proteins (22).

Analysis of Peroxynitrite-treated Prx2 Overoxidation—2-Cys Prx sensitivity to overoxidation can be followed by nonreducing SDS-PAGE (33, 34). As shown in Fig. 3, and consistent with results in Fig. 2, overoxidation was detected at lower H_2O_2 concentrations for the nontreated Prx2 than for the peroxynitrite-treated enzyme. Addition of increasing concentrations of H_2O_2 to reduced control or peroxynitrite-treated Prx2 caused the transition from reduced monomer (M) to mono-disulfide dimer (D_{SS}) and di-disulfide dimer ($D_{SS/SS}$), with high H_2O_2 concentrations rendering overoxidized disulfide dimer (D_{SS}) and overoxidized monomer (M). As observed previously (33, 35), substoichiometric addition of H_2O_2 was enough to overoxidize the enzyme in these conditions, leading to the formation of dimers containing a disulfide and an overoxidized C_P, whereas high concentrations of the oxidant were not able to completely overoxidize the enzyme to its monomers. This result supports the idea of asymmetry of the homodimer active sites, suggesting that, under noncatalytic conditions, the redox state of one C_P affects overoxidation of the second one, as discussed previously by others (35–38). Moreover, nitration protected Prx2 from overoxidation, as the treated enzyme showed less overoxidation after H_2O_2 treatment than the control under noncatalytic conditions, suggesting a structural connection between tyrosine nitration and overoxidation of the peroxidatic cysteine.
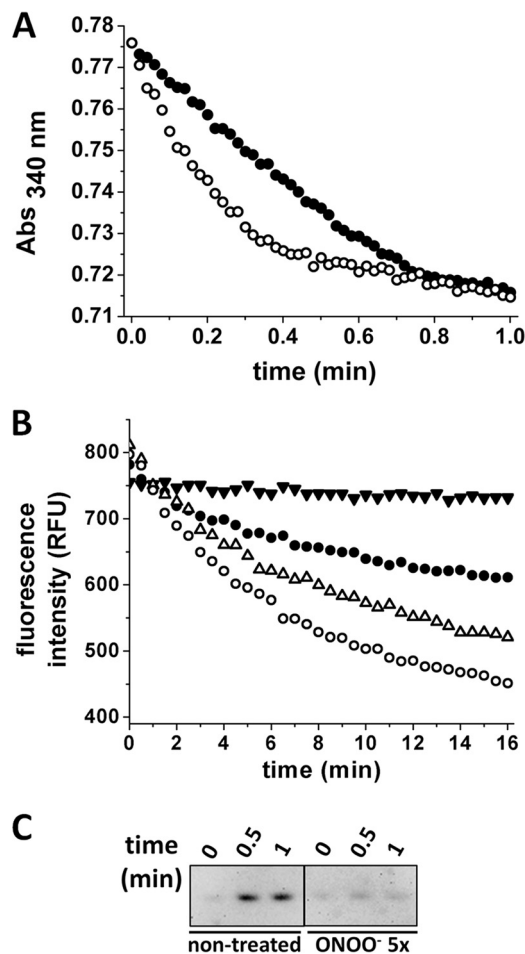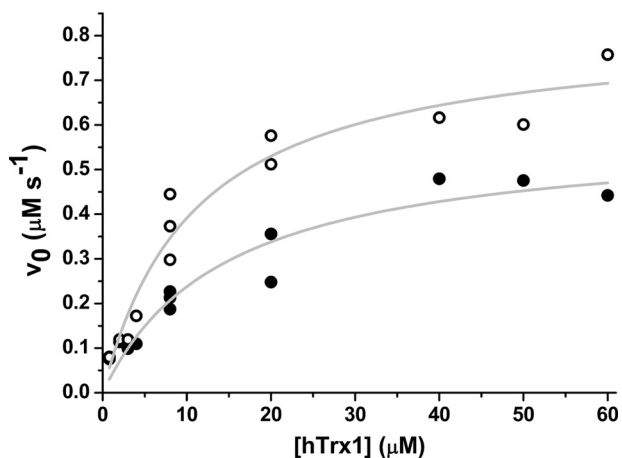

FIGURE 4. **Effect of nitration on Prx2 peroxidase activity and overoxidation.** *A*, NADPH-linked peroxidase activity. 0.5 μM reverse-order addition (●) or peroxynitrite-treated (○) Prx2 was incubated with 8 μM hTrx1, 0.4 μM *Eg*TR, and 160 μM NADPH in 50 mM sodium phosphate buffer, pH 7.4, 150 mM NaCl, 0.l mM DTPA. The reaction was started by the addition of H_2O_2 (10 μM final concentration), and consumption of NADPH was followed at 340 nm. *B*, *Ec*Trx1 fluorescence-linked Prx2 peroxidase activity. Oxidation of *Ec*Trx1 was followed at λ_{exc} = 280 nm, λ_{em} = 340 nm, in 50 mM sodium phosphate buffer, pH 7.4, 0.1 mM DTPA, 150 mM NaCl, with 10 μM reduced *Ec*Trx1. and 50 nM Prx2. ●, nontreated Prx2; △, Prx2 treated with 1-fold or (○) 5-fold excess peroxynitrite; ▼, control run (no Prx2 added). The reaction was started by the addition of 7 μM H_2O_2. *C*, Western blot analysis against C_P-$SO_{2/3}H$. Aliquots were taken at 0, 0.5, and 1 min after H_2O_2 addition in the presence of Trx, TR, and NADPH. Catalase (0.3 mg/ml) was added to eliminate residual H_2O_2 and NEM (26 mM) to block remaining thiols. 80 ng of Prx2 was loaded on each *lane* and resolved by reducing SDS-PAGE.

Treatment of Prx2 with Peroxynitrite Affects Its Peroxidase Activity—Peroxidase activity was measured following the consumption of NADPH at 340 nm after addition of H_2O_2 to a system containing Prx2, hTrx1, *Eg*TR, and NADPH (Fig. 4A). Treated Prx2 showed a higher rate of H_2O_2 reduction than the ROA control. The gain in peroxidase activity was confirmed by following NADPH consumption in a stopped-flow spectrophotometer, demonstrating that the change in peroxidase activity precedes oxidative inactivation of the enzyme (data not shown), as well as following the loss of reduced *Ec*Trx1 fluorescence at 340 nm (λ_{exc} = 280 nm) as it was oxidized by Prx2/H_2O_2 (Fig. 4B). The inactivation during turnover was clear for the native Prx2, whereas the peroxynitrite-treated enzyme suffered less overoxidation in turnover, as indicated by Western blot analysis (Fig. 4C).

Effects of Nitration on Prx2 Functionality

Interaction of Nitrated Prx2 with hTrx1 Does Not Explain the Increase in Peroxidase Activity—To understand the gain in Prx2 peroxidase activity after treatment with peroxynitrite, we measured peroxidase activity using increasing concentrations of hTrx1 at a fixed concentration of H_2O_2 (Fig. 5). Interestingly, when low concentrations of hTrx1 were used, control and treated-Prx2 showed no clear differences in their peroxidase activity, whereas increasing hTrx1 concentrations enhanced their differences. As shown in Fig. 5, even in the presence of high concentrations of hTrx1 (>10-fold the reported K_m^{app} (19)), a significant difference between untreated and peroxynitrite-treated Prx2 activity was observed. Fitting the data from Fig. 5 to the Michaelis-Menten equation, V_{max} can be calculated, obtaining a higher value for the peroxynitrite-treated enzyme than for control Prx2.

Mapping of the Modified Residues Reveals Nitration of Tyr-193—Analysis of digested Prx2 in an LTQ mass spectrometer mapped four of the seven tyrosine residues of the polypeptidic chain. From these peptides, three of the residues (Tyr-33, Tyr-126, and Tyr-193) were detected as nitro-tyrosines after peroxynitrite treatment, whereas Tyr-115 was found as native in every experiment. Table 1 shows the theoretical and experimental mass values for the modified tyrosine-containing peptides detected. Among these, Tyr-193 is part of the YF motif located in the C terminus region of the protein that has been related to Prx sensitivity to overoxidation (Fig. 6) (2), and the environment of the YF loop has been recently described to have a great impact on C_P overoxidation (35).

DISCUSSION

The peroxidatic cysteine of Prx reacts with H_2O_2 at 10^3- to 10^6-fold faster than most protein cysteines (13), but at ordinary rates with any other thiol reagent (39). Prx seem to be designed to specifically reduce peroxides, which place them not only as efficient antioxidant enzymes but also as key players in the mechanism of H_2O_2-induced redox signaling (40, 41). The catalysis of H_2O_2 reduction depends on a conserved Cys residue within a highly conserved active site pocket that adequately stabilizes the transition state. In addition, an important conformational change is needed for 2-Cys Prx to complete the oxidative part of the cycle, including the local unfolding of the helix that harbors C_P and the displacement of secondary structure elements that contain the C_R residue (2). Stabilization of the FF form of the enzyme has been associated with a slower rate of disulfide formation favoring the reaction of C_P-SOH with H_2O_2 to form the inactive sulfinic derivative (C_P-SO_2H). This inactivation by overoxidation has been postulated as a mechanism of regulating intracellular H_2O_2 levels, critical for redox signaling (2, 14, 42–44).

MS analysis of disulfide Prx2 treated with a 5-fold excess of peroxynitrite revealed that the main polypeptidic modification was nitration of tyrosine residues yielding mainly mononitrated and dinitrated species (Fig. 2A). Nitration of Prx2 rendered an enzyme less susceptible to overoxidation by H_2O_2 (Figs. 3 and 4C). This could be due either to a slower reaction with the second H_2O_2 molecule to yield the sulfinic derivative (step 5 in Fig. 1) or to a faster formation of the intermolecular disulfide (steps 2 and 3 in Fig. 1), thus unfavoring the overoxidation reaction.

FIGURE 5. **Dependence of Prx2 peroxidase activity with thioredoxin concentration.** Nontreated (●) or 5-fold excess peroxynitrite-treated (○) Prx2 activity was measured following NADPH consumption at 340 nm. The reaction was started with the addition of 10 μM H_2O_2 to a mixture containing 160 μM NADPH, 0.4 μM EgTR, varying concentrations of hTrx1 (0.8–60 μM), and 0.5 μM Prx2.

FIGURE 6. **Structural model of Prx2 active site.** View of human erythrocyte Prx2 active site. One monomer shows the C_P residue in sulfinic acid form (*blue*) whereas the other subunit (*gray*) shows the C_R, as well as the YF motif containing Tyr-193. The image was constructed with PyMOL from PDB 1QMV (6).

TABLE 1

Identification of modified tyrosine-containing peptides after treatment with peroxynitrite

Control and peroxynitrite-treated Prx2 were digested with trypsin after 15% SDS-PAGE. Samples were subjected to HPLC-MS/MS using an LTQ mass spectrometer as detailed under "Experimental Procedures." Sequences of modified tyrosine-containing peptides identified by MS are shown, with their corresponding theoretical and observed masses.
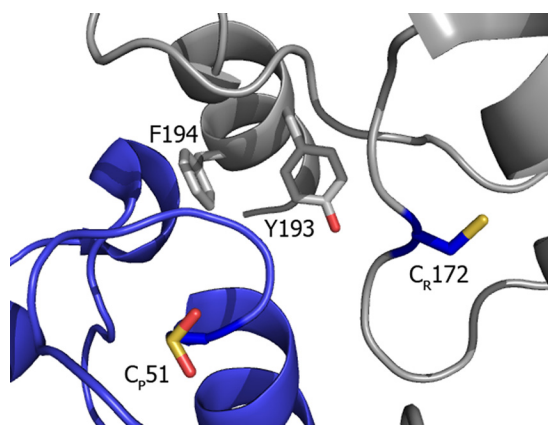
Peptide	Theoretical mass $[(M + H)^+]$	Theoretical mass + 45[a] $[(M + H)^+]$	Observed masses	Assigned sequence	Nitrated tyrosine
	Da	*Da*	*Da*		
1	625.3	670.3	670.2	[30]LSD[33]YK[34]	Tyr-33
2	673.3	718.3	718.2	[192]E[193]YFSK[196]	Tyr-193
3	924.4	969.4	969.3	[120]TDEGIA[126]YR[127]	Tyr-126

[a] Addition of a nitro (-NO_2) group results in a molecular mass increase of 45 Da.

Surprisingly, the peroxynitrite-treated enzyme was more active than the native enzyme (Fig. 4). Given the modified enzyme is more resistant to overoxidation, one possible explanation for the observed gain in activity could be less inactivation in turnover (as seen in Fig. 4C). However, measurement of activity by stopped-flow spectrophotometry showed a higher rate for the nitrated enzyme from the very beginning of the run (0.277 ± 0.006 μmol/min *versus* 0.213 ± 0.002 μmol/min for the untreated enzyme; data not shown), indicating the differences in activity preceded overoxidation in turnover.

The reaction of C_P with H_2O_2, the first step in catalysis, is so fast ($k_2 = 10^7$–10^8 M^{-1} s^{-1}) that it is safe to assume C_P-SOH formation will not be the limiting step (19, 39). Thus, under the experimental conditions employed, the gain in peroxidase activity should reside in disulfide formation between C_P-SOH and C_R and/or the reduction of the intermolecular disulfide by thioredoxin (Fig. 1). The first option will be kinetically limited by the conformational change needed to get together both cysteines (the FF-LU transition (8)) whereas the second is limited by the kinetics of protein-protein interaction (Fig. 1). As shown in Fig. 5, at a fixed saturating concentration of H_2O_2, initial NADPH consumption rates were very close for control and peroxynitrite-treated Prx2 at low concentrations of hTrx1, whereas a significant difference appeared at higher hTrx1 concentrations. Although a faster dissociation of the ternary complex between hTrx1 and Prx2 to yield reduced Prx2 could explain the observed differences in V_{max}, it cannot explain the resistance to overoxidation of the nitrated enzyme. Therefore, it can be affirmed that, at high hTrx1 concentrations, the velocity of NADPH consumption is limited by disulfide formation. From V_{max} and Prx2 concentration, the rate constant of this step, k_{cat}, can be estimated, obtaining a value of (1.2 ± 0.1) s^{-1} for the ROA control enzyme and (1.6 ± 0.1) s^{-1} for the peroxynitrite-treated Prx2. Very similar results were obtained when using *Ec*TR and *Ec*Trx1 (data not shown), supporting the idea that the observed changes in V_{max} are not due to differences in the interaction between Prx2 and Trx. The faster the intermolecular disulfide bond is formed, the lower the chance for C_P to get overoxidized by H_2O_2. These differences in k_{cat} explain the differences in activity as well as the different susceptibility to overoxidation. Thus, this PTM transforms a sensitive Prx into a more robust peroxidase.

It has been observed that eukaryotic Prx, generally more sensitive to overoxidation than prokaryotic Prx, present a YF motif at the C terminus (Fig. 6) that packs over the active site in the FF form of the protein and delays the conformational change that brings together C_P and C_R, therefore slowing down the disulfide formation and favoring the overoxidation reaction (3, 8, 33, 35). In addition, different susceptibility toward overoxidation was found between different mammalian 2-Cys Prx isoforms. Human mitochondrial Prx3 is more resistant to this modification than cytosolic Prx2 (33). Recent work by Haynes *et al.* (35) demonstrated that residues near the C_R at the C terminus modulate the extent of C_P overoxidation. The substitution of residues at the C terminus of Prx3 resulted in a Prx2-like enzyme, more susceptible to overoxidation (35). Moreover, truncation of the C terminus containing the YF motif was reported to decrease overoxidation of Prx (45, 46). The YF sequence motif

in the C-terminal helix of one subunit covers helix $\alpha 2$ containing the C_P of the adjacent subunit, stabilizing the FF form, thus making difficult the unfolding of the C_P-containing $\alpha 2$ to reach C_R (2). Tyr-193, which was nitrated by peroxynitrite treatment (Table 1) belongs to this YF motif and is most likely responsible for the resistance to overoxidation of the nitrated enzyme (Fig. 6). It is interesting to note that in *in vitro* experiments where Jurkat cell lysates were treated with peroxynitrite, the YF motif tyrosine of Prx1 was identified as nitrated (47).

Prx are key enzymes for detoxifying H_2O_2 as well as sensing H_2O_2 in redox signaling. In this context, the modulation of Prx peroxidase activity and interaction with other proteins is critical. Modification of the reactive cysteine causes inactivation of the peroxidase activity as seen for overoxidation to sulfinic/sulfonic acid. Glutathionylation and *S*-nitrosation of C_P have also been reported (48–50). Interestingly, phosphorylation of noncatalytic residues in Prx1 and Prx2 could decrease, as well as increase, their peroxidase activity, suggesting a fine interplay between H_2O_2- and kinase-driven signaling pathways (51–54). Similar to our results, *N*-acetylation of Lys-196 in Prx2 causes an increase in peroxidase activity and a decrease in overoxidation susceptibility (55). Again, modification of residues at the C terminus, adjacent to C_R (Lys-196, Thr-194, and Tyr-193 in this work) can affect activity and the extent of overoxidation.

Nitration of tyrosine residues has an impact on protein structure and activity (in general, inactivation, although a gain of function has also been reported) and is linked to a variety of pathological conditions such as neurodegenerative and cardiovascular diseases (56, 57). Nitration of typical 2-Cys Prx has been reported *in vitro* and *in vivo* (20, 47, 58). In particular, Prx2 was identified in a proteomic analysis as one of the nitrated brain proteins in early Alzheimer disease (20). This could have an impact on intracellular H_2O_2-induced signaling cascades, including Prx2-protein interactions, which still remains to be explored. Our work characterizes the nitrated form of Prx2 as a more active and robust peroxidase by favoring the intermolecular disulfide formation, placing tyrosine nitration as another mechanism of modulating Prx in the complex network of redox signaling.

REFERENCES

1. Rhee, S. G., Chae, H. Z., and Kim, K. (2005) Peroxiredoxins: a historical overview and speculative preview of novel mechanisms and emerging concepts in cell signaling. *Free Radic. Biol. Med.* **38,** 1543–1552
2. Wood, Z. A., Poole, L. B., and Karplus, P. A. (2003) Peroxiredoxin evolution and the regulation of hydrogen peroxide signaling. *Science* **300,** 650–653
3. Wood, Z. A., Schröder, E., Robin Harris, J., and Poole, L. B. (2003) Structure, mechanism and regulation of peroxiredoxins. *Trends Biochem. Sci.* **28,** 32–40

4. Hofmann, B., Hecht, H. J., and Flohé, L. (2002) Peroxiredoxins. *Biol. Chem.* **383,** 347–364

5. Copley, S. D., Novak, W. R., and Babbitt, P. C. (2004) Divergence of function in the thioredoxin fold suprafamily: evidence for evolution of peroxiredoxins from a thioredoxin-like ancestor. *Biochemistry* **43,** 13981–13995

6. Schröder, E., Littlechild, J. A., Lebedev, A. A., Errington, N., Vagin, A. A., and Isupov, M. N. (2000) Crystal structure of decameric 2-Cys peroxiredoxin from human erythrocytes at 1.7 Å resolution. *Structure* **8,** 605–615

7. Wood, Z. A., Poole, L. B., Hantgan, R. R., and Karplus, P. A. (2002) Dimers to doughnuts: redox-sensitive oligomerization of 2-cysteine peroxiredoxins. *Biochemistry* **41,** 5493–5504

8. Perkins, A., Nelson, K. J., Williams, J. R., Parsonage, D., Poole, L. B., and Karplus, P. A. (2013) The sensitive balance between fully folded and locally unfolded conformations of a model peroxiredoxin. *Biochemistry* **52,** 8708–8721

9. Biteau, B., Labarre, J., and Toledano, M. B. (2003) ATP-dependent reduction of cysteine-sulphinic acid by *S. cerevisiae* sulphiredoxin. *Nature* **425,** 980–984

10. Jönsson, T. J., Murray, M. S., Johnson, L. C., and Lowther, W. T. (2008) Reduction of cysteine sulfinic acid in peroxiredoxin by sulfiredoxin proceeds directly through a sulfinic phosphoryl ester intermediate. *J. Biol. Chem.* **283,** 23846–23851

11. Winterbourn, C. C., and Hampton, M. B. (2008) Thiol chemistry and specificity in redox signaling. *Free Radic. Biol. Med.* **45,** 549–561

12. Flohé, L., and Ursini, F. (2008) Peroxidase: a term of many meanings. *Antioxid. Redox Signal.* **10,** 1485–1490

13. Ferrer-Sueta, G., Manta, B., Botti, H., Radi, R., Trujillo, M., and Denicola, A. (2011) Factors affecting protein thiol reactivity and specificity in peroxide reduction. *Chem. Res. Toxicol.* **24,** 434–450

14. Randall, L. M., Ferrer-Sueta, G., and Denicola, A. (2013) Peroxiredoxins as preferential targets in H$_2$O$_2$-induced signaling. *Methods Enzymol.* **527,** 41–63

15. Sobotta, M. C., Barata, A. G., Schmidt, U., Mueller, S., Millonig, G., and Dick, T. P. (2013) Exposing cells to H$_2$O$_2$: a quantitative comparison between continuous low-dose and one-time high-dose treatments. *Free Radic. Biol. Med.* **60,** 325–335

16. Lowther, W. T, and Haynes, A. C. (2011) Reduction of cysteine sulfinic acid in eukaryotic, typical 2-Cys peroxiredoxins by sulfiredoxin. *Antioxid. Redox Signal.* **15,** 99–109

17. Moore, R. B., Mankad, M. V., Shriver, S. K., Mankad, V. N., and Plishker, G. A. (1991) Reconstitution of Ca^{2+}-dependent K$^+$ transport in erythrocyte membrane vesicles requires a cytoplasmic protein. *J. Biol. Chem.* **266,** 18964–18968

18. Cho, C. S., Kato, G. J., Yang, S. H., Bae, S. W., Lee, J. S., Gladwin, M. T., and Rhee, S. G. (2010) Hydroxyurea-induced expression of glutathione peroxidase 1 in red blood cells of individuals with sickle cell anemia. *Antioxid. Redox Signal.* **13,** 1–11

19. Manta, B., Hugo, M., Ortiz, C., Ferrer-Sueta, G., Trujillo, M., and Denicola, A. (2009) The peroxidase and peroxynitrite reductase activity of human erythrocyte peroxiredoxin 2. *Arch. Biochem. Biophys.* **484,** 146–154

20. Reed, T. T., Pierce, W. M., Jr., Turner, D. M., Markesbery, W. R., and Butterfield, D. A. (2009) Proteomic identification of nitrated brain proteins in early Alzheimer's disease inferior parietal lobule. *J. Cell. Mol. Med.* **13,** 2019–2029

21. Denicola, A., Alvarez, B., and Thomson, L. (2008) *Free Radical Pathophysiology* (Alvarez, S. and Evelson, P., eds) pp. 39–55, Transworld Research Network, India

22. Radi, R. (2004) Nitric oxide, oxidants, and protein tyrosine nitration. *Proc. Natl. Acad. Sci. U.S.A.* **101,** 4003–4008

23. Trujillo, M., Ferrer-Sueta, G., and Radi, R. (2008) Peroxynitrite detoxification and its biologic implications. *Antioxid. Redox Signal.* **10,** 1607–1620

24. Trujillo, M., Alvarez, B., Souza, J. M., Romero, N., Castro, L., Thomson, L., and Radi, R. (2010) *Nitric Oxide Biology and Pathobiology* (Ignarro, L. J., ed) pp. 61–102, Academic Press, Orlando, FL

25. Beckman, J. S., Beckman, T. W., Chen, J., Marshall, P. A., and Freeman, B. A. (1990) Apparent hydroxyl radical production by peroxynitrite: implications for endothelial injury from nitric oxide and superoxide. *Proc.*

26. Romero, N., Radi, R., Linares, E., Augusto, O., Detweiler, C. D., Mason, R. P., and Denicola, A. (2003) Reaction of human hemoglobin with peroxynitrite: isomerization to nitrate and secondary formation of protein radicals. *J. Biol. Chem.* **278,** 44049–44057

27. Poole, L. B., Godzik, A., Nayeem, A., and Schmitt, J. D. (2000) AhpF can be dissected into two functional units: tandem repeats of two thioredoxin-like folds in the N-terminus mediate electron transfer from the thioredoxin reductase-like C-terminus to AhpC. *Biochemistry* **39,** 6602–6615

28. Bonilla, M., Denicola, A., Marino, S. M., Gladyshev, V. N., and Salinas, G. (2011) Linked thioredoxin-glutathione systems in platyhelminth parasites: alternative pathways for glutathione reduction and deglutathionylation. *J. Biol. Chem.* **286,** 4959–4967

29. Pace, C. N., Vajdos, F., Fee, L., Grimsley, G., and Gray, T. (1995) How to measure and predict the molar absorption coefficient of a protein. *Protein Sci.* **4,** 2411–2423

30. Egwim, I. O., and Gruber, H. J. (2001) Spectrophotometric measurement of mercaptans with 4,4′-dithiodipyridine. *Anal. Biochem.* **288,** 188–194

31. Brito, C., Naviliat, M., Tiscornia, A. C., Vuillier, F., Gualco, G., Dighiero, G., Radi, R., and Cayota, A. M. (1999) Peroxynitrite inhibits T lymphocyte activation and proliferation by promoting impairment of tyrosine phosphorylation and peroxynitrite-driven apoptotic death. *J. Immunol.* **162,** 3356–3366

32. Jörnvall, H., and Jollès, P. (2000) Protein structure analysis of today: proteomics in functional genomics. *EXS* **88,** XI–XIII

33. Peskin, A. V., Dickerhof, N., Poynton, R. A., Paton, L. N., Pace, P. E., Hampton, M. B., and Winterbourn, C. C. (2013) Hyperoxidation of peroxiredoxins 2 and 3: rate constants for the reactions of the sulfenic acid of the peroxidatic cysteine. *J. Biol. Chem.* **288,** 14170–14177

34. Nelson, K. J., Parsonage, D., Karplus, P. A., and Poole, L. B. (2013) Evaluating peroxiredoxin sensitivity toward inactivation by peroxide substrates. *Methods Enzymol.* **527,** 21–40

35. Haynes, A. C., Qian, J., Reisz, J. A., Furdui, C. M., and Lowther, W. T. (2013) Molecular basis for the resistance of human mitochondrial 2-Cys peroxiredoxin 3 to hyperoxidation. *J. Biol. Chem.* **288,** 29714–29723

36. Yuan, Y., Knaggs, M., Poole, L., Fetrow, J., and Salsbury, F., Jr. (2010) Conformational and oligomeric effects on the cysteine pK_a of tryparedoxin peroxidase. *J. Biomol. Struct. Dyn.* **28,** 51–70

37. Salsbury, F. R., Jr., Yuan, Y., Knaggs, M. H., Poole, L. B., and Fetrow, J. S. (2012) Structural and electrostatic asymmetry at the active site in typical and atypical peroxiredoxin dimers. *J. Phys. Chem. B* **116,** 6832–6843

38. Budde, H., Flohé, L., Hecht, H. J., Hofmann, B., Stehr, M., Wissing, J., and Lünsdorf, H. (2003) Kinetics and redox-sensitive oligomerisation reveal negative subunit cooperativity in tryparedoxin peroxidase of *Trypanosoma brucei brucei. Biol. Chem.* **384,** 619–633

39. Peskin, A. V., Low, F. M., Paton, L. N., Maghzal, G. J., Hampton, M. B., and Winterbourn, C. C. (2007) The high reactivity of peroxiredoxin 2 with H$_2$O$_2$ is not reflected in its reaction with other oxidants and thiol reagents. *J. Biol. Chem.* **282,** 11885–11892

40. Fomenko, D. E., Koc, A., Agisheva, N., Jacobsen, M., Kaya, A., Malinouski, M., Rutherford, J. C., Siu, K. L., Jin, D. Y., Winge, D. R., and Gladyshev, V. N. (2011) Thiol peroxidases mediate specific genome-wide regulation of gene expression in response to hydrogen peroxide. *Proc. Natl. Acad. Sci. U.S.A.* **108,** 2729–2734

41. Oláhová, M, Taylor, S. R., Khazaipoul, S., Wang, J., Morgan, B. A., Matsumoto, K., Blackwell, T. K., and Veal, E. A. (2008) A redox-sensitive peroxiredoxin that is important for longevity has tissue- and stress-specific roles in stress resistance. *Proc. Natl. Acad. Sci. U.S.A.* **105,** 19839–19844

42. Day, A. M., Brown, J. D., Taylor, S. R., Rand, J. D., Morgan, B. A., and Veal, E. A. (2012) Inactivation of a peroxiredoxin by hydrogen peroxide is critical for thioredoxin-mediated repair of oxidized proteins and cell survival. *Mol. Cell* **45,** 398–408

43. Veal, E. A., Day, A. M., and Morgan, B. A. (2007) Hydrogen peroxide sensing and signaling. *Mol. Cell* **26,** 1–14

44. Rhee, S. G. (2006) Cell signaling: H$_2$O$_2$, a necessary evil for cell signaling. *Science* **312,** 1882–1883

45. Koo, K. H., Lee, S., Jeong, S. Y., Kim, E. T., Kim, H. J., Kim, K., Song, K., and Chae, H. Z. (2002) Regulation of thioredoxin peroxidase activity by C-ter-

minal truncation. *Arch. Biochem. Biophys.* **397,** 312–318

46. Sayed, A. A., and Williams, D. L. (2004) Biochemical characterization of 2-Cys peroxiredoxins from *Schistosoma mansoni. J. Biol. Chem.* **279,** 26159–26166

47. Ghesquière, B., Colaert, N., Helsens, K., Dejager, L., Vanhaute, C., Verleysen, K., Kas, K., Timmerman, E., Goethals, M., Libert, C., Vandekerckhove, J., and Gevaert, K. (2009) *In vitro* and *in vivo* protein-bound tyrosine nitration characterized by diagonal chromatography. *Mol. Cell. Proteomics* **8,** 2642–2652

48. Park, J. W., Piszczek, G., Rhee, S. G., and Chock, P. B. (2011) Glutathionylation of peroxiredoxin I induces decamer to dimers dissociation with concomitant loss of chaperone activity. *Biochemistry* **50,** 3204–3210

49. Fang, J., Nakamura, T., Cho, D. H., Gu, Z., and Lipton, S. A. (2007) *S*-Nitrosylation of peroxiredoxin 2 promotes oxidative stress-induced neuronal cell death in Parkinson's disease. *Proc. Natl. Acad. Sci. U.S.A.* **104,** 18742–18747

50. Engelman, R., Weisman-Shomer, P., Ziv, T., Xu, J., Arnér, E. S., and Benhar, M. (2013) Multilevel regulation of 2-Cys peroxiredoxin reaction cycle by *S*-nitrosylation. *J. Biol. Chem.* **288,** 11312–11324

51. Jang, H. H., Kim, S. Y., Park, S. K., Jeon, H. S., Lee, Y. M., Jung, J. H., Lee, S. Y., Chae, H. B., Jung, Y. J., Lee, K. O., Lim, C. O., Chung, W. S., Bahk, J. D., Yun, D. J., Cho, M. J., and Lee, S. Y. (2006) Phosphorylation and concomitant structural changes in human 2-Cys peroxiredoxin isotype I differentially regulate its peroxidase and molecular chaperone functions. *FEBS Lett.* **580,** 351–355

52. Woo, H. A., Yim, S. H., Shin, D. H., Kang, D., Yu, D. Y., and Rhee, S. G. (2010) Inactivation of peroxiredoxin I by phosphorylation allows localized H_2O_2 accumulation for cell signaling. *Cell* **140,** 517–528

53. Zykova, T. A., Zhu, F., Vakorina, T. I., Zhang, J., Higgins, L. A., Urusova, D. V., Bode, A. M., and Dong, Z. (2010) T-LAK cell-originated protein kinase (TOPK) phosphorylation of Prx1 at Ser-32 prevents UVB-induced apoptosis in RPMI7951 melanoma cells through the regulation of Prx1 peroxidase activity. *J. Biol. Chem.* **285,** 29138–29146

54. Chang, T. S., Jeong, W., Choi, S. Y., Yu, S., Kang, S. W., and Rhee, S. G. (2002) Regulation of peroxiredoxin I activity by Cdc2-mediated phosphorylation. *J. Biol. Chem.* **277,** 25370–25376

55. Parmigiani, R. B., Xu, W. S., Venta-Perez, G., Erdjument-Bromage, H., Yaneva, M., Tempst, P., and Marks, P. A. (2008) HDAC6 is a specific deacetylase of peroxiredoxins and is involved in redox regulation. *Proc. Natl. Acad. Sci. U.S.A.* **105,** 9633–9638

56. Perry, G., Raina, A. K., Nunomura, A., Wataya, T., Sayre, L. M., and Smith, M. A. (2000) How important is oxidative damage? Lessons from Alzheimer's disease. *Free Radic. Biol. Med.* **28,** 831–834

57. Leite, P. F., Liberman, M., Sandoli de Brito, F., and Laurindo, F. R. (2004) Redox processes underlying the vascular repair reaction. *World J. Surg.* **28,** 331–336

58. Turko, I. V., Li, L., Aulak, K. S., Stuehr, D. J., Chang, J. Y., and Murad, F. (2003) Protein tyrosine nitration in the mitochondria from diabetic mouse heart: implications to dysfunctional mitochondria in diabetes. *J. Biol. Chem.* **278,** 33972–33977

3.2. Efecto de la nitración en la estructura de Prx2

3.2.1. Resumen

Las peroxirredoxinas son peroxidasas dependientes de cisteínas que participan de la detoxificación de peróxido y en la señalización mediada por H_2O_2. La Prx2 humana es una Prx de 2-Cys típica que se organiza como pentámeros de homodímeros cabeza-cola. Durante la catálisis, la cisteína reactiva (C_P) cicla entre el estado reducido tiolato, el oxidada ácido sulfénico y disulfuro, lo que a su vez involucra cambios conformacionales y oligoméricos. Varias modificaciones postraduccionales han mostrado tener efectos en la actividad de Prx2, en particular la sobreoxidación de la C_P que conduce a inactivación de la enzima. Recientemente, reportamos que la nitración de Prx2, una modificación postraduccional en residuos no-catalíticos, sorprendentemente aumenta su actividad peroxidasa y su resistencia a sobreoxidarse. Para elucidar la relación entre esta modificación postraduccional y la actividad de la enzima, investigamos los cambios estructurales de Prx2 luego de nitrarla. Para entender el vínculo entre los cambios en el estado de oxidación de la proteína durante la catálisis y la nitración de tirosinas, se utilizaron técnicas de ultracentrifugación analítica, absorción UV, dicroísmo circular, y fluorescencia en estado estacionario y resuelta en el tiempo. Nuestros resultados muestran que la Prx2 nitrada reducida se asemeja estructuralmente a la Prx2 sin tratar oxidada a disulfuro, favoreciendo una conformación localmente desplegada que facilita la formación del enlace disulfuro en el sitio activo. Estos resultados proveen base estructural para el análisis cinético previamente reportado, el aumento en la actividad peroxidasa y la resistencia a sobreoxidación de la enzima tratada con peroxinitrito.

3.2.2. Principales resultados obtenidos

- El tratamiento de Prx2 con peroxinitrito afecta su estructura cuaternaria, debilitando la interacción entre homodímeros en el decámero.

- La nitración de tirosinas en Prx2 apaga la emisión de fluorescencia a 340 nm, a la vez que disminuye el tiempo de vida media.

- El tratamiento de Prx2 con peroxinitrito afecta la estructura terciaria de la proteína, dando lugar a una proteína nitrada reducida que, estructuralmente, se asemeja más a la proteína sin tratar, oxidada a disulfuro. En particular, el entorno de los triptofanos de la proteína nitrada reducida se asemeja a los de la proteína nativa oxidada a disulfuro, como se observa por análisis de los espectros UV y de dicroismo circular en el UV cercano.

- Globalmente, estos resultados sugieren que la nitración de Prx2 favorece una conformación localmente desplegada, facilitando la formación del enlace disulfuro intermolecular, aumentando así su actividad enzimática y protegiéndola de la sobreoxidación.

3.2.3. Artículo publicado en Archives of Biochemistry and Biophysics

Structural changes upon peroxynitrite-mediated nitration of peroxiredoxin 2; nitrated Prx2 resembles its disulfide-oxidized form

Lía Randall [a, b], Bruno Manta [c, a, 1], Kimberly J. Nelson [d], Javier Santos [e], Leslie B. Poole [d], Ana Denicola [a, b, *]

[a] Laboratorio de Fisicoquímica Biológica, Instituto de Química Biológica, Facultad de Ciencias, Universidad de la República, Montevideo, Uruguay
[b] Center for Free Radical and Biomedical Research, Facultad de Medicina, Universidad de la República, Montevideo, Uruguay
[c] Laboratory Redox Biology of Trypanosomes, Institut Pasteur de Montevideo, Uruguay
[d] Department of Biochemistry, Wake Forest School of Medicine, Winston-Salem, NC, USA
[e] IQUIFIB (UBA-CONICET) and Departamento de Química Biológica, Facultad de Farmacia y Bioquímica, Universidad de Buenos Aires, Ciudad Autónoma de Buenos Aires, Argentina

ARTICLE INFO

ABSTRACT

Peroxiredoxins are cys-based peroxidases that function in peroxide detoxification and H_2O_2-induced signaling. Human Prx2 is a typical 2-Cys Prx arranged as pentamers of head-to-tail homodimers. During the catalytic mechanism, the active-site cysteine (C_P) cycles between reduced, sulfenic and disulfide state involving conformational as well as oligomeric changes. Several post-translational modifications were shown to affect Prx activity, in particular C_P overoxidation which leads to inactivation. We have recently reported that nitration of Prx2, a post-translational modification on non-catalytic tyrosines, unexpectedly increases its peroxidase activity and resistance to overoxidation. To elucidate the cross-talk between this post-translational modification and the enzyme catalysis, we investigated the structural changes of Prx2 after nitration. Analytical ultracentrifugation, UV absorption, circular dichroism, steady-state and time-resolved fluorescence were used to connect catalytically relevant redox changes with tyrosine nitration. Our results show that the reduced nitrated Prx2 structurally resembles the disulfide-oxidized native form of the enzyme favoring a locally unfolded conformation that facilitates disulfide formation. These results provide structural basis for the kinetic analysis previously reported, the observed increase in activity and the resistance to overoxidation of the peroxynitrite-treated enzyme.

© 2015 Elsevier Inc. All rights reserved.

1. Introduction

Peroxiredoxins (Prx) are a group of peroxidases whose catalytic cycle depends on a conserved cysteine residue included in a PXXXTXXC motif [1]. Peroxiredoxins belong to the Thioredoxin (Trx) fold superfamily and the catalytic cysteine (known as C_P, from "peroxidatic cysteine") occupies the position of the second cysteine residue in the canonical CxxC redox motif of the Trx-fold [2]. In addition, for most Prx the catalytic mechanism relies on the presence of a second cysteine residue (known as C_R, from "resolving cysteine") located in the same polypeptide (atypical 2-Cys Prx) or in another polypeptide forming a head-to-tail homodimer unit (typical 2-Cys Prx). In typical 2-Cys Prx (Prx 1–4 in mammals), the C_R is located in a large C-terminal extension that extends to reach the active site (containing C_P) of the opposite subunit of the homodimer [3]. This extension is not conserved among other members of the Trx-fold superfamily [1,2]. Additionally, typical 2-Cys Prx form multimeric species both in solution and during crystallization conditions as well as in vivo [4]. Mammalian Prx1 and Prx2, the most abundant cytosolic isoforms, exist as a mixture of homodimers (maintained by a B-type interface) and decamers (pentamers of dimers through an A-type interface) [5,6]. This dimer–decamer equilibrium depends on the redox state of the active site cysteines [7–13], post-translational modifications such as cysteine glutathionylation and threonine phosphorylation [14–17], protein concentration [9], pH [18–20] and ionic strength [18,21,22]. Moreover, overoxidation of C_P has been associated with

the formation of high molecular weight complexes with chaperone-like activity [12,23].

The catalytic cycle of mammalian Prx1-4 begins with the reaction of C_P with H_2O_2 to form a sulfenic acid derivative (C_P—SOH) that reacts with the C_R on the adjacent subunit forming a disulfide that is subsequently reduced by thioredoxin. Disulfide formation requires a conformational change in C_P and C_R regions (about 14 Å apart) to allow the C_P-SOH of one subunit to approach the C_R from the other subunit. This rearrangement involves the transition from the so-called fully-folded (FF) form to a locally unfolded (LU) conformation. This conformational change imposes a pause in the mechanism that, in the presence of high concentrations of H_2O_2, can result in the reaction of the sulfenic acid intermediate with a second molecule of the oxidant to form sulfinic acid (C_P—SO_2H, overoxidation or hyperoxidation). The sensitivity of eukaryotic enzymes to hyperoxidation is linked to the presence of an additional helix ($\alpha7$) occurring as a C-terminal extension and containing the conserved YF motif. Such a structural configuration is thought to hinder the FF to LU transition, thereby favoring hyperoxidation [13]. The overoxidized form of typical 2-Cys Prx is specifically reduced by sulfiredoxin (Srx) in an ATP-dependent mechanism, suggesting a signaling role for this reversible post-translational modification [24]. In particular, overoxidation of Prx has been proposed as a way to allow a temporary inactivation of the major H_2O_2 consuming system (the floodgate hypothesis) [13] as well as a mechanism to allow Trx to interact with other intracellular targets [25].

In typical 2-Cys Prx, increasing evidence suggests that disulfide formation and overoxidation are competing reactions, with a slow disulfide formation favoring overoxidation [26–28]. As the rate of disulfide formation has been proposed to depend on the velocity of FF-LU conversion, post-translational modifications that affect this conformational change or the reaction between C_P-SOH and C_R-SH may affect sensitivity of the enzyme to oxidative inactivation [27,29,30], as proposed for human Prx2 [28].

Human Prx2 is the most abundant cytosolic Prx in several tissues and is highly sensitive to oxidative inactivation [26,31]. Besides hydroperoxides, Prx2 is capable of reducing peroxynitrite,[2] a potent oxidant formed *in vivo* by the diffusion-controlled reaction between superoxide and nitric oxide, that has been shown to overoxidize as well as nitrate Prx2 during catalysis [9]. Tyrosine nitration can affect protein properties including activity and protein—protein interactions under nitroxidative stress conditions [32–36]. Nitration of typical 2-Cys Prx has been reported *in vitro* and *in vivo* [37–39]. In particular, nitrated Prx2 was identified in a proteomic analysis of early Alzheimer's disease brains [39] suggesting a possible pathophysiological role of this modification. We recently reported that peroxynitrite-mediated nitration of human Prx2 surprisingly increases its peroxidase activity and protects it from overoxidation by H_2O_2 [28] while most of the reported post-translational modifications (PTM) on Prx result in loss of peroxidase activity [15,40–42].

In this work we focus on the analysis of the structural changes occurring upon Prx2 nitration by peroxynitrite to search for correlations with the observed increase in peroxidase activity and resistance to overoxidation. Our results provide structural support for previous findings and a suitable explanation for this inter-oxidant crosstalk that could be widely distributed among eukaryotes.

2. Materials and methods

2.1. Chemicals

Dithiothreitol (DTT), 5′,5′-dithio-bis(2-nitrobenzoic acid) (DTNB) and reduced nicotinamide adenine dinucleotide phosphate (NADPH) were purchased from AppliChem (Germany). 4′,4'-dithiodipyridine (DTDP) was purchased from ACROS Organics, Fisher Scientific (USA). Hydrogen peroxide (H_2O_2) and diethylene-triaminepentaacetic acid (dtpa) were purchased from Sigma (USA). Peroxynitrite was synthesized as in [43]. All other reagents were of analytical grade and used as received.

2.2. Purification of proteins

Human Prx2 was purified from human erythrocytes according to [9].

2.3. Peroxide and protein quantification

The concentration of H_2O_2 stock solutions was measured at 240 nm ($\varepsilon_{240} = 43.6$ M^{-1} cm^{-1}). Peroxynitrite concentration was determined at 302 nm ($\varepsilon_{302} = 1670$ M^{-1} cm^{-1}) as in [43]. Protein concentration was measured by absorption at 280 nm in the assay buffer, using the corresponding ε determined for the oxidized proteins according to [44]: $\varepsilon_{280}(Prx2) = 19,380$ M^{-1} cm^{-1}.

2.4. Thiol quantification

Thiol concentration of Prx2 was measured according to [45] with minor modifications. Briefly, the protein was reduced with DTT (>10-fold molar excess for 30 min) and the remaining reductant was removed by buffer exchange with a HiTrap column coupled to a FPLC with online UV detection equilibrated in 50 mM potassium phosphate buffer pH 7.4, with 0.1 mM dtpa and 150 mM NaCl. An excess of DTDP was added to the protein sample in the assay buffer and absorption was measured at 324 nm ($\varepsilon_{324} = 21,400$ M^{-1} cm^{-1}).

2.5. Prx2 thiol reduction and oxidation

For reduction of purified Prx2, the enzyme was incubated with 1 mM DTT for 30 min at RT immediately before the experiment, and the mixture was passed twice through a Bio-Spin column (BioRad) pre-equilibrated with the assay buffer. Thiol concentration was determined just after elution from the column. Controlled oxidation of reduced Prx2 to its disulfide form was achieved with the addition of 0.6 equivalents of H_2O_2 (enough oxidant to form the disulfide but not enough to overoxidize to sulfinic acid) [28].

2.6. Nitration of Prx2 by peroxynitrite

Peroxynitrite has been shown to react with Prx2 C_P, overoxidizing it to its sulfinic and even sulfonic form [9]. To prevent these modifications of C_P, treatment with peroxynitrite was performed on the disulfide-oxidized enzyme. The corresponding molar excess of peroxynitrite was added as a flux-like addition that simulate generation of peroxynitrite *in vivo* (it is worth to note that nitration yields depend on rate of radicals production from peroxynitrite [33,46]). As a control, peroxynitrite was previously decomposed in the assay buffer and then added to the protein (reverse-order addition, ROA). After treatment with peroxynitrite or its decomposition products, Prx2 thiols were reduced with DTT and oxidized to disulfide when needed, as described in Section 2.5. The only PTM generated with this treatment was nitration of tyrosine residues as

---

[2] The term peroxynitrite is used to refer to the sum of peroxynitrite anion (ONOO⁻) and peroxynitrous acid (ONOOH) unless specified.

previously confirmed by MS and western blot analysis of the protein [28]. Nitration of Prx2 by peroxynitrite rendered a more active peroxidase and less sensitive to overoxidation (Fig.1S in Supplementary Material). In the present study, the structural changes on Prx2 upon peroxynitrite treatment were analyzed comparing Prx2 before treatment (native) and after peroxynitrite treatment (nitrated), and in both cases in the reduced (thiol cysteines) as well as the oxidized-to-disulfide (cystine) forms.

2.7. Size-exclusion chromatography analysis

Prx2 (600 μg) was loaded on a Superdex 200 10/300 GL equilibrated with 50 mM phosphate buffer with 0.1 mM dtpa and 150 mM NaCl, coupled to an AKTA FPLC system at 0.5 mL/min with online multiwavelength detection. The column was calibrated with molecular weight standards (29–700 kDa, GE) under identical buffer and flow conditions. Chromatograms were analyzed to calculate the fraction of dimeric or decameric Prx2 as in [9].

2.8. Analytical ultracentrifugation of Prx2

To determine the effects of nitration on Prx2 oligomeric state, samples were analyzed by sedimentation velocity at 42,000 rpm on an Optima XL-A analytical ultracentrifuge (Beckman Instruments) outfitted with UV/vis optics. Control and treated with peroxynitrite Prx2 were prepared as described above in 50 mM phosphate buffer pH 7.4, with 0.1 mM dtpa and 150 mM NaCl. Samples (5 μM) were loaded into double-sectored cells and equilibrated to 20 °C. Sedimentation data were collected every 4 min at a rotor speed of 42,000 rpm and a radial step size of 0.003 cm. From these data, sedimentation and diffusion coefficient values for each treatment were calculated using the DCDT+ software (version 2.3.4, Philo JS Analytical Biochemistry 354 (2006) 238–246) from John S. Philo (www.jphilo.mailway.com). A partial specific volume of 0.7409 cm^3/g was calculated based on the amino acid composition of Prx2. The buffer density of 1.0217 g/cm^3 was determined using a DA-310M precision density meter (MettlerToledo) at 20 °C.

2.9. Prx2 steady-state fluorescence spectra analysis

10 μM Prx2 samples were analyzed in 20 mM sodium phosphate buffer with 50 mM NaCl, pH 7.4, using an Aminco Bowman Series 2 spectrofluorimeter equipped with a thermostated cell holder equilibrated at 25 °C. Excitation was at 295 nm, with a bandpass of 4 nm for both monochromators. Spectra (305–450 nm) were obtained at a 2.45 nm/s scan speed, with a step size of 1 nm.

2.10. Prx2 time-resolved fluorescence analysis

Frequency domain time-resolved spectroscopy was conducted on an ISS Chronos FD Fluorometer using Marconi 2022A frequency synthesizers and 280 nm LED as the excitation light source. Modulation frequencies were chosen such that the phase delay stayed within the range of 15° to 75°. p-terphenyl ($\tau = 1.05$ ns) was used as a reference.

2.11. Fourth-derivative UV-absorption spectroscopy

At least 10 scans were recorded at intervals of 0.1 nm in the range 240–340 nm at a 20 nm/min scan speed, 1 cm path length quartz cuvettes, using a Jasco V-550 UV–visible spectrophotometer equipped with a peltier device equilibrated at 25 °C. Prx2 samples were prepared as described at a concentration of 31 μM in 20 mM sodium phosphate buffer with 50 mM NaCl, pH 7.4. A scan of buffer was acquired in the same conditions, properly smoothed and

subtracted to the averaged spectrum of each protein sample. An ad-hoc Excel® spreadsheet was used to transform the raw numerical data to the corresponding fourth-derivative spectra.

2.12. Prx2 circular dichroism (CD) spectra analysis

Spectra were acquired at 20 °C using a Jasco 810 spectropolarimeter equipped with a Jasco CDF-4265/15 peltier-effect device for temperature control. Scan speed was set to 20 and 50 nm/min for near-UV and far-UV respectively, with a 1 s response time, 1 nm data pitch and 1 nm bandwidth. Near- UV measurements were carried out in 1 cm cells containing 31 μM Prx2 in 20 mM sodium phosphate buffer with 50 mM NaCl, pH 7.4. For far-UV measurements, 0.1 cm cells were used, and protein samples were diluted to 5 μM in the same buffer. A scan of buffer was properly smoothed and subtracted from the corresponding averaged sample spectra.

3. Results

3.1. Treatment with peroxynitrite alters Prx2 dynamic quaternary structure

Oligomeric structure of Prx2 was analyzed by size-exclusion chromatography (SEC) showing an increase in the dimeric form of disulfide-oxidized, peroxynitrite-treated Prx2 in comparison to the control enzyme (Fig. 1A). High molecular weight species (HMW) also appeared after treatment with peroxynitrite, as seen in a previous report by Manta et al. [9]. It is interesting to note that, contrary to what is seen for other typical 2-Cys Prx like Prx1 [47], the Prx2 purified from red blood cells is not present as a pure dimer when oxidized to disulfide (Fig. 1A). The reduced as well as the overoxidized (not shown) Prx2 run as decamers, although treatment with peroxynitrite also formed high molecular weight species (Fig. 1B).

Sedimentation velocity analytical ultracentrifugation (AUC) of the disulfide form of Prx2 confirmed that nitration affects its quaternary structure. As shown in Fig. 2, treatment with peroxynitrite increased the proportion of dimer when looking at the disulfide oxidized enzyme. These results suggest the nitrated enzyme is a less stable decamer, i.e. the interface between homodimers is weakened, displacing the dimer–decamer equilibrium towards the former. In the same way, dimers were observed for the reduced nitrated enzyme, in contrast to native reduced Prx2, present as pure decamers, as has been previously described [9,12].

3.2. Nitration affects the environment of tryptophan residues in the active site

Prx2 sequence contains two Trp residues: W86 located in helix α3 in close proximity (~5 Å) to the peroxidatic cysteine C52, and W176 in the same unstructured loop that contains the resolving cysteine C172 only 4.5 Å away from it. As shown in Fig. 3, oxidation of the protein to form C_P-C_R disulfide decreased Trp fluorescence, indicating quenching by disulfide, with a minor red shift in emission ($\lambda_{max} = 339$ nm). After treatment of the enzyme with peroxynitrite, the reduced enzyme displayed a strong quench in Trp emission, providing evidence that the modified Tyr is close to the emitting Trp. Based on the atomic distances in the 3D structure of Prx2 (pdb 1QMV), four of the seven Tyr residues (Y43, Y126, Y164 and Y193) are within 10 Å of C_P and solvent exposed. Additionally, Y126 and Y193 are close to W176 and were identified as nitrated in a previous report [28]. However, nitration of Prx2 did not show a shift in λ_{max} of global emission, suggesting there is no big change in the polarity of Trp environments. Differences in emission between
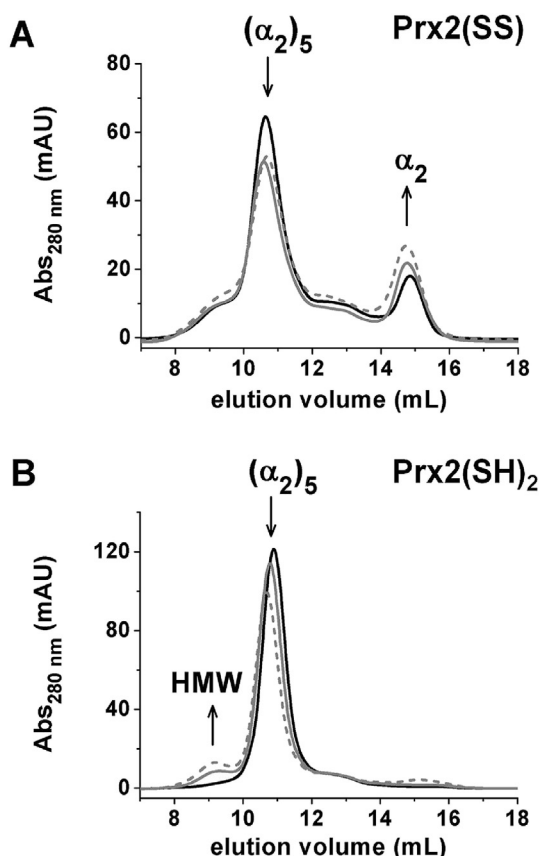
Fig. 1. Oligomerization state of Prx2 depends on peroxynitrite treatment. (A) Representative chromatograms of disulfide-oxidized Prx2 (black trace, solid), and Prx2 treated with a 5-fold (dark grey trace, solid) or a 10-fold excess peroxynitrite (dark grey trace, dashed) in their disulfide-oxidized form. (B) Representative chromatograms of reduced Prx2 (black trace, solid), Prx2 with 5-fold (dark grey trace, solid) or 10-fold excess peroxynitrite (dark grey trace, dashed), in their reduced form. For each run, 500 μg of Prx2 in 50 mM phosphate buffer pH 7.4 with 150 mM NaCl, 0.1 mM dtpa was loaded onto aSuperdex 200 10/300 GL column connected to a FPLC system, at a flow-rate of 0.5 mL/min, and the absorbance at 280 nm was monitored. Decamer $((\alpha_2)_5)$ eluted at ~10.8 mL while dimer (α_2) eluted at ~14.8 mL. HMW: high molecular weight species.

the reduced and the disulfide-oxidized forms were conserved for the nitrated enzyme. A closer look into the microenvironment of each Trp residue by time-resolved fluorescence revealed a long-lived emitting species ($\tau = 8.2 \pm 0.5$ ns) that contributes 50% to total emission and a shorter lifetime species of 4.9 ± 0.5 ns with 43% contribution (Table 1). Moreover, after oxidation of the enzyme to the disulfide form, a shift in lifetimes was observed suggesting an overall conformational change in the Trp surroundings that can be associated with the structural shift from the FF to the LU conformation. After nitration, the abundance-weighted lifetime shifted from 6.3 ns to 4.8 ns for the reduced enzyme (Table 1), with a slight decrease in the lifetime of the long-lived emitting species (from 8.2 ns to 7.1 ns) and a bigger change in the shorter lifetime species (from 4.9 ns to 3.3 ns).

Therefore, from the fluorescence spectroscopic analysis we conclude that Prx2 after peroxynitrite treatment undergoes a conformational change in the active site that affects the environment of both Trp residues. There is strong quenching due to the close presence of the nitro group, but a weak solvent relaxation denoting only subtle changes in the polarity of the Trp environments.

Potential changes in the microenvironments of Trp residues can also be assessed by near-UV absorption. Since the changes are

small, the fine structure of protein UV absorption can be visualized in second- or fourth-derivative spectra [48,49]. Fig. 4 shows the fourth-derivative spectra of Prx2 in the disulfide and reduced state, before and after treatment with peroxynitrite. Peaks in the region 265–285 nm correspond to Tyr–Trp transitions while above 285 nm there are exclusively Trp contributions. Bands around 290 nm can be safely assigned to ^1L_b transitions, that for Trp in solution are reported to peak at 288 nm, and significant red shifts (>2 nm) have been determined for Trp residues in a protein upon folding [50]. Thus, near-UV absorption evidenced a slightly higher exposure of Trp upon oxidation of Prx2 to disulfide with a 1 nm blue shift (from 289.4 nm to 288.4 nm). The fourth-derivative spectrum of the nitrated enzyme in the reduced state was more similar in wavelength to the disulfide form of the native Prx2 and did not change upon oxidation of the C_P (Fig. 4).

The near-UV CD spectrum of reduced Prx2 showed a significant contribution of aromatic residues, not only Trp but also Phe (250–265 nm), Tyr, and Tyr–Trp electronic interactions (265–285 nm) (Fig. 5). Upon oxidation of the C_P, the near-UV CD showed a striking change in overall conformation around aromatic residues (Fig. 5). Interestingly, near-UV CD spectra of nitrated (reduced or oxidized) Prx2 resemble the spectra of oxidized (disulfide) peroxiredoxin (Fig. 5, inset).

In addition, secondary structure analysis by far-UV CD showed a slight reduction in the alpha-helical content for the enzyme treated with peroxynitrite (Fig.2S in Supplementary Material).

4. Discussion

Peroxiredoxins are abundant, ubiquitous and efficient peroxidases, which places them not only as antioxidant enzymes but also as key players in the mechanism of H_2O_2-induced redox signaling [13,25,29,51–55]. In this context, the modulation of Prx peroxidase activity and interaction with other proteins is critical. Recently, we reported that nitration of Prx2 increases its peroxidase activity, and at the same time, reduces its susceptibility to inactivation by overoxidation [28]. The catalysis of H_2O_2 reduction depends on a conserved Cys residue within a highly conserved active site pocket that stabilizes the transition state [6,31,56]. An interesting feature of Prx2 is the conformational change at the active site that accompanies the catalytic cycle (FF − LU), as well as changes at the quaternary structure level that affects interactions with other proteins and potential roles as redox sensors in the cell [10].

Disulfide formation during catalysis requires the local unfolding of the C_P-loop to reach the resolving cysteine and form the disulfide to be reduced by thioredoxin [13]. Among these conformations, the FF form of the enzyme has been associated with the reduced enzyme in a decameric oligomeric state with high peroxidase activity, while the disulfide-oxidized LU form of the enzyme disassembles the decamer into dimers, potentially making it more accessible to reduction by thioredoxin [57]. Structural comparisons between reduced decamers and disulfide-oxidized dimers of different typical 2-Cys Prx led to the hypothesis that the C_P-loop functions as a molecular switch controlling decamerization [23]. Based on our results concerning quaternary structure analysis (Figs. 1 and 2), we propose nitration shifts the dimer–decamer equilibrium towards the dimer by promoting the local unfolding of the C_P-loop (LU conformation), thus facilitating disulfide bond formation with C_R (in line with the previously observed increase in peroxidase activity). Perturbation of this dynamic equilibrium could affect intracellular Prx2-protein interactions as well, since these oligomeric changes have been associated with regulation of Prx's interaction with other proteins. In particular, oligomeric Prx1 (and not the dimer) was shown to interact with the MST1 kinase and to be necessary for activation of this signaling pathway [58].
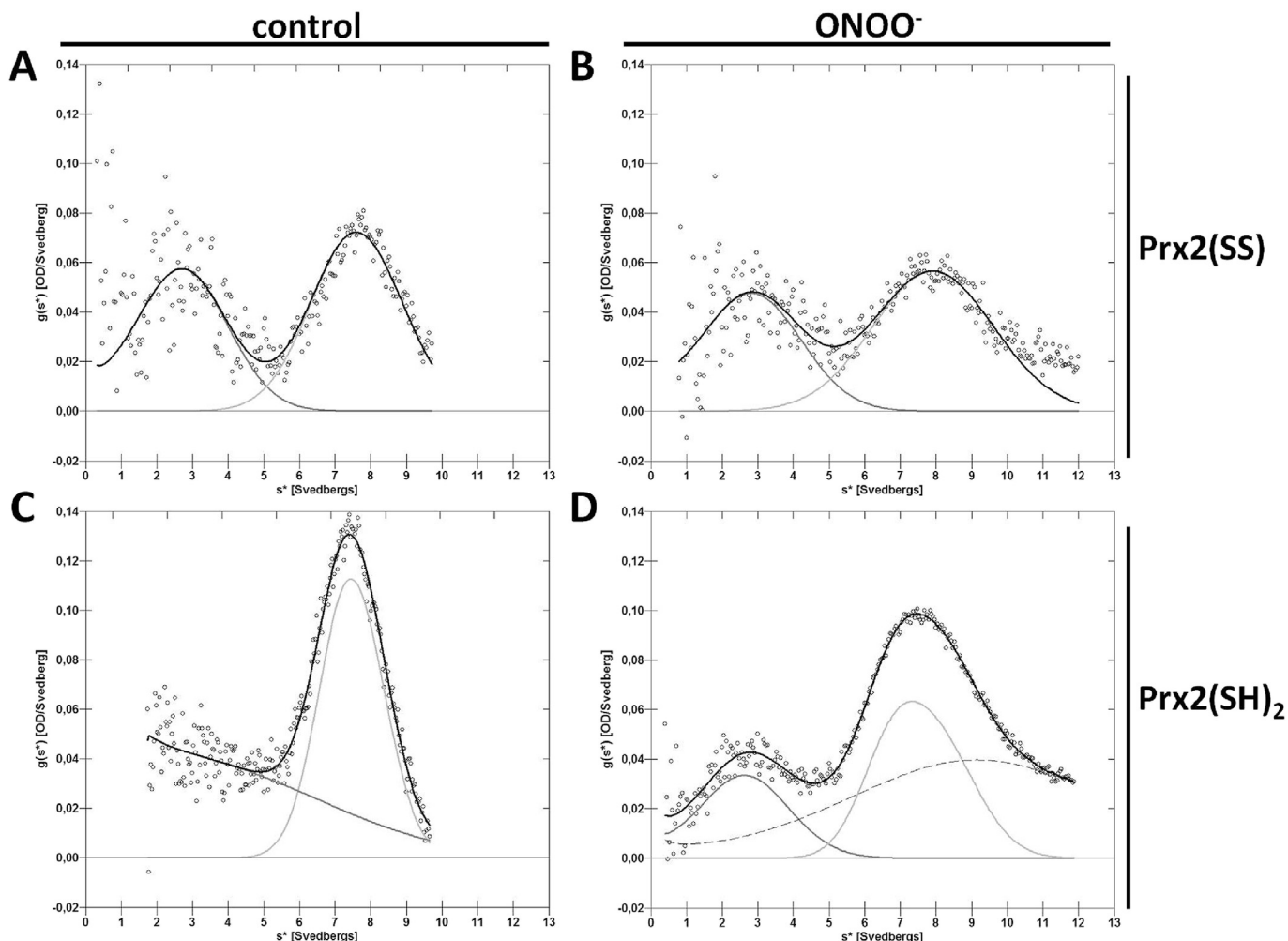
Fig. 2. Sedimentation velocity analysis of Prx2 treated with peroxynitrite. Analytical ultracentrifugation studies of 5 μM of disulfide oxidized (A and B) or reduced (C and D) Prx2 were carried out with centrifugation at 42,000 rpm (An-60 Ti rotor, Beckman), at 20 °C in 50 mM phosphate buffer with 0.1 mM dtpa and 150 mM NaCl, pH 7.4. A and C show representative runs for control Prx2, while B and D show representative traces for the enzyme previously treated with a 5-fold excess of peroxynitrite (ONOO⁻). Protein was detected at 230 nm. The data (circles) and curve fits (lines) are shown based on fits to either a two (A, B, and C) or a three species (D) model. The fits for the individual species are shown in dark gray (s*~2—3 S, dimer) and light gray (s*~7—8 S, decamer), and the combined fit is shown in black. In D, the dashed line represents the third species fit. Data were analyzed using the DCDT + software, as indicated in the experimental procedures section.
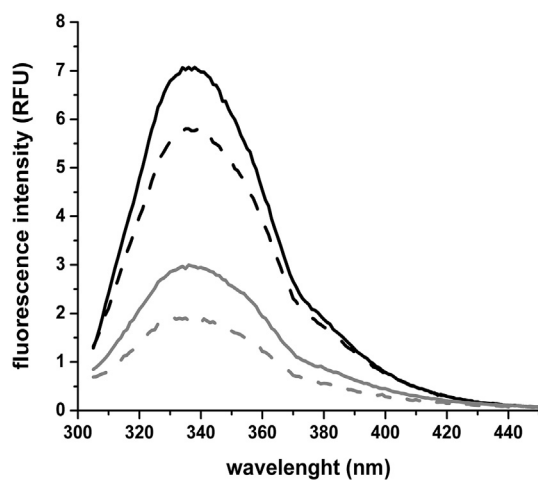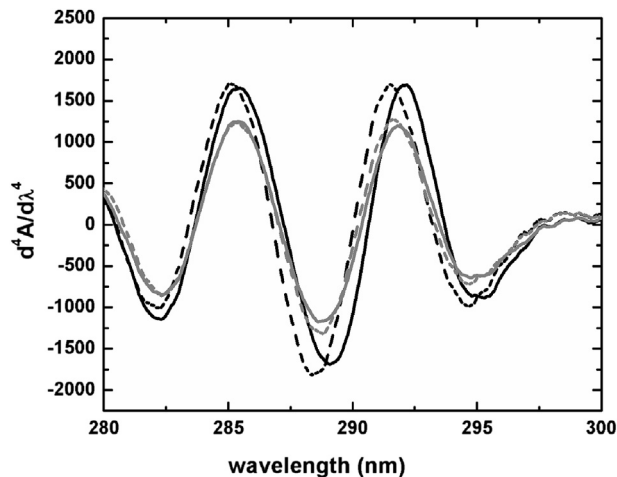

Fig. 3. Prx2 technical fluorescence emission spectra. 10 μM of reduced (black solid trace) or disulfide-oxidized control (black dashed trace), as well as Prx2 treated with peroxynitrite reduced (grey solid trace) or disulfide-oxidized (grey dashed trace) were analyzed by fluorescence spectroscopy. (λexc = 295 nm).

Table 1
Time-resolved fluorescence for Prx2. Lifetimes for native and peroxynitrite-treated Prx2 in their reduced (SH) and disulfide-oxidized (SS) forms are presented, as well as the relative abundance for each species. Experimental data were fitted to a discrete three-species model, and the global weighted lifetime ($<\tau>$) was calculated considering relative abundance of each species.

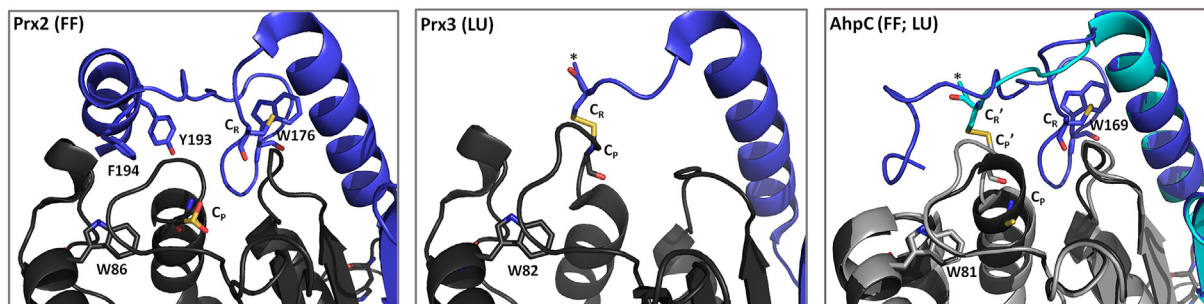|	τ_1 (ns)	%	τ_2 (ns)	%	τ_3 (ns)	%	$<\tau>$ (ns)
Prx2 (SH)	8.2 ± 0.5	50	4.9 ± 0.5	43	1.0 ± 0.1	7	6.3
Prx2 (SS)	7.6 ± 0.5	56	3.9 ± 0.5	33	1.1 ± 0.1	11	5.7
Prx2-NO₂ (SH)	7.1 ± 0.4	46	3.3 ± 0.4	42	0.8 ± 0.1	12	4.8
Prx2-NO₂ (SS)	7.0 ± 0.3	44	3.1 ± 0.3	44	0.7 ± 0.2	12	4.5

To further investigate potential changes in the active site conformation upon nitration, we performed near-UV spectroscopic analyses that are affected by the contribution of aromatic residues. Prx2 has two Trp residues (W86, W176), both located close to the active site (Fig. 6), that sense local changes after nitration as evidenced by UV absorption, CD and emission spectra (Figs. 4,5 and 3, respectively). Fig. 6 shows the crystal structure of Prx2 in the FF conformation and the LU conformation of Prx3 (the LU structure is not available for Prx2), as well as overlapped structures of AhpC, all

Fig. 4. Fourth-derivative near-UV absorption spectra analysis of Prx2. 31 μM of reduced (black solid trace) or disulfide-oxidized control (black dashed trace), as well as Prx2 treated with peroxynitrite in its reduced (grey solid trace) or disulfide-oxidized form (grey dashed trace) were analyzed by UV absorption spectroscopy and the fourth derivative of each spectrum was calculated.
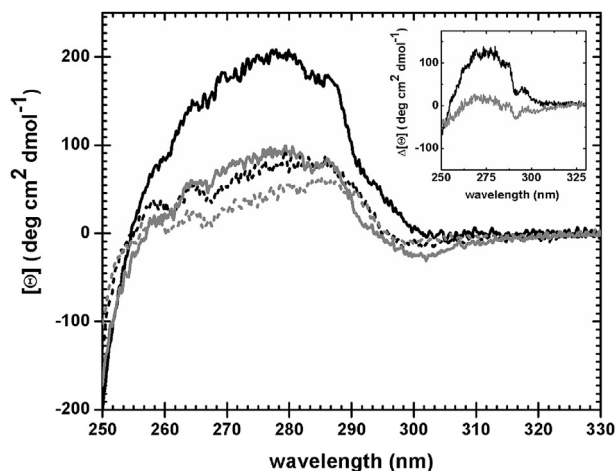
Fig. 5. Prx2 analysis by circular dichroism. 31 μM control Prx2 in its reduced (black solid trace) or disulfide-oxidized state (black dashed trace), and treated with peroxynitrite Prx2 in its reduced (grey solid trace) or disulfide-oxidized state (grey dashed trace), were analyzed by circular dichroism (CD) in the near UV. Inset. Differential spectra were calculated as reduced control Prx2 − disulfide Prx2 (black trace) and reduced nitrated Prx2 − disulfide Prx2 (grey trace).

of them typical 2-Cys Prx, although Prx2 and Prx3 are sensitive to overoxidation while AhpC is a robust Prx (lacking the YF motif). As shown in Fig. 6, W86 is closer to the C_P and doesn't seem to exhibit big changes in its environment after local unfolding of the C_P-loop and disulfide formation. On the other hand, W176 is part of the C-terminal extension that becomes disordered after disulfide formation, so, it is tempting to infer this is the Trp residue responsible for the spectroscopic changes observed. Importantly, all spectroscopic analyses showed that subtle conformational changes at the active site upon nitration converted the enzyme into a structure more similar to the disulfide form.

In summary, spectroscopic and hydrodynamic analyses of peroxynitrite-treated Prx2 showed that the nitrated enzyme resembles the disulfide oxidized form of Prx2. This post-translational modification on non-catalytical residues induces a conformational change that brings closer the active site cysteine residues C_P and C_R, favoring the local unfolding of the C_P-loop and facilitating the intermolecular disulfide formation, supporting the increase in peroxidase activity previously reported, as well as the higher resistance to overoxidation [28].

Acknowledgments

Appendix A. Supplementary data

Supplementary data related to this article can be found at http://dx.doi.org/10.1016/j.abb.2015.11.032.

References

[1] A. Perkins, K.J. Nelson, D. Parsonage, L.B. Poole, P.A. Karplus, Peroxiredoxins: guardians against oxidative stress and modulators of peroxide signaling, Trends Biochem. Sci. 40 (8, August 2015) 435–445.

Fig. 6. Active sites of human Prx2 (1QMV), bovine Prx3 (4MH3) and AhpC (FF, 1YEP and LU, 4MA9) in their fully-folded and locally unfolded conformations. For Prx2, C_P, C_R, and both tryptophan residues are labeled, as well as the YF motif. For disulfide-oxidized Prx3, the C-terminus of the protein moiety is disordered and could not be solved by crystallography (*). Both the fully-folded (dark grey and blue) and locally unfolded (light grey and cyan) conformations are presented for AhpC, with C_P and C_R shown for the FF conformation, and C_P' and C_R' for the LU conformation. (For interpretation of the references to colour in this figure legend, the reader is referred to the web version of this article.)

[2] S.D. Copley, W.R. Novak, P.C. Babbitt, Divergence of function in the thio-redoxin fold suprafamily: evidence for evolution of peroxiredoxins from a thioredoxin-like ancestor, Biochemistry 43 (2004) 13981–13995.

[3] D.E. Fomenko, V.N. Gladyshev, Identity and functions of CxxC-derived motifs, Biochemistry 42 (2003) 11214–11225.

[4] T. Seidel, B. Seefeldt, M. Sauer, K.J. Dietz, In vivo analysis of the 2-Cys per-oxiredoxin oligomeric state by two-step FRET, J. Biotechnol. 149 (2010) 272–279.

[5] G.N. Sarma, C. Nickel, S. Rahlfs, M. Fischer, K. Becker, P.A. Karplus, Crystal structure of a novel *Plasmodium falciparum* 1-Cys peroxiredoxin, J. Mol. Biol. 346 (2005) 1021–1034.

[6] A. Hall, K. Nelson, L.B. Poole, P.A. Karplus, Structure-based insights into the catalytic power and conformational dexterity of peroxiredoxins, Antioxid. Redox Signal 15 (2011) 795–815.

[7] S. Barranco-Medina, T. Krell, L. Bernier-Villamor, F. Sevilla, J.J. Lazaro, K.J. Dietz, Hexameric oligomerization of mitochondrial peroxiredoxin PrxIIF and for-mation of an ultrahigh affinity complex with its electron donor thioredoxin Trx-o, J. Exp. Bot. 59 (2008) 3259–3269.

[8] H.H. Jang, K.O. Lee, Y.H. Chi, B.G. Jung, S.K. Park, J.H. Park, J.R. Lee, S.S. Lee, J.C. Moon, J.W. Yun, Y.O. Choi, W.Y. Kim, J.S. Kang, G.W. Cheong, D.J. Yun, S.G. Rhee, M.J. Cho, S.Y. Lee, Two enzymes in one; two yeast peroxiredoxins display oxidative stress-dependent switching from a peroxidase to a molec-ular chaperone function, Cell 117 (2004) 625–635.

[9] B. Manta, M. Hugo, C. Ortiz, G. Ferrer-Sueta, M. Trujillo, A. Denicola, The peroxidase and peroxynitrite reductase activity of human erythrocyte per-oxiredoxin 2, Arch. Biochem. Biophys. 484 (2009) 146–154.

[10] J.C. Moon, Y.S. Hah, W.Y. Kim, B.G. Jung, H.H. Jang, J.R. Lee, S.Y. Kim, Y.M. Lee, M.G. Jeon, C.W. Kim, M.J. Cho, S.Y. Lee, Oxidative stress-dependent structural and functional switching of a human 2-Cys peroxiredoxin isotype II that en-hances HeLa cell resistance to H2O2-induced cell death, J. Biol. Chem. 280 (2005) 28775–28784.

[11] F. Saccoccia, P. Di Micco, G. Boumis, M. Brunori, I. Koutris, A.E. Miele, V. Morea, P. Sriratana, D.L. Williams, A. Bellelli, F. Angelucci, Moonlighting by different stressors: crystal structure of the chaperone species of a 2-Cys peroxiredoxin, Structure 20 (2012) 429–439.

[12] Z.A. Wood, L.B. Poole, R.R. Hantgan, P.A. Karplus, Dimers to doughnuts: redox-sensitive oligomerization of 2-cysteine peroxiredoxins, Biochemistry 41 (2002) 5493–5504.

[13] Z.A. Wood, L.B. Poole, P.A. Karplus, Peroxiredoxin evolution and the regulation of hydrogen peroxide signaling, Science 300 (2003) 650–653.

[14] H.H. Jang, S.Y. Kim, S.K. Park, H.S. Jeon, Y.M. Lee, J.H. Jung, S.Y. Lee, H.B. Chae, Y.J. Jung, K.O. Lee, C.O. Lim, W.S. Chung, J.D. Bahk, D.J. Yun, M.J. Cho, S.Y. Lee, Phosphorylation and concomitant structural changes in human 2-Cys per-oxiredoxin isotype I differentially regulate its peroxidase and molecular chaperone functions, FEBS Lett. 580 (2006) 351–355.

[15] J.W. Park, G. Piszczek, S.G. Rhee, P.B. Chock, Glutathionylation of peroxir-edoxin I induces decamer to dimers dissociation with concomitant loss of chaperone activity, Biochemistry 50 (2011) 3204–3210.

[16] D. Qu, J. Rashidian, M.P. Mount, H. Aleyasin, M. Parsanejad, A. Lira, E. Haque, Y. Zhang, S. Callaghan, M. Daigle, M.W. Rousseaux, R.S. Slack, P.R. Albert, I. Vincent, J.M. Woulfe, D.S. Park, Role of Cdk5-mediated phosphorylation of Prx2 in MPTP toxicity and Parkinson's disease, Neuron 55 (2007) 37–52.

[17] S. Salzano, P. Checconi, E.M. Hanschmann, C.H. Lillig, L.D. Bowler, P. Chan, D. Vaudry, M. Mengozzi, L. Coppo, S. Sacre, K.R. Atkuri, B. Sahaf, L.A. Herzenberg, L.A. Herzenberg, L. Mullen, P. Ghezzi, Linkage of inflamma-tion and oxidative stress via release of glutathionylated peroxiredoxin-2, which acts as a danger signal, Proc. Natl. Acad. Sci. U. S. A. 111 (2014) 12157–12162.

[18] L. Bernier-Villamor, E. Navarro, F. Sevilla, J.J. Lazaro, Cloning and character-ization of a 2-Cys peroxiredoxin from Pisum sativum, J. Exp. Bot. 55 (2004) 2191–2199.

[19] P. Kristensen, D.E. Rasmussen, B.I. Kristensen, Properties of thiol-specific anti-oxidant protein or calpromotin in solution, Biochem. Biophys. Res. Commun. 262 (1999) 127–131.

[20] M.A. Morais, P.O. Giuseppe, T.A. Souza, T.G. Alegria, M.A. Oliveira, L.E. Netto, M.T. Murakami, How pH modulates the dimer-decamer interconversion of 2-Cys peroxiredoxins from the Prx1 subfamily, J. Biol. Chem. 290 (2015) 8582–8590.

[21] K. Kitano, Y. Niimura, Y. Nishiyama, K. Miki, Stimulation of peroxidase activity by decamerization related to ionic strength: AhpC protein from Amphibacillus xylanus, J. Biochem. 126 (1999) 313–319.

[22] T. Matsumura, K. Okamoto, S.-I. Iwahara, H. Hori, Y. Takahashi, T. Nishino, Y. Abe, Dimer-oligomer interconversion of Wild-type and mutant rat 2-Cys peroxiredoxin, J. Biol. Chem. 283 (2008) 284–293.

[23] S. Barranco-Medina, J.J. Lazaro, K.J. Dietz, The oligomeric conformation of peroxiredoxins links redox state to function, FEBS Lett. 583 (2009) 1809–1816.

[24] B. Biteau, J. Labarre, M.B. Toledano, ATP-dependent reduction of cysteine-sulphinic acid by *S. cerevisiae* sulphiredoxin, Nature 425 (2003) 980–984.

[25] A.M. Day, J.D. Brown, S.R. Taylor, J.D. Rand, B.A. Morgan, E.A. Veal, Inactivation of a peroxiredoxin by hydrogen peroxide is critical for thioredoxin-mediated repair of oxidized proteins and cell survival, Mol. Cell 45 (2012) 398–408.

[26] A.V. Peskin, N. Dickerhof, R.A. Poynton, L.N. Paton, P.E. Pace, M.B. Hampton, C.C. Winterbourn, Hyperoxidation of peroxiredoxins 2 and 3: rate constants for the reactions of the sulfenic acid of the peroxidatic cysteine, J. Biol. Chem.

288 (2013) 14170–14177.

[27] A.C. Haynes, J. Qian, J.A. Reisz, C.M. Furdui, W.T. Lowther, Molecular basis for the resistance of human mitochondrial 2-Cys peroxiredoxin 3 to hyper-oxidation, J. Biol. Chem. 288 (2013) 29714–29723.

[28] L.M. Randall, B. Manta, M. Hugo, M. Gil, C. Batthyany, M. Trujillo, L.B. Poole, A. Denicola, Nitration transforms a sensitive peroxiredoxin 2 into a more active and robust peroxidase, J. Biol. Chem. 289 (2014) 15536–15543.

[29] L.M. Randall, G. Ferrer-Sueta, A. Denicola, Peroxiredoxins as preferential tar-gets in H2O2-induced signaling, Methods Enzymol. 527 (2013) 41–63.

[30] A. Hall, D. Parsonage, L.B. Poole, P.A. Karplus, Structural evidence that per-oxiredoxin catalytic power is based on transition-state stabilization, J. Mol. Biol. 402 (2010) 194–209.

[31] G. Ferrer-Sueta, B. Manta, H. Botti, R. Radi, M. Trujillo, A. Denicola, Factors affecting protein thiol reactivity and specificity in peroxide reduction, Chem. Res. Toxicol. 24 (2011) 434–450.

[32] B. Alvarez, A. Denicola, L. Thomson, 3-Nitrotyrosine, a post-translational modification associated with nitroxidative stress, in: S. Alvarez, P. Evelson (Eds.), Free Radical Patophysiology, 2008, p. 39.

[33] R. Radi, Nitric oxide, oxidants, and protein tyrosine nitration, Proc. Natl. Acad. Sci. U. S. A. 101 (2004) 4003–4008.

[34] M. Trujillo, G. Ferrer-Sueta, R. Radi, Peroxynitrite detoxification and its bio-logic implications, Antioxid. Redox Signal 10 (2008) 1607–1620.

[35] M. Trujillo, J.M. Souza, N. Romero, L. Castro, L. Thomson, R. Radi, Mechanisms and biological consequences of peroxynitrite-dependent protein oxidation and nitration, in: L.J. Ignarro (Ed.), Nitric Oxide Biology and Pathobiology, 2010, pp. 61–102.

[36] J.S. Beckman, T.W. Beckman, J. Chen, P.A. Marshall, B.A. Freeman, Apparent hydroxyl radical production by peroxynitrite: implications for endothelial injury from nitric oxide and superoxide, Proc. Natl. Acad. Sci. U. S. A. 87 (1990) 1620–1624.

[37] B. Ghesquiere, N. Colaert, K. Helsens, L. Dejager, C. Vanhaute, K. Verleysen, K. Kas, E. Timmerman, M. Goethals, C. Libert, J. Vandekerckhove, K. Gevaert, In vitro and in vivo protein-bound tyrosine nitration characterized by diagonal chromatography, Mol. Cell Proteomics 8 (2009) 2642–2652.

[38] I.V. Turko, L. Li, K.S. Aulak, D.J. Stuehr, J.Y. Chang, F. Murad, Protein tyrosine nitration in the mitochondria from diabetic mouse heart. Implications to dysfunctional mitochondria in diabetes, J. Biol. Chem. 278 (2003) 33972–33977.

[39] T.T. Reed, W.M. Pierce Jr., D.M. Turner, W.R. Markesbery, D.A. Butterfield, Proteomic identification of nitrated brain proteins in early Alzheimer's disease inferior parietal lobule, J. Cell Mol. Med. 13 (2009) 2019–2029.

[40] J. Fang, T. Nakamura, D.H. Cho, Z. Gu, S.A. Lipton, S-nitrosylation of peroxir-edoxin 2 promotes oxidative stress-induced neuronal cell death in Parkinson's disease, Proc. Natl. Acad. Sci. U. S. A. 104 (2007) 18742–18747.

[41] H.A. Woo, S.H. Yim, D.H. Shin, D. Kang, D.Y. Yu, S.G. Rhee, Inactivation of peroxiredoxin I by phosphorylation allows localized H(2)O(2) accumulation for cell signaling, Cell 140 (2010) 517–528.

[42] K.S. Yang, S.W. Kang, H.A. Woo, S.C. Hwang, H.Z. Chae, K. Kim, S.G. Rhee, Inactivation of human peroxiredoxin I during catalysis as the result of the oxidation of the catalytic site cysteine to cysteine-sulfinic acid, J. Biol. Chem. 277 (2002) 38029–38036.

[43] N. Romero, R. Radi, E. Linares, O. Augusto, C.D. Detweiler, R.P. Mason, A. Denicola, Reaction of human hemoglobin with peroxynitrite. Isomerization to nitrate and secondary formation of protein radicals, J. Biol. Chem. 278 (2003) 44049–44057.

[44] C.N. Pace, F. Vajdos, L. Fee, G. Grimsley, T. Gray, How to measure and predict the molar absorption coefficient of a protein, Protein Sci. 4 (1995) 2411–2423.

[45] I.O. Egwim, H.J. Gruber, Spectrophotometric measurement of mercaptans with 4,4'-dithiodipyridine, Anal. Biochem. 288 (2001) 188–194.

[46] C. Batthyany, J.M. Souza, R. Duran, A. Cassina, C. Cervenansky, R. Radi, Time course and site(s) of cytochrome c tyrosine nitration by peroxynitrite, Biochemistry 44 (2005) 8038–8046.

[47] W. Lee, K.S. Choi, J. Riddell, C. Ip, D. Ghosh, J.H. Park, Y.M. Park, Human per-oxiredoxin 1 and 2 are not duplicate proteins: the unique presence of CYS83 in Prx1 underscores the structural and functional differences between Prx1 and Prx2, J. Biol. Chem. 282 (2007) 22011–22022.

[48] E.M. Clerico, M.R. Ermacora, Tryptophan mutants of intestinal fatty acid-binding protein: ultraviolet absorption and circular dichroism studies, Arch. Biochem. Biophys. 395 (2001) 215–224.

[49] H. Mach, C.R. Middaugh, Simultaneous monitoring of the environment of tryptophan, tyrosine, and phenylalanine residues in proteins by near-ultraviolet second-derivative spectroscopy, Anal. Biochem. 222 (1994) 323–331.

[50] T.A. Bewley, C.H. Li, Conformational comparison of human pituitary growth hormone and human chorionic somatomammotropin (human placental lac-togen) by second-order absorption spectroscopy, Arch. Biochem. Biophys. 233 (1984) 219–227.

[51] S.G. Rhee, H.Z. Chae, K. Kim, Peroxiredoxins: a historical overview and spec-ulative preview of novel mechanisms and emerging concepts in cell signaling, Free Radic. Biol. Med. 38 (2005) 1543–1552.

[52] E.A. Veal, A.M. Day, B.A. Morgan, Hydrogen peroxide sensing and signaling, Mol. Cell 26 (2007) 1–14.

[53] C.C. Winterbourn, M.B. Hampton, Thiol chemistry and specificity in redox signaling, Free Radic. Biol. Med. 45 (2008) 549–561.

[54] L. Flohe, Changing paradigms in thiology from antioxidant defense toward

redox regulation, Methods Enzymol. 473 (2010) 1–39.

[55] D.E. Fomenko, A. Koc, N. Agisheva, M. Jacobsen, A. Kaya, M. Malinouski, J.C. Rutherford, K.L. Siu, D.Y. Jin, D.R. Winge, V.N. Gladyshev, Thiol peroxidases mediate specific genome-wide regulation of gene expression in response to hydrogen peroxide, Proc. Natl. Acad. Sci. U. S. A. 108 (2011) 2729–2734.

[56] S. Portillo-Ledesma, F. Sardi, B. Manta, M.V. Tourn, A. Clippe, B. Knoops, B. Alvarez, E.L. Coitino, G. Ferrer-Sueta, Deconstructing the catalytic efficiency of peroxiredoxin-5 peroxidatic cysteine, Biochemistry 53 (2014) 6113–6125.

[57] T.S. Chang, W. Jeong, S.Y. Choi, S. Yu, S.W. Kang, S.G. Rhee, Regulation of peroxiredoxin I activity by Cdc2-mediated phosphorylation, J. Biol. Chem. 277 (2002) 25370–25376.

[58] A. Morinaka, Y. Funato, K. Uesugi, H. Miki, Oligomeric peroxiredoxin-I is an essential intermediate for p53 to activate MST1 kinase and apoptosis, Oncogene 30 (2011) 4208–4218.

Supplementary Material

Structural changes upon peroxynitrite-mediated nitration of peroxiredoxin 2; nitrated Prx2 resembles its disulfide-oxidized form

Lía Randall[‡⊥], Bruno Manta[¶‡], Kimberly J. Nelson*, Javier Santos[§], Leslie B. Poole*, Ana Denicola[‡⊥1]

[‡] Laboratorio de Fisicoquímica Biológica, Instituto de Química Biológica, Facultad de Ciencias, Universidad de la República, Montevideo, Uruguay.
[⊥] Center for Free Radical and Biomedical Research, Facultad de Medicina, Universidad de la República, Montevideo, Uruguay.
[¶] Laboratory Redox Biology of Trypanosomes, Institut Pasteur de Montevideo, Uruguay.
* Department of Biochemistry, Wake Forest School of Medicine, Winston-Salem, North Carolina, USA.
[§] IQUIFIB (UBA-CONICET) and Departamento de Química Biológica, Facultad de Farmacia y Bioquímica, Universidad de Buenos Aires, Ciudad Autónoma de Buenos Aires, Argentina

The aim of the present work is the analysis of the structural changes occurring upon Prx2 nitration by peroxynitrite in order to search for correlations with the observed increase in peroxidase activity and resistance to overoxidation. We recently reported that peroxynitrite-mediated nitration of human Prx2 surprisingly increases its peroxidase activity and protects it from overoxidation by H_2O_2 [1] while most of the reported post-translational modifications (PTM) on Prx result in loss of peroxidase activity [2, 3-5]. Figure 1S is a representative run of peroxidase activity measured with a coupled assay described below, where Prx2 previously treated with peroxynitrite displayed a 30% increase in specific activity compared with native Prx2 (ROA as a control). The inset of Figures 1S shows that peroxynitrite-treated Prx2 was nitrated while the control Prx2 (ROA) was not. At the same time, at the end of the run, the nitrated Prx2 was less overoxidized than the untreated Prx2 (ROA).
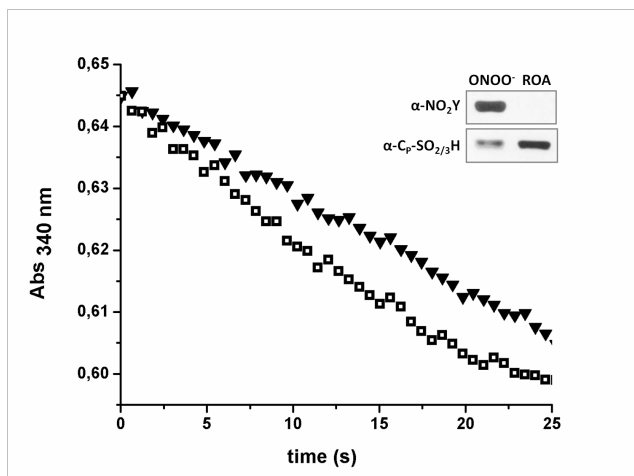
Figure 1S. Treatment of Prx2 with peroxynitrite renders a nitrated and more active form of the enzyme. Peroxidase activity was measured using a coupled assay (0.5 µM Prx2, 8 µM Trx, 1 µM TR, 120 µM NADPH in 50 mM phosphate buffer pH 7.4) starting the reaction with 10 µM H_2O_2 and following NADPH consumption at 340 nm, for non-treated Prx2 (black triangles) and peroxynitrite (5x)-treated Prx2 (open squares). *Inset.* Western blot of Prx2 treated with peroxynitrite (ONOO⁻) or the control treatment (reverse-order addition, ROA) at the end of the run, probed for nitrotyrosine residues (α-NO$_2$Y) and overoxidized C$_P$ (α-C$_P$-SO$_{2/3}$H).

The biophysical characterization of nitrated Prx2 included analytical ultracentrifugation, UV absorption, CD, steady-state and time-resolved fluorescence. A change in quaternary structure (dimer-decamer equilibrium displaced towards the former) as well as changes in tertiary structure around the active site were observed.

Secondary structure analysis by far-UV CD showed a slight reduction in the alpha-helical content for the enzyme treated with peroxynitrite; the elipticity at the 222 nm minimum increased and the value at the 195 nm maximum decreased (Figure 2S).
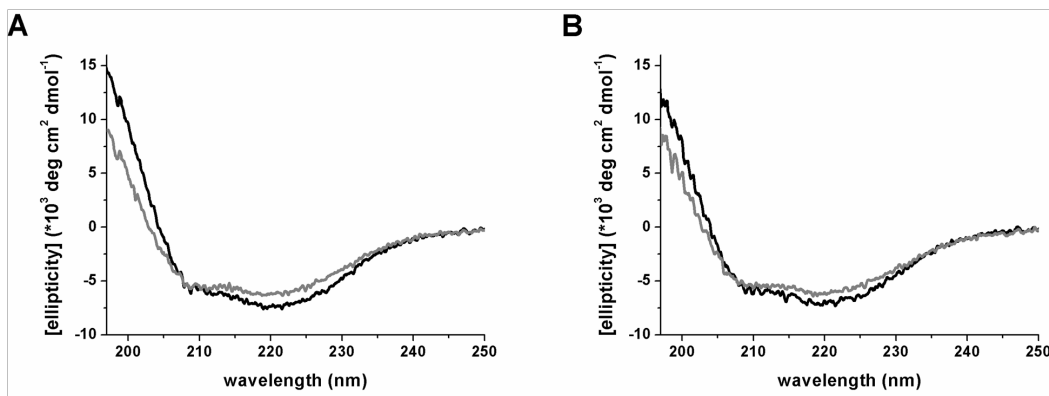
Figure 2S. Prx2 analysis by circular dichroism. 5 μM Prx2 in its (**A**) reduced or (**B**) disulfide-oxidized form was studied for the control enzyme (black trace), or after treatment with peroxynitrite (grey trace) by circular dichroism (CD) in the far UV.

Even though the observed differences are small, big differences were not expected since denaturation is not occurring and the peroxidase activity is not only preserved but actually increased after treatment. Thus, the active site overall structure was expected to be conserved.

Once again, more pronounced differences were observed between the reduced and disulfide-oxidized forms of the native enzyme while the structure of the nitrated Prx2 is closer to the disulfide form (Figure 2S).

In addition, the results on far-UV CD are in line with all the other spectroscopic studies.

Methods

Purification of proteins. Human Prx2 was purified from human erythrocytes according to [6]. Recombinant *E. coli* thioredoxin 1 (*Ec*Trx1) and recombinant *E. coli* thioredoxin reductase (*Ec*TR) were produced and purified as reported in [6] and [7], respectively.

Peroxide and protein quantification. The concentration of H_2O_2 stock solutions was measured at 240 nm ($\varepsilon_{240} = 43.6$ M^{-1} cm^{-1}). Peroxynitrite concentration was determined

at 302 nm (ε_{302} = 1,670 M^{-1} cm^{-1}) as in [8]. Protein concentration was measured by absorption at 280 nm in the assay buffer, using the corresponding ε determined for the oxidized proteins according to [9]: ε_{280}(Prx2) = 19,380 M^{-1} cm^{-1}, ε_{280}(EcTrx) = 14,060 M^{-1} cm^{-1} and ε_{280}(EcTR) = 19,160 M^{-1} cm^{-1}.

Nitration of Prx2 by peroxynitrite. Peroxynitrite has been shown to react with Prx2 C_P, overoxidizing it to its sulfinic and even sulfonic form [6]. To prevent these modifications of C_P, treatment with peroxynitrite was performed on the disulfide-oxidized enzyme. The corresponding molar excess of peroxynitrite was added as a flux-like addition that simulate generation of peroxynitrite in vivo (it is worth to note that nitration yields depend on rate of radicals production from peroxynitrite [10,11]). As a control, peroxynitrite was previously decomposed in the assay buffer and then added to the protein (reverse-order addition, ROA). The only PTM generated with this treatment was nitration of tyrosine residues as previously confirmed by MS and western blot analysis of the protein [1]. After treatment with peroxynitrite or its decomposition products (ROA), Prx2 cysteine residues were reduced with DTT (to gain a potentially active enzyme) and peroxidase activity was measured with the coupled assay described below.

NADPH-linked peroxidase activity (coupled assay). NADPH consumption was followed spectrophotometrically at 340 nm in a Cary 50 spectrophotometer (Varian, Australia). Prx2 (0.5 µM) was mixed with 120 µM NADPH, 1 µM EcTR, 8 µM EcTrx in 50 mM phosphate buffer pH 7.4 containing 150 mM NaCl, 0.1 mM dtpa, and the reaction was started with the addition of 10 µM H_2O_2.

Overoxidation of Prx2 by H_2O_2. To study the overoxidation of Prx2, disulfide-oxidized Prx2 was treated with peroxynitrite for nitration, Prx2 was reduced as described, and after removal of DTT the enzyme was treated with a 5-fold excess of

H_2O_2. Samples were resolved in 15 % SDS-PAGE under non-reducing conditions, transferred to a PVDF membrane and blotted with specific α-Prx2-C_P-$SO_{2/3}H$ antibody (AbFrontier, Korea).

Prx2 far-UV circular dichroism (CD) spectra analysis. Spectra were acquired at 20 °C using a Jasco 810 spectropolarimeter equipped with a Jasco CDF-4265/15 peltier-effect device for temperature control. Scan speed was set to 50 nm/min for far-UV, with a 1 s response time, 1 nm data pitch and 1 nm bandwidth. Far- UV measurements were carried out in 0.1 cm cells containing 5 μM Prx2 in 20 mM sodium phosphate buffer with 50 mM NaCl, pH 7.4. A scan of buffer was properly smoothed and subtracted from the corresponding averaged sample spectra.

References

[1] L.M. Randall, B. Manta, M. Hugo, M. Gil, C. Batthyany, M. Trujillo, L.B. Poole, A. Denicola, Nitration transforms a sensitive peroxiredoxin 2 into a more active and robust peroxidase, J Biol Chem 289 (2014) 15536-15543.

[2] J.W. Park, G. Piszczek, S.G. Rhee, P.B. Chock, Glutathionylation of peroxiredoxin I induces decamer to dimers dissociation with concomitant loss of chaperone activity, Biochemistry 50 (2011) 3204-3210.

[3] J. Fang, T. Nakamura, D.H. Cho, Z. Gu, S.A. Lipton, S-nitrosylation of peroxiredoxin 2 promotes oxidative stress-induced neuronal cell death in Parkinson's disease, Proc Natl Acad Sci U S A 104 (2007) 18742-18747.

[4] H.A. Woo, S.H. Yim, D.H. Shin, D. Kang, D.Y. Yu, S.G. Rhee, Inactivation of peroxiredoxin I by phosphorylation allows localized H(2)O(2) accumulation for cell signaling, Cell 140 (2010) 517-528.

[5] K.S. Yang, S.W. Kang, H.A. Woo, S.C. Hwang, H.Z. Chae, K. Kim, S.G. Rhee, Inactivation of human peroxiredoxin I during catalysis as the result of the oxidation of the catalytic site cysteine to cysteine-sulfinic acid, J Biol Chem 277 (2002) 38029-38036.

[6] B. Manta, M. Hugo, C. Ortiz, G. Ferrer-Sueta, M. Trujillo, A. Denicola, The peroxidase and peroxynitrite reductase activity of human erythrocyte peroxiredoxin 2, Arch Biochem Biophys 484 (2009) 146-154.

[7] L.B. Poole, A. Godzik, A. Nayeem, J.D. Schmitt, AhpF can be dissected into two functional units: tandem repeats of two thioredoxin-like folds in the N-terminus mediate

electron transfer from the thioredoxin reductase-like C-terminus to AhpC, Biochemistry, 39 (2000) 6602-6615.

[8] N. Romero, R. Radi, E. Linares, O. Augusto, C.D. Detweiler, R.P. Mason, A. Denicola, Reaction of human hemoglobin with peroxynitrite. Isomerization to nitrate and secondary formation of protein radicals, J Biol Chem, 278 (2003) 44049-44057.

[9] C.N. Pace, F. Vajdos, L. Fee, G. Grimsley, T. Gray, How to measure and predict the molar absorption coefficient of a protein, Protein Sci, 4 (1995) 2411-2423.

[10] R. Radi, Nitric oxide, oxidants, and protein tyrosine nitration, Proc Natl Acad Sci U S A 101 (2004) 4003-4008.

[11] C. Batthyany, J.M. Souza, R. Duran, A. Cassina, C. Cervenansky, R. Radi, Time course and site(s) of cytochrome c tyrosine nitration by peroxynitrite, Biochemistry 44 (2005) 8038-8046.

3.3. Prx2 como sensor de H_2O_2; el paso crítico de resolución (oxidación a disulfuro o sobreoxidación)

3.3.1. Resumen

Las Prx de 2-cisteínas tienen un ciclo catalítico en 3 pasos, que consiste en (1) reducción del peróxido y formación de ácido cisteinsulfénico en la enzima, (2) condensación del ácido cisteinsulfénico con un tiol para formar un enlace disulfuro, también conocido como resolución, y (3) reducción del disulfuro por una proteína reductora. Siguiendo los cambios en la fluorescencia intrínseca, se estudió la dependencia con el pH de la reacción 2 en las peroxirredoxinas humanas 1, 2 y 5 y en la AhpC de *Salmonella typhimurium* obteniendo las constantes cinéticas para la reacción, así como valores de pK_a para el tiol y el ácido cisteinsulfénico para cada sistema. Las constantes de reacción obtenidas varían en 2 órdenes de magnitud, pero en todos los casos la reacción 2 parece ser lenta comparándola con la misma reacción entre reactantes, indicando que las velocidades obtenidas experimentalmente están limitadas por características conformacionales de las proteínas. Para cada Prx, la reacción 2 se volverá limitante a partir de una concentración de H_2O_2, a partir de la cual se produce la acumulación de Prx en ácido cisteinsulfénico. Cuando esto ocurre, una Prx alternativa y con mayor velocidad de resolución (u otra peroxidasa) puede pasar a hacerse cargo de esta función antioxidante. La acumulación de Prx en sulfénico a distintas concentraciones de H_2O_2 depende de las limitaciones cinéticas del ciclo catalítico y podrían constituir las bases de una vía de señalización redox mediada por H_2O_2 independiente de inactivación y modificaciones postraduccionales. Las diferencias en las constantes de resolución entre las Prx coexistiendo en un mismo compartimiento subcelular podrían explicar en parte su complementación en la función antioxidante y en la percepción diferencial del H_2O_2.

3.3.2. Principales resultados obtenidos

- Se obtuvieron los perfiles de constante cinética de resolución en función del pH para tres Prx humanas (Prx1, Prx2 y Prx5) y para *St*AhpC.

- Mediante simulaciones se constató que la reacción de resolución (formación del disulfuro) es particularmente lenta, o sea que el entorno del sitio catalítico de estas Prx, así como favorece a una reacción de la C_P con H_2O_2 muy rápida, también desfavorece el encuentro con C_R para formar el disulfuro.

- Se determinaron los valores de pK_a para el tiol de la cisteína resolutiva y para el ácido cisteinsulfénico de la C_P de estas cuatro Prx.

- A partir de los valores obtenidos y de modelos matemáticos se propone un modelo de señalización redox por H_2O_2 y Prx independiente de modificaciones postraduccionales e inactivación de Prx. Este modelo podría explicar la presencia no redundante de más de una Prx en un mismo compartimiento subcelular.

3.3.3. Artículo publicado en Biochemistry

Differential Kinetics of Two-Cysteine Peroxiredoxin Disulfide Formation Reveal a Novel Model for Peroxide Sensing

Stephanie Portillo-Ledesma,[†,‡,§] Lía M. Randall,[†,§,‖] Derek Parsonage,[⊥] Joaquín Dalla Rizza,[†,§]
P. Andrew Karplus,[@] Leslie B. Poole,[⊥] Ana Denicola,[†,§] and Gerardo Ferrer-Sueta*[,†,§]

[†]Laboratorio de Fisicoquímica Biológica and [‡]Laboratorio de Química Teórica y Computacional, Instituto de Química Biológica, Facultad de Ciencias, and [§]Center for Free Radical and Biomedical Research, Universidad de la República, Montevideo, Uruguay

[‖]Laboratorio de I+D de Moléculas Bioactivas, CENUR Litoral Norte, Universidad de la República, Paysandú, Uruguay

[⊥]Department of Biochemistry and Centers for Structural Biology and for Redox Biology and Medicine, Wake Forest School of Medicine, Winston-Salem, North Carolina 27157, United States

[@]Department of Biochemistry and Biophysics, Oregon State University, 2011 Agricultural & Life Sciences Building, Corvallis, Oregon 97331, United States

S *Supporting Information*

ABSTRACT: Two-cysteine peroxiredoxins (Prx) have a three-step catalytic cycle consisting of (1) reduction of peroxide and formation of sulfenic acid on the enzyme, (2) condensation of the sulfenic acid with a thiol to form disulfide, also known as resolution, and (3) reduction of the disulfide by a reductant protein. By following changes in protein fluorescence, we have studied the pH dependence of reaction 2 in human peroxiredoxins 1, 2, and 5 and in *Salmonella typhimurium* AhpC and obtained rate constants for the reaction and pK_a values of the thiol and sulfenic acid involved for each system. The observed reaction 2 rate constant spans 2 orders of magnitude, but in all cases, reaction 2 appears to be slow compared to the same reaction in small-molecule systems, making clear the rates are limited by conformational features of the proteins. For each Prx, reaction 2 will become rate-limiting at some critical steady-state concentration of H_2O_2 producing the accumulation of Prx as sulfenic acid. When this happens, an alternative and faster-resolving Prx (or other peroxidase) may take over the antioxidant role. The accumulation of sulfenic acid Prx at distinct concentrations of H_2O_2 is embedded in the kinetic limitations of the catalytic cycle and may constitute the basis of a H_2O_2-mediated redox signal transduction pathway requiring neither inactivation nor posttranslational modification. The differences in the rate constants of resolution among Prx coexisting in the same compartment may partially explain their complementation in antioxidant function and stepwise sensing of H_2O_2 concentration.
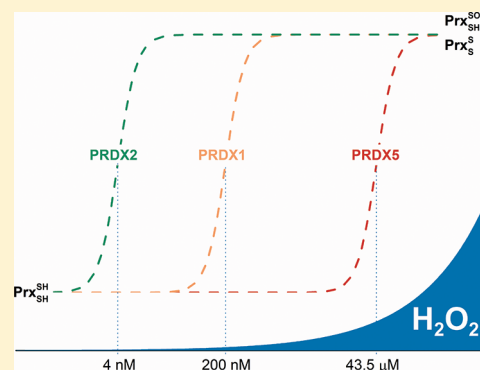
Peroxiredoxins (Prx) are enzymes capable of reducing hydroperoxides in remarkably rapid reactions using one or two cysteine residues as reductants. Reported rate constants for the reduction of H_2O_2 range from 9×10^3 M^{-1} s^{-1} for bacterioferritin comigrating protein[1] (now known as PrxQ) to 1×10^8 M^{-1} s^{-1} for human peroxiredoxin 2 (PRDX2).[2] It has been repeatedly pointed out that this is 4−8 orders of magnitude faster than the same reaction with a low-molecular weight thiol as a reductant,[3] and explanations for the accelerated reaction have been provided on the basis of structural approaches[4,5] and quantum mechanics/molecular mechanics calculations.[3,6,7]

Since the discovery of the enzymatic activity of Prx,[8,9] the emphasis on its catalytic characterization has been placed mostly on the exceptionally large rate constants of their reactions with hydroperoxides and peroxynitrous acid,[10−14] with less attention being paid to the rest of the reactions completing the catalytic cycle.

Among Prx, those that use two cysteine residues (2Cys Prx) have a three-step catalytic cycle described by reactions 1−3. Reduction of peroxide, albeit rapid, is only one of the steps. Situations in which peroxide formation is sustained for a long period of time require the enzymes to go through the whole catalytic cycle repeatedly. In reaction 1, a hydroperoxide is reduced and the peroxidatic cysteine (C_P) is oxidized to sulfenic acid, usually with a very high rate constant (k_{ROOH}). Reaction 2 is the condensation between the newly formed C_P sulfenic acid and a second cysteine thiol (the resolving cysteine or C_R). It is called the resolution reaction and is always first-order, even in the case of typical 2Cys Prx, in which C_P and C_R of the disulfide belong to different subunits, because of the

Table 1. Reaction Rate Constants of the Catalytic Cycle of Human Peroxiredoxins

		reaction 1	reaction 2	reaction 3	
Prx	localization	$k_{H_2O_2}$ (M^{-1} s^{-1})	k_{res} (s^{-1})	reductant[a]	k_3 (M^{-1} s^{-1})
PRDX1	cytosolic	3.8×10^7 [15]	9[15]	Trx1	ND
		1.1×10^8 [b]	12.9[b]		
PRDX2	cytosolic	0.13 to 1×10^8 [2]	2;[16] 0.25[15]	Trx1	ND
		1.6×10^8 [b]	0.64[b]		
PRDX3	mitochondrial	2×10^7 [17]	20[16]	Trx2	ND
PRDX4	endoplasmic reticulum	2.2×10^7 [18]	ND	PDI[19]	ND
PRDX5	mitochondrial, cytosolic, peroxisomal	$3-4 \times 10^5$ [3,20]	15[20]	Trx2	2×10^6 [20]
			18.7[b]		
PRDX6	cytosolic, lysosomal	3.4×10^7 [21,c]	not applicable[d]	π-GST + GSH[22]	ND

[a]The reductant usually invoked as part of the catalytic thiol peroxidase cycle. Other potential redox partners have been identified but not kinetically characterized. [b]The values in italics were determined in the work presented here (see Results). [c]This value was obtained with the rat protein. [d]PRDX6 is a 1Cys Prx and as such does not undergo a resolution reaction.

extreme stability of the dimers. Finally, reaction 3 is the reduction of the disulfide formed in the previous step, and the typical reductant is a thioredoxin or a similar thiol oxidoreductase.

$$\text{Prx}_{SH}^{SH} + \text{ROOH} \rightarrow \text{Prx}_{SH}^{SOH} + \text{ROH} \qquad (1)$$

$$\text{Prx}_{SH}^{SOH} \rightarrow \text{Prx}_{S_2} + \text{H}_2\text{O} \qquad (2)$$

$$\text{Prx}_{S_2} + \text{Trx}_{SH}^{SH} \rightarrow \text{Prx}_{SH}^{SH} + \text{Trx}_{S_2} \qquad (3)$$
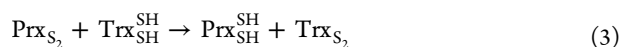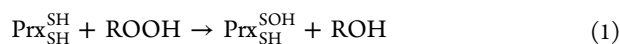
One aspect that is often overlooked in the study of Prx is their diversity, which is further complicated by the incomplete quantitative information about their reaction kinetics. As mentioned, the reaction rate constant with H$_2$O$_2$ in the Prx family spans 4 orders of magnitude. The rate constant of reaction 2 (k_{res}) is also different, even between very similar proteins. Finally, reaction 3 is largely understudied with very few direct determinations. The scenario is further complicated if additional phenomena like hyperoxidation, posttranslational modification, and oligomerization equilibria and dynamics are considered. Take for instance the six Prx present in human cells, for which the reported kinetic data, summarized in Table 1, has major gaps in the rate constants of reduction.

Because of their extreme rate of reduction of H$_2$O$_2$, Prx have often been implicated in signaling mediated by this peroxide. The large reaction rate constants and high concentrations make Prx the preferred target, accounting for the reduction of nearly all H$_2$O$_2$ formed or otherwise present in the same compartment as long as upstream reductants can keep up with demand.[23−25] Once oxidized, the Prx may relay the signal via thiol−disulfide exchange reactions with other proteins.[26−30] Some researchers consider that the signaling can be modulated via posttranslational modifications that affect the peroxidase activity, such as hyperoxidation[31] of the C$_P$, phosphorylation,[32] and glutathionylation.[33] In addition, transient inactivation of Prx is viewed by some authors as a means of allowing H$_2$O$_2$ to react with slower targets that would become the receptors of the H$_2$O$_2$ signal.[31,34] The two mechanisms (direct relay or modulation/inactivation via posttranslational modifications to permit the oxidation of slower targets) are not mutually exclusive, and they are theoretically possible but, again, suffer from a lack of quantitative information about the chemical and enzyme kinetics involved. Additionally, the apparent redundancy of different Prx coexisting in the same compartment evidenced in Table 1 is often disregarded.

The center of attention in this article is reaction 2, or "resolution", for which some rate constant (k_{res}) values have been published: 15 s^{-1} in human PRDX5,[20] 2 and 20 M^{-1} s^{-1} in human PRDX2 and PRDX3, respectively,[16] 9 s^{-1} in human PRDX1,[15] and 75 s^{-1} in *Salmonella typhimurium* AhpC.[35] One of the remarkable aspects of this reaction is that it requires an important conformational change, called the fully folded to locally unfolded or FF−LU transition, in which both C$_P$ and C$_R$ move to bridge the gap of 13−15 Å that separates them in the dithiol state according to the X-ray structures. The conformational dynamics of this process have been studied in *Arabidopsis thaliana* PrxQ, belonging to another subfamily of Prx. The authors reported a relatively fast conformational exchange rate (1650 s^{-1}) that, according to them, is not likely to be limiting for catalysis.[36] The chemical reaction itself, the condensation of sulfenic acid and thiol moieties, is known to be fast when low-molecular weight sulfenic acids and thiols are involved[37,38] but appears to be limited by the protein structure in Prx.

In this work, we study the pH dependence of the resolution process for four 2Cys Prx and find that all four of them show similar patterns, consistent with two ionizable reacting groups. Nevertheless, the rate constants are different, spanning 2 orders of magnitude that cannot be easily explained in terms of differences in reactivity of the sulfenic acids and thiols involved. We then explore how such evolutionarily conserved differences in the rates of the resolution step would allow differential accumulation of the sulfenic acid of certain Prx so that they could play direct roles in peroxide signaling.

■ **EXPERIMENTAL PROCEDURES**

Proteins. Human PRDX2 was purified from red blood cells, as previously described.[2] Recombinant human PRDX5 and *S. typhimurium* AhpC were expressed and purified as previously described.[20,39] The coding sequence of PRDX1 (GenBank accession number NM_001202431), including an N-terminal His tag and TEV protease cleavage site, was synthesized and cloned into a pET28a plasmid with *Nco*I and *Hind*III by Genscript.

BL21(DE3) cells, harboring the PRDX1pET-28a vector, were grown in Luria broth (LB) medium containing kanamycin (50 μg/mL) at 37 °C to an OD$_{600}$ of ∼0.6. Expression was induced by adding isopropyl β-D-1-thiogalactopyranoside to a final concentration of 0.5 mM at 20 °C. The next morning cultured cells were harvested by centrifugation and suspended in buffer A [50 mM sodium phosphate (pH 7.4) and 150 mM
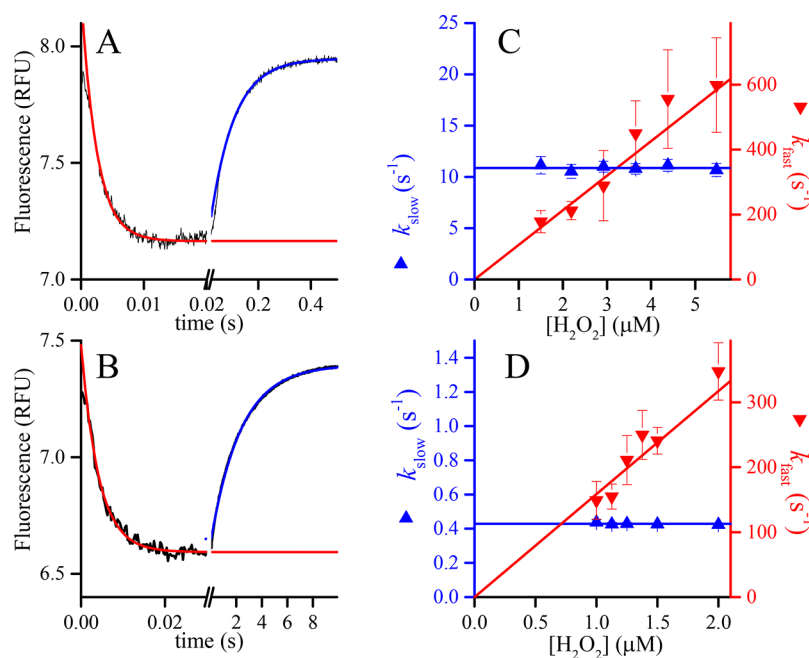
Figure 1. Kinetics of oxidation of PRDX1 and PRDX2 by H_2O_2. Time courses of the changes in intrinsic fluorescence of (A) 0.25 μM reduced PRDX1 upon reaction with 2.9 μM H_2O_2 at pH 6.7 and (B) 0.2 μM reduced PRDX2 upon reaction with 1.5 μM H_2O_2 at pH 7.4. Note the different time scales. The two phases were fitted independently to single-exponential functions to obtain first-order rate constants. The dependence of the rate constants on H_2O_2 concentration, k_{fast}, corresponding to the descending phase of the reaction (down triangles, right y axis) depends linearly on H_2O_2 concentration, whereas the rate constant of the ascending phase (k_{slow}, up triangles, left y axis) is apparently independent of H_2O_2 concentration for both (C) PRDX1 and (D) PRDX2.

NaCl] with 5 mM phenylmethanesulfonyl fluoride and 1 mg/mL lysozyme. The cell suspension was sonicated, and the supernatant was separated by centrifugation. Histidine-tagged PRDX1 was purified using a HisTrap immobilized metal ion affinity chromatography (IMAC) column (GE Healthcare) equilibrated with buffer A with 20 mM imidazole. Elution was achieved with an imidazole gradient from 20 to 500 mM. To remove the His tag, 2 mg of TEV protease was added to the collected fractions, and they were extensively dialyzed against buffer A with 0.5 mM EDTA and 1 mM dithiothreitol (DTT) at 4 °C. The cleaved His tag and TEV protease were removed with a second IMAC column. Finally, the protein was concentrated, reduced with DTT for 30 min at room temperature, and injected onto a HiLoad 16/60 Superdex 200 column (GE Healthcare) equilibrated with buffer A with 0.1 mM diethylenetriamine pentaacetic acid (DTPA). Fractions with PRDX1 were pooled, concentrated, and stored at −80 °C. Purity was evaluated by sodium dodecyl sulfate−polyacrylamide gel electrophoresis.

Buffer System. Unless otherwise indicated, for kinetic determinations we used a wide-range buffer solution at a constant ionic strength (I = 0.15) independent of the pH as proposed by Ellis and Morrison,[40] consisting of 30 mM Tris, 15 mM MES, and 15 mM acetic acid; the buffer also contained 120 mM NaCl and 0.1 mM DTPA.

Kinetic Studies. The change in fluorescence of PRDX1, PRDX2, and AhpC upon oxidation with excess H_2O_2 was used to measure the rate constant of the oxidation ($k_{H_2O_2}$, reaction 1) and the resolution reaction (k_{res}, reaction 2). Time courses are biphasic, with a faster phase that is first-order in H_2O_2 concentration and a slower phase independent of H_2O_2 concentration and assigned to reaction 2 in the case of AhpC.[35] Thus, k_{res} was measured in the presence of excess

H_2O_2 (5 μM for PDRX1 and PRDX2 and 50 μM for AhpC) as the slower phase of the fluorescence time course, which was fitted to a single-exponential function. In some instances, a much slower decay in fluorescence was apparent at longer times, which was at least partially due to photolysis of the tryptophans; this was considered but essentially affected neither the fitting process nor its results (Figure S1).

The behavior of PRDX5 fluorescence upon oxidation is different, likely because it has only one tryptophan (W85) <6 Å from the C_P and none near C_R. Additionally, the oxidation to sulfenic acid causes an increase in fluorescence emission, and the resolution reaction apparently does not produce any change in fluorescence, as evidenced by the study of the C_R mutant.[20] Therefore, k_{res} was measured as previously described, as the asymptotic limit of the rate constant of oxidation at high H_2O_2 concentrations.[20] We studied the dependence of k on H_2O_2 concentration at three different pHs in the range 5.84−8.94 and chose 200 μM H_2O_2 as a concentration close enough to the asymptotic limit.

Cysteine pK_a Determination. The pK_a values of C_P and C_R of PRDX2 were determined through the pH dependence of the rate of alkylation by monobromobimane as previously described.[41]

■ RESULTS AND DISCUSSION

Kinetics of the resolution reaction were previously reported at single pH values (pH 7−7.4) for PRDX5,[20] AhpC,[35] and PRDX1[15] measured through the changes in fluorescence of the proteins caused by oxidation, but independent of H_2O_2 concentration. The reported rate constant for resolution of PRDX2 was previously obtained through a combination of competition kinetics of reaction 2 with the hyperoxidation

reaction (reaction 4) monitored by SDS−PAGE and competition kinetics between reaction 4 and catalase.[16]

$$\text{Prx}_{SH}^{SOH} + H_2O_2 \rightarrow \text{Prx}_{SH}^{SO_2H} + H_2O \qquad (4)$$
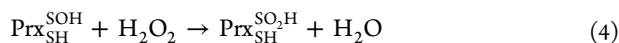
In this work, we monitored reaction 2 directly through changes in the intrinsic fluorescence of the Prx. As seen for AhpC and PRDX1, when PRDX2 reacts with H_2O_2 the time course of fluorescence changes shows two distinct phases (Figure 1). The rate constant of the faster phase depends linearly on H_2O_2 concentration, and the calculated second-order rate constant $[(1.59 \pm 0.06) \times 10^8 \ M^{-1} \ s^{-1}]$ agrees reasonably well with previous values of $k_{H_2O_2}$ obtained by competition with HRP.[2,14]

On the other hand, the rate constant of the slower phase is independent of H_2O_2 concentration in the range used and is interpreted here as the k_{res}.

The time courses of oxidation of PRDX5 by H_2O_2 are single exponentials, in which the rate constant tends asymptotically to the value of k_{res} at high H_2O_2 concentrations.[3] Because the oxidation and the resolution cannot be discriminated from the time courses alone, as they can be for AhpC and PRDX2, we studied the kinetics of oxidation at different pHs and in a range of H_2O_2 concentrations to make sure we could select a concentration close enough to the plateau in rate constant. Experiments performed at pH 5.84, 7.08, and 8.94 showed that with 200 μM H_2O_2 the rate constant was practically indistinguishable from the asymptote (Figure 2).
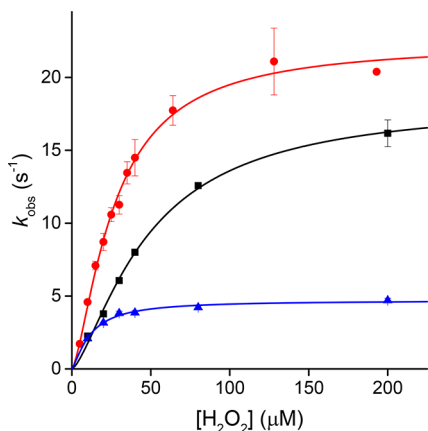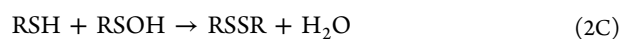

Figure 2. Kinetics of oxidation of PRDX5 by H_2O_2. The reaction rate constants were measured through the change in intrinsic fluorescence of the protein at different concentrations of H_2O_2, at 25 °C and pH 5.84 (black squares), pH 7.08 (red circles), and pH 8.94 (blue triangles).

We then measured the apparent rate constants of resolution of each peroxiredoxin at a single excess concentration of H_2O_2 in the pH range from 5 to 9. The pH profiles of k_{res}^{app} are bell-shaped as expected for reactions with two acid−base groups involved. We posit that the C_R thiol and C_P sulfenic acid would be the groups whose pK_a values could most affect the rate constant (Figure 3).

Taking into account the protonation states of the two reacting groups, reaction 2 can be considered as four possible combinations. Considering that RS^- is the best nucleophile and RSOH is the best electrophile, we can order the combinations of protonation states in reactions from faster to slower as

$$RS^- + RSOH \rightarrow RSSR + OH^- \qquad (2A)$$
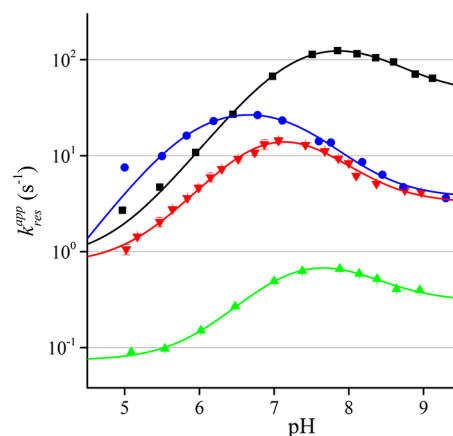
Figure 3. pH profiles of the rate constant of resolution of AhpC (black squares), PRDX1 (red triangles), PRDX2 (green triangles), and PRDX5 (blue circles). The lines represent the fits to eq 5.

$$RS^- + RSO^- + H^+ \rightarrow RSSR + OH^- \qquad (2B)$$

$$RSH + RSOH \rightarrow RSSR + H_2O \qquad (2C)$$

$$RSH + RSO^- \rightarrow RSSR + OH^- \qquad (2D)$$

In this order, we have assumed that the nucleophilicity of the thiolate is more important than the electrophilicity of the sulfenic acid in determining the rate constant.

The general rate law of the reaction would be

$$v = k[RS(H)]_T[RSO(H)]_T$$

where $[RS(H)]_T$ and $[RSO(H)]_T$ are the total concentrations of thiol plus thiolate and sulfenic acid plus sulfenate, respectively. The rate of the reaction is the sum of the rates of the four possible combinations (2A−2D) that are pH-dependent according to the pH distribution of the species involved. For instance, the rate law of reaction 2A would be

$$v = k_{2A}[RS^-][RSOH]$$

or

$$v = k_{2A}[RS(H)]_T\left(\frac{K_a^{SH}}{[H^+] + K_a^{SH}}\right)[RSO(H)]_T$$

$$\times \left(\frac{[H^+]}{[H^+] + K_a^{SOH}}\right)$$

where K_a^{SH} and K_a^{SOH} are the ionization constants of the C_R thiol and the C_P sulfenic acid, respectively. Thus, the apparent rate constant would be

$$k_{2A}^{app} = k_{2A}\left(\frac{K_a^{SH}}{[H^+] + K_a^{SH}}\right)\left(\frac{[H^+]}{[H^+] + K_a^{SOH}}\right)$$

$$= k_{2A}\left[\frac{[H^+]K_a^{SH}}{[H^+]^2 + [H^+](K_a^{SH} + K_a^{SOH}) + K_a^{SH}K_a^{SOH}}\right]$$

The apparent rate constants of reactions 2B−2D can be analogously derived (see the Supporting Information). As the four combinations happen simultaneously, the overall rate constant of the resolution would be the sum of the apparent rate constants:

$$k_{res}^{app} = k_{2A}^{app} + k_{2B}^{app} + k_{2C}^{app} + k_{2D}^{app}$$

Table 2. Best Fit Values of eq 5 to the Apparent Rate Constants of Resolution Shown in Figure 3 and Values of Cysteine pK_a Obtained by Other Experimental Approaches for Comparison

	AhpC	PRDX1	PRDX2	PRDX5
k_{2A}	2410 ± 725	113 ± 49	10.5 ± 5.5	1032 ± 425
k_{2B}	44 ± 4.7	3.2 ± 0.3	0.30 ± 0.03	3.7 ± 0.5
k_{2C}	1.1 ± 1.2	0.7 ± 0.2	0.06 ± 0.01	0 ± 3.1
$pK_a^{SOH}(C_P)$	7.22 ± 0.06	6.8 ± 0.1	7.0 ± 0.1	5.9 ± 0.1
$pK_a^{SH}(C_R)$	8.3 ± 0.1	7.4 ± 0.2	8.0 ± 0.2	7.35 ± 0.09
$pK_a^{SH}(C_P)$	5.84 ± 0.02[42]	not determined	4.8 ± 0.1	5.2 ± 0.2[20]
$pK_a^{SH}(C_R)$	8.7 ± 0.1[42]	not determined	8.5 ± 0.2	8.8 ± 0.1[41]

or

$$k_{res}^{app} = \left[\frac{k_{2A}[H^+]K_a^{SH} + k_{2B}K_a^{SH}K_a^{SOH} + k_{2C}[H^+]^2 + k_{2D}[H^+]K_a^{SOH}}{[H^+]^2 + [H^+](K_a^{SH} + K_a^{SOH}) + K_a^{SH}K_a^{SOH}} \right] \quad (5)$$

The resolution reaction is first-order, because C_P and C_R are contained in the same protein chain (PRDX5) or belong to dimers that do not dissociate (PRDX1, PRDX2, and AhpC). Nevertheless, the pH dependence is the same as in a bimolecular reaction.

The pH profiles of Figure 3 were fitted to eq 5 using Origin 8.6, and to simplify the fitting, the value of the least likely rate constant (k_{2D}) was fixed to 0. Results of the best fits are listed in Table 2.

The values in Table 2 show, as expected, that reaction 2A is the main contributor to the overall reaction rate; reaction 2B has some minor relevance, mostly because its relative contribution to k_{res}^{app} will be perceived only when pH > $pK_a^{SH}(C_R)$. The rate constant of reaction 2C makes a negligible contribution to the overall reaction rate.

There are two pK_a values reported in the literature for the sulfenic acid of C_P in Prx (pK_a^{SOH}); a value of 6.6 was determined for *Mycobacterium tuberculosis* AhpE,[43] and a value of 6.1 was determined for *S. typhimurium* AhpC C165S.[44] The latter is significantly lower than the value determined herein for wild-type AhpC (7.22 ± 0.06). Remarkably, the values of pK_a^{SH} for C_R determined through fitting of the resolution reaction are significantly lower than those previously measured by alkylation in refs 41 and 42 or in this work (Figure S1). The shift in the pK_a values of both sulfenic acid and thiol points to a potential alteration of the protein environment of both C_P and C_R upon formation of the sulfenic acid that may occur in a manner independent of the conformational change that enables disulfide bond formation.

In comparison with the C_P thiol/thiolate present in the reduced form of these enzymes, the sulfenic acid/sulfenate is bulkier, significantly less acidic,[20,42] and potentially much better at forming hydrogen bonds because of its oxygen atom. These steric, electrostatic, and interaction properties will alter the environment of the active site and could result in a destabilization of the FF conformer and may accelerate the FF → LU transition.

Reactivity of the Residues versus Encounter Frequency of the Reacting Moieties. Sulfenic acids in the presence of thiols are short-lived. They react to yield a disulfide that is much more stable than the reactants; thus, measuring the kinetics of condensation through partial oxidation of a thiol is difficult. This difficulty was evident in a recent debate in the literature[37,38] about the rate constant of reaction of Cys with Cys sulfenic acid at pH 6.0 to form a disulfide (k_{CysSS}). One

group reported a value of 720 M^{-1} s^{-1},[37] and the other set a lower limit of 10^5 M^{-1} s^{-1};[38] both rate constants indicate relatively fast reactions. There is nevertheless a detailed kinetic study of a sulfenic acid reacting with thiols in aqueous solution; the proton pump inhibitor omeprazole produces a sulfenic acid by a rearrangement in acidic medium in the absence of thiols, and the sulfenic acid is in fast equilibrium with a cyclic sulfenylamide. The mixture of sulfenic and cyclic sulfenylamide reacts with β-mercaptoethanol with a diffusion-limited rate,[45] in line with the highest rate constant obtained in the cysteine studies. In any case, both reported rate constants of the condensation of cysteine with cysteine sulfenic acid can be compared to the resolution reactions of the four Prx studied here. To make the comparison, we need to calculate effective molarities as k_{res}^{app}/k_{CysSS} (Table 3). A simple model assuming

Table 3. Resolution Rate Constants at pH 6.0 and Effective Molarities Estimated as the Resolution Rate Constant Divided by the Reported Bimolecular Rate Constant of the Condensation between Cys and Cys Sulfenic Acid (k_{res}^{app}/k_{CysSS})

Prx	k_{res}^{app} (s^{-1} at pH 6.0)[a]	effective molarity [k_{res}^{app}/k_{CysSS} (M)]	
		$k_{CysSS} = 720$ M^{-1} s^{-1}	$k_{CysSS} > 10^5$ M^{-1} s^{-1}
AhpC	11.8	2.71×10^{-2}	$<1.95 \times 10^{-4}$
PRDX1	4.61	6.4×10^{-3}	$<4.61 \times 10^{-5}$
PRDX2	0.15	2.08×10^{-4}	$<1.50 \times 10^{-6}$
PRDX5	19.5	1.64×10^{-2}	$<1.18 \times 10^{-4}$

[a]Values interpolated from Figure 3, using pH 6 to compare the results with those of small-molecule studies.

that both C_P sulfenic acid and C_R thiol are constrained to move in a sphere with a 30 Å radius (twice the distance between the residues in the reduced enzyme) produces an effective molarity of 0.68 M, much higher than those calculated even with the smallest rate constant. It follows that the encounter probability of the two residues is restricted by the protein structure; i.e., the Prx structure limits the resolution reaction rate and thus may limit the overall turnover of the enzyme. One of the secondary effects of the slow resolution is the differential propensity to hyperoxidation previously observed among different Prx.[31]

The FF active site of Prx is an extremely conserved structure;[5,46,47] thus, the sulfenic acids of the C_P are formed in similar environments in the four Prx studied. Also, the C_R thiol appears to be a regular cysteine in terms of reactivity, with the expected pK_a for a surface Cys and not particularly fast in any of the reactions studied so far. However, 2 orders of magnitude separate the apparent rate constants of PRDX2 and AhpC. Thus, it appears, particularly in the case of PRDX2, that the resolution rate is limited not by the reactivity of the thiol—

sulfenic acid pair but by a structural restriction that hinders the access to the LU conformation.

Furthermore, according to the estimates in Table 2, the resolution reaction is slower than expected in all four cases. This evidence supports the hypothesis that the protein structure restricts the rate of resolution, not necessarily by affecting the reactivity of the groups involved but by sequestering or stabilizing them in the FF conformation and limiting their productive encounters.

Stabilization of the LU conformation happens in nitrated PRDX2[48] and results in faster overall catalysis. Additional evidence of this structural limitation of the rate comes from another thiol peroxidase from the GPx family. In a recent report on a mycothiol peroxidase from *Corynebacterium glutamicum* (Mpx),[49] the authors show that the resolution reaction happens at a rate on par with that of AhpC (k_{res} = 111 s^{-1}) but a C64S mutation makes the reaction 5-fold faster (k_{res} = 559 s^{-1}). Because C64 is not involved in the reaction and seems to be too far from either C_P or C_R (according to structural models) to affect the reactivity of either, the best hypothesis is that the C64S mutation helps stabilize the conformation where the reaction is possible.

The sole example of the dynamics of the FF–LU transition studied by nuclear magnetic resonance in a Prx indicates a rather fast process,[36] but even if the conformational transition is fast, it could limit the overall rate of resolution. The reaction sequence, including the conformational transition, would be

$$(Prx_{SH}^{SOH})_{FF} \underset{k_{FF}}{\overset{k_{LU}}{\rightleftharpoons}} (Prx_{SH}^{SOH})_{LU} \overset{k_2}{\rightarrow} (Prx_{S_2})_{LU} + H_2O \qquad (6)$$
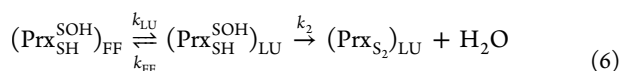
The rate law of the system can be approximated using any of the three simplified approaches, namely, steady state, prior equilibrium, or improved prior equilibrium,[50] described in Table 4.

Table 4. Approximate Solutions for the Kinetic System of Resolution Described in eq 6

	steady state	prior equilibrium	improved prior equilibrium
$k_{res} \approx$	$\dfrac{k_{LU}k_2}{k_{FF}+k_2}$	$\dfrac{k_{LU}k_2}{k_{LU}+k_{FF}}$	$\dfrac{k_{LU}k_2}{k_{LU}+k_{FF}+k_2}$

In all three cases, the approximate rate constant of product buildup (k_{res}) includes k_{LU} and k_{FF}, with k_{FF} always being in the denominator. Then, regardless of the approximation, assuming that the LU conformation is less stable than FF ($k_{LU} \ll k_{FF}$),[51] the conformational change will limit the rate of resolution by restricting the available concentration of the LU conformer. In

other words, the FF → LU transition does not need to be slow to decelerate the resolution reaction; as long as the transition in the LU direction is slower than its reverse, k_{res} will be lower than the rate constant of the chemical process (k_2).

Stoichiometric versus Catalytic Consumption of H$_2$O$_2$ and the Sensing of Peroxide Flux. Limitation of the catalytic turnover of Prx by the resolution reaction could have profound consequences in terms of the sensing of peroxides. The rate of peroxide consumption by Prx depends crucially on the concentration of enzyme and the rate of H$_2$O$_2$ generation. If the enzyme is in the dithiol state and in excess, and H$_2$O$_2$ is introduced suddenly into the system, as in a bolus addition, the consumption of peroxide will obey the rate law of reaction 1 (Table 5). This stoichiometric consumption of H$_2$O$_2$ is extremely rapid, particularly by PRDX1, PRDX2, and AhpC that are abundant and have large rate constants. As a result, under these conditions, the enzymes will consume H$_2$O$_2$ very fast. Nevertheless, if H$_2$O$_2$ is produced constantly, the excess reduced Prx will be eventually depleted, and further H$_2$O$_2$ reduction can be possible only if the enzyme goes through the complete catalytic cycle. In this case, reaction 2 or 3 may become rate-limiting. Using the values of Prx rate constants, we calculated the steady-state concentrations of the oxidant ($[H_2O_2]_{ss}$) and reductant (either Trx or AhpF, $[Red]_{ss}$) that make all three steps in the catalytic cycle proceed at the same rate (Table 5). The calculated $[H_2O_2]_{ss}$ in the case of PRDX2 is remarkably low (4 nM) and separated from that of PRDX1 and PRDX5, enzymes that coexist in the cytosolic compartment. Interestingly, the range of $[H_2O_2]_{ss}$ between the two main cytosolic Prx (PRDX1 and PRDX2) coincides with the range described recently as physiological, or "oxidative eustress".[52]

In the case in which a sustained influx of H$_2$O$_2$ oxidizes the Prx and forces it to consume the peroxide catalytically through multiple turnovers (i.e., when $[H_2O_2]_{ss}$ exceeds the critical values of Table 5 for each Prx), the actual rate of consumption of H$_2$O$_2$ by said Prx will not increase with an increasing $[H_2O_2]_{ss}$, as reaction 2 or 3 will become rate-limiting. For instance, if the H$_2$O$_2$ influx is sufficient to sustain $[H_2O_2]_{ss} > 4$ nM, PRDX2 will accumulate as either sulfenic acid or disulfide and will not be able to consume H$_2$O$_2$ any faster, thus forfeiting its antioxidant function. An alternative, faster Prx present in the same compartment can then perform the catalytic reduction of H$_2$O$_2$ below their respective critical $[H_2O_2]_{ss}$, namely up to 120 nM for PRDX1 and up to 43.5 μM for PRDX5. In summary, in a cytosolic compartment where PRDX1, PRDX2, and PRDX5 coexist, in the range of $[H_2O_2]_{ss}$ of ≤4 nM all three Prx contribute to the catalytic reduction of peroxide. From 4 to 120 nM, PRDX1 and PRDX5 will be the catalytic antioxidant

Table 5. Calculated Steady-State Concentrations of Substrates Making All Three Steps in the Catalytic Cycle of Prx Equally Fast at pH 7.4^a

	reaction 1		reaction 2	reaction 3	
	$\nu = k_{H_2O_2}[H_2O_2][Prx(SH)_2]$		$\nu = k_{res}[Prx_{SH}^{SOH}]$	$\nu = k_{red}[Red][PrxS_2]$	
	$k_{H_2O_2}$ (M^{-1} s^{-1})	$[H_2O_2]_{ss}$	k_{res} (s^{-1})	k_{red} (M^{-1} s^{-1})	$[Red]_{ss}$ (μM)
AhpC	1.36×10^{8b}	0.77 μM	104.8	2.00×10^{7b}	5.24
PRDX1	1.1×10^8	0.12 μM	12.9	not determined	not determined
PRDX2	1.6×10^8	4 nM	0.64	not determined	not determined
PRDX5	4.3×10^5	43.5 μM	18.7	2.00×10^6	9.35

^{a}$k_{H_2O_2}$ and k_{red} were taken from refs 2, 20, and 35, and k_{res} values were interpolated from Figure 3. ^{b}These values were obtained at pH 7 but are a good approximation of the values at pH 7.4.

whereas PRDX2 will accumulate as sulfenic acid and/or disulfide (depending on the rate of reaction 3). When $[H_2O_2]_{ss} > 120$ nM, only PRDX5 will continue functioning as the antioxidant. Of course, in the same compartment there may be other peroxidases (glutathione peroxidase, PRDX6, and catalase) sharing the burden of reducing H_2O_2; nevertheless, the ranges of steady-state concentrations are embedded in each 2Cys Prx through the rate-limiting step that reaction 2 may become (Figure 4).
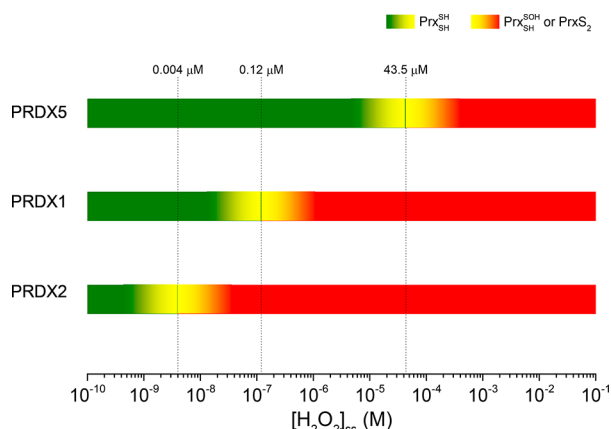
Figure 4. Ranges of H_2O_2 concentration and PRDX roles. Below the $[H_2O_2]_{ss}$ threshold imposed for each PRDX by their resolution reaction, the enzymes act as fast peroxidases consuming most of the peroxide and keeping its concentration low. Once the flux of H_2O_2 overcomes the maximal flux of consumption by a Prx, resolution or reduction reactions become rate-limiting, and the enzyme accumulates as sulfenic acid or disulfide and may acquire the role of reporting the increased H_2O_2 flux (i.e., as a threshold sensor). The other Prx continue the peroxidase function until the $[H_2O_2]_{ss}$ reaches their respective critical points. Other peroxidases such as catalase and GPx also contribute to the consumption of H_2O_2 and may prove to be important for preventing hyperoxidation, a reaction that needs a rather high $[H_2O_2]_{ss}$.

There is the additional possibility of reaction 3 becoming the rate-limiting step, for instance, because of low reducing partner concentrations. In those cases, the critical $[H_2O_2]_{ss}$ will be lower than those in Table 5 and the Prx will accumulate as the disulfide, instead of as the sulfenic acid.

Above each critical $[H_2O_2]_{ss}$, the catalytic capability of one Prx is overwhelmed and the next one takes over with the possibility of setting a stepwise sensing system with hard-wired detection points at specific concentrations of the oxidant. At each critical point, and in a very narrow range of concentrations, the Prx will switch from mostly reduced to mostly oxidized, providing a recognizable target in a signaling pathway. As each 2Cys Prx has a unique combination of rate constants, several such switches are possible in compartments where multiple 2Cys Prx exist.

One reaction that is usually invoked in systems where Prx turnover occurs with excess H_2O_2 is hyperoxidation of the C_P to render the catalytically inactive sulfinic and sulfonic forms[53,54] (reaction 4). To gain a better quantitative perspective on the importance of hyperoxidation, we can make some simple calculations at one of the critical $[H_2O_2]_{ss}$ values listed in Table 5. What fraction of PRDX2, the most sensitive Prx, will be inactivated through hyperoxidation at 120 nM, the point at which PRDX1 switches from a catalytic antioxidant to a signaling sulfenic acid or disulfide? The

reported rate constant of reaction 4 is 12000 M^{-1} s^{-1};[16] then at 120 nM, the rate of reaction 4 would be

$$v_4 = k_4[H_2O_2][Prx_{SH}^{SOH}] = 12000 \times 1.2 \times 10^{-7}[Prx_{SH}^{SOH}]$$
$$= 1.44 \times 10^{-3}[Prx_{SH}^{SOH}]$$

Meanwhile, with the turnover of PRDX2 limited by the resolution reaction, its rate would be

$$v_{res} = k_{res} \times [Prx_{SH}^{SOH}] = 0.64[Prx_{SH}^{SOH}]$$

The quotient v_4/v_{res} tells us that under these conditions PRDX2 is inactivated at a rate of once every 440 turnovers. Of course, because v_4 increases with increasing H_2O_2 concentrations, it may become more prevalent under conditions of higher H_2O_2 concentrations, and hyperoxidized protein could accumulate under such conditions.

Other reactions of the sulfenic acid may be even more important than hyperoxidation, e.g., glutathionylation of the C_P. The rate constant of that reaction has been reported as 500 M^{-1} s^{-1};[55] then, assuming a conservative glutathione concentration of 1 mM, the rate would be

$$v_{GSH} = k_{GSH}[GSH][Prx_{SH}^{SOH}] = 500 \times 1 \times 10^{-3}[Prx_{SH}^{SOH}]$$
$$= 0.5[Prx_{SH}^{SOH}]$$

In this case, a v_{GSH}/v_{res} ratio of 1.28 indicates that a very important fraction of PRDX2 may become glutathionylated in the system and its return to the basic catalytic cycle will depend on the action of glutaredoxins or other enzymatic systems.[55]

We still do not know whether or under what circumstances the Prx present as sulfenic acid, as disulfide, gluthionylated, or as the hyperoxidized sulfinic acid (or all of them) would serve as the recognizable transducer of the signal for H_2O_2 concentration. Recent results point to the involvement of C_P sulfenic acid in the formation of mixed disulfides of target protein thiols with PRDX1 and PRDX2 in cells subject to mild H_2O_2 exposure.[27] The involvement of the reduction reaction, by thioredoxin or alternative reductants, in the modulation of the distribution of the three catalytic species of Prx (thiol, sulfenic acid, and disulfide) requires further research. Detailed kinetic studies are needed, beginning with the systems of reduction of Prx by thioredoxins and exploring further the alternative redox partners that may relay the signal. In any case, we currently know that the Prx properties (i.e., structures, dynamics, and kinetic rate constants) are clearly tunable and have been adapted to fulfill their biological niche in ways that we are just beginning to understand.

In summary, by evaluating the disulfide bond formation rate constant across a pH range among a set of Prx with distinct features and roles in biology, we have determined the functional pK_a values of both the C_P sulfenic acid and C_R thiol for each. As expected, disulfide bond formation proceeding by the nucleophilic attack of the deprotonated C_R on the protonated, electrophilic C_P sulfenic acid is the most efficient (by >30-fold) versus the next fastest reaction (between the C_R thiolate and C_P sulfenate), while the contributions of reactions involving the protonated C_R are negligibly small. In all four Prx studied (PRDX1, PRDX2, PRDX5, and AhpC), the maximal potential rate of disulfide bond formation is never reached because of the higher pK_a of the C_R thiol relative to that of the C_P sulfenic acid (limiting the maximal observed rate constant to approximately 12−30-fold lower than the rate constant of the optimal redox forms of C_P and C_R). Where the disulfide bond formation rate

is slowest, in PRDX2, stoichiometric amounts of H_2O_2 can still be rapidly reduced (comparable to the case for the other major cytosolic Prx, PRDX1), but as H_2O_2 concentrations increase and turnover of the system is required, disulfide bond formation rapidly becomes a bottleneck that favors flux through PRDX1 rather than PRDX2, even if reductant availability becomes an issue. This supports the possibility that PRDX2 redox status, which is strongly shifted at $[H_2O_2]_{ss}$ values of >4 nM, is used by the cell as a threshold sensor of H_2O_2 levels for the purpose of regulating cell signaling processes.

■ ASSOCIATED CONTENT

Ⓢ Supporting Information

The Supporting Information is available free of charge on the ACS Publications website at DOI: 10.1021/acs.biochem.8b00188.

> Derivation of kinetic equations for fitting Figure 3, alternative fittings to the fluorescence time courses (Figure S1), and determination of the pK_a of PRDX2 using the reaction with mBBr (Figure S2) (PDF)

■ AUTHOR INFORMATION

Corresponding Author

*Laboratorio de Fisicoquímica Biológica, Facultad de Ciencias, Universidad de la República, Iguá 4225, 11400 Montevideo, Uruguay. E-mail: gfe@fmed.edu.uy. Telephone and fax: 598 2525 0749.

ORCID Ⓘ

Gerardo Ferrer-Sueta: 0000-0002-8663-8480

Author Contributions

S.P.-L. and L.M.R. contributed equally to this work.

Funding

Notes

The authors declare no competing financial interest.

■ REFERENCES

(1) Reeves, S. A., Parsonage, D., Nelson, K. J., and Poole, L. B. (2011) Kinetic and thermodynamic features reveal that *Escherichia coli* BCP is an unusually versatile peroxiredoxin. *Biochemistry 50*, 8970−8981.

(2) Manta, B., Hugo, M., Ortiz, C., Ferrer-Sueta, G., Trujillo, M., and Denicola, A. (2009) The peroxidase and peroxynitrite reductase activity of human erythrocyte peroxiredoxin 2. *Arch. Biochem. Biophys. 484*, 146−154.

(3) Portillo-Ledesma, S., Sardi, F., Manta, B., Tourn, M. V., Clippe, A., Knoops, B., Alvarez, B., Coitiño, E. L., and Ferrer-Sueta, G. (2014) Deconstructing the Catalytic Efficiency of Peroxiredoxin-5 Peroxidatic Cysteine. *Biochemistry 53*, 6113−6125.

(4) Hall, A., Nelson, K., Poole, L. B., and Karplus, P. A. (2011) Structure-based insights into the catalytic power and conformational dexterity of peroxiredoxins. *Antioxid. Redox Signaling 15*, 795−815.

(5) Perkins, A., Parsonage, D., Nelson, K. J., Ogba, O. M., Cheong, P. H., Poole, L. B., and Karplus, P. A. (2016) Peroxiredoxin Catalysis at Atomic Resolution. *Structure 24*, 1668−1678.

(6) Zeida, A., Reyes, A. M., Lebrero, M. C., Radi, R., Trujillo, M., and Estrin, D. A. (2014) The extraordinary catalytic ability of peroxiredoxins: a combined experimental and QM/MM study on the fast thiol oxidation step. *Chem. Commun. (Cambridge, U. K.) 50*, 10070−10073.

(7) Nagy, P., Karton, A., Betz, A., Peskin, A. V., Pace, P., O'Reilly, R. J., Hampton, M. B., Radom, L., and Winterbourn, C. C. (2011) Model for the exceptional reactivity of peroxiredoxins 2 and 3 with hydrogen peroxide: a kinetic and computational study. *J. Biol. Chem. 286*, 18048−18055.

(8) Jacobson, F. S., Morgan, R. W., Christman, M. F., and Ames, B. N. (1989) An alkyl hydroperoxide reductase from Salmonella typhimurium involved in the defense of DNA against oxidative damage. Purification and properties. *J. Biol. Chem. 264*, 1488−1496.

(9) Chae, H. Z., Chung, S. J., and Rhee, S. G. (1994) Thioredoxin-dependent peroxide reductase from yeast. *J. Biol. Chem. 269*, 27670−27678.

(10) Bryk, R., Griffin, P., and Nathan, C. (2000) Peroxynitrite reductase activity of bacterial peroxiredoxins. *Nature 407*, 211−215.

(11) Ogusucu, R., Rettori, D., Munhoz, D. C., Soares Netto, L. E., and Augusto, O. (2007) Reactions of yeast thioredoxin peroxidases I and II with hydrogen peroxide and peroxynitrite: rate constants by competitive kinetics. *Free Radical Biol. Med. 42*, 326−334.

(12) Jaeger, T., Budde, H., Flohe, L., Menge, U., Singh, M., Trujillo, M., and Radi, R. (2004) Multiple thioredoxin-mediated routes to detoxify hydroperoxides in *Mycobacterium tuberculosis*. *Arch. Biochem. Biophys. 423*, 182−191.

(13) Parsonage, D., Youngblood, D. S., Sarma, G. N., Wood, Z. A., Karplus, P. A., and Poole, L. B. (2005) Analysis of the link between enzymatic activity and oligomeric state in AhpC, a bacterial peroxiredoxin. *Biochemistry 44*, 10583−10592.

(14) Peskin, A. V., Low, F. M., Paton, L. N., Maghzal, G. J., Hampton, M. B., and Winterbourn, C. C. (2007) The high reactivity of peroxiredoxin 2 with H(2)O(2) is not reflected in its reaction with other oxidants and thiol reagents. *J. Biol. Chem. 282*, 11885−11892.

(15) Carvalho, L. A. C., Truzzi, D. R., Fallani, T. S., Alves, S. V., Toledo, J. C., Jr., Augusto, O., Netto, L. E. S., and Meotti, F. C. (2017) Urate hydroperoxide oxidizes human peroxiredoxin 1 and peroxiredoxin 2. *J. Biol. Chem. 292*, 8705−8715.

(16) Peskin, A. V., Dickerhof, N., Poynton, R. A., Paton, L. N., Pace, P. E., Hampton, M. B., and Winterbourn, C. C. (2013) Hyperoxidation of peroxiredoxins 2 and 3: rate constants for the reactions of the sulfenic acid of the peroxidatic cysteine. *J. Biol. Chem. 288*, 14170−14177.

(17) Cox, A. G., Peskin, A. V., Paton, L. N., Winterbourn, C. C., and Hampton, M. B. (2009) Redox potential and peroxide reactivity of human peroxiredoxin 3. *Biochemistry 48*, 6495−6501.

(18) Wang, X., Wang, L., Wang, X. e., Sun, F., and Wang, C.-c. (2012) Structural insights into the peroxidase activity and inactivation of human peroxiredoxin 4. *Biochem. J. 441*, 113−118.

(19) Tavender, T. J., Springate, J. J., and Bulleid, N. J. (2010) Recycling of peroxiredoxin IV provides a novel pathway for disulphide formation in the endoplasmic reticulum. *EMBO J. 29*, 4185−4197.

(20) Trujillo, M., Clippe, A., Manta, B., Ferrer-Sueta, G., Smeets, A., Declercq, J. P., Knoops, B., and Radi, R. (2007) Pre-steady state kinetic characterization of human peroxiredoxin 5: taking advantage of Trp84 fluorescence increase upon oxidation. *Arch. Biochem. Biophys. 467*, 95−106.

(21) Toledo, J. C., Jr., Audi, R., Ogusucu, R., Monteiro, G., Netto, L. E., and Augusto, O. (2011) Horseradish peroxidase compound I as a tool to investigate reactive protein-cysteine residues: from quantification to kinetics. *Free Radical Biol. Med. 50*, 1032−1038.

(22) Manevich, Y., Feinstein, S. I., and Fisher, A. B. (2004) Activation of the antioxidant enzyme 1-CYS peroxiredoxin requires glutathionylation mediated by heterodimerization with pi GST. *Proc. Natl. Acad. Sci. U. S. A. 101*, 3780−3785.

(23) Ferrer-Sueta, G., Manta, B., Botti, H., Radi, R., Trujillo, M., and Denicola, A. (2011) Factors affecting protein thiol reactivity and specificity in peroxide reduction. *Chem. Res. Toxicol. 24*, 434−450.

(24) Cox, A. G., Winterbourn, C. C., and Hampton, M. B. (2010) Mitochondrial peroxiredoxin involvement in antioxidant defence and redox signalling. *Biochem. J. 425*, 313−325.

(25) Randall, L. M., Ferrer-Sueta, G., and Denicola, A. (2013) Peroxiredoxins as preferential targets in H2O2-induced signaling. *Methods Enzymol.* 527, 41−63.

(26) Sobotta, M. C., Liou, W., Stocker, S., Talwar, D., Oehler, M., Ruppert, T., Scharf, A. N., and Dick, T. P. (2015) Peroxiredoxin-2 and STAT3 form a redox relay for H2O2 signaling. *Nat. Chem. Biol.* 11, 64−70.

(27) Stocker, S., Maurer, M., Ruppert, T., and Dick, T. P. (2018) A role for 2-Cys peroxiredoxins in facilitating cytosolic protein thiol oxidation. *Nat. Chem. Biol.* 14, 148−155.

(28) Winterbourn, C. C. (2018) Biological Production, Detection and Fate of Hydrogen Peroxide. *Antioxid. Redox Signaling*, DOI: 10.1089/ars.2017.7425.

(29) Jarvis, R. M., Hughes, S. M., and Ledgerwood, E. C. (2012) Peroxiredoxin 1 functions as a signal peroxidase to receive, transduce, and transmit peroxide signals in mammalian cells. *Free Radical Biol. Med.* 53, 1522−1530.

(30) Stocker, S., Van Laer, K., Mijuskovic, A., and Dick, T. P. (2018) The Conundrum of Hydrogen Peroxide Signaling and the Emerging Role of Peroxiredoxins as Redox Relay Hubs. *Antioxid. Redox Signaling* 28, 558−573.

(31) Wood, Z. A., Poole, L. B., and Karplus, P. A. (2003) Peroxiredoxin evolution and the regulation of hydrogen peroxide signaling. *Science* 300, 650−653.

(32) Woo, H. A., Yim, S. H., Shin, D. H., Kang, D., Yu, D. Y., and Rhee, S. G. (2010) Inactivation of peroxiredoxin I by phosphorylation allows localized H(2)O(2) accumulation for cell signaling. *Cell* 140, 517−528.

(33) Park, J. W., Piszczek, G., Rhee, S. G., and Chock, P. B. (2011) Glutathionylation of peroxiredoxin I induces decamer to dimers dissociation with concomitant loss of chaperone activity. *Biochemistry* 50, 3204−3210.

(34) Rhee, S. G., Woo, H. A., and Kang, D. (2018) The Role of Peroxiredoxins in the Transduction of H2O2 Signals. *Antioxid. Redox Signaling* 28, 537−557.

(35) Parsonage, D., Nelson, K. J., Ferrer-Sueta, G., Alley, S., Karplus, P. A., Furdui, C. M., and Poole, L. B. (2015) Dissecting peroxiredoxin catalysis: separating binding, peroxidation, and resolution for a bacterial AhpC. *Biochemistry* 54, 1567−1575.

(36) Aden, J., Wallgren, M., Storm, P., Weise, C. F., Christiansen, A., Schroder, W. P., Funk, C., and Wolf-Watz, M. (2011) Extraordinary μs-ms backbone dynamics in *Arabidopsis thaliana* peroxiredoxin Q. *Biochim. Biophys. Acta, Proteins Proteomics* 1814, 1880−1890.

(37) Luo, D., Smith, S. W., and Anderson, B. D. (2005) Kinetics and mechanism of the reaction of cysteine and hydrogen peroxide in aqueous solution. *J. Pharm. Sci.* 94, 304−316.

(38) Ashby, M. T., and Nagy, P. (2007) Revisiting a proposed kinetic model for the reaction of cysteine and hydrogen peroxide via cysteine sulfenic acid. *Int. J. Chem. Kinet.* 39, 32−38.

(39) Poole, L. B., and Ellis, H. R. (1996) Flavin-dependent alkyl hydroperoxide reductase from *Salmonella typhimurium*. 1. Purification and enzymatic activities of overexpressed AhpF and AhpC proteins. *Biochemistry* 35, 56−64.

(40) Ellis, K. J., and Morrison, J. F. (1982) Buffers of constant ionic strength for studying pH-dependent processes. *Methods Enzymol.* 87, 405−426.

(41) Sardi, F., Manta, B., Portillo-Ledesma, S., Knoops, B., Comini, M. A., and Ferrer-Sueta, G. (2013) Determination of acidity and nucleophilicity in thiols by reaction with monobromobimane and fluorescence detection. *Anal. Biochem.* 435, 74−82.

(42) Nelson, K. J., Parsonage, D., Hall, A., Karplus, P. A., and Poole, L. B. (2008) Cysteine pK(a) values for the bacterial peroxiredoxin AhpC. *Biochemistry* 47, 12860−12868.

(43) Hugo, M., Turell, L., Manta, B., Botti, H., Monteiro, G., Netto, L. E., Alvarez, B., Radi, R., and Trujillo, M. (2009) Thiol and sulfenic acid oxidation of AhpE, the one-cysteine peroxiredoxin from Mycobacterium tuberculosis: kinetics, acidity constants, and conformational dynamics. *Biochemistry* 48, 9416−9426.

(44) Poole, L. B., and Ellis, H. R. (2002) Identification of cysteine sulfenic acid in AhpC of alkyl hydroperoxide reductase. *Methods Enzymol.* 348, 122−136.

(45) Brändström, A., Lindberg, P., Bergman, N., Tekenbergs-Hjelte, L., and Ohlson, K. (1989) Chemical Reactions of Omeprazole and Omeprazole Analogues. IV. Reactions of Compounds of the Omeprazole System with 2-Mercaptoethanol. *Acta Chem. Scand.* 43, 577−586.

(46) Hall, A., Parsonage, D., Poole, L. B., and Karplus, P. A. (2010) Structural evidence that peroxiredoxin catalytic power is based on transition-state stabilization. *J. Mol. Biol.* 402, 194−209.

(47) Soito, L., Williamson, C., Knutson, S. T., Fetrow, J. S., Poole, L. B., and Nelson, K. J. (2011) PREX: PeroxiRedoxin classification indEX, a database of subfamily assignments across the diverse peroxiredoxin family. *Nucleic Acids Res.* 39, D332−337.

(48) Randall, L. M., Manta, B., Hugo, M., Gil, M., Batthyany, C., Trujillo, M., Poole, L. B., and Denicola, A. (2014) Nitration transforms a sensitive peroxiredoxin 2 into a more active and robust peroxidase. *J. Biol. Chem.* 289, 15536−15543.

(49) Pedre, B., Van Molle, I., Villadangos, A. F., Wahni, K., Vertommen, D., Turell, L., Erdogan, H., Mateos, L. M., and Messens, J. (2015) The *Corynebacterium glutamicum* mycothiol peroxidase is a reactive oxygen species-scavenging enzyme that shows promiscuity in thiol redox control. *Mol. Microbiol.* 96, 1176−1191.

(50) Espenson, J. H. (1995) *Chemical Kinetics and Reaction Mechanisms*, McGraw-Hill, New York.

(51) Perkins, A., Nelson, K. J., Williams, J. R., Parsonage, D., Poole, L. B., and Karplus, P. A. (2013) The sensitive balance between the fully folded and locally unfolded conformations of a model peroxiredoxin. *Biochemistry* 52, 8708−8721.

(52) Sies, H. (2017) Hydrogen peroxide as a central redox signaling molecule in physiological oxidative stress: Oxidative eustress. *Redox Biol.* 11, 613−619.

(53) Rabilloud, T., Heller, M., Gasnier, F., Luche, S., Rey, C., Aebersold, R., Benahmed, M., Louisot, P., and Lunardi, J. (2002) Proteomics analysis of cellular response to oxidative stress. Evidence for in vivo overoxidation of peroxiredoxins at their active site. *J. Biol. Chem.* 277, 19396−19401.

(54) Yang, K. S., Kang, S. W., Woo, H. A., Hwang, S. C., Chae, H. Z., Kim, K., and Rhee, S. G. (2002) Inactivation of human peroxiredoxin I during catalysis as the result of the oxidation of the catalytic site cysteine to cysteine-sulfinic acid. *J. Biol. Chem.* 277, 38029−38036.

(55) Peskin, A. V., Pace, P. E., Behring, J. B., Paton, L. N., Soethoudt, M., Bachschmid, M. M., and Winterbourn, C. C. (2016) Glutathionylation of the Active Site Cysteines of Peroxiredoxin 2 and Recycling by Glutaredoxin. *J. Biol. Chem.* 291, 3053−3062.

Differential Kinetics of Two-Cysteine Peroxiredoxin Disulfide Formation Reveal a Novel Model for Peroxide Sensing

Stephanie Portillo-Ledesma[a,b,c] [#], Lía M. Randall[a,c,d] [#], Derek Parsonage[e,f], Joaquín Dalla Rizza[a,b], P. Andrew Karplus[g], Leslie B. Poole[e,f], Ana Denicola[a,c] and Gerardo Ferrer-Sueta[a,c] [*]

[a]Laboratorio de Fisicoquímica Biológica and [b]Laboratorio de Química Teórica y Computacional, Instituto de Química Biológica, Facultad de Ciencias, and [c]Center for Free Radical and Biomedical Research, Universidad de la República, Montevideo, Uruguay. [d]Laboratorio de I+D de Moléculas Bioactivas, CENUR Litoral Norte, Universidad de la República, Paysandú, Uruguay [e]Department of Biochemistry and [f]Centers for Structural Biology and for Redox Biology and Medicine, Wake Forest School of Medicine, Winston-Salem, North Carolina 27157. [g]Department of Biochemistry and Biophysics, Oregon State University, 2011 AG Life Sciences Building, Corvallis, Oregon 97331.

Derivation of kinetic equations for fitting Figure 3

Using the mass balance and the expression of the equilibrium constant we can reach the pH-distribution of each species
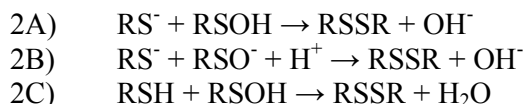
$$[RS(H)]_T = [RSH] + [RS^-] \qquad\qquad K_a^{SH} = \frac{[RS^-][H^+]}{[RSH]}$$

$$[RS(H)]_T = \frac{[RS^-][H^+]}{K_a^{SH}} + [RS^-] = [RS^-]\left(\frac{[H^+] + K_a^{SH}}{K_a^{SH}}\right)$$

$$[RS^-] = [RS(H)]_T \left(\frac{K_a^{SH}}{[H^+] + K_a^{SH}}\right) \tag{S1}$$

$$[RS(H)]_T = \frac{[RSH]K_a^{SH}}{[H^+]} + [RSH] = [RSH]\left(\frac{[H^+] + K_a^{SH}}{[H^+]}\right)$$

$$[RSH] = [RS(H)]_T \left(\frac{[H^+]}{[H^+] + K_a^{SH}}\right) \tag{S2}$$

$$[RSO(H)]_T = [RSOH] + [RSO^-] \qquad K_a^{SOH} = \frac{[RSO^-][H^+]}{[RSOH]}$$

$$[RSO(H)]_T = \frac{[RSO^-][H^+]}{K_a^{SOH}} + [RSO^-] = [RSO^-]\left(\frac{[H^+] + K_a^{SOH}}{K_a^{SOH}}\right)$$

$$[RSO^-] = [RSO(H)]_T \left(\frac{K_a^{SOH}}{[H^+] + K_a^{SOH}}\right) \tag{S3}$$

$$[RSO(H)]_T = \frac{[RSOH]K_a^{SOH}}{[H^+]} + [RSOH] = [RSOH]\left(\frac{[H^+] + K_a^{SOH}}{[H^+]}\right)$$

$$[RSOH] = [RSO(H)]_T \left(\frac{[H^+]}{[H^+] + K_a^{SOH}}\right) \tag{S4}$$

Taking into account the protonation states of thiol and sulfenic acid, there are four possible reactions leading to disulfide formation. Considering that RS$^-$ is the best nucleophile and RSOH is the best electrophile, in order of likelihood of being fast, those are:

2A) $RS^- + RSOH \rightarrow RSSR + OH^-$
2B) $RS^- + RSO^- + H^+ \rightarrow RSSR + OH^-$
2C) $RSH + RSOH \rightarrow RSSR + H_2O$

2D) $RSH + RSO^- \rightarrow RSSR + OH^-$

The general rate law of the reaction is:

$v = k\,[RS(H)]_T\,[RSO(H)]_T$

Which in turn is the sum of the rates of the four reactions (A − D) that are pH-dependent according to the pH distribution of the species involved, thus, the rate law of reaction A would be:

$v = k_{2A}\,[RS^-][RSOH]$

or, using equations S1 and S4 above,

$v = k_{2A}\,[RS(H)]_T\left(\frac{K_a^{SH}}{[H^+]+K_a^{SH}}\right)\,[RSO(H)]_T\left(\frac{[H^+]}{[H^+]+K_a^{SOH}}\right)$

with an apparent rate constant of

$k_{2A}^{app} = k_{2A}\left(\frac{K_a^{SH}}{[H^+]+K_a^{SH}}\right)\left(\frac{[H^+]}{[H^+]+K_a^{SOH}}\right) = k_{2A}\left(\frac{[H^+]K_a^{SH}}{[H^+]^2 + [H^+](K_a^{SH}+K_a^{SOH}) + K_a^{SH}K_a^{SOH}}\right)$

A similar process leads to the other apparent rate constants

$k_{2B}^{app} = k_{2B}\left(\frac{K_a^{SH}}{[H^+]+K_a^{SH}}\right)\left(\frac{K_a^{SOH}}{[H^+]+K_a^{SOH}}\right) = k_{2B}\left(\frac{K_a^{SH}K_a^{SOH}}{[H^+]^2 + [H^+](K_a^{SH}+K_a^{SOH}) + K_a^{SH}K_a^{SOH}}\right)$

$k_{2C}^{app} = k_{2C}\left(\frac{[H^+]}{[H^+]+K_a^{SH}}\right)\left(\frac{[H^+]}{[H^+]+K_a^{SOH}}\right) = k_{2C}\left(\frac{[H^+]^2}{[H^+]^2 + [H^+](K_a^{SH}+K_a^{SOH}) + K_a^{SH}K_a^{SOH}}\right)$

$k_{2D}^{app} = k_{2D}\left(\frac{[H^+]}{[H^+]+K_a^{SH}}\right)\left(\frac{K_a^{SOH}}{[H^+]+K_a^{SOH}}\right) = k_{2D}\left(\frac{[H^+]K_a^{SOH}}{[H^+]^2 + [H^+](K_a^{SH}+K_a^{SOH}) + K_a^{SH}K_a^{SOH}}\right)$

The overall apparent rate constant would be the sum:

$k_{res}^{app} = k_{2A}^{app} + k_{2B}^{app} + k_{2C}^{app} + k_{2D}^{app}$

Or

$$k_{res}^{app} = \left(\frac{k_{2A}[H^+]K_a^{SH} + k_{2B}K_a^{SH}K_a^{SOH} + k_{2C}[H^+]^2 + k_{2D}[H^+]K_a^{SOH}}{[H^+]^2 + [H^+](K_a^{SH}+K_a^{SOH}) + K_a^{SH}K_a^{SOH}}\right) \tag{S5}$$

The equation used to fit (equation 4 in the main text) actually considers $k_{2D} = 0$, *i.e.*

$$k_{res}^{app} = \left(\frac{k_{2A}[H^+]K_a^{SH} + k_{2B}K_a^{SH}K_a^{SOH} + k_{2C}[H^+]^2}{[H^+]^2 + [H^+](K_a^{SH} + K_a^{SOH}) + K_a^{SH}K_a^{SOH}}\right)$$

k_{2D} was fixed as 0 not only because it makes chemical sense but to avoid the convergence in the fitting process to an statistically equivalent solution where $k_{2A}K_a^{SH}$ and $k_{2D}K_a^{SOH}$ are exchanged. It can be seen in eq. S5 that the dependence of k_{res}^{app} is symmetrical for those products.

In the fitting process we forced the condition $K_a^{SOH} < K_a^{SH}$ based on the available evidence that the sulfenic acid was more acidic than the resolving thiol. Finally, the fitting is highly dependent on the values of k_{2A}, K_a^{SOH} and K_a^{SH}, and not so much on k_{2B}. The value of k_{2C} can be fixed as zero without affecting too much the quality of the fit or the value of the remaining parameters.

S3
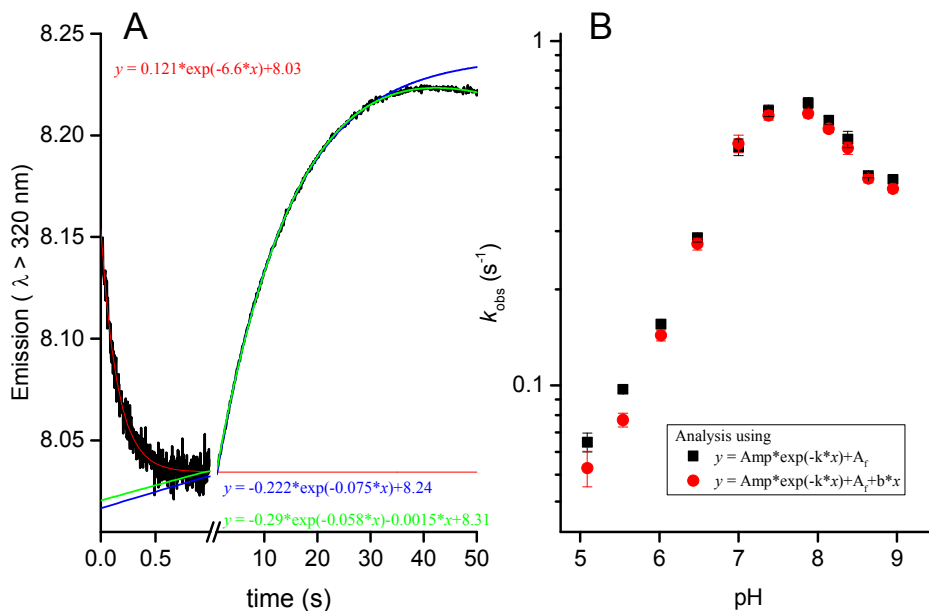
Figure S1. A. Averaged time course (ten runs) and fitting of the fluorescence of PRDX2 (0.5 μM) reacting with 5 μM H_2O_2 at pH 5.09. The two phases of the time course were fitted independently (red and blue lines), each to a single exponential function. The ascending phase was fitted from 2 to 35 s to avoid interference with the slow decay of fluorescence observed at longer times. Alternatively, a linear decrease term was included to account for the slow drift of the endpoint (green line). **B.** The rate constants obtained by fitting to either function are not significantly different and yield essentially the same pH profile.
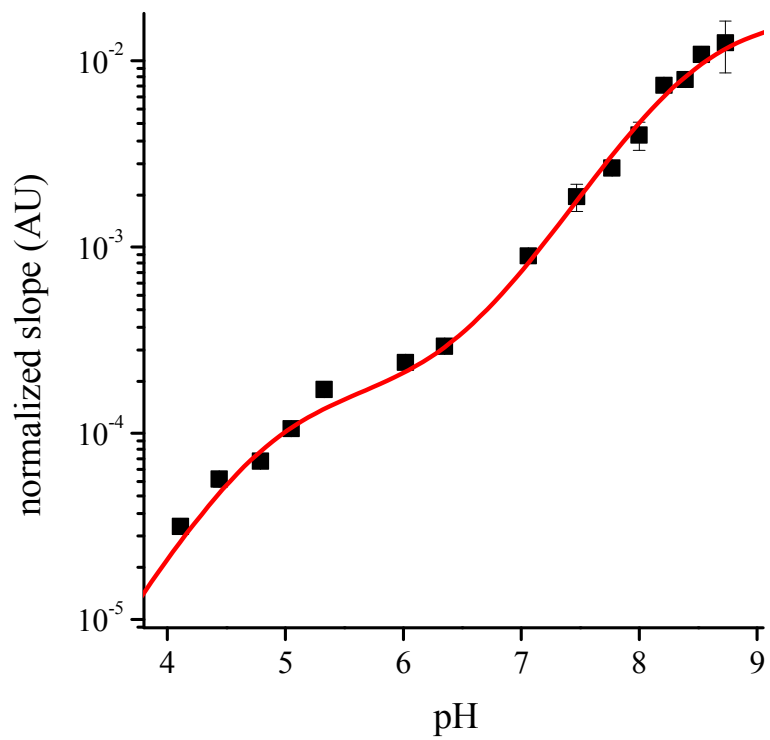
Figure S2. pH profile of the reaction rate of PRDX2 with mBBr. The data are fitted to a two pK_a function as previously described[41]. Best fit pK_a values are 4.8 ± 0.1 and 8.5 ± 0.2.

3.4. Rol de la Y193 en la resistencia a la sobreoxidación luego del tratamiento con peroxinitrito

3.4.1. Resumen

Las peroxirredoxinas son enzimas que reducen eficientemente hidroperóxidos mediante la participación de cisteínas (C_P, C_R). El primer paso en la catálisis, la reducción del peróxido sustrato, es rápido; 1×10^8 M^{-1} s^{-1} para la Prx2 humana. Por otra parte, la alta concentración intracelular de las Prx las posiciona no sólo como buenos antioxidantes sino también como protagonistas en las vías de señalización redox. Estas funciones biológicas pueden verse afectadas por modificaciones postraduccionales que puedan alterar su actividad peroxidasa y/o su interacción con otras proteínas. En particular, la inactivación por sobreoxidación de la C_P, que ocurre cuando una segunda molécula de peróxido reacciona con el ácido cisteinsulfénico de la C_P, modula su participación en vías de señalización redox. La mayor sensibilidad a sobreoxidarse de las Prx de 2-Cys típicas eucariotas comparado con las procariotas ha sido vinculada a la presencia de motivos estructurales que desfavorecen la formación del disulfuro en el sitio activo, dejando C_P-SOH más disponible para sobreoxidarse. Anteriormente reportamos que el tratamiento de Prx2 humana con peroxinitrito da lugar a una proteína con tirosinas nitradas, una modificación postraduccional en residuos no catalíticos, generándose una enzima con más actividad peroxidasa y mayor resistencia a sobreoxidarse. En este trabajo, se produjeron distintas mutantes de Prx2 humana para descifrar el efecto que tiene la nitración de tirosinas en la actividad peroxidasa de la enzima. En particular, se generaron variantes nitradas cotraduccionalmente en sitios específicos. Los resultados obtenidos confirman que Y193, perteneciente al motivo YF del extremo C-terminal de las Prx eucariotas, es necesaria para observar un aumento en la actividad peroxidasa y una mayor resistencia a sobreoxidarse luego del tratamiento con peroxinitrito. Los resultados apoyan el rol crítico de este motivo estructural en la velocidad de formación del disulfuro que determinará la participación diferencial de las Prx en las vías de señalización redox.

3.4.2. Principales resultados obtenidos

- El tratamiento de la Prx2 humana recombinante con peroxinitrito produce una enzima más activa y más robusta, al igual que lo obtenido para la enzima purificada de glóbulos rojos humanos.

- La incorporación de un residuo de nitrotirosina co-traduccionalmente en las posiciones 33, 43 y 126 permite obtener muestras con 100% de nitración en un único sitio, obteniendo así muestras homogéneas. Sin embargo, la incorporación de un grupo nitro en dichas posiciones no reproduce los efectos observados al tratar a la enzima con peroxinitrito.

- La incorporación co-traduccional de un residuo de tirosina en la posición 193 no fue posible, pero el tratamiento con peroxinitrito de la enzima sin Y193 (Y193F) da como resultado una enzima menos activa, o sea, no reproduce el efecto observado con la enzima *wild type*.

- El análisis computacional del efecto de una mutación puntual en la posición 193 sobre la estabilidad de la enzima y en particular la flexibilidad del C-terminal indica que fenilalanina en esa posición rigidiza mientras que glicina flexibiliza el loop. La mutante Y193G resulta en una enzima más activa como peroxidasa con menor sensibilidad a sobreoxidarse, lo que sugiere que flexibilizando ese extremo de la proteína se obtienen los mismos resultados que al nitrarla con peroxinitrito.

- En conjunto, los resultados apuntan a la nitración de Y193 como responsable del aumento de actividad y resistencia a la sobreoxidación observados y afirman el rol protagónico del motivo YF en la modulación de la actividad Prx2 humana por peroxinitrito.

3.4.2. Artículo publicado en Free Radical Biology and Medicine

Original article

Unraveling the effects of peroxiredoxin 2 nitration; role of C-terminal tyrosine 193

Lía M. Randall[a,b,c,1], Joaquín Dalla Rizza[b,c,1], Derek Parsonage[d], Javier Santos[e,f], Ryan A. Mehl[g], W. Todd Lowther[d], Leslie B. Poole[d,**], Ana Denicola[b,c,*]

[a] Laboratorio I+D de Moléculas Bioactivas, CENUR Litoral Norte, Universidad de la República, Paysandú, Uruguay
[b] Laboratorio de Fisicoquímica Biológica, Facultad de Ciencias, Universidad de la República, Montevideo, Uruguay
[c] Centro de Investigaciones Biomédicas, Universidad de la República, Uruguay
[d] Department of Biochemistry and Center for Redox Biology and Medicine, Wake Forest School of Medicine, Winston-Salem, NC, USA
[e] Departamento de Fisiología y Biología Molecular y Celular, Facultad de Ciencias Exactas y Naturales, Universidad de Buenos Aires, Buenos Aires, Argentina
[f] Instituto de Química y Fisicoquímica Biológicas (UBA-CONICET), Buenos Aires, Argentina
[g] Department of Biochemistry and Biophysics, Oregon State University, Corvallis, OR, USA

ABSTRACT

Peroxiredoxins (Prx) are enzymes that efficiently reduce hydroperoxides through active participation of cysteine residues (C_P, C_R). The first step in catalysis, the reduction of peroxide substrate, is fast, $10^7 - 10^8 \, M^{-1} s^{-1}$ for human Prx2. In addition, the high intracellular concentration of Prx positions them not only as good antioxidants but also as central players in redox signaling pathways. These biological functions can be affected by post-translational modifications that could alter the peroxidase activity and/or interaction with other proteins. In particular, inactivation by hyperoxidation of C_P, which occurs when a second molecule of peroxide reacts with the C_P in the sulfenic acid form, modulates their participation in redox signaling pathways. The higher sensitivity to hyperoxidation of some Prx has been related to the presence of structural motifs that disfavor disulfide formation at the active site, making the C_P sulfenic acid more available for hyperoxidation or interaction with a redox protein target. We previously reported that treatment of human Prx2 with peroxynitrite results in tyrosine nitration, a post-translational modification on non-catalytic residues, yielding a more active peroxidase with higher resistance to hyperoxidation. In this work, studies on various mutants of hPrx2 confirm that the presence of the tyrosyl side-chain of Y193, belonging to the C-terminal YF motif of eukaryotic Prx, is necessary to observe the increase in Prx2 resistance to hyperoxidation. Moreover, our results underline the critical role of this structural motif on the rate of disulfide formation that determines the differential participation of Prx in redox signaling pathways.

1. Introduction

Peroxiredoxins (Prx) are enzymes that efficiently reduce hydroperoxides through active participation of one or two cysteine residues [1]. The catalytic cycle can be divided into three steps: 1) the reduction of peroxide via oxidation of the peroxidatic cysteine (C_P-SH) to sulfenic acid (C_P–SOH), 2) the resolution step, that for typical 2-Cys Prx involves the condensation of the sulfenic acid with the resolving cysteine (C_R-SH) to form an intersubunit disulfide, and 3) the reduction of the disulfide at the expense of thioredoxin or other reductant. The resolution step demands a conformational change to bring both cysteine residues together in order to make the disulfide bond, the so-called FF (fully-folded) to LU (locally-unfolded) transition. The C_P-SOH has a second potential fate; it can either react with the resolving cysteine C_R-SH (which requires the FF to LU transition) or (in FF) with a second peroxide molecule forming cysteine sulfinic acid C_P-SO$_2$H (hyperoxidation).

The first step in catalysis, the reduction of peroxide substrate, is fast. In particular, the rate constant for the reduction of hydrogen peroxide (H_2O_2) by the peroxidatic cysteine of human Prx2 (a typical 2-Cys Prx) is $1 \times 10^8 \, M^{-1} s^{-1}$ [2], more than a million times faster than the reaction of H_2O_2 with a low molecular weight thiol [3]. Structural and

---

computational studies have helped uncover the particular active site architecture that explains this extraordinary acceleration [4–7]. In addition, the intracellular concentration of Prx is high (10–400 μM), positioning them not only as good antioxidants but also as central players in redox signaling pathways [8,9].

These biological functions can be affected by post-translational modifications (PTM) that could alter aspects of the peroxidase activity and/or the interaction with other proteins. The latter would be extremely important in the transduction of the signal in a redox-relay mechanism and in the reduction step of the catalytic cycle [10,11]. Any covalent modification of the C_P will inactivate the enzyme, as observed before for nitrosation or glutathionylation [12–14]. Hyperoxidation of C_P also leads to inactivation of Prx2, at least during a period of time before the slow sulfiredoxin-dependent reduction of C_P-SO_2H takes place [15]. It was noted that the bacterial Prx were more resistant to hyperoxidation than the eukaryotic counterparts which led to a classification into robust *vs* sensitive Prx. Early comparative structural analysis revealed that sensitive Prx present YF and GGLG motifs close to the active site that are largely absent in prokaryotes [16,17]. The YF sequence motif in the C-terminal helix of one subunit covers helix α2 containing the C_P of the adjacent subunit, hindering the unfolding of the C_P-containing α2 to reach C_R and form the disulfide. More recently, additional molecular determinants were discovered, motifs A and B, that even discriminate distinct levels of sensitivity to hyperoxidation amongst the sensitive Prx [18].

We have previously reported that treatment of human Prx2 with peroxynitrite results in tyrosine nitration, a PTM on non-catalytic residues [19]. Even though Prx2 is a peroxynitrite reductase, the enzyme gets nitrated (on tyrosine residues) as well as hyperoxidized (on its peroxidatic cysteine) in turnover [2,20]. Under conditions of high oxidant flux, most of intracellular Prx is found in the disulfide-oxidized form, and in this form, it is more easily modified on tyrosine residues by peroxynitrite. Nitration of tyrosines after peroxynitrite treatment of the disulfide-containing Prx2 surprisingly resulted in an enzyme more active as a peroxidase, with higher resistance to hyperoxidation [19].

Protein tyrosine nitration is a common PTM occurring under conditions of nitroxidative stress, which alters the structure and function of the modified protein. The biological mechanism of protein nitration is a radical mechanism involving the one-electron oxidation of a tyrosine residue to form the tyrosyl radical followed by addition of nitrogen dioxide ($NO_2^•$) to yield 3-nitrotyrosine [21,22]. The radicals derived from peroxynitrite homolysis represent a major source of tyrosine nitration *in vivo* [23]. Although non-enzymatically catalyzed, specificity in protein nitration is achieved *in vivo* [24]. Proteomic analysis revealed the presence of 3-nitrotyrosine on select proteins as well as specific tyrosine residues. PrxII E from *Arabidopsis thaliana* was found nitrated after inducing oxidative stress in plants [25] and Prx1 was found nitrated (on Y194) on Jurkat cells exposed to peroxynitrite [26]. Nitrated proteins have been detected in plasma and tissues of patients with oxidative stress-associated pathologies and aging. In particular, nitrated Prx2 was found in patients with early Alzheimer's disease [27] and mitochondrial Prx3 was found nitrated in diabetic mice hearts [28].

Human Prx2 is a decamer composed of five head-to-tail homodimers and each monomer contains seven tyrosine residues, all of them at least somewhat exposed to the solvent (Fig. 1). Mass spectrometry analysis of disulfide-containing Prx2 treated with peroxynitrite revealed that tyrosine nitration was the main modification on the protein and nitration of three residues (Y33, Y126 and Y193) was confirmed [19]. Although peroxynitrite treatments could be adjusted to limit modification of the Prx2 protein molecules to 1–1.5 sites of nitration on average, all preparations were undoubtedly complex mixtures with up to two sites modified, potentially also on different tyrosine residues within the mixture. Despite this, the peroxynitrite-treated Prx2 always behaved as a more robust Prx compared with the non-treated enzyme.

Herein, mutants of human Prx2 were produced in order to unravel the effects of tyrosine nitration on the activity of this protein, which
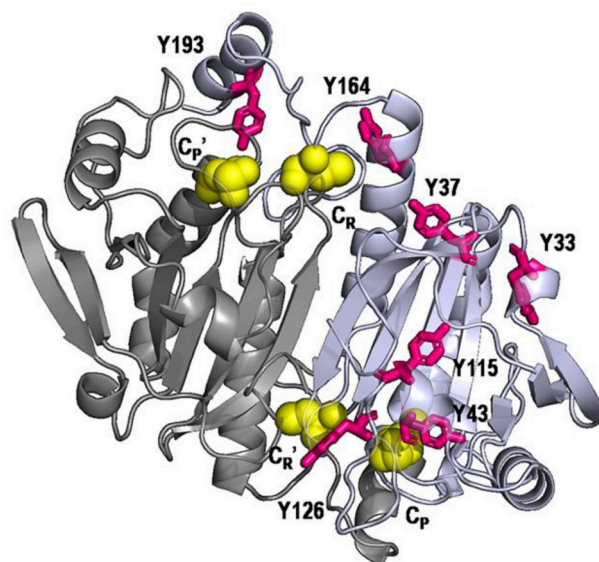
Fig. 1. Representation of the human Prx2 dimer. The 7 tyrosine residues (magenta) from chain A (light gray) are shown, as well as the cysteine residues of both active sites of the dimer: C_P and C_R of chain A (light gray); and C_P' and C_R' of chain B (dark gray); C_P is C51, C_R is C172. Figure constructed using Pymol from pdb 1QMV.

could impact on its role as a H_2O_2 sensor/transducer. In particular, specific co-translationally nitrated variants of the protein on different tyrosine residues were generated using genetic code expansion technology to incorporate unnatural amino acids. Together, our results confirm that the presence of Y193 is necessary to observe an increase in peroxidase activity and a more robust Prx2 after nitration by peroxynitrite. The results underline the critical role of this C-terminal residue on the rate of disulfide formation that affects the fate of Prx2 in redox signaling pathways.

2. Materials and methods

2.1. Chemicals

Dithiothreitol (DTT), N-ethylmaleimide (NEM) and reduced nicotinamide adenine dinucleotide phosphate (NADPH) were purchased from AppliChem (Germany). Hydrogen peroxide (H_2O_2), 3-nitro-L-tyrosine and diethylenetriaminepentaacetic acid (DTPA) were purchased from Sigma-Aldrich (USA).4,4′-Dithiodipyridine (DTDPy) was from Acros Organics (Fisher Scientific, USA). Peroxynitrite was synthesized as in Ref. [29]. All other reagents were of analytical grade and used as received.

2.2. Methods

2.2.1. Peroxide and protein quantification

The concentration of H_2O_2 was measured at 240 nm ($\epsilon_{240} = 39.4\,M^{-1}\,cm^{-1}$) [30], peroxynitrite concentration was determined at alkaline pH at 302 nm ($\epsilon_{302} = 1670\,M^{-1}\,cm^{-1}$) [31] and *E. coli* thioredoxin reductase (TR) concentration was measured at 280 nm ($\epsilon_{280} = 51,700\,M^{-1}\,cm^{-1}$) [32]. Prx2 wild-type, mutants and *E. coli* thioredoxin 1 (Trx) were quantified by the absorption at 280 nm, using the corresponding ϵ determined with https://web.expasy.org/protparam/: $\epsilon_{280} = 21,555\,M^{-1}\,cm^{-1}$ for $(Prx2)_{SS}$, $(Prx2\ Y193F)_{SS}$, and $(Prx2\ Y193M)_{SS}$, $\epsilon_{280} = 21,430\,M^{-1}\,cm^{-1}$ for $(Prx2)_{SH}$, $(Prx2\ Y193F)_{SH}$, $(Prx2\ Y93G)_{SH}$, and $\epsilon_{280}\ (EcTrx)_{SH} = 14,060\,M^{-1}\,cm^{-1}$. The co-translationally nitrated variants of Prx2 (NO_2Y33, NO_2Y43 and NO_2Y126 Prx2) were quantified using the Bradford method and BSA for the calibration curve.

2.2.2. Protein expression and purification

2.2.2.1. Wild-type Prx2, Y193F, Y193G and Y193 M Prx2 mutants. Recombinant proteins were expressed with two different constructs; non-tagged recombinant wild-type Prx2 and the Y193F mutant were expressed and purified as in Ref. [33] using a pET17 vector in BL21-Gold (DE3) with the modification that lactose autoinduction media, ZYM-5052, containing $100 \,\mu g \, ml^{-1}$ ampicillin, was used for expression overnight at 25 °C [34]. The QuikChange mutagenesis protocol was used to create the Y193F mutation in the wild-type vector. On the other hand, Y193G and Y193 M Prx2 were expressed and purified as reported for PRDX1 in Ref. [35] using a pET28a plasmid containing the coding sequence of wild type *Hs*Prx2 fused to a His-tag and a cleavage site for the protease TEV at the N-terminus (synthesized and codon-optimized by Genscript). Mutagenesis was performed using a QuikChangeTM site-directed mutagenesis kit (Stratagene). All of the site-directed mutations were confirmed by DNA sequencing.

Purified proteins were concentrated and stored at -20 °C in buffer A (50 mM sodium phosphate and 150 mM NaCl, 0.1 mM DTPA, pH 7.4). Purity was evaluated by SDS-PAGE.

2.2.2.2. Co-translationally nitrated Prx2 variants. The pET17 clone containing the gene for wild-type Prx2 was mutated to convert the native amber TAG stop codon to TAA, an ochre stop codon. Individual Tyr codons at positions 33, 43, 126 and 193 were then mutated to a TAG amber codon. BL21-ai (arabinose inducible) competent cells were co-transformed with one of these mutated plasmids and pDule2-3nY-5B, a plasmid expressing mutated tRNA and aminoacyl-tRNA synthetase genes which direct nitrotyrosine incorporation at TAG codons [36]. Protein expression was carried out in the arabinose induction media described by Hammill et al. [37] modified to include a final concentration of 1 mM 3-nitrotyrosine from a $50 \, mg \, ml^{-1}$ stock dissolved in 1 M HCl. Overnight growth at 37 °C was found to be optimal for expression of Prx2 containing nitrotyrosine. Purification of nitrotyrosine-containing Prx2 was carried out as described above for non-tagged, wild-type Prx2. Attempted expression of Prx2 with nitrotyrosine incorporation at codon 193 consistently gave a mix of truncated as well as successfully extended protein, which could not be separated during the purification steps. Re-engineering of the expression vector to include cleavable fusion proteins at the C-terminus was also unsuccessful in generating the nitrated protein at Y193.

2.2.2.3. Proteins for the coupled activity assay. E. coli thioredoxin 1 (*Ec*Trx) was expressed and purified according to Ref. [38] and *E. coli* thioredoxin reductase (*Ec*TR) as reported in Ref. [39]. Protein purity was evaluated by SDS-PAGE.

2.2.3. Prx2 thiol reduction and oxidation

For reduction of purified Prx2, the enzyme was incubated with 1 mM DTT for 30 min at room temperature immediately before the experiment, and the mixture was passed twice through a Vivaspin ultrafiltration spin column (5 kDa MWCO, GE Healthcare) pre-equilibrated with the assay buffer. Thiol concentration was determined immediately after recovery of the protein. Controlled oxidation of reduced Prx2 to its disulfide form was achieved with the addition of 0.6 equivalents of H_2O_2 per thiol, probed to be enough oxidant to form the disulfide without hyperoxidation to sulfinic acid [19].

2.2.4. Nitration of Prx2 with peroxynitrite

Peroxynitrite has been shown to react with Prx2 C_P, hyperoxidizing it to its sulfinic and even sulfonic acid form [2]. To prevent these modifications of C_P, treatment with peroxynitrite was performed on the disulfide-oxidized enzyme. Disulfide-oxidized Prx2 (130 μM) was treated with a five-fold excess peroxynitrite in a flux-like addition, as described in Ref. [19]. This protocol had to be followed rigorously in

order to obtain reproducible results after nitration, considering that nitration yields depend on the rate of radicals production from peroxynitrite [21,40]. As a control, peroxynitrite was previously decomposed in the assay buffer and then added to the protein (reverse-order addition, ROA). After treatment with peroxynitrite or its decomposition products, Prx2 thiols were reduced with DTT and oxidized to disulfide when needed, as described above.

2.2.5. NADPH-linked peroxidase activity (coupled assay)

Peroxidase activity was measured spectrophotometrically through a coupled assay following the NADPH consumption at 340 nm $(\epsilon_{340} = 6.2 \, mM^{-1} \, cm^{-1})$ in a cuvette containing 200 μM NADPH, 1 μM *Ec*TR, 8 μM *Ec*Trx1 and 0.5 μM Prx in buffer A. The reaction was started by adding the specified amount of H_2O_2. All spectrophotometric measurements were made with a Cary 50 spectrophotometer (Varian, Australia).

2.2.6. Determination of $C_{hyp1\%}$ in turnover

Using the NADPH-linked peroxidase activity assay, $C_{hyp1\%}$ (as the peroxide concentration at which 1 out of every 100 Prx molecules would be inactivated per turnover) was determined for wild type and Prx2 mutants according to Ref. [41].

2.2.7. Kinetics followed by intrinsic fluorescence

Reaction of pre-reduced enzymes with H_2O_2 was detected by following the change in their intrinsic fluorescence as described in Ref. [35] in an Applied Photophysics SX20 stopped-flow fluorimeter with a mixing time of less than 2 m s, with $\lambda_{ex} = 280$ nm, measuring the total emission above 320 nm. Prx (0.25 μM) in buffer A was reacted with different concentrations of H_2O_2 diluted in buffer A. At low oxidant concentrations ($< 10 \, \mu M$) the time courses were biphasic (a fast drop, followed by a slow increase in the signal) and fit to a double exponential function. The fast phase, rapid decrease in fluorescence was associated to the reaction Prx-C_P-SH + $H_2O_2 \rightarrow$ Prx-C_P-SOH ($k_{fast} = k_{H2O2}$). When working at higher H_2O_2 concentrations, the downward phase became faster than the dead time of mixing (thus hard to register), and the slower phase was fit to a monoexponential decay (k_{slow}). This slower recovery of fluorescence, k_{slow}, was associated with the two processes competing for C_P-SOH: disulfide formation (k_{res}) and hyperoxidation to C_P-SO_2H (k_{hyp}).

$$k_{slow} = k_{res} + k_{hyp}[H_2O_2] \qquad (1)$$

From the curve k_{slow} *vs* $[H_2O_2]$, the bimolecular rate constant of hyperoxidation, k_{hyp} (slope), and the first-order rate constant of re-solution, k_{res} (y-axis intercept) were determined for each protein assayed.

2.2.8. Direct determination of $C_{hyp1\%}$

Knowing the rate constants of the two competing processes, k_{res} and k_{hyp}, the fraction of inactive sulfinylated Prx, f_{inact}, at specific concentrations of H_2O_2 can be estimated as:

$$f_{inact} \approx k_{hyp} \, [H_2O_2] \, / \, k_{res} \qquad (2)$$

The value of $C_{hyp1\%}$ as the concentration of H_2O_2 that yields 1% inactivated/hyperoxidized Prx can be calculated from $f_{inact} = 0.01$, thus:

$$C_{hyp1\%} = 0.01 \times k_{res} \, / \, k_{hyp} \qquad (3)$$

2.2.9. Prx2 circular dichroism (CD) spectra analysis

Spectra of Prx2 wild-type, mutants and nitro variants were acquired at 20 °C using a Jasco 810 spectropolarimeter (with a Jasco CDF-4265/15 Peltier-effect device). Near- UV measurements were carried out in 1 cm cells containing 40 μM Prx2 in buffer A. For far-UV measurements, 0.1 cm cells were used, and protein samples were diluted to 4 μM in the
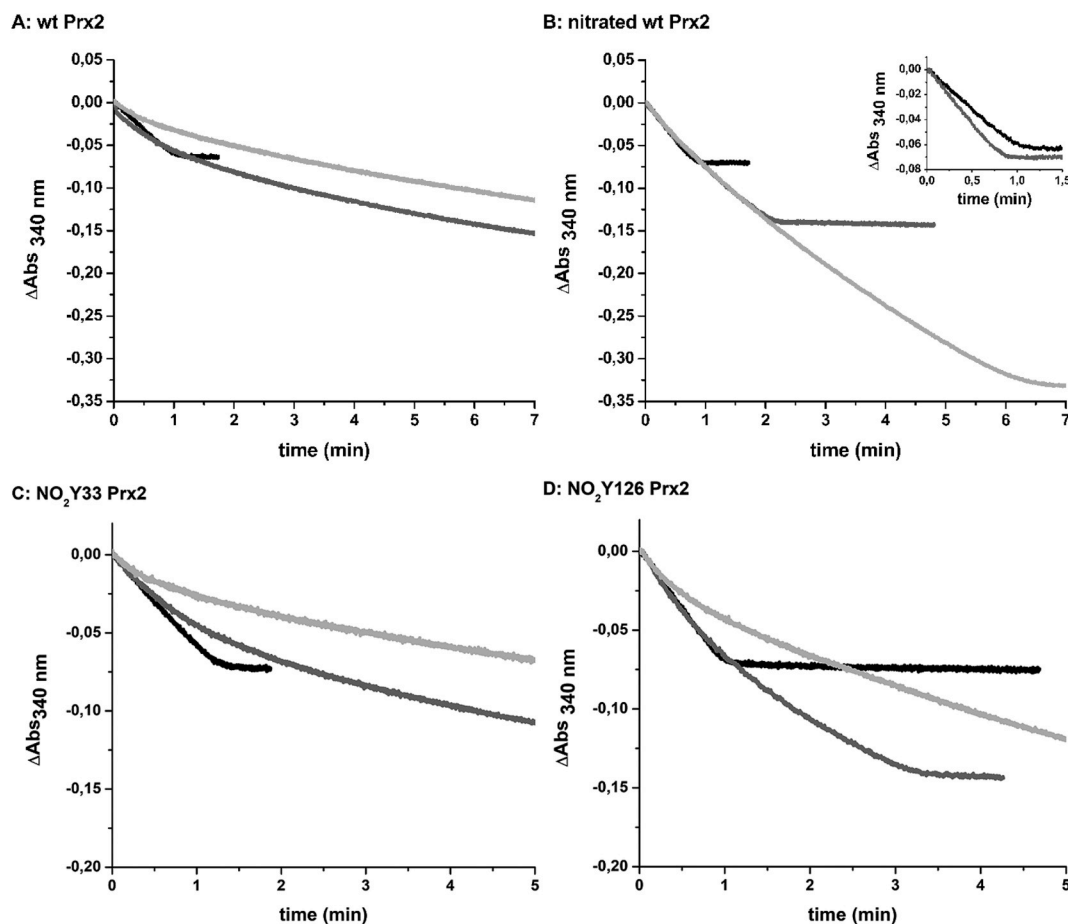
Fig. 2. Peroxidase activity of recombinant wild-type Prx2, with and without peroxynitrite treatment, and specific nitro variants. (**A**) Coupled assay of peroxidase activity of wild type Prx2. For activity measurements, 200 μM NADPH, 1 μM *Ec*TR, 8 μM *Ec*Trx1 and 0.5 μM Prx2 were used, and reaction was started with 10 μM H_2O_2 (black), 20 μM H_2O_2 (dark gray) or 50 μM H_2O_2 (light gray). Consumption of NADPH was followed at 340 nm. (**B**) Coupled assay peroxidase activity of nitrated wild-type Prx2 in the same conditions used in A. **Inset.** Coupled assay peroxidase activity of wild-type Prx2 non-treated (black) or treated with a 5-fold excess peroxynitrite (gray) using 10 μM H_2O_2. (**C**) Coupled assay peroxidase activity of nitro-variant NO_2Y33 Prx2 and (**D**) NO_2Y126 Prx2, in the same conditions used in A.

same buffer. Scans of buffer were properly smoothed and subtracted from the corresponding averaged sample spectra.

2.2.10. Bioinformatics and conformational stability predictions

The contribution of a given side chain to the global stability of the Prx2 was explored by means of two different computational methods: FOLDX [42,43] and *Dynamut* [44]. The former is based on an empirical physic force field, whereas the latter is based on a statistical force field which additionally introduces the dynamics component to mutation analysis. In both cases the calculation of the free energy contribution was carried out using the high-resolution 3D structure of a Prx2 (PDB ID: 1QMV) in which the hyperoxidized Cys 51 residue was first converted to Cys and then, the routine 'repair' tool from FOLDX was run in order to minimize the energy of the model (side-chains with wrong torsion angles or van der Waals' clashes were identified and corrected by changing the side-chain rotamers). In addition, the calculations were performed using the dimer AB and the mutation was introduced only in chain A. The $\Delta\Delta G^o_{NU} = \Delta G^o_{NU\ wild-type} - \Delta G^o_{NU\ mutant}$ was considered for the interpretation of the calculations.

The dimer AB from Prx2 structure PDB ID: 1QMV was examined using *Frustratometer* [45] in order to infer the localization of energetic frustration in the native protein structure. Frustration is a measure of how favorable a particular contact is relative to sets of possible interactions. The individual contacts can be classified regarding their frustration index values in contacts minimally, neutral, or highly frustrated.

Mutational frustration was evaluated, that is: how favorable the native residues are relative to other possible residues in that location. *Frustatometer* evaluates every possible mutation of the amino acid pair that forms a particular contact in a fixed structure. Importantly, the energy change observed comes from the particular contact probed but also from interactions of each residue with other residues of the protein.

2.2.11. Molecular dynamics (MD) simulations

The coordinates corresponding to Prx2 structure (PDB ID: 1QMV) were used as starting structure for classical molecular dynamics simulation. Given that C_P is oxidized to sulfinic acid, it was in silico transformed to Cys (thiolate state). Additionally, Y193G, Y193M and Y193F mutants were prepared. Mutations were performed in every chain of the decamer. Each system was solvated with TIP3P water molecules [46] and a standard minimization protocol was applied. The systems were heated up from 100 K to 300 K, using the Berendsen thermostat and subsequently switched to a constant isotropic pressure to allow the density to equilibrate. The SHAKE algorithm was applied and a 2 fs time step was settled. Unrestrained MD simulations were performed with the Amber 16 software [47] and all used residue parameters corresponding to the ff14SB force field [48]. Production MDs were run at 300 K for 100 ns Analysis was performed using Amber Tools package.

2.2.12. Thermal-induced denaturation

Heat-induced denaturation of Prx2 wild-type and mutants was

carried out in a Chronos FD fluorimeter (ISS, USA) equipped with a Peltier-type temperature controller. Thermal denaturation was recorded following changes in fluorescence spectra (excitation at 280 nm, emission from 310 nm to 450 nm) from 25 °C to 65 °C at 5 °C intervals and allowing 10 min for equilibration at each temperature. The protein concentration was 2 μM in 50 mM phosphate buffer, pH 7.4, 150 mM NaCl, 0.1 mM DTPA, 1 mM DTT and 1 M urea (to reduce temperature of melting and avoid aggregation).

3. Results

Our previous studies on nitration of human Prx2 were performed on the enzyme purified from red blood cells, thus, the first step was to obtain the human recombinant protein in order to generate different mutations on its tyrosine residues. Importantly, the same peroxynitrite-dependent effects were observed on the recombinant protein as on protein purified from red blood cells, i.e. the peroxidase activity increased with a decrease in hyperoxidation sensitivity (Fig. 2A and B). The analysis of steady-state kinetics (coupled assay) at different H_2O_2 concentrations allows in a simple graphical way, easy comparison of the sensitivity of these enzymes to oxidative inactivation. Given the low apparent K_m of Prx2 for H_2O_2 and the catalytic mechanism of this protein [2,8], it is expected that, at low peroxide concentrations, all the substrate is consumed at maximum velocity as observed when 10 μM H_2O_2 is used (Fig. 2A). However, for a sensitive enzyme like Prx2, the peroxide consumption rate at a concentration as low as 20 μM already significantly decreases during turnover (Fig. 2A), which has been associated with inactivation by hyperoxidation of its peroxidatic cysteine [41]. Nitration of Prx2 by peroxynitrite yields an enzyme able to work at maximal activity at higher H_2O_2 concentrations over many turnovers, i.e. more resistant to hyperoxidation (Fig. 2B).

3.1. Co-translational incorporation and kinetic analysis of specific nitro-tyrosine residues

Treatment of native Prx2 with peroxynitrite resulted in detectable nitration of three of the seven tyrosine residues of the protein (Y33, Y126 and Y193, Fig. 1), but this nitration was shown to be non-stoichiometric and complex [19,49]. One approach to study the role of tyrosine nitration on Prx2 functionality was to use the elegant method developed by R. Mehl's group that uses genetic code expansion to site-specifically incorporate non-canonical amino acids into proteins [50,51]. We succeeded in producing homogeneous, high-quality nitrated forms of Prx2 on residues Y33 and Y126, as confirmed by ESI-TOF MS (Fig. 1S) and UV–vis absorption spectra (Fig. 2S). Far-UV CD spectra (Fig. 3S) confirmed that the nitro variants displayed essentially the same secondary structure as the wild type in the reduced as well as the oxidized form [49]. The near-UV CD spectra showed a notable decrease of the signal around 280 nm after disulfide formation as

observed before for the wild type enzyme [49].

Peroxidase activity of these nitro variants was measured using the coupled assay following NADPH consumption at 340 nm, as shown in Fig. 2C and D. Interestingly, both nitro variants were active peroxidases in the conditions of our assay, although differences in the susceptibility to hyperoxidation were observed. Again, the activity using the coupled assay was measured at three different H_2O_2 concentrations, giving a sense of the differential susceptibility to hyperoxidation. While NO_2Y33 showed a decrease in peroxidase activity at a H_2O_2 concentration as low as 20 μM (Fig. 2C), NO_2Y126 Prx2 was more resistant to hyperoxidation, not showing loss of activity until 50 μM H_2O_2 (Fig. 2D). Importantly, none of the mononitrated variants assayed were as robust as the peroxynitrite-treated enzyme (Fig. 2B).

In addition, NO_2Y43 Prx2 was expressed and successfully purified. Although Y43 was not detected as nitrated by MS after peroxynitrite treatment of Prx2 [19], it is located in a critical position in proximity to the interface between dimers and accessible to the solvent (Fig. 1). As seen for the other nitrovariants, the mononitrated variant on Y43 did not behave as the nitrated wtPrx2 (Fig. 4S).

Unfortunately, homogenous NO_2Y193 Prx2 could not be adequately expressed since during synthesis in E. coli this variant was prone to becoming prematurely truncated, a result observed by other authors when trying to incorporate modified amino acid residues at the C-terminus of a protein [52]. The obtained mixture of full-length protein presumably containing 3-nitrotyrosine along with protein truncated at the C-terminus could not be resolved during purification, suggesting that dimerization of the Prx2 is not significantly affected by the truncation. As described in more detail below, however, the characterization of a panel of site-directed mutants at position Y193 did prove to be useful.

3.2. Characterization of Prx2 Y193 mutants

Since the NO_2Y193 variant could not be obtained, point mutations were designed to test the important structural/functional role of this residue at position 193. The first approach was to delete the tyrosine residue at that position and the mutant Y193F was generated. Although the mutant Y193F Prx2 showed higher peroxidase activity than the wild type enzyme in the NADPH-linked coupled assay (Fig. 3A), (probably due to the fact that the C-terminus was modified, which has repeatedly been related to changes in activity for typical 2-Cys Prx [53–56]), the effect of peroxynitrite treatment on this mutant was totally different than for the wild type enzyme (Fig. 3A). Disulfide-containing Y193F Prx2 treated with peroxynitrite yielded a nitrated protein on tyrosine residues other than Y193, as shown in Fig. 3C. However, the nitrated Y193F Prx2 was a less active peroxidase, still sensitive to inactivation by hyperoxidation (Fig. 3A and B). It is worth noting that peroxynitrite is capable of nitrating tyrosine and tryptophan residues but not phenylalanine [57].
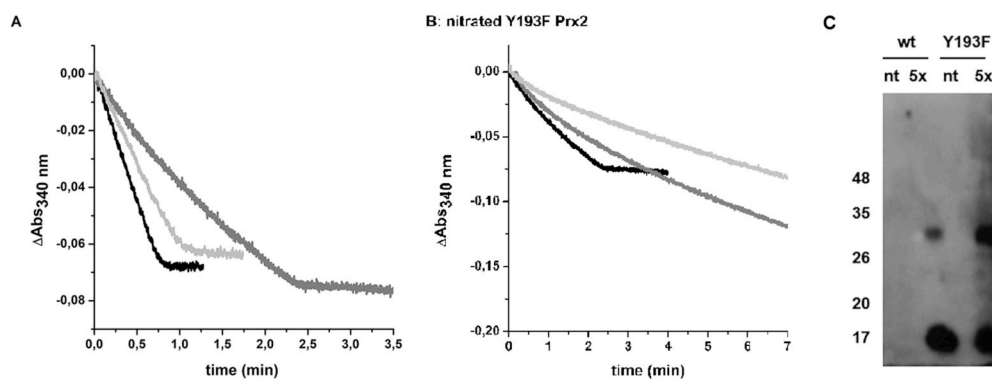
Fig. 3. Effect of nitration on NADPH-linked peroxidase activity of wild type vs Y193F Prx2. (**A**) Non-treated Y193F Prx2 is shown in black while protein treated with a 5-fold excess of peroxynitrite is shown in dark gray. Wild type Prx2 activity is shown in light gray. To start the reactions, 10 μM H_2O_2 was added and consumption of NADPH was followed at 340 nm. (**B**) The same treatments and assays were done with nitrated Y193F Prx2 using increasing concentrations of H_2O_2 [10 μM H_2O_2 (black), 20 μM H_2O_2 (dark gray) or 50 μM H_2O_2 (light gray)]. (**C**) Western blot of wild-type and Y193F Prx2, non-treated or treated with 5-fold excess peroxynitrite were resolved by a 12% reducing SDS-PAGE. A polyclonal antibody against nitrated tyrosine residues [58] was used in a 1/5000 dilution and a secondary antibody conjugated to HRP was used in a 1/100,000 dilution.
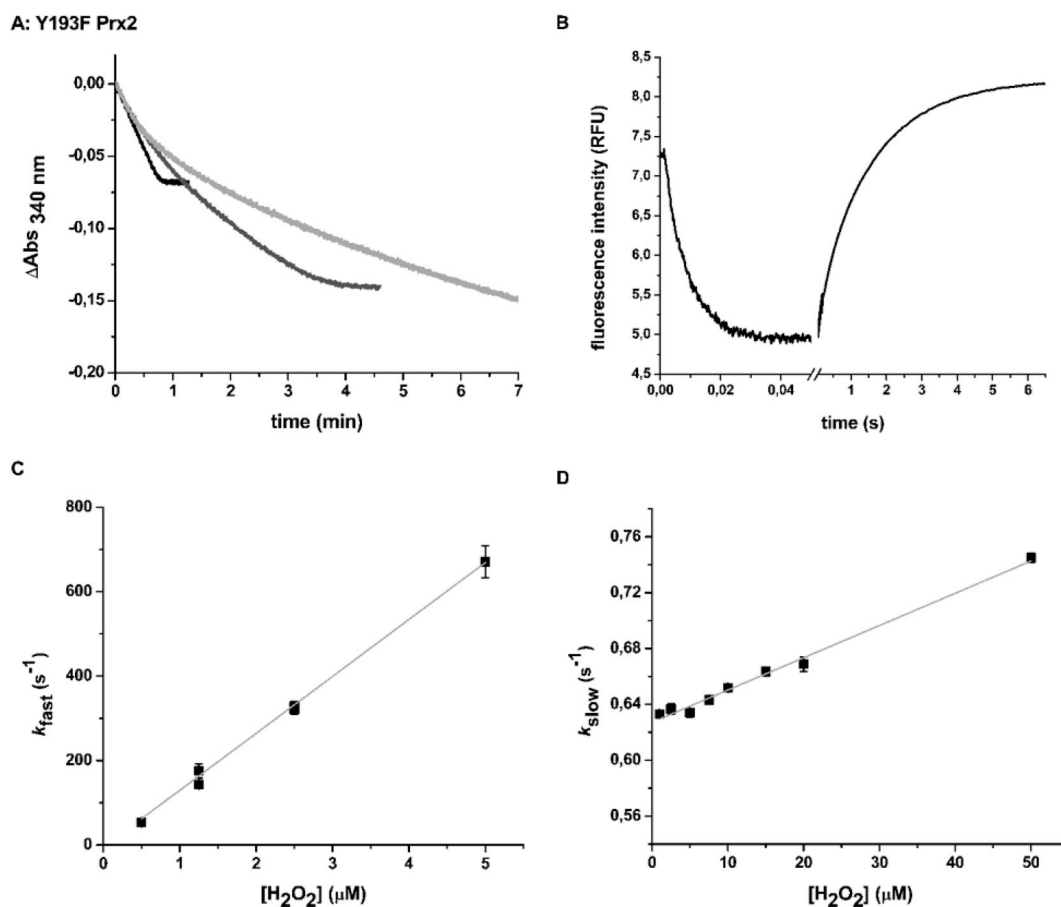
Fig. 4. Kinetic analysis of the reaction of H_2O_2 with Y193F Prx2. (**A**) NADPH-linked peroxidase activity of Y193F Prx2. Reaction was started with the addition of 10 μM H_2O_2 (black), 20 μM H_2O_2 (dark gray) or 50 μM H_2O_2 (light gray). (**B**) Intrinsic fluorescence profile of the reaction of 0.5 μM Y193F Prx2 with 1 μM H_2O_2. (**C**) Fast phase kinetic constant determined using different H_2O_2 concentrations. (**D**) Dependence of the kinetic constant of the second (slow) phase on H_2O_2 concentration. λ_{ex} = 295 nm.

Table 1
Kinetic constants for disulfide formation and hyperoxidation and determination of $C_{hyp1\%}$ value of different Prx.

	k_{res} (s^{-1})	k_{hyp} ($M^{-1} s^{-1}$)	*direct* $C_{hyp1\%}$ (μM)	$C_{hyp1\%}$ (μM)
$Prx2_{RBC}$	0.419 ± 0.004[a]	$(2.6 \pm 0.4) \times 10^3$[a]	1.61	
	2.0[b]	1.2×10^4[b]	1.67	
wt Prx2	0.197 ± 0.001	$(1.73 \pm 0.06) \times 10^3$	1.14	5[d]
	0.20[c]	2.0×10^3[c]	1.00	
Nitrated wt Prx2	¥	¥		136
Y193F Prx2	0.627 ± 0.002	$(2.31 \pm 0.09) \times 10^3$	2.71	
Y193G Prx2	76 ± 1	$(1.3 \pm 0.2) \times 10^3$	585	
AhpC	77 ± 1	$(0.41 \pm 0.03) \times 10^3$	1880	> 5000[d]
Prx1	11[c]	1.7×10^3[c]	65	50[d]
				62[e]
Prx3	20[b]	1.2×10^4[b]	17	127[e]
	2[f]	1.1×10^3[f]	18	

¥ could not be determined by intrinsic fluorescence kinetics.

$C_{hyp1\%}$ refers to the parameter defined in Nelson et al. [41].

direct $C_{hyp1\%}$ was calculated using equation (3).

Values shown from the literature were used to calculate *direct* $C_{hyp1\%}$ for $Prx2_{RBC}$, wt Prx2, Prx1 and Prx3 as indicated.

The k_{res} and k_{hyp} values from this work were obtained following changes in intrinsic fluorescence in a SF spectrophotometer. All experiments were performed in buffer A (pH 7.4).

  [a] Randall et al., unpublished results.
  [b] Peskin et al. [63].
  [c] Dalla Rizza et al. [20].
  [d] Bolduc et al. [62].
  [e] Nelson et al. [41].
  [f] De Armas et al. [60].

Steady-state kinetics (coupled assay) at different H_2O_2 concentrations showed that Y193F Prx2 was more sensitive to hyperoxidation than the wild type (Fig. 4A). In addition, a separate kinetic analysis was performed by stopped-flow spectrofluorimetry following changes in intrinsic fluorescence after mixture of the reduced enzyme with various concentrations of H_2O_2 (Fig. 4B). As reported previously for Prx oxidation by peroxides [6,20,41,59,60], two phases of fluorescence changes were observed, a fast decrease in emission associated with the oxidation step, followed by a slower recovery of fluorescence associated with the resolution step (Fig. 4B). For Y193F Prx2, from the fast peroxide-dependent phase, a second-order rate constant of $1.3 \times 10^8 \, M^{-1} s^{-1}$ was determined for the reaction of C_P-SH with H_2O_2 (Fig. 4C), a value similar to the previously reported for different Prx isoforms [2,20,]. However, the slow phase, associated with the competition between the two pathways the sulfenic form of the enzyme could follow, hyperoxidation or disulfide formation (resolution step), behaved differently than the wild type enzyme with a higher k_{res} (0.64 vs 0.2 s^{-1}) but the same $k_{hyp} = 1.2 \times 10^3 \, M^{-1} s^{-1}$ (Fig. 4D, Table 1). The faster resolution rate constant obtained for the variant Y193F is in accordance with a slightly faster peroxidase activity and a modestly more robust enzyme. These results suggest that removing a hydroxyl group in the C-terminal region of Prx2 is sufficient to lead to dynamic or conformational changes in the enzyme that can alter its catalytic activity.

Computational analysis regarding the contribution of different side-chains in position 193 to the global stability of Prx2 suggested that a glycine residue in that position would significantly destabilize the protein, while a phenylalanine would rigidize the region (Fig. 5A). Mutation of position 193 to Met was predicted as neutral or modestly destabilizing, with a small enhancement in flexibility. In addition, the energetics of Prx2 dimer structure were explored by means of the Frustratometer tool (Fig. 5B). Briefly, for a contact between two residues defined as highly frustrated, it means that most other amino acid pairs at that location would be more favorable for folding than those found in Prx2 sequence (the native ones). Even though the core of the dimer seems to be unfrustrated, some regions of the protein present clusters of highly frustrated contacts. Among them, the C-terminal region is shown to be highly frustrated. In particular, residue Tyr 193 showed the highest frustration index value (Fig. 5B). This fact suggests that this residue may not necessarily provide stability to the protein but would potentially contribute to the Prx2 function. Thus, a Gly residue at position 193 is expected to increase the local backbone flexibility, whereas a Phe residue would rigidify this α-helical stretch, as judged by the Dynamut analysis (Fig. 5A). In fact, preliminary molecular dynamics simulations show that residues at the C-terminal of the mutant Y193G display more fluctuations than the rest of the backbone chain compared to the wt Prx2 (Fig. 5S), suggesting a higher flexibility of this loop when glycine (and not phenylalanine) is in position 193, as predicted.

Following up on these computational results, the mutants Y193G and Y193 M were generated, since the first one would theoretically yield a much more destabilized protein than the latter (Fig. 5). As shown in Fig. 6, insertion of a Met residue in position 193 gave an inactive Prx2, while Y193G was a more active and robust variant of the enzyme.

Interestingly, the mutant Y193G Prx2, displaying a more unstable C-terminal region (Fig. 5C and Fig. 5S) behaved very similarly to the nitrated enzyme, showing higher peroxidase activity and higher robustness than the wild type enzyme (Fig. 6B). Availability of this pure, single site variant also enabled evaluation of rate constants by intrinsic fluorescence kinetics (Fig. 6C), revealing a faster resolution step ($k_{res} = 76 \, s^{-1}$) and a similar hyperoxidation rate constant, $k_{hyp} = 1.3 \times 10^3 \, M^{-1} s^{-1}$ (Table 1).

3.3. Analysis of hyperoxidation sensitivity and structural features of Y193F and Y193G

The parameter $C_{hyp1\%}$ is the concentration of H_2O_2 that yields 1% of inactivated Prx per turnover, previously described as a quantitative measure of Prx susceptibility toward peroxide-mediated hyperoxidation [41]. Herein, a straightforward way to calculate this parameter is described using the rate constants of the two competing reactions for C_P-SOH, disulfide formation or hyperoxidation, as determined during the stopped flow kinetic analysis (equation (3)). For Y193G Prx2 we obtained a value of $C_{hyp1\%}$ higher than 500 μM to achieve 1% inactivation per turnover, compared to ~1.6 μM for the wild type enzyme (Table 1) supporting the higher robustness of this mutant to H_2O_2-induced inactivation. For Y193F Prx2 analyzed by this approach, $C_{hyp1\%}$ was only slightly increased compared to wild type enzyme, ~3 μM (Table 1). Rate constants for the nitrated wild type Prx2 could not be determined using stopped flow fluorimetry due to heterogeneity of the sample and quenched Trp fluorescence, but using the coupled assay and previous approach [41] $C_{hyp1\%}$ was determined to be ~136 μM (Table 1).

In addition, as observed before for the peroxynitrite-treated Prx2 [49], the near-UV CD spectra of the reduced form of Y193G resembles its disulfide-oxidized form (Fig. 7A and B), while Y193F only modestly exhibited this perturbation. The fluorescence spectra (Fig. 7C) show a red shift of the maximum emission and a decreased in intensity for Y193G mutant (center mass of 352 nm compared to 349 nm for the wild type protein), indicating a shift of tryptophan residues to a more polar environment. Prx2 has two tryptophan residues, W86 close to C_P, and W176 at the C-terminal region; W176 is probably the one being more exposed in the Y193G Prx2 structure. Global protein stability of the Prx2 wild type and mutant proteins was also assessed by monitoring fluorescence changes during thermal denaturation. A lower apparent melting temperature of denaturation was obtained for the Y193G mutant compared to wild type (Fig. 7D) indicating a decrease in global stability by insertion of a glycine at position 193, while Y193F mutant
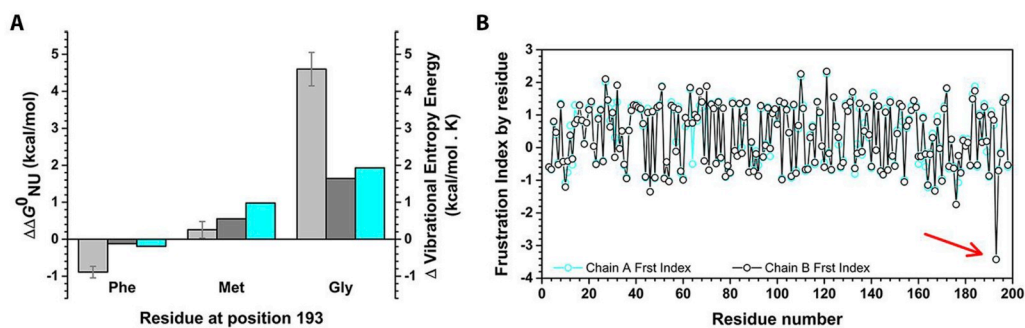
Fig. 5. Energetics and dynamics of Prx2 and mutants. **(A)** Predictions of the contribution of residue 193 to the conformational stability of Prx2: FOLDX and Dynamut were used to test the effect of point mutations at position 193 in chain A (light and dark gray, respectively). In addition, Dynamut was used to evaluate the effect of these mutations on dynamics (cyan). **(B)** Frustration by residue for chains A and B (cyan and black, respectively). Positive (> 0.55) values indicate residues minimally frustrated and nega-

tive (< −1) values indicate residues highly frustrated. The arrow indicates residue Y193 All the calculations were carried out using the dimer AB from PDB ID: 1QMV, in which hyperoxidized Cys was previously mutated to Cys using FOLDX. (For interpretation of the references to colour in this figure legend, the reader is referred to the Web version of this article.)
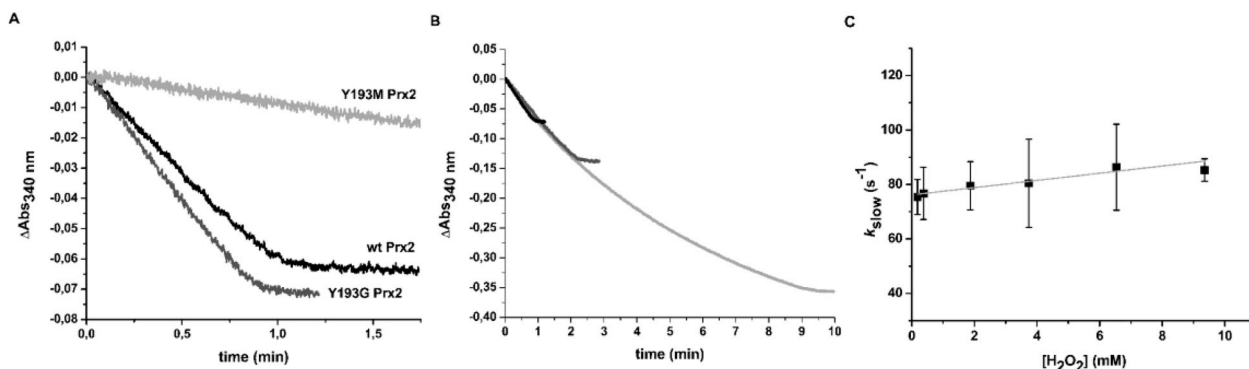
Fig. 6. Kinetic analysis of the reduction of H_2O_2 by wild type, Y193G and Y193 M Prx2. (**A**) NADPH-linked peroxidase activity of wild-type Prx2 is shown in black, Y193G Prx2 in dark gray and Y193 M Prx2 in light gray. Ten µM H_2O_2 was added to start the reactions and consumption of NADPH was followed at 340 nm. (**B**) NADPH-linked peroxidase activity was followed for the Y193G Prx2 mutant in the same conditions, using 10 µM H_2O_2 (black), 20 µM H_2O_2 (dark gray) or 50 µM H_2O_2 (light gray). (**C**) Oxidation of Y193G Prx2 followed by intrinsic fluorescence. Dependence of the kinetic constant of the slow phase on H_2O_2 concentration.

displayed an intermediate stability.

3.4. Nitration of AhpC, a model robust Prx

AhpC, a very well characterized robust Prx, lacks the YF motif present in the sensitive enzymes. As previously reported [61], the kinetics of H_2O_2 reaction with AhpC from *Salmonella typhimurium* followed by intrinsic fluorescence showed similar behavior to other 2-Cys

Prx. More specifically, AhpC behaved most like mutant Y193G Prx2, displaying a slow recovery of fluorescence after the initial fast drop, from which k_{res} and k_{hyp}, as well as a $C_{hyp1\%}$ value of ~1.9 mM, were obtained herein (Table 1, Fig. 6S). The same described peroxynitrite treatment of human Prx2 (using a 5-fold excess of peroxynitrite) was performed on AhpC, protecting its cysteine residues by first forming the disulfide bond in the active site. After treatment, nitration on tyrosine residues was confirmed by Western blot analysis (not shown), and the
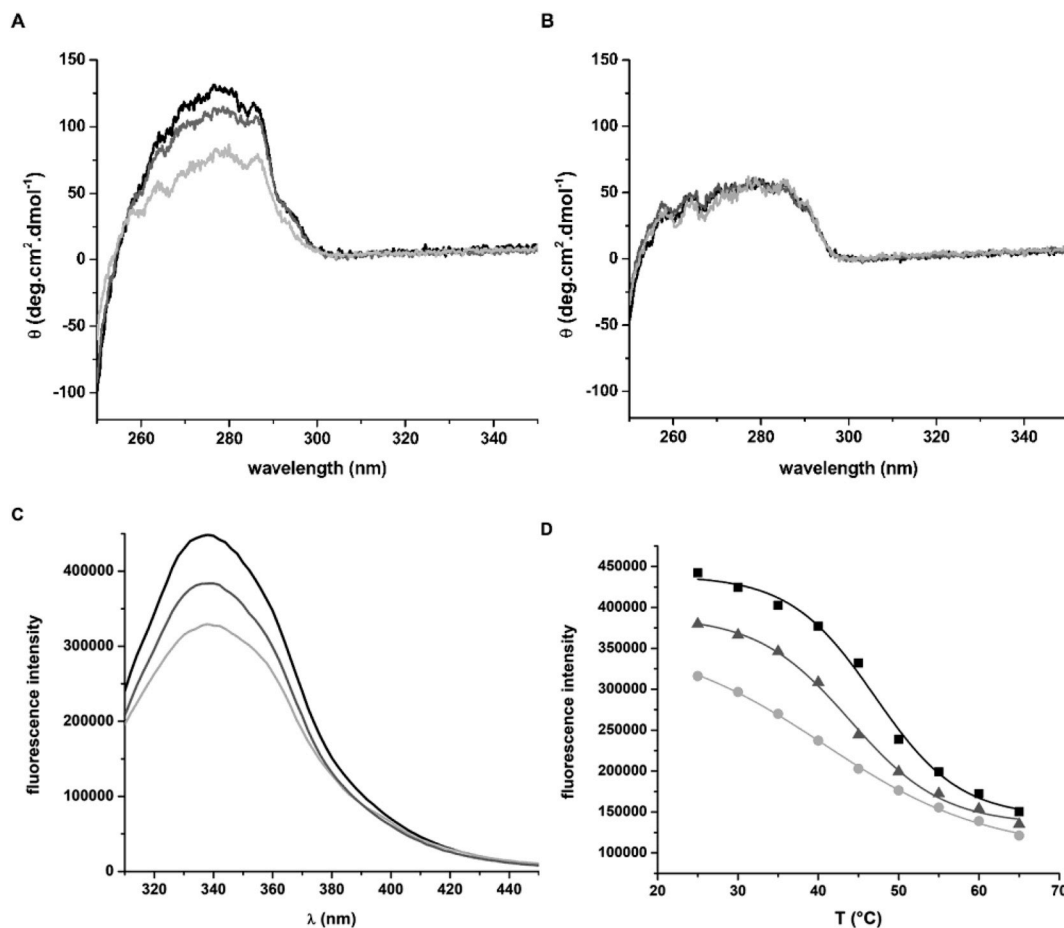
Fig. 7. Spectroscopic analysis of Prx2 mutants Y193F and Y193G. (**A**) Near UV-CD spectra of the reduced form of wild type Prx2 (black), Y193F (dark gray) and Y193G (light gray). (**B**) Near UV-CD spectra of disulfide-oxidized wild type Prx2 (black), Y193F (dark gray) and Y193G (light gray). (**C**) Emission spectra of wild type Prx2 (black), Y193F (dark gray) and Y193G (light gray) mutants in phosphate buffer pH 7.4, 1 mM DTT, 1 M urea, λ_{ex} = 280 nm. (**D**) Thermal-induced denaturation followed by intrinsic fluorescence (λ_{ex} = 280 nm, λ_{em} = 340 nm). Apparent melting temperatures of 47 °C, 44 °C and 40 °C were obtained for wt Prx2 (black), Y193F (dark gray), and Y193G (light gray), respectively.

peroxidase activity was assessed using the coupled assay (Fig. 7S). Interestingly, nitration of AhpC, a Prx lacking a tyrosine residue at the C-terminus, did not increase the enzyme activity; on the contrary, it rendered AhpC moderately less active as a peroxidase, which is the same effect as observed for the nitrated Y193F Prx2 mutant, also lacking Y193 at the C-terminal. Nitration of AhpC was never reported before and revealed a different behavior for this pathogen-derived Prx compared to the mammalian host counterpart Prx2.

4. Discussion

We previously reported that nitration of human Prx2 transforms this sensitive enzyme into a more robust peroxidase, less sensitive to hyperoxidation, and our results pointed to Y193 nitration as likely responsible for that effect [19]. In order to unravel the molecular mechanism for this modulation, Prx2 variants with a co-translationally incorporated nitrotyrosine residue were envisioned. In practice, three proteins with a unique nitration site per monomer were obtained, NO_2Y33, NO_2Y43 and NO_2Y126 (Figs. 1S, 2S and 3S). This elegant approach enabled studies with homogeneous samples, which cannot be achieved by protein treatment with peroxynitrite, however, none of these nitro variants behaved as the nitrated wild type (Figs. 2 and 4S) [22]. Unfortunately, it was not possible to effectively incorporate a nitrotyrosine into position 193 belonging to the YF motif linked to eukaryotic Prx sensitivity to hyperoxidation. On the other hand, the effects on conformation and function of the chemical alteration of side-chain 193 were explored by site-directed mutagenesis. Different mutants for this position were prepared and studied. Surprisingly, a neutral substitution of Y193 by phenylalanine resulted in a variant slightly more resistant to hyperoxidation than the wild type (Fig. 3A), underlying the importance of this structural motif for Prx2 functional modulation. Given this first interesting result, other mutants at this position that would stabilize or destabilize the protein were designed based on theoretical calculations (Fig. 5). Preliminary molecular dynamics simulations suggest that incorporation of glycine at position 193 increases the fluctuations of the protein backbone in the C-terminal region more than observed for the wild type Prx2 (Fig. 5S). As expected, this mutant with a more flexible C-terminal loop that favors the transition to the LU conformation, displayed a higher rate of disulfide formation, thus, more resistance to hyperoxidation (Fig. 6, Table 1). Interestingly, while none of the nitro variants produced herein behaved like the nitrated wild type enzyme, the incorporation of a glycine in place of tyrosine at position 193 very much resembled it. In addition, peroxynitrite treatment of Y193F Prx2 (lacking a tyrosine residue at the C-terminal) yielded a protein nitrated on tyrosine residues but less active and still sensitive to hyperoxidation, contrary to what was observed for the wild type enzyme. Altogether, these results confirm that, although *in vitro*, Prx2 can get nitrated on other Tyr residues, the tyrosyl side-chain at position 193 is necessary for the observed increase in peroxidase activity and hyperoxidation resistance after peroxynitrite treatment. This effect is likely achieved by increased flexibility of the C-terminal loop so that the C_P sulfenic acid can more easily reach the resolving cysteine to form the disulfide bond and protect the enzyme from hyperoxidation.

The results obtained for the Prx2 mutants have allowed a direct correlation between time courses of the coupled assay at increasing H_2O_2 concentrations and stopped-flow kinetics analysis (Figs. 3, 4 and 6). With the rate constants obtained by intrinsic fluorescence, a value of $C_{hyp1\%}$ was calculated as a measure of inactivation sensitivity, which mostly agree with the reported ones obtained in turnover (Table 1) [41,62]. The faster the disulfide is formed (higher k_{res}), the more resistant the enzyme is to hyperoxidation as long as the reactivity of the C_P-SOH with H_2O_2 does not change significantly, and this is reflected in a higher concentration of H_2O_2 needed to inactivate 1% of the protein ($C_{hyp1\%}$). For instance, Prx2 showed a decrease in peroxidase activity during turnover with H_2O_2 concentrations as low as 20 μM, while Prx1

needs higher H_2O_2 concentrations to become inactivated [20]. This correlates well with lower k_{res} and $C_{hyp1\%}$ values for Prx2 compared to Prx1 (Table 1). Unfortunately, peroxynitrite-treated Prx2 could not be reasonably analyzed by changes in intrinsic fluorescence, due to the heterogeneity of the sample combined with quenching of Trp fluorescence emission [19,49]. However, $C_{hyp1\%}$ in turnover was determined, yielding a value of 136 μM H_2O_2 (Figure 8S and Table 1), consistent with the desensitization of the enzyme by nitration as shown directly by the coupled assay (Fig. 2).

These functional studies correlate with the near-UV CD spectra results, in which the conformational change occurring during oxidation of the active site can be detected (Fig. 7). As previously reported, proteins less sensitive to oxidative inactivation by H_2O_2 also have a lower CD signal around 280 nm, already resembling the disulfide oxidized form even in their reduced state [49], which relates to the k_{res} values discussed in this work. That is, with a more readily displaced C-terminus, the FF to LU transition of C_P-SOH is facilitated and the disulfide can more readily form.

As previously pointed out [9,20], the kinetic pause at the resolution step opens different pathways for Prx to participate in redox signaling. The longer the lifetime of the sulfenic acid, higher the chance to get hyperoxidized but also to react with other protein thiols to translate the signal through a redox relay. On the other hand, a faster resolution step favors disulfide Prx formation, which can also function in a redox relay, probably interacting with a different set of targets.

In conclusion, our results not only confirm Y193 as a critical residue in modulation of Prx2 activity by peroxynitrite, but also highlight the importance of the YF motif at the C-terminus as a sensitive structural point that determines the fate of Prx2 in redox signaling pathways.

Conflicts of interest

The authors declare that they have no conflicts of interest with the contents of this article.

Acknowledgements

Appendix A. Supplementary data

Supplementary data to this article can be found online at https://doi.org/10.1016/j.freeradbiomed.2019.07.016.

References

[1] Z.A. Wood, E. Schroder, R.J. Harris, L.B. Poole, Structure, mechanism and regulation of peroxiredoxins, Trends Biochem. Sci. 28 (2003) 32–40.

[2] B. Manta, M. Hugo, C. Ortiz, G. Ferrer-Sueta, M. Trujillo, A. Denicola, The peroxidase and peroxynitrite reductase activity of human erythrocyte peroxiredoxin 2, Arch. Biochem. Biophys. 484 (2009) 146–154.

[3] C.C. Winterbourn, D. Metodiewa, Reactivity of biologically important thiol compounds with superoxide and hydrogen peroxide, Free Radical Biol. Med. 27 (1999) 322–328.

[4] A. Hall, D. Parsonage, L.B. Poole, P.A. Karplus, Structural evidence that peroxiredoxin catalytic power is based on transition-state stabilization, J. Mol. Biol. 402 (2010) 194–209.

[5] P. Nagy, A. Karton, A. Betz, A.V. Peskin, P. Pace, R.J. O'Reilly, M.B. Hampton, L. Radom, C.C. Winterbourn, Model for the exceptional reactivity of peroxiredoxins

2 and 3 with hydrogen peroxide: a kinetic and computational study, J. Biol. Chem. 286 (2011) 18048–18055.

[6] S. Portillo-Ledesma, F. Sardi, B. Manta, M.V. Tourn, A. Clippe, B. Knoops, B. Alvarez, E.L. Coitino, G. Ferrer-Sueta, Deconstructing the catalytic efficiency of peroxiredoxin-5 peroxidatic cysteine, Biochemistry 53 (2014) 6113–6125.

[7] A. Zeida, A.M. Reyes, M.C. Lebrero, R. Radi, M. Trujillo, D.A. Estrin, The extra-ordinary catalytic ability of peroxiredoxins: a combined experimental and QM/MM study on the fast thiol oxidation step, Chem. Commun. 50 (2014) 10070–10073.

[8] G. Ferrer-Sueta, B. Manta, H. Botti, R. Radi, M. Trujillo, A. Denicola, Factors affecting protein thiol reactivity and specificity in peroxide reduction, Chem. Res. Toxicol. 24 (2011) 434–450.

[9] L.M. Randall, G. Ferrer-Sueta, A. Denicola, Peroxiredoxins as preferential targets in H2O2-induced signaling, Methods Enzymol. 527 (2013) 41–63.

[10] P.E. Pace, A.V. Peskin, A. Konigstorfer, C.J. Jasoni, C.C. Winterbourn, M.B. Hampton, Peroxiredoxin interaction with the cytoskeletal-regulatory protein CRMP2: investigation of a putative redox relay, Free Radical Biol. Med. 129 (2018) 383–393.

[11] M.C. Sobotta, W. Liou, S. Stocker, D. Talwar, M. Oehler, T. Ruppert, A.N. Scharf, T.P. Dick, Peroxiredoxin-2 and STAT3 form a redox relay for H2O2 signaling, Nat. Chem. Biol. 11 (2015) 64–70.

[12] R. Engelman, P. Weisman-Shomer, T. Ziv, J. Xu, E.S. Arner, M. Benhar, Multilevel regulation of 2-Cys peroxiredoxin reaction cycle by S-nitrosylation, J. Biol. Chem. 288 (2013) 11312–11324.

[13] J. Fang, T. Nakamura, D.H. Cho, Z. Gu, S.A. Lipton, S-nitrosylation of peroxiredoxin 2 promotes oxidative stress-induced neuronal cell death in Parkinson's disease, Proc. Natl. Acad. Sci. U. S. A. 104 (2007) 18742–18747.

[14] J.W. Park, G. Piszczek, S.G. Rhee, P.B. Chock, Glutathionylation of peroxiredoxin I induces decamer to dimers dissociation with concomitant loss of chaperone activity, Biochemistry 50 (2011) 3204–3210.

[15] W.T. Lowther, A.C. Haynes, Reduction of cysteine sulfinic acid in eukaryotic, typical 2-Cys peroxiredoxins by sulfiredoxin, Antioxidants Redox Signal. 15 (2011) 99–109.

[16] A. Hall, P.A. Karplus, L.B. Poole, Typical 2-Cys peroxiredoxins-structures, mechanisms and functions, FEBS J. 276 (2009) 2469–2477.

[17] A. Perkins, K.J. Nelson, D. Parsonage, L.B. Poole, P.A. Karplus, Peroxiredoxins: guardians against oxidative stress and modulators of peroxide signaling, Trends Biochem. Sci. 40 (2015) 435–445.

[18] J.A. Bolduc, K.J. Nelson, A.C. Haynes, J. Lee, J.A. Reisz, A.H. Graff, J.E. Clodfelter, D. Parsonage, L.B. Poole, C.M. Furdui, W.T. Lowther, Novel hyperoxidation resistance motifs in 2-Cys peroxiredoxins, J. Biol. Chem. 293 (2018) 11901–11912.

[19] L.M. Randall, B. Manta, M. Hugo, M. Gil, C. Batthyany, M. Trujillo, L.B. Poole, A. Denicola, Nitration transforms a sensitive peroxiredoxin 2 into a more active and robust peroxidase, J. Biol. Chem. 289 (2014) 15536–15543.

[20] J. Dalla Rizza, L.M. Randall, J. Santos, G. Ferrer-Sueta, A. Denicola, Differential Parameters between Cytosolic 2-Cys Peroxiredoxins, PRDX1 and PRDX2. Protein Science, vol. 28, (2019), pp. 191–201.

[21] R. Radi, Nitric oxide, oxidants, and protein tyrosine nitration, Proc. Natl. Acad. Sci. U. S. A. 101 (2004) 4003–4008.

[22] M. Trujillo, G. Ferrer-Sueta, R. Radi, Peroxynitrite detoxification and its biologic implications, Antioxidants Redox Signal. 10 (2008) 1607–1620.

[23] M. Trujillo, B. Alvarez, J.M. Souza, N. Romero, L. Castro, L. Thomson, R. Radi, Nitric Oxide and Pathobiology, Academic Press, Orlando, FL, 2010.

[24] A. Denicola, B. Alvarez, L. Thomson, 3-Nitrotyrosine, a Post-translational Modification Associated with Nitroxidative Stress, Free Radical Pahtophysiology Transworlk Research Network, India, 2008, pp. 39–55.

[25] M. Takahashi, J. Shigeto, A. Sakamoto, S. Izumi, K. Asada, H. Morikawa, Dual selective nitration in Arabidopsis: almost exclusive nitration of PsbO and PsbP, and highly susceptible nitration of four non-PSII proteins, including peroxiredoxin II E, Electrophoresis 36 (2015) 2569–2578.

[26] B. Ghesquiere, N. Colaert, K. Helsens, L. Dejager, C. Vanhaute, K. Verleysen, K. Kas, E. Timmerman, M. Goethals, C. Libert, J. Vandekerckhove, K. Gevaert, In vitro and in vivo protein-bound tyrosine nitration characterized by diagonal chromatography, Mol. Cell. Proteom. : MCP 8 (2009) 2642–2652.

[27] T.T. Reed, W.M. Pierce Jr., D.M. Turner, W.R. Markesbery, D.A. Butterfield, Proteomic identification of nitrated brain proteins in early Alzheimer's disease inferior parietal lobule, J. Cell Mol. Med. 13 (2009) 2019–2029.

[28] I.V. Turko, L. Li, K.S. Aulak, D.J. Stuehr, J.Y. Chang, F. Murad, Protein tyrosine nitration in the mitochondria from diabetic mouse heart. Implications to dysfunctional mitochondria in diabetes, J. Biol. Chem. 278 (2003) 33972–33977.

[29] N. Romero, R. Radi, E. Linares, O. Augusto, C.D. Detweiler, R.P. Mason, A. Denicola, Reaction of human hemoglobin with peroxynitrite. Isomerization to nitrate and secondary formation of protein radicals, J. Biol. Chem. 278 (2003) 44049–44057.

[30] D.P. Nelson, L.A. Kiesow, Enthalpy of decomposition of hydrogen peroxide by catalase at 25 degrees C (with molar extinction coefficients of H2O2 solutions in the UV), Anal. Biochem. 49 (1972) 474–478.

[31] R. Radi, J.S. Beckman, K.M. Bush, B.A. Freeman, Peroxynitrite oxidation of sulfhydryls. The cytotoxic potential of superoxide and nitric oxide, J. Biol. Chem. 266 (1991) 4244–4250.

[32] P.F. Wang, D.M. Veine, S.H. Ahn, C.H. Williams Jr., A stable mixed disulfide between thioredoxin reductase and its substrate, thioredoxin: preparation and characterization, Biochemistry 35 (1996) 4812–4819.

[33] A.C. Haynes, J. Qian, J.A. Reisz, C.M. Furdui, W.T. Lowther, Molecular basis for the resistance of human mitochondrial 2-Cys peroxiredoxin 3 to hyperoxidation, J. Biol. Chem. 288 (2013) 29714–29723.

[34] F.W. Studier, Protein production by auto-induction in high density shaking cultures, Protein Expr. Purif. 41 (2005) 207–234.

[35] S. Portillo-Ledesma, L.M. Randall, D. Parsonage, J. Dalla Rizza, P.A. Karplus, L.B. Poole, A. Denicola, G. Ferrer-Sueta, Differential kinetics of two-cysteine peroxiredoxin disulfide formation reveal a novel model for peroxide sensing, Biochemistry 57 (2018) 3416–3424.

[36] R.B. Cooley, J.L. Feldman, C.M. Driggers, T.A. Bundy, A.L. Stokes, P.A. Karplus, R.A. Mehl, Structural basis of improved second-generation 3-nitro-tyrosine tRNA synthetases, Biochemistry 53 (2014) 1916–1924.

[37] J.T. Hammill, S. Miyake-Stoner, J.L. Hazen, J.C. Jackson, R.A. Mehl, Preparation of site-specifically labeled fluorinated proteins for 19F-NMR structural characterization, Nat. Protoc. 2 (2007) 2601–2607.

[38] J. Santos, C. Marino-Buslje, C. Kleinman, M.R. Ermacora, J.M. Delfino, Consolidation of the thioredoxin fold by peptide recognition: interaction between E. coli thioredoxin fragments 1-93 and 94-108, Biochemistry 46 (2007) 5148–5159.

[39] S.B. Mulrooney, Application of a single-plasmid vector for mutagenesis and high-level expression of thioredoxin reductase and its use to examine flavin cofactor incorporation, Protein Expr. Purif. 9 (1997) 372–378.

[40] C. Batthyany, J.M. Souza, R. Duran, A. Cassina, C. Cervenansky, R. Radi, Time course and site(s) of cytochrome c tyrosine nitration by peroxynitrite, Biochemistry 44 (2005) 8038–8046.

[41] K.J. Nelson, D. Parsonage, P.A. Karplus, L.B. Poole, Evaluating peroxiredoxin sensitivity toward inactivation by peroxide substrates, Methods Enzymol. 527 (2013) 21–40.

[42] J. Schymkowitz, J. Borg, F. Stricher, R. Nys, F. Rousseau, L. Serrano, The FoldX web server: an online force field, Nucleic Acids Res. 33 (2005) W382–W388.

[43] J. Van Durme, J. Delgado, F. Stricher, L. Serrano, J. Schymkowitz, F. Rousseau, A graphical interface for the FoldX forcefield, Bioinformatics 27 (2011) 1711–1712.

[44] C.H. Rodrigues, D.E. Pires, D.B. Ascher, DynaMut: predicting the impact of mutations on protein conformation, flexibility and stability, Nucleic Acids Res. 46 (2018) W350–W355.

[45] R.G. Parra, N.P. Schafer, L.G. Radusky, M.Y. Tsai, A.B. Guzovsky, P.G. Wolynes, D.U. Ferreiro, Protein Frustratometer 2: a tool to localize energetic frustration in protein molecules, now with electrostatics, Nucleic Acids Res. 44 (2016) W356–W360.

[46] W.L. Jorgensen, J, C, J.D. Madura, R.W. Impey, M.L. Klein, Comparison of simple potential functions for simulating liquid water, J. Chem. Phys. 79 (1983) 926–935.

[47] R. Salomon-Ferrer, A.W. Gotz, D. Poole, S. Le Grand, R.C. Walker, Routine microsecond molecular dynamics simulations with AMBER on GPUs. 2. Explicit solvent particle mesh ewald, J. Chem. Theory Comput. 9 (2013) 3878–3888.

[48] J.A. Maier, C. Martinez, K. Kasavajhala, L. Wickstrom, K.E. Hauser, C. Simmerling, ff14SB: improving the accuracy of protein side chain and backbone parameters from ff99SB, J. Chem. Theory Comput. 11 (2015) 3696–3713.

[49] L. Randall, B. Manta, K.J. Nelson, J. Santos, L.B. Poole, A. Denicola, Structural changes upon peroxynitrite-mediated nitration of peroxiredoxin 2; nitrated Prx2 resembles its disulfide-oxidized form, Arch. Biochem. Biophys. 590 (2016) 101–108.

[50] H. Neumann, J.L. Hazen, J. Weinstein, R.A. Mehl, J.W. Chin, Genetically encoding protein oxidative damage, J. Am. Chem. Soc. 130 (2008) 4028–4033.

[51] J.J. Porter, R.A. Mehl, Genetic code expansion: a powerful tool for understanding the physiological consequences of oxidative stress protein modifications, Oxidative Med. Cell. Longev. 2018 (2018) 7607463.

[52] T. Mukai, H. Hoshi, K. Ohtake, M. Takahashi, A. Yamaguchi, A. Hayashi, S. Yokoyama, K. Sakamoto, Highly reproductive Escherichia coli cells with no specific assignment to the UAG codon, Sci. Rep. 5 (2015) 9699.

[53] T.S. Chang, W. Jeong, S.Y. Choi, S. Yu, S.W. Kang, S.G. Rhee, Regulation of peroxiredoxin I activity by Cdc2-mediated phosphorylation, J. Biol. Chem. 277 (2002) 25370–25376.

[54] R.B. Parmigiani, W.S. Xu, G. Venta-Perez, H. Erdjument-Bromage, M. Yaneva, P. Tempst, P.A. Marks, HDAC6 is a specific deacetylase of peroxiredoxins and is involved in redox regulation, Proc. Natl. Acad. Sci. U. S. A. 105 (2008) 9633–9638.

[55] H.A. Woo, S.H. Yim, D.H. Shin, D. Kang, D.Y. Yu, S.G. Rhee, Inactivation of peroxiredoxin I by phosphorylation allows localized H(2)O(2) accumulation for cell signaling, Cell 140 (2010) 517–528.

[56] T.A. Zykova, F. Zhu, T.I. Vakorina, J. Zhang, L.A. Higgins, D.V. Urusova, A.M. Bode, Z. Dong, T-LAK cell-originated protein kinase (TOPK) phosphorylation of Prx1 at Ser-32 prevents UVB-induced apoptosis in RPMI7951 melanoma cells through the regulation of Prx1 peroxidase activity, J. Biol. Chem. 285 (2010) 29138–29146.

[57] B. Alvarez, H. Rubbo, M. Kirk, S. Barnes, B.A. Freeman, R. Radi, Peroxynitrite-dependent tryptophan nitration, Chem. Res. Toxicol. 9 (1996) 390–396.

[58] C. Brito, M. Naviliat, A.C. Tiscornia, F. Vuillier, G. Gualco, G. Dighiero, R. Radi, A.M. Cayota, Peroxynitrite inhibits T lymphocyte activation and proliferation by promoting impairment of tyrosine phosphorylation and peroxynitrite-driven apoptotic death, J. Immunol. 162 (1999) 3356–3366.

[59] L.A.C. Carvalho, D.R. Truzzi, T.S. Fallani, S.V. Alves, J.C. Toledo Jr., O. Augusto, L.E.S. Netto, F.C. Meotti, Urate hydroperoxide oxidizes human peroxiredoxin 1 and peroxiredoxin 2, J. Biol. Chem. 292 (2017) 8705–8715.

[60] M.I. De Armas, R. Esteves, N. Viera, A.M. Reyes, M. Mastrogiovanni, T.G.P. Alegria, L.E.S. Netto, V. Tortora, R. Radi, M. Trujillo, Rapid peroxynitrite reduction by human peroxiredoxin 3: implications for the fate of oxidants in mitochondria, Free Radical Biol. Med. 130 (2019) 369–378.

[61] D. Parsonage, K.J. Nelson, G. Ferrer-Sueta, S. Alley, P.A. Karplus, C.M. Furdui, L.B. Poole, Dissecting peroxiredoxin catalysis: separating binding, peroxidation, and resolution for a bacterial AhpC, Biochemistry 54 (2015) 1567–1575.

[62] J.A. Bolduc, K.J. Nelson, A.C. Haynes, J. Lee, J.A. Reisz, A.H. Graff, J.E. Clodfelter, D. Parsonage, L.B. Poole, C.M. Furdui, W.T. Lowther, Novel hyperoxidation resistance motifs in 2-Cys peroxiredoxins, J. Biol. Chem. (2018).

[63] A.V. Peskin, N. Dickerhof, R.A. Poynton, L.N. Paton, P.E. Pace, M.B. Hampton, C.C. Winterbourn, Hyperoxidation of peroxiredoxins 2 and 3: rate constants for the reactions of the sulfenic acid of the peroxidatic cysteine, J. Biol. Chem. 288 (2013) 14170–14177.

Supporting information
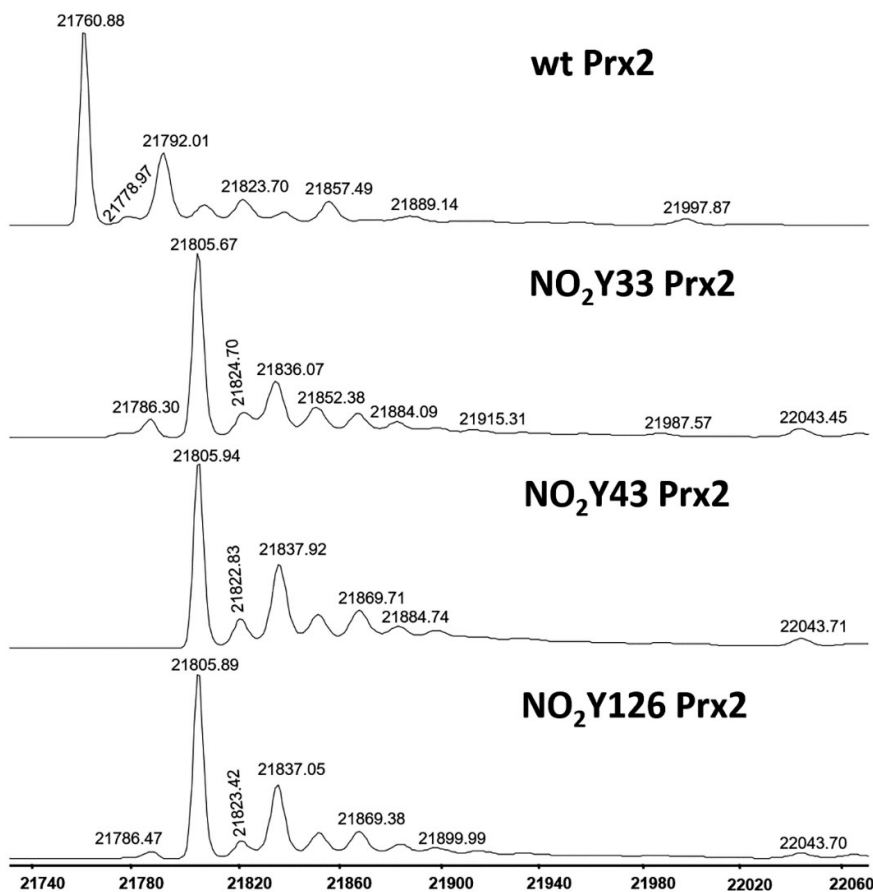
Figure 1S. MS analysis of Prx2 nitro variants. NO_2Y33, NO_2Y43 and NO_2Y126 Prx2 were reduced with DTT, with excess DTT removed by gel filtration and samples exchanged into 0.1% formic acid, then analyzed by ESI-MS. The main peak ($m/z=$ 21760) corresponds to the reduced monomer of wild type Prx2, and the increase in +45 amu ($m/z=$ 21805) confirms the incorporation of one nitrotyrosine residue into each variant. The minor species with $m/z=$ 21837 detected in all the samples corresponds to the hyperoxidized form of Prx2 (C_P-SO_2H) since thiols were not protected by alkylation with NEM.

Tyrosine 33, 126 and 193 were found nitrated after treatment of Prx2 with peroxynitrite. Nitro variant at Y43, a residue close to the helix in the interface between dimers, was also included.
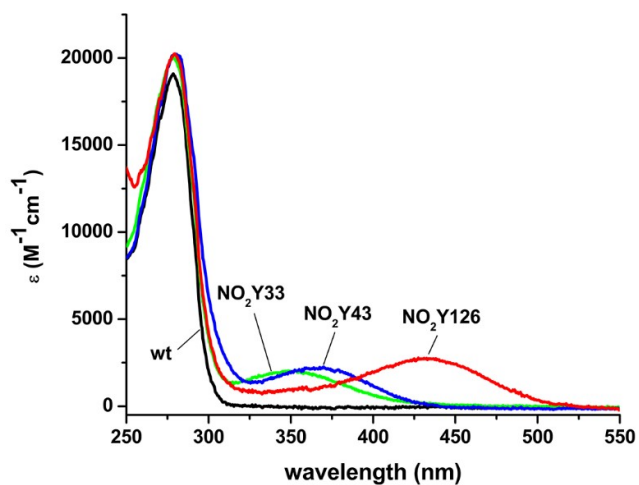
Figure 2S. UV-vis spectra of wtPrx2 and variants NO_2Y33, NO_2Y43 and NO_2Y126 Prx2. Protein samples were diluted in buffer A and assayed for protein content (Bradford method). Spectra were measured and corrected to molar concentration.The absorbance peaks of NO_2-Y33 (334 nm) and NO_2-Y126 (432 nm) are characteristic of protonated and deprotonated 3-NO_2-Tyr respectively (48).
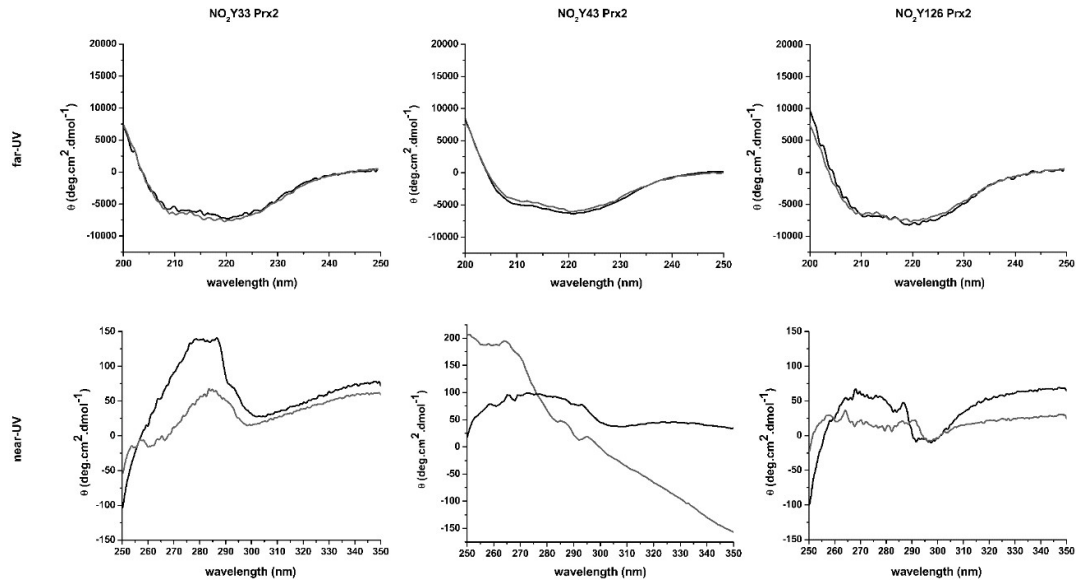
Figure 3S. Far-UV and near-UV CD spectra of NO$_2$Y33 Prx2, NO$_2$Y43 Prx2 and NO$_2$Y126 Prx2. The spectra of the reduced proteins are shown in black and the spectra of the oxidized to disulfide species are shown in gray.
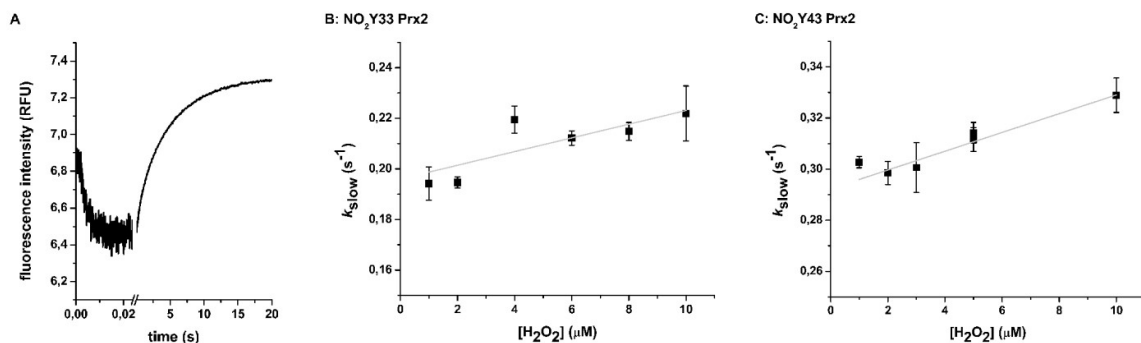
Figure 4S. Oxidation kinetics of co-translationally nitrated Prx2 variants by H_2O_2. (**A**) Intrinsic fluorescence change of 0.25 µM reduced NO_2Y33 Prx2 after addition of 2 µM H_2O_2. The slower phase was fit to a monoexponential decay and the first-order rate constant plotted against H_2O_2 concentration for (**B**) NO_2Y33 Prx2 and (**C**) NO_2Y43 Prx2.According to equation 1, a value for the second-order rate constant of hyperoxidation was determined from the slope ($k_{hyp} = 3.5 \times 10^3$ M^{-1} s^{-1} and 3.0×10^3 M^{-1} s^{-1} for NO_2Y33 and NO_2Y43, respectively). The y-axis intercept yielded the rate of disulfide formation, $k_{res} = 0.19$ s^{-1} and 0.30 s^{-1} for NO_2Y33 and NO_2Y43, respectively. From the k_{res} and k_{hyp} values obtained, a $C_{hyp1\%}$ of 0.72 µM and 0.81µM was calculated (using equation 3) for NO_2Y33 Prx2 and NO_2Y43 Prx2, very close to the value obtained for wt Prx2 (1 µM).

Reaction of H_2O_2 with NO_2Y126 Prx2 could not be followed by intrinsic fluorescence, probably due to a higher quenching of the signal by the NO_2 group in that position.
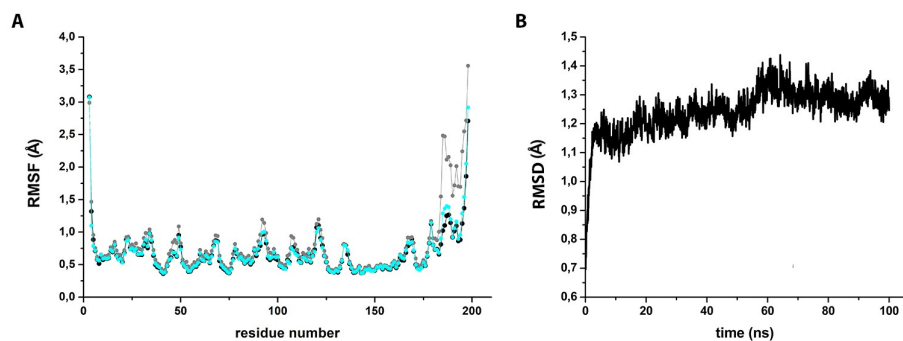
Figure 5S. Molecular dynamics of Prx2 mutants. **(A)** RMSF (Root Mean Square Fluctuation) plot of wild type (black), Y193F (cyan) and Y193G (gray) Prx2 Cα atoms along the 100 ns simulation period. The structures were stable along the last 90 ns simulation period as shown by RMSD (Root mean square deviation) values **(B)**.
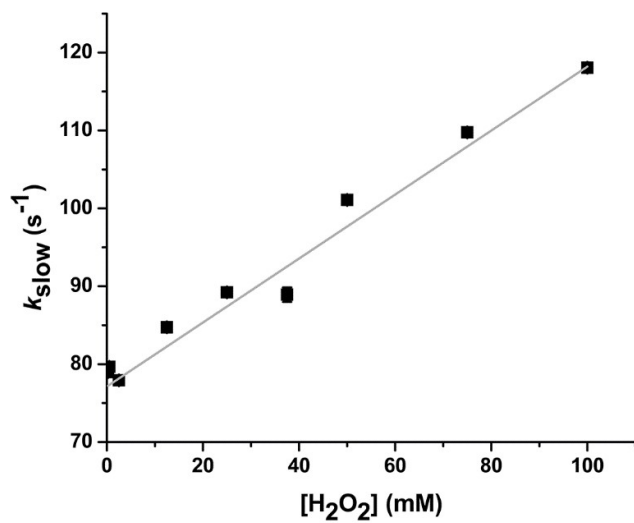
Figure 6S. Kinetics of H_2O_2 reaction with AhpC followed by changes in intrinsic fluorescence. Determination of the kinetic constant of the slow phase using increasing H_2O_2 concentrations. $\lambda_{ex} = 295$ nm. From the y-axis intercept, k_{res} was obtained, and from the slope, k_{hyp} reported on Table 1.
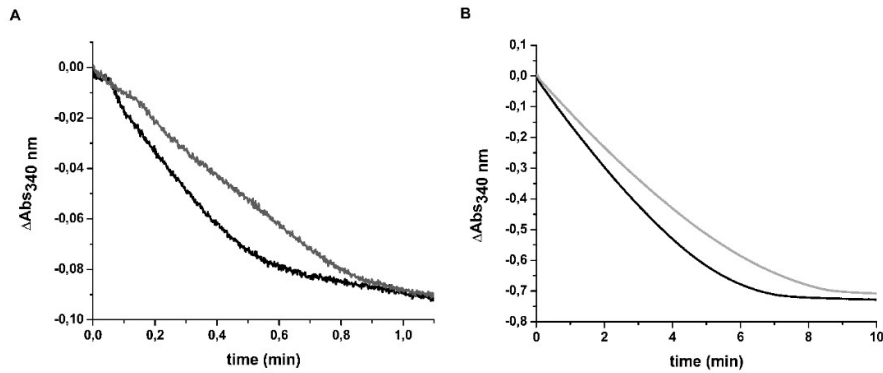
Figure 7S. Effect of nitration on NADPH-linked peroxidase activity of *St*AhpC. Peroxidase activity was measured for non-treated AhpC (black) or AhpC treated with 5-fold excess of peroxynitrite (gray). The assay was started with the addition of (**A**) 10 µM H_2O_2 or (**B**) 100 µM H_2O_2, and the consumption of NADPH was followed at 340 nm.
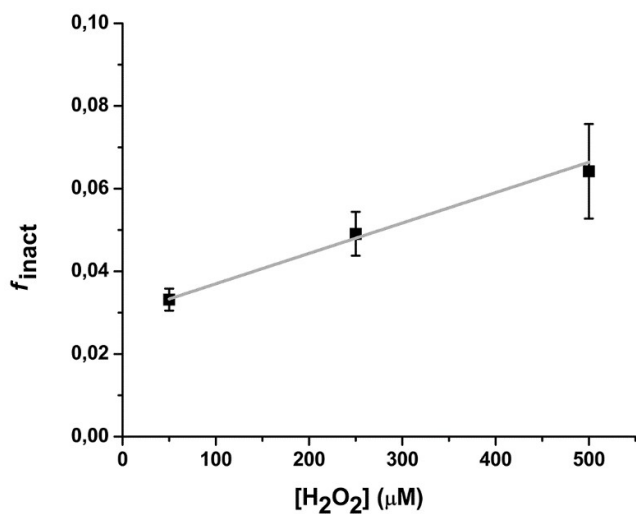
Figure 8S. Determination of $C_{hyp}1\%$ in turnover of nitrated wtPrx2 (recombinant Prx2 treated with peroxynitrite as detailed under Materials and Methods). f_{inact} of nitrated wtPrx2 was determined using the coupled assay as described above, at H_2O_2 concentrations between 50 and 500 μM. The analysis of the data was done following (33,46) and f_{inact} was plotted against [H_2O_2]. Fromtheslope, $C_{hyp}1\%$ wascalculated (Table 1).

4. Discusión general

En el año 2009 nuestro grupo reportó que la Prx2 de glóbulo rojo humano no sólo posee actividad peroxinitrito reductasa, sino que además es sensible a sobreoxidarse y a nitrarse en catálisis por este oxidante (82). A su vez, en el año 2009 un estudio proteómico de muestras tomadas de cerebros de pacientes con Alzheimer temprano detectaba Prx2 nitrada. Este resultado, sumado a la evidencia acumulada que vincula al estrés nitroxidativo con las patologías neurodegenerativas (98,191-196), aparece como una posible implicación fisiopatológica de esta modificación en Prx2. Es entonces que nos planteamos la siguiente pregunta: ¿cuál es el vínculo entre sobreoxidacion y nitración de Prx2? Con eso en mente surge este proyecto, que se enfoca en el estudio *in vitro* de las relaciones entre estructura y función en la Prx2 humana nitrada utilizando herramientas de biofísica de proteínas, cinética enzimática, modificación química y biología molecular.

Además del ampliamente reportado rol como antioxidantes, más recientemente aparece un nuevo papel para las Prx que las coloca como enzimas clave en las vías de señalización redox intracelulares. En la última década han ido apareciendo sucesivas evidencias apoyando esta teoría, entre las cuales se encuentra el elegante experimento del grupo de Gladishev (245), en el que al eliminar todas las peroxidasas de la levadura *Saccharomyces cerevisiae* dejan de detectar oxidación de las proteínas señalizadoras, confirmando el protagonismo de la Prx en estos procesos. A su vez, se ha demostrado -tanto *in vitro* como *in vivo*- la modulación de la actividad y el estado oligomérico de estas proteínas por diversas modificaciones postraduccionales (29,136).

A pesar de que la nitración de tirosinas suele asociarse con la pérdida de función y degradación proteica (172,177,179), el tratamiento con peroxinitrito de la Prx2 humana en su forma disulfuro resulta en una enzima nitrada en residuos de tirosinas, más activa como peroxidasa y menos sensible a sobreoxidarse por H_2O_2 (109). Los estudios biofísicos realizados demuestran que la nitración de la Prx2 conduce a una estructura de la enzima que en su forma reducida se parece más a la forma oxidada a disulfuro sugiriendo que la nitración favorece la población de un subestado energético más cercano a la forma oxidada de la enzima, pero ya desde el estado reducido. En particular, se observó que las formas oxidadas a disulfuro tanto de la enzima tratada con peroxinitrito como de la *wild type*, presentaban menos señal en el CD en el UV cercano, sugiriendo un cambio en el entorno de triptofanos y consecuente cambio de estructura terciaria. Estos resultados se vieron respaldados

también por una leve pérdida de estructura de alfa-hélice inferida a partir de la comparación de espectros de CD en el UV lejano. Como se describió en la Introducción, para que se forme el disulfuro intermolecular en el sitio activo de esta enzima, tiene que ocurrir un desplegado local de la hélice C-terminal de la proteína, permitiendo entonces que C_PSOH y C_R se acerquen y reaccionen. Es interesante notar que las formas oxidadas a disulfuro de la *wild type* y de la nitrada son superponibles, resultado coherente con la formación del disulfuro como estructura final (252).

Estos cambios espectrales al pasar de la forma reducida a la forma oxidada a disulfuro en el CD-UV cercano se observaron también en la mayoría de las mutantes generadas, a excepción de Prx2 NO_2Y43, en la que el CD cercano no sigue esta tendencia, probablemente porque la presencia de un grupo nitro en esa tirosina altera otros motivos estructurales que no permiten visualizar estos cambios entre la forma reducida y la oxidada a disulfuro (253).

Por otra parte, los distintos estudios cinéticos de la enzima nitrada y de diversas mutantes de Prx2 permitieron orientar los efectos observados luego del tratamiento con peroxinitrito hacia cambios en la velocidad de resolución del disulfuro (253). Una mayor velocidad de formación del disulfuro permite a la enzima permanecer menos tiempo en sulfénico, y protegerse así de la sobreoxidación a sulfínico. Asimismo, al ser la resolución el paso limitante de la velocidad en el ciclo catalítico *in vitro*, aumentar su velocidad permite aumentar la velocidad de consumo de H_2O_2. Esta asociación entre la velocidad de cierre del disulfuro y la sensibilidad a sobreoxidación por peróxido ya ha sido reportada y demostrada en la literatura, como se detalló en la Introducción. En particular, el motivo YF perteneciente al extremo C-terminal de las Prx eucariotas ha sido vinculado a la sensibilidad a inactivarse de estas enzimas.

En estudios de mapeo de las tirosinas modificadas por peroxinitrito en Prx2 se encontraron tres tirosinas nitradas: Y33, Y126 e Y193 (109). A raíz de este resultado se pudieron purificar las variantes NO_2Y33 y NO_2Y126 Prx2 obtenidas por incorporación cotraduccional del residuo de nitro-tirosina, sin embargo, la actividad peroxidasa de ambas no coincidió con lo observado luego de la nitración de Prx2 por peroxinitrito (253). Lamentablemente, la variante nitrada co-traduccionalmente en la Y193 aún no pudo obtenerse, debiendo utilizarse otro encare para su estudio. Se generó entonces la mutante Y193F, que al ser tratada con peroxinitrito ya no presenta mayor actividad peroxidasa sino inactivación, demostrando el rol fundamental de este residuo en los efectos del tratamiento con peroxinitrito en la actividad de la enzima (253). Por otra parte, la sustitución de la tirosina en esa posición por glicina que desestabiliza la estructura proteica, a juzgar por los resultados de estabilidad

obtenidos mediante el programa FOLDX, dio lugar a una enzima más activa y robusta, con mayor velocidad de resolución, simulando la forma nitrada (253).

Con la intención de entender los factores que determinan la velocidad de formación del enlace disulfuro de las Prx, determinamos los pK_a de las especies involucradas en la reacción de resolución (C_P-SOH y C_R-SH) (254). Los resultados obtenidos en este trabajo colocan al cambio conformacional FF-LU como determinante de la resolución, paso crítico en la velocidad de catálisis y por lo tanto en la modulación de la actividad de estas enzimas. El efecto observado luego del tratamiento con peroxinitrito de la Prx2 puede explicarse entonces como que esta modificación favorece una conformación más cercana a la LU, acelerando así la formación del enlace disulfuro.

Es interesante que la acetilación de la K196 de Prx2 y de K197 en Prx1 da como resultado enzimas más robustas y más activas como peroxidasas que las *wild type* (170). La acetilación de K196, que también pertenece al extremo C-terminal de estas proteínas, podría, al igual que la nitración de Y193, estar favoreciendo la apertura del loop C-terminal al que pertenecen, acelerando la formación del enlace disulfuro. Esta modificación se asemeja además a la nitración en el sentido en que el residuo de Lys pierde su carga positiva al ser modificado, y podría así estar desestabilizando esta porción proteica como consecuencia de un desbalance local de cargas (173,175).

Por otra parte, un trabajo reporta que la fosforilación de Y194 en Prx1 (residuo análogo a Y193 en Prx2), provoca una disminución de la actividad peroxidasa de la enzima, resultado que atribuyen a las cargas negativas aportadas por el grupo fosfato, apoyados en la menor actividad que presenta la mutante Y194D (255). Sin embargo, los autores no profundizan en elucidar si la disminución de actividad peroxidasa registrada en el ensayo acoplado está vinculada a una menor reactividad del sitio activo con el peróxido (lo que sería difícil de visualizar por esta técnica), por cambios en la velocidad de resolución, o por cambios en la reducción del disulfuro por la Trx. Como no parece inactivarse la enzima por sobreoxidación, sino que aparentemente demora más en reducir la misma cantidad de peróxido, podría descartarse la menor velocidad de resolución. En este sentido, entender cuál de los pasos del ciclo catalítico se ve afectado por la fosforilación de Y194 podría esclarecer el efecto diferencial que tiene esta PTM comparada con la nitración y la acetilación de residuos cercanos.

La nitración de Prx2 aparece entonces como un mecanismo más de modulación de la actividad peroxidasa de la enzima, así como su estructura

oligomérica, pudiendo afectar *in vivo* su interacción con otras proteínas intracelulares. Por otro lado, los efectos de la nitración observados para las demás Prx ensayadas -todas de la subfamilia Prx1/AhpC- reafirman la idea de que no existe redundancia en tener varias Prx, sino que son enzimas que cumplen distintas funciones en la señalización redox. En particular, como se reporta en el trabajo de Dalla Rizza et al. (84) (Anexo 1), realizado en colaboración con esta tesis, la presencia de la C83 en Prx1 compite por el peroxinitrito oxidándose y dando lugar a una enzima inactiva. Es así que la sola presencia de esta cisteína adicional determina el efecto diferencial del peroxinitrito en ambas proteínas. La Prx3, en cambio, no presenta este residuo de cisteína adicional y su nitración resulta en una enzima con menor actividad peroxidasa, pero más robusta (resultados no publicados). La Prx3 ya ha presentado en trabajos previos resultados que no son los esperados según el comportamiento tradicional de las Prx de 2-Cys típicas, y en ese entonces los autores lo asociaron a asimetría de los sitios catalíticos dentro de un dímero, favoreciéndose diferencialmente la sobreoxidación de uno sobre el otro (111). En este sentido, sería interesante profundizar en el estudio de esta enzima nitrada para tratar de elucidar el mecanismo por el cual, a pesar de perder actividad peroxidasa, se vuelve más robusta luego del tratamiento con peroxinitrito.

En nuestro último trabajo (253) se describe la determinación del parámetro $C_{hyp}1\%$ de manera más directa, siguiendo la reacción de oxidación por los cambios en la fluorescencia intrínseca de estas proteínas en equipo de flujo detenido. El poder determinar de manera cuantitativa la sensibilidad a sobreoxidarse de las Prx de manera sencilla como lo es utilizando el $C_{hyp}1\%$ descrito en (249) o en (253), permite avanzar en la generación de una base de datos que facilite eventualmente modelar estos sistemas complejos y desentramar la participación de las Prx en las vías de señalización redox intracelulares.

En la Tabla 1 de (253) se reportan los valores de $C_{hyp}1\%$ así como los valores de k_{ox}, k_{res} y k_{hyp} publicados hasta el momento para las Prx estudiadas. De este estudio se destaca que las diferencias mayores entre las Prx estudiadas se observan a nivel de la velocidad de formación del disulfuro, y no tanto a nivel de la velocidad de sobreoxidación del ácido cisteinsulfénico de la C_P. Estos resultados cinéticos acompañan la gran variedad de evidencias estructurales y experimentales que señalan este paso como determinante del destino del sulfénico hacia sulfínico o disulfuro. Experimentalmente se constató que la reacción de resolución (formación del disulfuro) es particularmente lenta en relación con lo esperado teóricamente, es decir que el entorno del sitio catalítico de estas Prx, así como favorece a una reacción de la C_P con

H_2O_2 muy rápida, también desfavorece el encuentro con C_R para formar el disulfuro (254). Esto sugiere que existe algún tipo de restricción estructural a nivel de la proteína, evolutivamente favorecido, que explica la permanencia relativamente prolongada del sulfénico de la C_P favoreciendo su sobreoxidación.

A su vez, esta tesis abre nuevas interrogantes, desde cuál es el efecto de la nitración en la actividad chaperona de la enzima, hasta cómo afecta su interacción con distintas proteínas en las vías de señalización redox. Entender cómo se afectan estas interacciones podría ayudar a esclarecer el rol que juega esta modificación en el contexto de las patologías neurodegenerativas en que se ha visto. Aunque no queda claro que la nitración sea en sí un mecanismo de señalización, hay evidencias de que participa en las vías de señalización redox modulando la actividad de las Prx *in vivo* en condiciones fisiopatólogicas asociadas a estrés nitroxidativo crónico. En este sentido nuestros aportes pretenden ser un estímulo para seguir generando preguntas que permitan elucidar la participación de estas enzimas en la intrincada red de interacciones y reacciones intracelulares de manera de poder encontrar eventualmente puntos de control que permitan tratar estas patologías en un futuro.

5. PERSPECTIVAS

Esta tesis abre nuevas interrogantes en relación con el efecto de la nitración en la actividad de Prx2 en las células y en las vías de señalización en las que participa esta proteína. En este sentido, quedaron postergados objetivos inicialmente planteados como estudiar el efecto de esta modificación sobre la actividad chaperona de Prx2 y en la reducción de la forma sobreoxidada de la enzima por Srx así como en la interacción entre ambas proteínas.

Por otra parte, obtener la variante NO_2Y193 Prx2 nitrada cotraduccionalmente, permitiría realizar su caracterización estructural y funcional trabajando con una muestra homogénea. Asimismo, el estudio de las mutantes Y193D, Y193E, permitiría profundizar en el efecto que tiene la nitración de Y193 en la estructura de la proteína vinculado a la incorporación de una carga negativa en ese sitio.

Varias preguntas surgen del efecto de la nitración sobre la estructura cuaternaria de Prx2. En particular, estudiar el impacto de la alteración de la dinámica del estado de oligomerización sobre el ciclo catalítico permitiría profundizar en la comprensión de los mecanismos que vinculan oligomerización y actividad de la enzima.

Por último, la evaluación *in vitro* del efecto de la nitración en la interacción de Prx2 con otras proteínas, y en particular el estudio de interacciones descritas en enfermedades neurodegenerativas donde se ha reportado la nitración de Prx2, contribuiría a esclarecer la participación de esta proteína en los mecanismos fisiopatológicos subyacentes a estas patologías.

6. BIBLIOGRAFÍA

1. Anbar, A. D. (2008) Oceans. Elements and evolution. *Science* **322**, 1481-1483
2. Bekker, A., Holland, H. D., Wang, P. L., Rumble, D., 3rd, Stein, H. J., Hannah, J. L., Coetzee, L. L., and Beukes, N. J. (2004) Dating the rise of atmospheric oxygen. *Nature* **427**, 117-120
3. Drews, G. (2011) The evolution of cyanobacteria and photosynthesis. in *Bioenergetic processes of cyanobacteria* (G.A., P. ed.), Springer, Netherlands. pp 265-284
4. Knoll, A.H. (2003) The geological consequences of evolution. *Geobiology* **1**, 3-14
5. Castresana, J., and Saraste, M. (1995) Evolution of energetic metabolism: the respiration-early hypothesis. *Trends in biochemical sciences* **20**, 443-448
6. Kim, H. J., Ha, S., Lee, H. Y., and Lee, K. J. (2015) ROSics: chemistry and proteomics of cysteine modifications in redox biology. *Mass spectrometry reviews* **34**, 184-208
7. Jenney, F. E., Jr., Verhagen, M. F., Cui, X., and Adams, M. W. (1999) Anaerobic microbes: oxygen detoxification without superoxide dismutase. *Science* **286**, 306-309
8. Balsera, M., and Buchanan, B. B. (2019) Evolution of the thioredoxin system as a step enabling adaptation to oxidative stress. *Free radical biology & medicine*
9. Valentine, J. S., Wertz, D. L., Lyons, T. J., Liou, L. L., Goto, J. J., and Gralla, E. B. (1998) The dark side of dioxygen biochemistry. *Current opinion in chemical biology* **2**, 253-262
10. Apel, K., and Hirt, H. (2004) Reactive oxygen species: metabolism, oxidative stress, and signal transduction. *Annual review of plant biology* **55**, 373-399
11. Balaban, R. S., Nemoto, S., and Finkel, T. (2005) Mitochondria, oxidants, and aging. *Cell* **120**, 483-495
12. Hole, P. S., Darley, R. L., and Tonks, A. (2011) Do reactive oxygen species play a role in myeloid leukemias? *Blood* **117**, 5816-5826
13. Bedard, K., and Krause, K. H. (2007) The NOX family of ROS-generating NADPH oxidases: physiology and pathophysiology. *Physiological reviews* **87**, 245-313
14. Sheng, Y., Abreu, I. A., Cabelli, D. E., Maroney, M. J., Miller, A. F., Teixeira, M., and Valentine, J. S. (2014) Superoxide dismutases and superoxide reductases. *Chemical reviews* **114**, 3854-3918
15. Liu, Y., Fiskum, G., and Schubert, D. (2002) Generation of reactive oxygen species by the mitochondrial electron transport chain. *Journal of neurochemistry* **80**, 780-787
16. Winterbourn, C. C. (2013) The biological chemistry of hydrogen peroxide. *Methods in enzymology* **528**, 3-25
17. Winterbourn, C. C. (2018) Biological Production, Detection, and Fate of Hydrogen Peroxide. *Antioxidants & redox signaling* **29**, 541-551
18. Dickinson, B. C., and Chang, C. J. (2011) Chemistry and biology of reactive oxygen species in signaling or stress responses. *Nature chemical biology* **7**, 504-511
19. Gough, D. R., and Cotter, T. G. (2011) Hydrogen peroxide: a Jekyll and Hyde signalling molecule. *Cell death & disease* **2**, e213
20. Veal, E. A., Day, A. M., and Morgan, B. A. (2007) Hydrogen peroxide sensing and signaling. *Molecular cell* **26**, 1-14
21. Sies, H. (2017) Hydrogen peroxide as a central redox signaling molecule in physiological oxidative stress: Oxidative eustress. *Redox Biol* **11**, 613-619

22. Imlay, J. A. (2008) Cellular defenses against superoxide and hydrogen peroxide. *Annual review of biochemistry* **77**, 755-776

23. Möller, M. N., Lancaster Jr, J.R., and Denicola, A. (2008) The interaction of reactive oxygen species and nitrogen species with membranes. *Current Topics in Membranes* **61**, 23-42

24. Makino, N., Sasaki, K., Hashida, K., and Sakakura, Y. (2004) A metabolic model describing the H2O2 elimination by mammalian cells including H2O2 permeation through cytoplasmic and peroxisomal membranes: comparison with experimental data. *Biochimica et biophysica acta* **1673**, 149-159

25. Bienert, G. P., Moller, A. L., Kristiansen, K. A., Schulz, A., Moller, I. M., Schjoerring, J. K., and Jahn, T. P. (2007) Specific aquaporins facilitate the diffusion of hydrogen peroxide across membranes. *The Journal of biological chemistry* **282**, 1183-1192

26. Straube, R., and Ridgway, D. (2009) Investigating the effects of molecular crowding on Ca2+ diffusion using a particle-based simulation model. *Chaos* **19**, 037110

27. Randall, L. M., Ferrer-Sueta, G., and Denicola, A. (2013) Peroxiredoxins as preferential targets in H2O2-induced signaling. *Methods in enzymology* **527**, 41-63

28. Ferrer-Sueta, G., Manta, B., Botti, H., Radi, R., Trujillo, M., and Denicola, A. (2011) Factors affecting protein thiol reactivity and specificity in peroxide reduction. *Chemical research in toxicology* **24**, 434-450

29. Netto, L. E., and Antunes, F. (2016) The Roles of Peroxiredoxin and Thioredoxin in Hydrogen Peroxide Sensing and in Signal Transduction. *Molecules and cells* **39**, 65-71

30. Beckman, J. S., Beckman, T. W., Chen, J., Marshall, P. A., and Freeman, B. A. (1990) Apparent hydroxyl radical production by peroxynitrite: implications for endothelial injury from nitric oxide and superoxide. *Proceedings of the National Academy of Sciences of the United States of America* **87**, 1620-1624

31. Ischiropoulos, H., Zhu, L., Chen, J., Tsai, M., Martin, J. C., Smith, C. D., and Beckman, J. S. (1992) Peroxynitrite-mediated tyrosine nitration catalyzed by superoxide dismutase. *Archives of biochemistry and biophysics* **298**, 431-437

32. Radi, R., Beckman, J. S., Bush, K. M., and Freeman, B. A. (1991) Peroxynitrite-induced membrane lipid peroxidation: the cytotoxic potential of superoxide and nitric oxide. *Archives of biochemistry and biophysics* **288**, 481-487

33. Ferrer-Sueta, G., and Radi, R. (2009) Chemical biology of peroxynitrite: kinetics, diffusion, and radicals. *ACS Chem Biol* **4**, 161-177

34. Pacher, P., Beckman, J. S., and Liaudet, L. (2007) Nitric oxide and peroxynitrite in health and disease. *Physiological reviews* **87**, 315-424

35. Szabo, C., Ischiropoulos, H., and Radi, R. (2007) Peroxynitrite: biochemistry, pathophysiology and development of therapeutics. *Nature reviews. Drug discovery* **6**, 662-680

36. Trujillo, M., Alvarez, B., Souza, J.M., Romero, N., Castro, L., Thomson, L. and Radi, R. (2010) *Nitric Oxide and Pathobiology*, Academic Press, Orlando, FL

37. Torreilles, F., Salman-Tabcheh, S., Guerin, M., and Torreilles, J. (1999) Neurodegenerative disorders: the role of peroxynitrite. *Brain research. Brain research reviews* **30**, 153-163

38. Uppu, R. M., Nossaman, B. D., Greco, A. J., Fokin, A., Murthy, S. N., Fonseca, V. A., and Kadowitz, P. J. (2007) Cardiovascular effects of peroxynitrite. *Clinical and experimental pharmacology & physiology* **34**, 933-937

39. Wattanapitayakul, S. K., Weinstein, D. M., Holycross, B. J., and Bauer, J. A. (2000) Endothelial dysfunction and peroxynitrite formation are early events in angiotensin-induced cardiovascular disorders. *FASEB journal : official publication of the Federation of American Societies for Experimental Biology* **14**, 271-278

40.   Arora, M., Kumar, A., Kaundal, R. K., and Sharma, S. S. (2008) Amelioration of neurological and biochemical deficits by peroxynitrite decomposition catalysts in experimental diabetic neuropathy. *European journal of pharmacology* **596**, 77-83

41.   Zou, M. H., Cohen, R., and Ullrich, V. (2004) Peroxynitrite and vascular endothelial dysfunction in diabetes mellitus. *Endothelium : journal of endothelial cell research* **11**, 89-97

42.   Cross, A. H., Manning, P. T., Stern, M. K., and Misko, T. P. (1997) Evidence for the production of peroxynitrite in inflammatory CNS demyelination. *Journal of neuroimmunology* **80**, 121-130

43.   Sandhu, J. K., Robertson, S., Birnboim, H. C., and Goldstein, R. (2003) Distribution of protein nitrotyrosine in synovial tissues of patients with rheumatoid arthritis and osteoarthritis. *The Journal of rheumatology* **30**, 1173-1181

44.   Oates, J. C., Christensen, E. F., Reilly, C. M., Self, S. E., and Gilkeson, G. S. (1999) Prospective measure of serum 3-nitrotyrosine levels in systemic lupus erythematosus: correlation with disease activity. *Proceedings of the Association of American Physicians* **111**, 611-621

45.   Goldstein, S., and Czapski, G. (1995) The reaction of NO. with O2.- and HO2.: a pulse radiolysis study. *Free radical biology & medicine* **19**, 505-510

46.   Huie, R. E., and Padmaja, S. (1993) The reaction of no with superoxide. *Free radical research communications* **18**, 195-199

47.   Kissner, R., Nauser, T., Bugnon, P., Lye, P. G., and Koppenol, W. H. (1997) Formation and properties of peroxynitrite as studied by laser flash photolysis, high-pressure stopped-flow technique, and pulse radiolysis. *Chemical research in toxicology* **10**, 1285-1292

48.   Pryor, W. A., and Squadrito, G. L. (1995) The chemistry of peroxynitrite: a product from the reaction of nitric oxide with superoxide. *The American journal of physiology* **268**, L699-722

49.   Denicola, A., Souza, J. M., and Radi, R. (1998) Diffusion of peroxynitrite across erythrocyte membranes. *Proceedings of the National Academy of Sciences of the United States of America* **95**, 3566-3571

50.   Marla, S. S., Lee, J., and Groves, J. T. (1997) Peroxynitrite rapidly permeates phospholipid membranes. *Proceedings of the National Academy of Sciences of the United States of America* **94**, 14243-14248

51.   Lymar, S. V., and Hurst, J. K. (1998) Radical nature of peroxynitrite reactivity. *Chemical research in toxicology* **11**, 714-715

52.   Ferrer-Sueta, G., Campolo, N., Trujillo, M., Bartesaghi, S., Carballal, S., Romero, N., Alvarez, B., and Radi, R. (2018) Biochemistry of Peroxynitrite and Protein Tyrosine Nitration. *Chemical reviews* **118**, 1338-1408

53.   Carballal, S., Bartesaghi, S., and Radi, R. (2014) Kinetic and mechanistic considerations to assess the biological fate of peroxynitrite. *Biochimica et biophysica acta* **1840**, 768-780

54.   Romero, N., Radi, R., Linares, E., Augusto, O., Detweiler, C. D., Mason, R. P., and Denicola, A. (2003) Reaction of human hemoglobin with peroxynitrite. Isomerization to nitrate and secondary formation of protein radicals. *The Journal of biological chemistry* **278**, 44049-44057

55.   Trujillo, M., Ferrer-Sueta, G., and Radi, R. (2008) Peroxynitrite detoxification and its biologic implications. *Antioxidants & redox signaling* **10**, 1607-1620

56.   Radi, R., Beckman, J. S., Bush, K. M., and Freeman, B. A. (1991) Peroxynitrite oxidation of sulfhydryls. The cytotoxic potential of superoxide and nitric oxide. *The Journal of biological chemistry* **266**, 4244-4250

57.   Koppenol, W. H., Moreno, J. J., Pryor, W. A., Ischiropoulos, H., and Beckman, J. S. (1992) Peroxynitrite, a cloaked oxidant formed by nitric oxide and superoxide. *Chemical research in toxicology* **5**, 834-842

58. Trujillo, M., and Radi, R. (2002) Peroxynitrite reaction with the reduced and the oxidized forms of lipoic acid: new insights into the reaction of peroxynitrite with thiols. *Archives of biochemistry and biophysics* **397**, 91-98

59. Winterbourn, C. C., and Metodiewa, D. (1999) Reactivity of biologically important thiol compounds with superoxide and hydrogen peroxide. *Free radical biology & medicine* **27**, 322-328

60. Fomenko, D. E., Marino, S. M., and Gladyshev, V. N. (2008) Functional diversity of cysteine residues in proteins and unique features of catalytic redox-active cysteines in thiol oxidoreductases. *Molecules and cells* **26**, 228-235

61. Skaff, O., Pattison, D. I., and Davies, M. J. (2009) Hypothiocyanous acid reactivity with low-molecular-mass and protein thiols: absolute rate constants and assessment of biological relevance. *The Biochemical journal* **422**, 111-117

62. Peskin, A. V., and Winterbourn, C. C. (2001) Kinetics of the reactions of hypochlorous acid and amino acid chloramines with thiols, methionine, and ascorbate. *Free radical biology & medicine* **30**, 572-579

63. Baker, L. M., Baker, P. R., Golin-Bisello, F., Schopfer, F. J., Fink, M., Woodcock, S. R., Branchaud, B. P., Radi, R., and Freeman, B. A. (2007) Nitro-fatty acid reaction with glutathione and cysteine. Kinetic analysis of thiol alkylation by a Michael addition reaction. *The Journal of biological chemistry* **282**, 31085-31093

64. Hill, B. G., Reily, C., Oh, J. Y., Johnson, M. S., and Landar, A. (2009) Methods for the determination and quantification of the reactive thiol proteome. *Free radical biology & medicine* **47**, 675-683

65. Aebi, H. (1984) Catalase in vitro. *Methods in enzymology* **105**, 121-126

66. Chance, B., Sies, H., and Boveris, A. (1979) Hydroperoxide metabolism in mammalian organs. *Physiological reviews* **59**, 527-605

67. Winternitz, M. C., and Meloy, C. R. (1908) On the Occurrence of Catalase in Human Tissues and Its Variations in Diseases. *The Journal of experimental medicine* **10**, 759-781

68. https://www.brenda-enzymes.org/

69. Glorieux, C., and Calderon, P. B. (2017) Catalase, a remarkable enzyme: targeting the oldest antioxidant enzyme to find a new cancer treatment approach. *Biological chemistry* **398**, 1095-1108

70. Gebicka, L., and Didik, J. (2009) Catalytic scavenging of peroxynitrite by catalase. *Journal of inorganic biochemistry* **103**, 1375-1379

71. Heinzelmann, S., and Bauer, G. (2010) Multiple protective functions of catalase against intercellular apoptosis-inducing ROS signaling of human tumor cells. *Biological chemistry* **391**, 675-693

72. Flohe, L., Gunzler, W. A., and Schock, H. H. (1973) Glutathione peroxidase: a selenoenzyme. *FEBS letters* **32**, 132-134

73. Stadtman, T. C. (1974) Selenium biochemistry. *Science* **183**, 915-922

74. Flohé, L. (1982) Glutathione peroxidase brought into focus. in *Free Radicals in Biology* (Pryor, W. A. ed.), Ed. Academic Press. pp 223-254

75. Brigelius-Flohe, R., and Maiorino, M. (2013) Glutathione peroxidases. *Biochimica et biophysica acta* **1830**, 3289-3303

76. Selles, B., Hugo, M., Trujillo, M., Srivastava, V., Wingsle, G., Jacquot, J. P., Radi, R., and Rouhier, N. (2012) Hydroperoxide and peroxynitrite reductase activity of poplar thioredoxin-dependent glutathione peroxidase 5: kinetics, catalytic mechanism and oxidative inactivation. *The Biochemical journal* **442**, 369-380

77. Sies, H., Sharov, V. S., Klotz, L. O., and Briviba, K. (1997) Glutathione peroxidase protects against peroxynitrite-mediated oxidations. A new function for selenoproteins as peroxynitrite reductase. *The Journal of biological chemistry* **272**, 27812-27817

78. Flohé L., B.-F. R. (2016) Basics and news on glutathione peroxidases. in *Selenium, its molecular biology and role in human health* (Hatfield D.L., S. U., Tsuji P.A., Gladyshev V.N. ed.), 4th Ed., Springer, New York. pp

79. Chae, H. Z., Chung, S. J., and Rhee, S. G. (1994) Thioredoxin-dependent peroxide reductase from yeast. *The Journal of biological chemistry* **269**, 27670-27678

80. Chae, H. Z., Robison, K., Poole, L. B., Church, G., Storz, G., and Rhee, S. G. (1994) Cloning and sequencing of thiol-specific antioxidant from mammalian brain: alkyl hydroperoxide reductase and thiol-specific antioxidant define a large family of antioxidant enzymes. *Proceedings of the National Academy of Sciences of the United States of America* **91**, 7017-7021

81. Bryk, R., Griffin, P., and Nathan, C. (2000) Peroxynitrite reductase activity of bacterial peroxiredoxins. *Nature* **407**, 211-215

82. Manta, B., Hugo, M., Ortiz, C., Ferrer-Sueta, G., Trujillo, M., and Denicola, A. (2009) The peroxidase and peroxynitrite reductase activity of human erythrocyte peroxiredoxin 2. *Archives of biochemistry and biophysics* **484**, 146-154

83. De Armas, M. I., Esteves, R., Viera, N., Reyes, A. M., Mastrogiovanni, M., Alegria, T. G. P., Netto, L. E. S., Tortora, V., Radi, R., and Trujillo, M. (2019) Rapid peroxynitrite reduction by human peroxiredoxin 3: Implications for the fate of oxidants in mitochondria. *Free radical biology & medicine* **130**, 369-378

84. Dalla Rizza, J., Randall, L. M., Santos, J., Ferrer-Sueta, G., and Denicola, A. (2019) Differential parameters between cytosolic 2-Cys peroxiredoxins, PRDX1 and PRDX2. *Protein Sci* **28**, 191-201

85. Dubuisson, M., Vander Stricht, D., Clippe, A., Etienne, F., Nauser, T., Kissner, R., Koppenol, W. H., Rees, J. F., and Knoops, B. (2004) Human peroxiredoxin 5 is a peroxynitrite reductase. *FEBS letters* **571**, 161-165

86. Trujillo, M., Clippe, A., Manta, B., Ferrer-Sueta, G., Smeets, A., Declercq, J. P., Knoops, B., and Radi, R. (2007) Pre-steady state kinetic characterization of human peroxiredoxin 5: taking advantage of Trp84 fluorescence increase upon oxidation. *Archives of biochemistry and biophysics* **467**, 95-106

87. Toledo, J. C., Jr., Audi, R., Ogusucu, R., Monteiro, G., Netto, L. E., and Augusto, O. (2011) Horseradish peroxidase compound I as a tool to investigate reactive protein-cysteine residues: from quantification to kinetics. *Free radical biology & medicine* **50**, 1032-1038

88. Trujillo, M., Budde, H., Pineyro, M. D., Stehr, M., Robello, C., Flohe, L., and Radi, R. (2004) Trypanosoma brucei and Trypanosoma cruzi tryparedoxin peroxidases catalytically detoxify peroxynitrite via oxidation of fast reacting thiols. *The Journal of biological chemistry* **279**, 34175-34182

89. Reyes, A. M., Hugo, M., Trostchansky, A., Capece, L., Radi, R., and Trujillo, M. (2011) Oxidizing substrate specificity of Mycobacterium tuberculosis alkyl hydroperoxide reductase E: kinetics and mechanisms of oxidation and overoxidation. *Free radical biology & medicine* **51**, 464-473

90. Loumaye, E., Ferrer-Sueta, G., Alvarez, B., Rees, J. F., Clippe, A., Knoops, B., Radi, R., and Trujillo, M. (2011) Kinetic studies of peroxiredoxin 6 from Arenicola marina: rapid oxidation by hydrogen peroxide and peroxynitrite but lack of reduction by hydrogen sulfide. *Archives of biochemistry and biophysics* **514**, 1-7

91. Pineyro, M. D., Arcari, T., Robello, C., Radi, R., and Trujillo, M. (2011) Tryparedoxin peroxidases from Trypanosoma cruzi: high efficiency in the catalytic elimination of hydrogen peroxide and peroxynitrite. *Archives of biochemistry and biophysics* **507**, 287-295

92. Ogusucu, R., Rettori, D., Munhoz, D. C., Netto, L. E., and Augusto, O. (2007) Reactions of yeast thioredoxin peroxidases I and II with hydrogen peroxide and

peroxynitrite: rate constants by competitive kinetics. *Free radical biology & medicine* **42**, 326-334

93. Su, T., Si, M., Zhao, Y., Liu, Y., Yao, S., Che, C., and Chen, C. (2018) A thioredoxin-dependent peroxiredoxin Q from Corynebacterium glutamicum plays an important role in defense against oxidative stress. *PloS one* **13**, e0192674

94. Hugo, M., Turell, L., Manta, B., Botti, H., Monteiro, G., Netto, L. E., Alvarez, B., Radi, R., and Trujillo, M. (2009) Thiol and sulfenic acid oxidation of AhpE, the one-cysteine peroxiredoxin from Mycobacterium tuberculosis: kinetics, acidity constants, and conformational dynamics. *Biochemistry* **48**, 9416-9426

95. Staudacher, V., Djuika, C. F., Koduka, J., Schlossarek, S., Kopp, J., Buchler, M., Lanzer, M., and Deponte, M. (2015) Plasmodium falciparum antioxidant protein reveals a novel mechanism for balancing turnover and inactivation of peroxiredoxins. *Free radical biology & medicine* **85**, 228-236

96. Romero-Puertas, M. C., Laxa, M., Matte, A., Zaninotto, F., Finkemeier, I., Jones, A. M., Perazzolli, M., Vandelle, E., Dietz, K. J., and Delledonne, M. (2007) S-nitrosylation of peroxiredoxin II E promotes peroxynitrite-mediated tyrosine nitration. *Plant Cell* **19**, 4120-4130

97. Pedrajas, J. R., Carreras, A., Valderrama, R., and Barroso, J. B. (2010) Mitochondrial 1-Cys-peroxiredoxin/thioredoxin system protects manganese-containing superoxide dismutase (Mn-SOD) against inactivation by peroxynitrite in Saccharomyces cerevisiae. *Nitric oxide : biology and chemistry* **23**, 206-213

98. Hattori, F., Murayama, N., Noshita, T., and Oikawa, S. (2003) Mitochondrial peroxiredoxin-3 protects hippocampal neurons from excitotoxic injury in vivo. *Journal of neurochemistry* **86**, 860-868

99. Chae, H. Z., Kim, H. J., Kang, S. W., and Rhee, S. G. (1999) Characterization of three isoforms of mammalian peroxiredoxin that reduce peroxides in the presence of thioredoxin. *Diabetes Res Clin Pract* **45**, 101-112

100. Park, J. W., Piszczek, G., Rhee, S. G., and Chock, P. B. (2011) Glutathionylation of peroxiredoxin I induces decamer to dimers dissociation with concomitant loss of chaperone activity. *Biochemistry* **50**, 3204-3210

101. Cho, C. S., Kato, G. J., Yang, S. H., Bae, S. W., Lee, J. S., Gladwin, M. T., and Rhee, S. G. (2010) Hydroxyurea-induced expression of glutathione peroxidase 1 in red blood cells of individuals with sickle cell anemia. *Antioxidants & redox signaling* **13**, 1-11

102. Moore, R. B., Mankad, M. V., Shriver, S. K., Mankad, V. N., and Plishker, G. A. (1991) Reconstitution of Ca(2+)-dependent K+ transport in erythrocyte membrane vesicles requires a cytoplasmic protein. *The Journal of biological chemistry* **266**, 18964-18968

103. Jang, H. H., Lee, K. O., Chi, Y. H., Jung, B. G., Park, S. K., Park, J. H., Lee, J. R., Lee, S. S., Moon, J. C., Yun, J. W., Choi, Y. O., Kim, W. Y., Kang, J. S., Cheong, G. W., Yun, D. J., Rhee, S. G., Cho, M. J., and Lee, S. Y. (2004) Two enzymes in one; two yeast peroxiredoxins display oxidative stress-dependent switching from a peroxidase to a molecular chaperone function. *Cell* **117**, 625-635

104. Rhee, S. G., and Woo, H. A. (2011) Multiple functions of peroxiredoxins: peroxidases, sensors and regulators of the intracellular messenger H(2)O(2), and protein chaperones. *Antioxidants & redox signaling* **15**, 781-794

105. Hall, A., Parsonage, D., Poole, L. B., and Karplus, P. A. (2010) Structural evidence that peroxiredoxin catalytic power is based on transition-state stabilization. *Journal of molecular biology* **402**, 194-209

106. Poole, L. B., and Nelson, K. J. (2016) Distribution and Features of the Six Classes of Peroxiredoxins. *Molecules and cells* **39**, 53-59

107. Hall, A., Nelson, K., Poole, L. B., and Karplus, P. A. (2011) Structure-based insights into the catalytic power and conformational dexterity of peroxiredoxins. *Antioxidants & redox signaling* **15**, 795-815

108. Perkins, A., Nelson, K. J., Parsonage, D., Poole, L. B., and Karplus, P. A. (2015) Peroxiredoxins: guardians against oxidative stress and modulators of peroxide signaling. *Trends in biochemical sciences* **40**, 435-445

109. Randall, L. M., Manta, B., Hugo, M., Gil, M., Batthyany, C., Trujillo, M., Poole, L. B., and Denicola, A. (2014) Nitration transforms a sensitive peroxiredoxin 2 into a more active and robust peroxidase. *The Journal of biological chemistry* **289**, 15536-15543

110. Wood, Z. A., Poole, L. B., and Karplus, P. A. (2003) Peroxiredoxin evolution and the regulation of hydrogen peroxide signaling. *Science* **300**, 650-653

111. Haynes, A. C., Qian, J., Reisz, J. A., Furdui, C. M., and Lowther, W. T. (2013) Molecular basis for the resistance of human mitochondrial 2-Cys peroxiredoxin 3 to hyperoxidation. *The Journal of biological chemistry* **288**, 29714-29723

112. Bolduc, J. A., Nelson, K. J., Haynes, A. C., Lee, J., Reisz, J. A., Graff, A. H., Clodfelter, J. E., Parsonage, D., Poole, L. B., Furdui, C. M., and Lowther, W. T. (2018) Novel hyperoxidation resistance motifs in 2-Cys peroxiredoxins. *The Journal of biological chemistry* **293**, 11901-11912

113. Agarwal, P. K., Doucet, N., Chennubhotla, C., Ramanathan, A., and Narayanan, C. (2016) Conformational Sub-states and Populations in Enzyme Catalysis. *Methods in enzymology* **578**, 273-297

114. Baldwin, A. J., and Kay, L. E. (2009) NMR spectroscopy brings invisible protein states into focus. *Nature chemical biology* **5**, 808-814

115. Faraj, S. (2016) *Dinámica molecular y consolidación estructural de la frataxina humana.* Ph.D., Universidad de Buenos Aires

116. Li, J., Kanekiyo, T., Shinohara, M., Zhang, Y., LaDu, M. J., Xu, H., and Bu, G. (2012) Differential regulation of amyloid-beta endocytic trafficking and lysosomal degradation by apolipoprotein E isoforms. *The Journal of biological chemistry* **287**, 44593-44601

117. Gilbert, H. F. (1990) Molecular and cellular aspects of thiol-disulfide exchange. *Advances in enzymology and related areas of molecular biology* **63**, 69-172

118. Trujillo, M., Ferrer-Sueta, G., Thomson, L., Flohe, L., and Radi, R. (2007) Kinetics of peroxiredoxins and their role in the decomposition of peroxynitrite. *Sub-cellular biochemistry* **44**, 83-113

119. Zeida, A., Guardia, C. M., Lichtig, P., Perissinotti, L. L., Defelipe, L. A., Turjanski, A., Radi, R., Trujillo, M., and Estrin, D. A. (2014) Thiol redox biochemistry: insights from computer simulations. *Biophys Rev* **6**, 27-46

120. Wood, Z. A., Schroder, E., Harris, R. J., and Poole, L. B. (2003) Structure, mechanism and regulation of peroxiredoxins. *Trends in biochemical sciences* **28**, 32-40

121. Nelson, K. J., Knutson, S. T., Soito, L., Klomsiri, C., Poole, L. B., and Fetrow, J. S. (2011) Analysis of the peroxiredoxin family: using active-site structure and sequence information for global classification and residue analysis. *Proteins* **79**, 947-964

122. Hall, A., Karplus, P. A., and Poole, L. B. (2009) Typical 2-Cys peroxiredoxins-- structures, mechanisms and functions. *The FEBS journal* **276**, 2469-2477

123. Rhee, S. G., Woo, H. A., Kil, I. S., and Bae, S. H. (2012) Peroxiredoxin functions as a peroxidase and a regulator and sensor of local peroxides. *The Journal of biological chemistry* **287**, 4403-4410

124. Chae, H. Z., Oubrahim, H., Park, J. W., Rhee, S. G., and Chock, P. B. (2012) Protein glutathionylation in the regulation of peroxiredoxins: a family of thiol-specific peroxidases that function as antioxidants, molecular chaperones, and signal modulators. *Antioxidants & redox signaling* **16**, 506-523

125. Lowther, W. T., and Haynes, A. C. (2011) Reduction of cysteine sulfinic acid in eukaryotic, typical 2-Cys peroxiredoxins by sulfiredoxin. *Antioxidants & redox signaling* **15**, 99-109

126. Dietz, K. J. (2011) Peroxiredoxins in plants and cyanobacteria. *Antioxidants & redox signaling* **15**, 1129-1159

127. Saccoccia, F., Di Micco, P., Boumis, G., Brunori, M., Koutris, I., Miele, A. E., Morea, V., Sriratana, P., Williams, D. L., Bellelli, A., and Angelucci, F. (2012) Moonlighting by different stressors: crystal structure of the chaperone species of a 2-Cys peroxiredoxin. *Structure* **20**, 429-439

128. Harris, J. R., Schroder, E., Isupov, M. N., Scheffler, D., Kristensen, P., Littlechild, J. A., Vagin, A. A., and Meissner, U. (2001) Comparison of the decameric structure of peroxiredoxin-II by transmission electron microscopy and X-ray crystallography. *Biochimica et biophysica acta* **1547**, 221-234

129. Phalen, T. J., Weirather, K., Deming, P. B., Anathy, V., Howe, A. K., van der Vliet, A., Jonsson, T. J., Poole, L. B., and Heintz, N. H. (2006) Oxidation state governs structural transitions in peroxiredoxin II that correlate with cell cycle arrest and recovery. *The Journal of cell biology* **175**, 779-789

130. Barranco-Medina, S., Kakorin, S., Lazaro, J. J., and Dietz, K. J. (2008) Thermodynamics of the dimer-decamer transition of reduced human and plant 2-cys peroxiredoxin. *Biochemistry* **47**, 7196-7204

131. Wood, Z. A., Poole, L. B., Hantgan, R. R., and Karplus, P. A. (2002) Dimers to doughnuts: redox-sensitive oligomerization of 2-cysteine peroxiredoxins. *Biochemistry* **41**, 5493-5504

132. Lee, W., Choi, K. S., Riddell, J., Ip, C., Ghosh, D., Park, J. H., and Park, Y. M. (2007) Human peroxiredoxin 1 and 2 are not duplicate proteins: the unique presence of CYS83 in Prx1 underscores the structural and functional differences between Prx1 and Prx2. *The Journal of biological chemistry* **282**, 22011-22022

133. Matsumura, T., Okamoto, K., Iwahara, S., Hori, H., Takahashi, Y., Nishino, T., and Abe, Y. (2008) Dimer-oligomer interconversion of wild-type and mutant rat 2-Cys peroxiredoxin: disulfide formation at dimer-dimer interfaces is not essential for decamerization. *The Journal of biological chemistry* **283**, 284-293

134. Chuang, M. H., Wu, M. S., Lo, W. L., Lin, J. T., Wong, C. H., and Chiou, S. H. (2006) The antioxidant protein alkylhydroperoxide reductase of Helicobacter pylori switches from a peroxide reductase to a molecular chaperone function. *Proceedings of the National Academy of Sciences of the United States of America* **103**, 2552-2557

135. Jang, H. H., Kim, S. Y., Park, S. K., Jeon, H. S., Lee, Y. M., Jung, J. H., Lee, S. Y., Chae, H. B., Jung, Y. J., Lee, K. O., Lim, C. O., Chung, W. S., Bahk, J. D., Yun, D. J., Cho, M. J., and Lee, S. Y. (2006) Phosphorylation and concomitant structural changes in human 2-Cys peroxiredoxin isotype I differentially regulate its peroxidase and molecular chaperone functions. *FEBS letters* **580**, 351-355

136. Veal, E. A., Underwood, Z. E., Tomalin, L. E., Morgan, B. A., and Pillay, C. S. (2018) Hyperoxidation of Peroxiredoxins: Gain or Loss of Function? *Antioxidants & redox signaling* **28**, 574-590

137. Morais, M. A., Giuseppe, P. O., Souza, T. A., Alegria, T. G., Oliveira, M. A., Netto, L. E., and Murakami, M. T. (2015) How pH modulates the dimer-decamer interconversion of 2-Cys peroxiredoxins from the Prx1 subfamily. *The Journal of biological chemistry* **290**, 8582-8590

138. Neumann, C. A., Krause, D. S., Carman, C. V., Das, S., Dubey, D. P., Abraham, J. L., Bronson, R. T., Fujiwara, Y., Orkin, S. H., and Van Etten, R. A. (2003) Essential role for the peroxiredoxin Prdx1 in erythrocyte antioxidant defence and tumour suppression. *Nature* **424**, 561-565

139. Lee, T. H., Kim, S. U., Yu, S. L., Kim, S. H., Park, D. S., Moon, H. B., Dho, S. H., Kwon, K. S., Kwon, H. J., Han, Y. H., Jeong, S., Kang, S. W., Shin, H. S.,

Lee, K. K., Rhee, S. G., and Yu, D. Y. (2003) Peroxiredoxin II is essential for sustaining life span of erythrocytes in mice. *Blood* **101**, 5033-5038

140. Cox, A. G., Pearson, A. G., Pullar, J. M., Jonsson, T. J., Lowther, W. T., Winterbourn, C. C., and Hampton, M. B. (2009) Mitochondrial peroxiredoxin 3 is more resilient to hyperoxidation than cytoplasmic peroxiredoxins. *The Biochemical journal* **421**, 51-58

141. Carvalho, L. A. C., Truzzi, D. R., Fallani, T. S., Alves, S. V., Toledo, J. C., Jr., Augusto, O., Netto, L. E. S., and Meotti, F. C. (2017) Urate hydroperoxide oxidizes human peroxiredoxin 1 and peroxiredoxin 2. *The Journal of biological chemistry* **292**, 8705-8715

142. Schroder, E., Littlechild, J. A., Lebedev, A. A., Errington, N., Vagin, A. A., and Isupov, M. N. (2000) Crystal structure of decameric 2-Cys peroxiredoxin from human erythrocytes at 1.7 A resolution. *Structure* **8**, 605-615

143. Kim, S. U., Jin, M. H., Kim, Y. S., Lee, S. H., Cho, Y. S., Cho, K. J., Lee, K. S., Kim, Y. I., Kim, G. W., Kim, J. M., Lee, T. H., Lee, Y. H., Shong, M., Kim, H. C., Chang, K. T., Yu, D. Y., and Lee, D. S. (2011) Peroxiredoxin II preserves cognitive function against age-linked hippocampal oxidative damage. *Neurobiology of aging* **32**, 1054-1068

144. Peskin, A. V., Dickerhof, N., Poynton, R. A., Paton, L. N., Pace, P. E., Hampton, M. B., and Winterbourn, C. C. (2013) Hyperoxidation of peroxiredoxins 2 and 3: rate constants for the reactions of the sulfenic acid of the peroxidatic cysteine. *The Journal of biological chemistry* **288**, 14170-14177

145. Sarma, G. N., Nickel, C., Rahlfs, S., Fischer, M., Becker, K., and Karplus, P. A. (2005) Crystal structure of a novel Plasmodium falciparum 1-Cys peroxiredoxin. *Journal of molecular biology* **346**, 1021-1034

146. Cheah, F. C., Peskin, A. V., Wong, F. L., Ithnin, A., Othman, A., and Winterbourn, C. C. (2014) Increased basal oxidation of peroxiredoxin 2 and limited peroxiredoxin recycling in glucose-6-phosphate dehydrogenase-deficient erythrocytes from newborn infants. *FASEB journal : official publication of the Federation of American Societies for Experimental Biology* **28**, 3205-3210

147. Low, F. M., Hampton, M. B., Peskin, A. V., and Winterbourn, C. C. (2007) Peroxiredoxin 2 functions as a noncatalytic scavenger of low-level hydrogen peroxide in the erythrocyte. *Blood* **109**, 2611-2617

148. O'Neill, J. S., and Reddy, A. B. (2011) Circadian clocks in human red blood cells. *Nature* **469**, 498-503

149. Feliciano, A., Vaz, F., Torres, V. M., Valentim-Coelho, C., Silva, R., Prosinecki, V., Alexandre, B. M., Carvalho, A. S., Matthiesen, R., Malhotra, A., Pinto, P., Barbara, C., and Penque, D. (2017) Evening and morning peroxiredoxin-2 redox/oligomeric state changes in obstructive sleep apnea red blood cells: Correlation with polysomnographic and metabolic parameters. *Biochimica et biophysica acta. Molecular basis of disease* **1863**, 621-629

150. Day, A. M., Brown, J. D., Taylor, S. R., Rand, J. D., Morgan, B. A., and Veal, E. A. (2012) Inactivation of a peroxiredoxin by hydrogen peroxide is critical for thioredoxin-mediated repair of oxidized proteins and cell survival. *Molecular cell* **45**, 398-408

151. Biteau, B., Labarre, J., and Toledano, M. B. (2003) ATP-dependent reduction of cysteine-sulphinic acid by S. cerevisiae sulphiredoxin. *Nature* **425**, 980-984

152. Park, J. W., Mieyal, J. J., Rhee, S. G., and Chock, P. B. (2009) Deglutathionylation of 2-Cys peroxiredoxin is specifically catalyzed by sulfiredoxin. *The Journal of biological chemistry* **284**, 23364-23374

153. Peskin, A. V., Pace, P. E., Behring, J. B., Paton, L. N., Soethoudt, M., Bachschmid, M. M., and Winterbourn, C. C. (2016) Glutathionylation of the Active Site Cysteines of Peroxiredoxin 2 and Recycling by Glutaredoxin. *The Journal of biological chemistry* **291**, 3053-3062

154. Astier, J., and Lindermayr, C. (2012) Nitric oxide-dependent posttranslational modification in plants: an update. *International journal of molecular sciences* **13**, 15193-15208

155. Begara-Morales, J. C., Sanchez-Calvo, B., Chaki, M., Valderrama, R., Mata-Perez, C., Padilla, M. N., Corpas, F. J., and Barroso, J. B. (2016) Antioxidant Systems are Regulated by Nitric Oxide-Mediated Post-translational Modifications (NO-PTMs). *Frontiers in plant science* **7**, 152

156. Corpas, F. J., Bergara-Morales, J.C., Sánchez-Calvo, B., Chaki, M. and Barroso, J.B. (2015) Nitration and S-Nitrosylation: two post-translational modifications (PTMs) mediated by reactive nitrogen species (RNS) and their role in signalling processes of plant cells. in *Reactive oxygen and nitrogen species signaling and communication in plants* (A.U., G. K. J. a. I. ed.), Springer, Berlin. pp 267-281

157. Hess, D. T., Matsumoto, A., Kim, S. O., Marshall, H. E., and Stamler, J. S. (2005) Protein S-nitrosylation: purview and parameters. *Nature reviews. Molecular cell biology* **6**, 150-166

158. Astier, J., Rasul, S., Koen, E., Manzoor, H., Besson-Bard, A., Lamotte, O., Jeandroz, S., Durner, J., Lindermayr, C., and Wendehenne, D. (2011) S-nitrosylation: an emerging post-translational protein modification in plants. *Plant science : an international journal of experimental plant biology* **181**, 527-533

159. Gaston, B., Reilly, J., Drazen, J. M., Fackler, J., Ramdev, P., Arnelle, D., Mullins, M. E., Sugarbaker, D. J., Chee, C., Singel, D. J., and et al. (1993) Endogenous nitrogen oxides and bronchodilator S-nitrosothiols in human airways. *Proceedings of the National Academy of Sciences of the United States of America* **90**, 10957-10961

160. Durner, J., Gow, A. J., Stamler, J. S., and Glazebrook, J. (1999) Ancient origins of nitric oxide signaling in biological systems. *Proceedings of the National Academy of Sciences of the United States of America* **96**, 14206-14207

161. Leitner, M., Vandelle, E., Gaupels, F., Bellin, D., and Delledonne, M. (2009) NO signals in the haze: nitric oxide signalling in plant defence. *Current opinion in plant biology* **12**, 451-458

162. Benhar, M., Forrester, M. T., Hess, D. T., and Stamler, J. S. (2008) Regulated protein denitrosylation by cytosolic and mitochondrial thioredoxins. *Science* **320**, 1050-1054

163. Kneeshaw, S., Gelineau, S., Tada, Y., Loake, G. J., and Spoel, S. H. (2014) Selective protein denitrosylation activity of Thioredoxin-h5 modulates plant Immunity. *Molecular cell* **56**, 153-162

164. Feechan, A., Kwon, E., Yun, B. W., Wang, Y., Pallas, J. A., and Loake, G. J. (2005) A central role for S-nitrosothiols in plant disease resistance. *Proceedings of the National Academy of Sciences of the United States of America* **102**, 8054-8059

165. Fang, J., Nakamura, T., Cho, D. H., Gu, Z., and Lipton, S. A. (2007) S-nitrosylation of peroxiredoxin 2 promotes oxidative stress-induced neuronal cell death in Parkinson's disease. *Proceedings of the National Academy of Sciences of the United States of America* **104**, 18742-18747

166. Sunico, C. R., and Moreno-Lopez, B. (2010) Evidence for endothelial nitric oxide as a negative regulator of Schwann cell dedifferentiation after peripheral nerve injury. *Neuroscience letters* **471**, 119-124

167. Sunico, C. R., Sultan, A., Nakamura, T., Dolatabadi, N., Parker, J., Shan, B., Han, X., Yates, J. R., 3rd, Masliah, E., Ambasudhan, R., Nakanishi, N., and Lipton, S. A. (2016) Role of sulfiredoxin as a peroxiredoxin-2 denitrosylase in human iPSC-derived dopaminergic neurons. *Proceedings of the National Academy of Sciences of the United States of America* **113**, E7564-E7571

168. Akter, S., Fu, L., Jung, Y., Conte, M. L., Lawson, J. R., Lowther, W. T., Sun, R., Liu, K., Yang, J., and Carroll, K. S. (2018) Chemical proteomics reveals new

targets of cysteine sulfinic acid reductase. *Nature chemical biology* **14**, 995-1004

169. Qu, D., Rashidian, J., Mount, M. P., Aleyasin, H., Parsanejad, M., Lira, A., Haque, E., Zhang, Y., Callaghan, S., Daigle, M., Rousseaux, M. W., Slack, R. S., Albert, P. R., Vincent, I., Woulfe, J. M., and Park, D. S. (2007) Role of Cdk5-mediated phosphorylation of Prx2 in MPTP toxicity and Parkinson's disease. *Neuron* **55**, 37-52

170. Parmigiani, R. B., Xu, W. S., Venta-Perez, G., Erdjument-Bromage, H., Yaneva, M., Tempst, P., and Marks, P. A. (2008) HDAC6 is a specific deacetylase of peroxiredoxins and is involved in redox regulation. *Proceedings of the National Academy of Sciences of the United States of America* **105**, 9633-9638

171. Seo, J. H., Lim, J. C., Lee, D. Y., Kim, K. S., Piszczek, G., Nam, H. W., Kim, Y. S., Ahn, T., Yun, C. H., Kim, K., Chock, P. B., and Chae, H. Z. (2009) Novel protective mechanism against irreversible hyperoxidation of peroxiredoxin: Nalpha-terminal acetylation of human peroxiredoxin II. *The Journal of biological chemistry* **284**, 13455-13465

172. Radi, R. (2004) Nitric oxide, oxidants, and protein tyrosine nitration. *Proceedings of the National Academy of Sciences of the United States of America* **101**, 4003-4008

173. Gow, A. J., Farkouh, C. R., Munson, D. A., Posencheg, M. A., and Ischiropoulos, H. (2004) Biological significance of nitric oxide-mediated protein modifications. *American journal of physiology. Lung cellular and molecular physiology* **287**, L262-268

174. Moller, M. N., Li, Q., Vitturi, D. A., Robinson, J. M., Lancaster, J. R., Jr., and Denicola, A. (2007) Membrane "lens" effect: focusing the formation of reactive nitrogen oxides from the *NO/O2 reaction. *Chemical research in toxicology* **20**, 709-714

175. Turko, I. V., Li, L., Aulak, K. S., Stuehr, D. J., Chang, J. Y., and Murad, F. (2003) Protein tyrosine nitration in the mitochondria from diabetic mouse heart. Implications to dysfunctional mitochondria in diabetes. *The Journal of biological chemistry* **278**, 33972-33977

176. Abello, N., Kerstjens, H. A., Postma, D. S., and Bischoff, R. (2009) Protein tyrosine nitration: selectivity, physicochemical and biological consequences, denitration, and proteomics methods for the identification of tyrosine-nitrated proteins. *Journal of proteome research* **8**, 3222-3238

177. Souza, J. M., Peluffo, G., and Radi, R. (2008) Protein tyrosine nitration--functional alteration or just a biomarker? *Free radical biology & medicine* **45**, 357-366

178. Radi, R. (2013) Protein tyrosine nitration: biochemical mechanisms and structural basis of functional effects. *Accounts of chemical research* **46**, 550-559

179. Souza, J. M., Choi, I., Chen, Q., Weisse, M., Daikhin, E., Yudkoff, M., Obin, M., Ara, J., Horwitz, J., and Ischiropoulos, H. (2000) Proteolytic degradation of tyrosine nitrated proteins. *Archives of biochemistry and biophysics* **380**, 360-366

180. Zhang, Y. J., Xu, Y. F., Chen, X. Q., Wang, X. C., and Wang, J. Z. (2005) Nitration and oligomerization of tau induced by peroxynitrite inhibit its microtubule-binding activity. *FEBS letters* **579**, 2421-2427

181. Gow, A. J., Duran, D., Malcolm, S., and Ischiropoulos, H. (1996) Effects of peroxynitrite-induced protein modifications on tyrosine phosphorylation and degradation. *FEBS letters* **385**, 63-66

182. Grune, T., Klotz, L. O., Gieche, J., Rudeck, M., and Sies, H. (2001) Protein oxidation and proteolysis by the nonradical oxidants singlet oxygen or peroxynitrite. *Free radical biology & medicine* **30**, 1243-1253

183. Gorg, B., Qvartskhava, N., Voss, P., Grune, T., Haussinger, D., and Schliess, F. (2007) Reversible inhibition of mammalian glutamine synthetase by tyrosine nitration. *FEBS letters* **581**, 84-90

184. Deeb, R. S., Nuriel, T., Cheung, C., Summers, B., Lamon, B. D., Gross, S. S., and Hajjar, D. P. (2013) Characterization of a cellular denitrase activity that reverses nitration of cyclooxygenase. *American journal of physiology. Heart and circulatory physiology* **305**, H687-698

185. Aulak, K. S., Koeck, T., Crabb, J. W., and Stuehr, D. J. (2004) Dynamics of protein nitration in cells and mitochondria. *American journal of physiology. Heart and circulatory physiology* **286**, H30-38

186. Koeck, T., Fu, X., Hazen, S. L., Crabb, J. W., Stuehr, D. J., and Aulak, K. S. (2004) Rapid and selective oxygen-regulated protein tyrosine denitration and nitration in mitochondria. *The Journal of biological chemistry* **279**, 27257-27262

187. Irie, Y., Saeki, M., Kamisaki, Y., Martin, E., and Murad, F. (2003) Histone H1.2 is a substrate for denitrase, an activity that reduces nitrotyrosine immunoreactivity in proteins. *Proceedings of the National Academy of Sciences of the United States of America* **100**, 5634-5639

188. Kamisaki, Y., Wada, K., Bian, K., Balabanli, B., Davis, K., Martin, E., Behbod, F., Lee, Y. C., and Murad, F. (1998) An activity in rat tissues that modifies nitrotyrosine-containing proteins. *Proceedings of the National Academy of Sciences of the United States of America* **95**, 11584-11589

189. Huang, J., Lin, S. C., Nadershahi, A., Watts, S. W., and Sarkar, R. (2008) Role of redox signaling and poly (adenosine diphosphate-ribose) polymerase activation in vascular smooth muscle cell growth inhibition by nitric oxide and peroxynitrite. *Journal of vascular surgery* **47**, 599-607

190. Thomson, L., Christie, J., Vadseth, C., Lanken, P. N., Fu, X., Hazen, S. L., and Ischiropoulos, H. (2007) Identification of immunoglobulins that recognize 3-nitrotyrosine in patients with acute lung injury after major trauma. *American journal of respiratory cell and molecular biology* **36**, 152-157

191. Smith, M. A., Richey Harris, P. L., Sayre, L. M., Beckman, J. S., and Perry, G. (1997) Widespread peroxynitrite-mediated damage in Alzheimer's disease. *The Journal of neuroscience : the official journal of the Society for Neuroscience* **17**, 2653-2657

192. Tohgi, H., Abe, T., Yamazaki, K., Murata, T., Ishizaki, E., and Isobe, C. (1999) Alterations of 3-nitrotyrosine concentration in the cerebrospinal fluid during aging and in patients with Alzheimer's disease. *Neuroscience letters* **269**, 52-54

193. Castegna, A., Thongboonkerd, V., Klein, J. B., Lynn, B., Markesbery, W. R., and Butterfield, D. A. (2003) Proteomic identification of nitrated proteins in Alzheimer's disease brain. *Journal of neurochemistry* **85**, 1394-1401

194. Hensley, K., Maidt, M. L., Yu, Z., Sang, H., Markesbery, W. R., and Floyd, R. A. (1998) Electrochemical analysis of protein nitrotyrosine and dityrosine in the Alzheimer brain indicates region-specific accumulation. *The Journal of neuroscience : the official journal of the Society for Neuroscience* **18**, 8126-8132

195. Su, J. H., Deng, G., and Cotman, C. W. (1997) Neuronal DNA damage precedes tangle formation and is associated with up-regulation of nitrotyrosine in Alzheimer's disease brain. *Brain research* **774**, 193-199

196. Good, P. F., Hsu, A., Werner, P., Perl, D. P., and Olanow, C. W. (1998) Protein nitration in Parkinson's disease. *Journal of neuropathology and experimental neurology* **57**, 338-342

197. Tohgi, H., Abe, T., Yamazaki, K., Murata, T., Ishizaki, E., and Isobe, C. (1999) Increase in oxidized NO products and reduction in oxidized glutathione in cerebrospinal fluid from patients with sporadic form of amyotrophic lateral sclerosis. *Neuroscience letters* **260**, 204-206

198. Cookson, M. R., and Shaw, P. J. (1999) Oxidative stress and motor neurone disease. *Brain pathology* **9**, 165-186

199. Hall, E. D., Detloff, M. R., Johnson, K., and Kupina, N. C. (2004) Peroxynitrite-mediated protein nitration and lipid peroxidation in a mouse model of traumatic brain injury. *Journal of neurotrauma* **21**, 9-20

200. Tanaka, K., Shirai, T., Nagata, E., Dembo, T., and Fukuuchi, Y. (1997) Immunohistochemical detection of nitrotyrosine in postischemic cerebral cortex in gerbil. *Neuroscience letters* **235**, 85-88

201. Walker, L. M., York, J. L., Imam, S. Z., Ali, S. F., Muldrew, K. L., and Mayeux, P. R. (2001) Oxidative stress and reactive nitrogen species generation during renal ischemia. *Toxicological sciences : an official journal of the Society of Toxicology* **63**, 143-148

202. Zou, M. H., and Bachschmid, M. (1999) Hypoxia-reoxygenation triggers coronary vasospasm in isolated bovine coronary arteries via tyrosine nitration of prostacyclin synthase. *The Journal of experimental medicine* **190**, 135-139

203. Reed, T. T., Pierce, W. M., Jr., Turner, D. M., Markesbery, W. R., and Butterfield, D. A. (2009) Proteomic identification of nitrated brain proteins in early Alzheimer's disease inferior parietal lobule. *J Cell Mol Med* **13**, 2019-2029

204. Takahashi, M., Shigeto, J., Sakamoto, A., Izumi, S., Asada, K., and Morikawa, H. (2015) Dual selective nitration in Arabidopsis: Almost exclusive nitration of PsbO and PsbP, and highly susceptible nitration of four non-PSII proteins, including peroxiredoxin II E. *Electrophoresis* **36**, 2569-2578

205. Ghesquiere, B., Colaert, N., Helsens, K., Dejager, L., Vanhaute, C., Verleysen, K., Kas, K., Timmerman, E., Goethals, M., Libert, C., Vandekerckhove, J., and Gevaert, K. (2009) In vitro and in vivo protein-bound tyrosine nitration characterized by diagonal chromatography. *Molecular & cellular proteomics : MCP* **8**, 2642-2652

206. Ghesquiere, B., Goethals, M., Van Damme, J., Staes, A., Timmerman, E., Vandekerckhove, J., and Gevaert, K. (2006) Improved tandem mass spectrometric characterization of 3-nitrotyrosine sites in peptides. *Rapid communications in mass spectrometry : RCM* **20**, 2885-2893

207. Stevens, S. M., Jr., Prokai-Tatrai, K., and Prokai, L. (2008) Factors that contribute to the misidentification of tyrosine nitration by shotgun proteomics. *Molecular & cellular proteomics : MCP* **7**, 2442-2451

208. Matsuzawa, A. (2017) Thioredoxin and redox signaling: Roles of the thioredoxin system in control of cell fate. *Archives of biochemistry and biophysics* **617**, 101-105

209. Jonsson, T. J., Johnson, L. C., and Lowther, W. T. (2008) Structure of the sulphiredoxin-peroxiredoxin complex reveals an essential repair embrace. *Nature* **451**, 98-101

210. Choi, M. H., Lee, I. K., Kim, G. W., Kim, B. U., Han, Y. H., Yu, D. Y., Park, H. S., Kim, K. Y., Lee, J. S., Choi, C., Bae, Y. S., Lee, B. I., Rhee, S. G., and Kang, S. W. (2005) Regulation of PDGF signalling and vascular remodelling by peroxiredoxin II. *Nature* **435**, 347-353

211. Cha, M. K., Yun, C. H., and Kim, I. H. (2000) Interaction of human thiol-specific antioxidant protein 1 with erythrocyte plasma membrane. *Biochemistry* **39**, 6944-6950

212. Moore, R. B., and Shriver, S. K. (1997) Protein 7.2b of human erythrocyte membranes binds to calpromotin. *Biochemical and biophysical research communications* **232**, 294-297

213. Pallotta, V., D'Alessandro, A., Rinalducci, S., and Zolla, L. (2013) Native protein complexes in the cytoplasm of red blood cells. *Journal of proteome research* **12**, 3529-3546

214. Bayer, S. B., Low, F. M., Hampton, M. B., and Winterbourn, C. C. (2016) Interactions between peroxiredoxin 2, hemichrome and the erythrocyte membrane. *Free radical research* **50**, 1329-1339

215. Ma, Q., An, L., Tian, H., Liu, J., Zhang, L., Li, X., Wei, C., Xie, C., Ding, H., Qin, W., and Su, Y. (2019) Interactions between human hemoglobin subunits and peroxiredoxin 2. *Frontiers in bioscience* **24**, 1085-1096

216. Lang, F., Abed, M., Lang, E., and Foller, M. (2014) Oxidative stress and suicidal erythrocyte death. *Antioxidants & redox signaling* **21**, 138-153

217. Sobotta, M. C., Liou, W., Stocker, S., Talwar, D., Oehler, M., Ruppert, T., Scharf, A. N., and Dick, T. P. (2015) Peroxiredoxin-2 and STAT3 form a redox relay for H2O2 signaling. *Nature chemical biology* **11**, 64-70

218. Pace, P. E., Peskin, A. V., Han, M. H., Hampton, M. B., and Winterbourn, C. C. (2013) Hyperoxidized peroxiredoxin 2 interacts with the protein disulfide-isomerase ERp46. *The Biochemical journal* **453**, 475-485

219. Gaetano, C., Matsuo, T., and Thiele, C. J. (1997) Identification and characterization of a retinoic acid-regulated human homologue of the unc-33-like phosphoprotein gene (hUlip) from neuroblastoma cells. *The Journal of biological chemistry* **272**, 12195-12201

220. Ricard, D., Rogemond, V., Charrier, E., Aguera, M., Bagnard, D., Belin, M. F., Thomasset, N., and Honnorat, J. (2001) Isolation and expression pattern of human Unc-33-like phosphoprotein 6/collapsin response mediator protein 5 (Ulip6/CRMP5): coexistence with Ulip2/CRMP2 in Sema3a- sensitive oligodendrocytes. *The Journal of neuroscience : the official journal of the Society for Neuroscience* **21**, 7203-7214

221. Gordon-Weeks, P. R. (2004) Microtubules and growth cone function. *Journal of neurobiology* **58**, 70-83

222. Vincent, P., Collette, Y., Marignier, R., Vuaillat, C., Rogemond, V., Davoust, N., Malcus, C., Cavagna, S., Gessain, A., Machuca-Gayet, I., Belin, M. F., Quach, T., and Giraudon, P. (2005) A role for the neuronal protein collapsin response mediator protein 2 in T lymphocyte polarization and migration. *Journal of immunology* **175**, 7650-7660

223. Rakhmetov, A. D., Pil, L. S., Ostapchenko, L. I., and Zoon, C. H. (2016) Prx II and CKBB proteins interaction under physiologic al and thermal stress conditions in A549 and HeLa cells. *Ukrainian biochemical journal* **88**, 61-68

224. Kang, D. H., Lee, D. J., Lee, S., Lee, S. Y., Jun, Y., Kim, Y., Kim, Y., Lee, J. S., Lee, D. K., Lee, S., Jho, E. H., Yu, D. Y., and Kang, S. W. (2017) Interaction of tankyrase and peroxiredoxin II is indispensable for the survival of colorectal cancer cells. *Nature communications* **8**, 40

225. Fernandez-Caggiano, M., Schroder, E., Cho, H. J., Burgoyne, J., Barallobre-Barreiro, J., Mayr, M., and Eaton, P. (2016) Oxidant-induced Interprotein Disulfide Formation in Cardiac Protein DJ-1 Occurs via an Interaction with Peroxiredoxin 2. *The Journal of biological chemistry* **291**, 10399-10410

226. Peskin, A. V., Low, F. M., Paton, L. N., Maghzal, G. J., Hampton, M. B., and Winterbourn, C. C. (2007) The high reactivity of peroxiredoxin 2 with H(2)O(2) is not reflected in its reaction with other oxidants and thiol reagents. *The Journal of biological chemistry* **282**, 11885-11892

227. Parsonage, D., Youngblood, D. S., Sarma, G. N., Wood, Z. A., Karplus, P. A., and Poole, L. B. (2005) Analysis of the link between enzymatic activity and oligomeric state in AhpC, a bacterial peroxiredoxin. *Biochemistry* **44**, 10583-10592

228. Reyes, A. M., Vazquez, D. S., Zeida, A., Hugo, M., Pineyro, M. D., De Armas, M. I., Estrin, D., Radi, R., Santos, J., and Trujillo, M. (2016) PrxQ B from Mycobacterium tuberculosis is a monomeric, thioredoxin-dependent and highly efficient fatty acid hydroperoxide reductase. *Free radical biology & medicine* **101**, 249-260

229. Cox, A. G., Peskin, A. V., Paton, L. N., Winterbourn, C. C., and Hampton, M. B. (2009) Redox potential and peroxide reactivity of human peroxiredoxin 3. *Biochemistry* **48**, 6495-6501

230. Portillo-Ledesma, S., Sardi, F., Manta, B., Tourn, M. V., Clippe, A., Knoops, B., Alvarez, B., Coitino, E. L., and Ferrer-Sueta, G. (2014) Deconstructing the catalytic efficiency of peroxiredoxin-5 peroxidatic cysteine. *Biochemistry* **53**, 6113-6125

231. Stocker, S., Van Laer, K., Mijuskovic, A., and Dick, T. P. (2018) The Conundrum of Hydrogen Peroxide Signaling and the Emerging Role of Peroxiredoxins as Redox Relay Hubs. *Antioxidants & redox signaling* **28**, 558-573

232. Stocker, S., Maurer, M., Ruppert, T., and Dick, T. P. (2018) A role for 2-Cys peroxiredoxins in facilitating cytosolic protein thiol oxidation. *Nature chemical biology* **14**, 148-155

233. Peskin, A. V., Cox, A. G., Nagy, P., Morgan, P. E., Hampton, M. B., Davies, M. J., and Winterbourn, C. C. (2010) Removal of amino acid, peptide and protein hydroperoxides by reaction with peroxiredoxins 2 and 3. *The Biochemical journal* **432**, 313-321

234. Winterbourn, C. C., and Hampton, M. B. (2008) Thiol chemistry and specificity in redox signaling. *Free radical biology & medicine* **45**, 549-561

235. Brown, J. D., Day, A. M., Taylor, S. R., Tomalin, L. E., Morgan, B. A., and Veal, E. A. (2013) A peroxiredoxin promotes H2O2 signaling and oxidative stress resistance by oxidizing a thioredoxin family protein. *Cell reports* **5**, 1425-1435

236. Bozonet, S. M., Findlay, V. J., Day, A. M., Cameron, J., Veal, E. A., and Morgan, B. A. (2005) Oxidation of a eukaryotic 2-Cys peroxiredoxin is a molecular switch controlling the transcriptional response to increasing levels of hydrogen peroxide. *The Journal of biological chemistry* **280**, 23319-23327

237. Jeong, W., Bae, S. H., Toledano, M. B., and Rhee, S. G. (2012) Role of sulfiredoxin as a regulator of peroxiredoxin function and regulation of its expression. *Free radical biology & medicine* **53**, 447-456

238. Kil, I. S., Ryu, K. W., Lee, S. K., Kim, J. Y., Chu, S. Y., Kim, J. H., Park, S., and Rhee, S. G. (2015) Circadian Oscillation of Sulfiredoxin in the Mitochondria. *Molecular cell* **59**, 651-663

239. Molin, M., Yang, J., Hanzen, S., Toledano, M. B., Labarre, J., and Nystrom, T. (2011) Life span extension and H(2)O(2) resistance elicited by caloric restriction require the peroxiredoxin Tsa1 in Saccharomyces cerevisiae. *Molecular cell* **43**, 823-833

240. Delaunay, A., Isnard, A. D., and Toledano, M. B. (2000) H2O2 sensing through oxidation of the Yap1 transcription factor. *Embo J* **19**, 5157-5166

241. Vivancos, A. P., Castillo, E. A., Biteau, B., Nicot, C., Ayte, J., Toledano, M. B., and Hidalgo, E. (2005) A cysteine-sulfinic acid in peroxiredoxin regulates H2O2-sensing by the antioxidant Pap1 pathway. *Proceedings of the National Academy of Sciences of the United States of America* **102**, 8875-8880

242. Trotter, E. W., Rand, J. D., Vickerstaff, J., and Grant, C. M. (2008) The yeast Tsa1 peroxiredoxin is a ribosome-associated antioxidant. *The Biochemical journal* **412**, 73-80

243. Findlay, V. J., Townsend, D. M., Morris, T. E., Fraser, J. P., He, L., and Tew, K. D. (2006) A novel role for human sulfiredoxin in the reversal of glutathionylation. *Cancer research* **66**, 6800-6806

244. Karplus, P. A. (2015) A primer on peroxiredoxin biochemistry. *Free radical biology & medicine* **80**, 183-190

245. Fomenko, D. E., Koc, A., Agisheva, N., Jacobsen, M., Kaya, A., Malinouski, M., Rutherford, J. C., Siu, K. L., Jin, D. Y., Winge, D. R., and Gladyshev, V. N. (2011) Thiol peroxidases mediate specific genome-wide regulation of gene

expression in response to hydrogen peroxide. *Proceedings of the National Academy of Sciences of the United States of America* **108**, 2729-2734

246. Gutscher, M., Sobotta, M. C., Wabnitz, G. H., Ballikaya, S., Meyer, A. J., Samstag, Y., and Dick, T. P. (2009) Proximity-based protein thiol oxidation by H2O2-scavenging peroxidases. *The Journal of biological chemistry* **284**, 31532-31540

247. Trujillo, M., Ferrer-Sueta, G., and Radi, R. (2008) Kinetic studies on peroxynitrite reduction by peroxiredoxins. *Methods in enzymology* **441**, 173-196

248. Radi, R. (1996) Kinetic analysis of reactivity of peroxynitrite with biomolecules. *Methods in enzymology* **269**, 354-366

249. Nelson, K. J., Parsonage, D., Karplus, P. A., and Poole, L. B. (2013) Evaluating peroxiredoxin sensitivity toward inactivation by peroxide substrates. *Methods in enzymology* **527**, 21-40

250. Parsonage, D., Nelson, K. J., Ferrer-Sueta, G., Alley, S., Karplus, P. A., Furdui, C. M., and Poole, L. B. (2015) Dissecting peroxiredoxin catalysis: separating binding, peroxidation, and resolution for a bacterial AhpC. *Biochemistry* **54**, 1567-1575

251. J.H., E. (1995) Chemical kinetics and reaction mechanisms. in *Series in advanced chemistry* (J.H., E. ed.), McGraw-Hill, New York. pp 46-49

252. Randall, L., Manta, B., Nelson, K. J., Santos, J., Poole, L. B., and Denicola, A. (2016) Structural changes upon peroxynitrite-mediated nitration of peroxiredoxin 2; nitrated Prx2 resembles its disulfide-oxidized form. *Archives of biochemistry and biophysics* **590**, 101-108

253. Randall L.M., D. R. J., Parsonage D., Mehl R.A., Lowther W.T., Santos J., Poole L.B., Denicola A. (2019) Unravelling the effects of nitration on human Prx2 activity. *Free radical biology & medicine* **Under revision**

254. Portillo-Ledesma, S., Randall, L. M., Parsonage, D., Dalla Rizza, J., Karplus, P. A., Poole, L. B., Denicola, A., and Ferrer-Sueta, G. (2018) Differential Kinetics of Two-Cysteine Peroxiredoxin Disulfide Formation Reveal a Novel Model for Peroxide Sensing. *Biochemistry* **57**, 3416-3424

255. Woo, H. A., Yim, S. H., Shin, D. H., Kang, D., Yu, D. Y., and Rhee, S. G. (2010) Inactivation of peroxiredoxin I by phosphorylation allows localized H(2)O(2) accumulation for cell signaling. *Cell* **140**, 517-528

7. ANEXO

Differential parameters between cytosolic 2-Cys peroxiredoxins, PRDX1 and PRDX2

Dalla Rizza J, Randall, LM; Santos J, Ferrer-Sueta G, Denicola A

Protein Science (2019) 28, 191-201.

Differential parameters between cytosolic 2-Cys peroxiredoxins, PRDX1 and PRDX2

Joaquín Dalla Rizza,[1,2] Lía M. Randall,[1,2,3] Javier Santos,[4] Gerardo Ferrer-Sueta,[1,2] and Ana Denicola ⓘ[1,2]*

[1]Laboratorio de Fisicoquímica Biológica, Instituto de Química Biológica, Facultad de Ciencias, Universidad de la República, Montevideo, Uruguay
[2]Center for Free Radical and Biomedical Research, Universidad de la República, Montevideo, Uruguay
[3]Laboratorio de I+D de Moléculas Bioactivas, CENUR Litoral Norte, Universidad de la República, Paysandú, Uruguay
[4]IQUIFIB (UBA-CONICET) and Departamento de Química Biológica, Facultad de Farmacia y Bioquímica, and Department of Physiology, Molecular and Cellular Biology, Universidad de Buenos Aires, Ciudad Autónoma de Buenos Aires, Argentina

Abstract: Peroxiredoxins are thiol-dependent peroxidases that function in peroxide detoxification and H_2O_2 induced signaling. Among the six isoforms expressed in humans, PRDX1 and PRDX2 share 97% sequence similarity, 77% sequence identity including the active site, subcellular localization (cytosolic) but they hold different biological functions albeit associated with their peroxidase activity. Using recombinant human PRDX1 and PRDX2, the kinetics of oxidation and hyperoxidation with H_2O_2 and peroxynitrite were followed by intrinsic fluorescence. At pH 7.4, the peroxidatic cysteine of both isoforms reacts nearly tenfold faster with H_2O_2 than with peroxynitrite, and both reactions are orders of magnitude faster than with most protein thiols. For both isoforms, the sulfenic acids formed are in turn oxidized by H_2O_2 with rate constants of *ca* 2×10^3 M^{-1} s^{-1} and by peroxynitrous acid significantly faster. As previously observed, a crucial difference between PRDX1 and PRDX2 is on the resolution step of the catalytic cycle, the rate of disulfide formation (11 s^{-1} for PRDX1, 0.2 s^{-1} for PRDX2, independent of the oxidant) which correlates with their different sensitivity to hyperoxidation. This kinetic pause opens different pathways on redox signaling for these isoforms. The longer lifetime of PRDX2 sulfenic acid allows it to react with other protein thiols to translate the signal via an intermediate mixed disulfide (involving its peroxidatic cysteine), whereas PRDX1 continues the cycle forming disulfide involving its resolving cysteine to function as a redox relay. In addition, the presence of C83 on PRDX1 imparts a difference on peroxidase activity upon peroxynitrite exposure that needs further study.

Keywords: peroxiredoxin 1; peroxiredoxin 2; hyperoxidation; redox signaling; hydrogen peroxide; peroxynitrite; kinetics

Introduction

Peroxiredoxins (Prx) are thiol-dependent peroxidases that efficiently reduce H_2O_2 and also organic hydroperoxides and peroxynitrous acid.[1,2] They have been mostly known as good antioxidants, scavengers of toxic levels of peroxides, and recently more attention is focused on their role in redox signaling considering their abundance and high rate constant of reaction with H_2O_2.[3,4]

A specialized cysteine residue called peroxidatic cysteine, C_P, is responsible for the reduction of the peroxide substrate (the oxidation step in the catalytic cycle, Fig. 1). The sulfenic acid formed (C_P-SOH) condenses with a cysteine residue from another subunit, the resolving cysteine, C_R, to form an intermolecular disulfide (the resolution step). Thus, each dimer contains two catalytic sites. The resolution step includes a crucial conformational change (from fully folded to locally unfolded or FF→LU) that makes the C_P side chain more accessible and in which both conformations are in dynamic equilibrium. The disulfide is finally reduced by an electron donor such as thioredoxin to regenerate the dithiol enzyme (the reduction step, Fig. 1). Any modification of the peroxidatic cysteine like protonation, alkylation or nitrosylation[5,6] will prevent reaction with the peroxide substrate rendering an inactive peroxidase. In addition, the reaction of C_P-SOH with another molecule of peroxide yields a sulfinic acid (Prx hyperoxidation, Fig. 1) inactivating the enzyme until sulfiredoxin (only expressed in eukaryotes) catalyzes its ATP-dependent reduction back to C_P-SOH.[7]

Prx were originally divided into three categories depending on the number and location of cysteine residues involved in catalysis: the 1-Cys, the typical 2-Cys and the atypical 2-Cys Prxs.[2,8] More recently, based on functional site sequence similarity, Prx have been classified into subgroups Prx1, Prx5, Prx6, Tpx, AhpE, and PrxQ.[9] Humans express six Prx isoforms, four in the Prx1 subgroup, one Prx5 and one in the Prx6 subgroup. Human PRDX1 and PRDX2 belong to the Prx1 subgroup, both are 2-Cys typical Prx, both are cytosolic and have more than 95% sequence similarity, even more, 77% sequence identity, but yet they hold different biological functions albeit associated with their peroxidase activity.

The redox state of these Prx has been associated with the oligomeric structure switching from the disulfide-oxidized homodimer to the reduced decamer (doughnut-shaped pentamer of dimers) as described before for bacterial AhpC, also a member of the Prx1 subgroup.[10] In addition to the catalytic cysteine residues C_P and C_R (C52 and C173 for PRDX1, C51 and C172 for PRDX2), both contain another Cys residue (C71, C70, respectively) that is poorly accessible and need SDS addition to be quantified or alkylated.[11] In addition, PRDX1 has a fourth Cys residue, C83, located in the dimer–dimer interface that can be alkylated and was reported glutathionylated favoring dimer formation.[12]

The relevance of these two cytosolic Prx isoforms in cell homeostasis, and at the same time their differential role, is underlined by the observation that knock-out mice in PRDX1 developed malignant tumors and die prematurely,[13] whereas knock-out
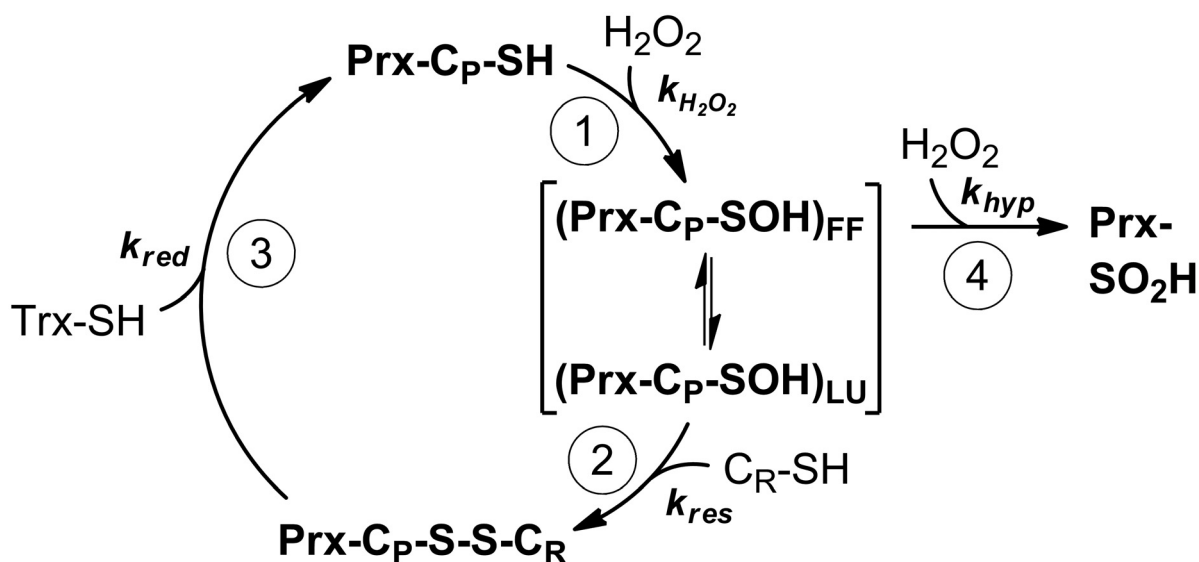
Figure 1. Catalytic cycle of peroxide reduction by 2-Cys Prx. (1) Oxidation. Reaction of Prx peroxidatic cysteine C_P with peroxide substrate yield the sulfenic acid. In brackets is represented the dynamic equilibrium between the LU and the FF structural conformations. (2) Resolution. Disulfide formation between C_P and C_R. (3) Reduction by thioredoxin to complete the cycle. (4) Hyperoxidation. Reaction of the sulfenic acid of C_P with H_2O_2, yielding a sulfinic acid which inactivates the enzyme. For each step, the associated rate constant is represented.
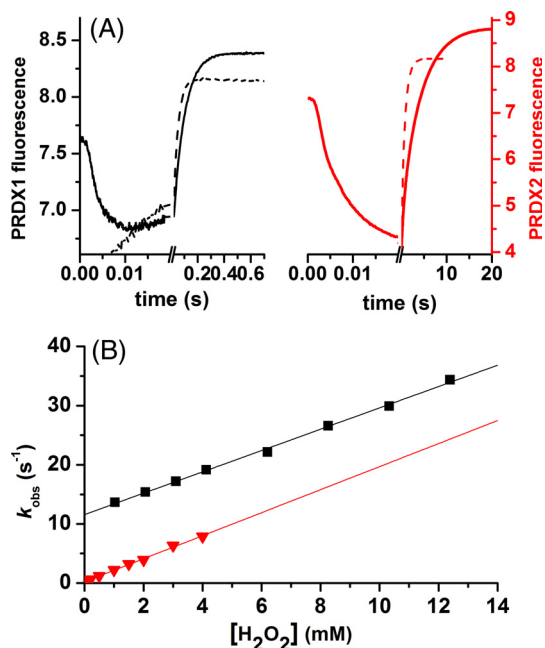
mice in PRDX2 were healthy and fertile but developed hemolytic anemia and splenomegalia.[14].

The aim of this work is to evaluate the kinetic differences between human PRDX1 and PRDX2 that contribute to understand their physiological role.

Results

Reduction of H₂O₂ by PRDX1 and PRDX2 followed by intrinsic fluorescence

The reaction of reduced Prx with H_2O_2 was followed by the change in fluorescence as previously described.[15–17] Two phases were observed, one rapid decrease in fluorescence and a slower increase [Fig. 2(a)]. The rate constant of the fast phase showed a linear dependence with H_2O_2 concentration and was assigned to the reaction of C_P-SH with H_2O_2, with a second-order rate constant of $k_{H2O2} = 1.1 \times 10^8$ M^{-1} s^{-1} for PRDX1 and 1.6×10^8 M^{-1} s^{-1} for PRDX2.[17] The slow phase was previously associated with the resolution step, the formation of disulfide Prx[16,17] but at higher concentrations of H_2O_2 the hyperoxidation reaction is competing for the same C_P-SOH. In fact, the slow phase was fitted to a single exponential function to obtain a first-order rate constant (k_{obs}, s^{-1}) that increased linearly with the concentration of H_2O_2 [Fig. 2(b)]. From the slope, a second-order rate constant for the reaction of C_P-SOH with H_2O_2, k_{hyp}, was obtained (1.8×10^3 M^{-1} s^{-1} for PRDX1

and 2×10^3 M^{-1} s^{-1} for PRDX2 at pH 7.4 and 25 °C). The intercepts represent the rate constant of disulfide formation, 11 s^{-1} for PRDX1 and 0.2 s^{-1} for PRDX2 [Fig. 2(b)] consistent with our previous report.[17]

Peroxidase activity of PRDX1 and PRDX2

Kinetic parameters were determined for the NAPDH-linked peroxidase activity using the coupled TR, Trx assay as before.[18] At a fixed concentration of H_2O_2 (saturating but not inactivating the enzyme) and varying the concentration of thioredoxin, the oxidation of NADPH was followed at 340 nm with saturating thioredoxin reductase so that the rate-limiting step was the reduction of Prx by Trx at low Trx concentrations. Initial rates as a function of Trx concentration [Fig. 3(a)] allowed the determination of K_m for *Escherichia coli* thioredoxin and k_{cat} values for both isoforms, summarized in Table .
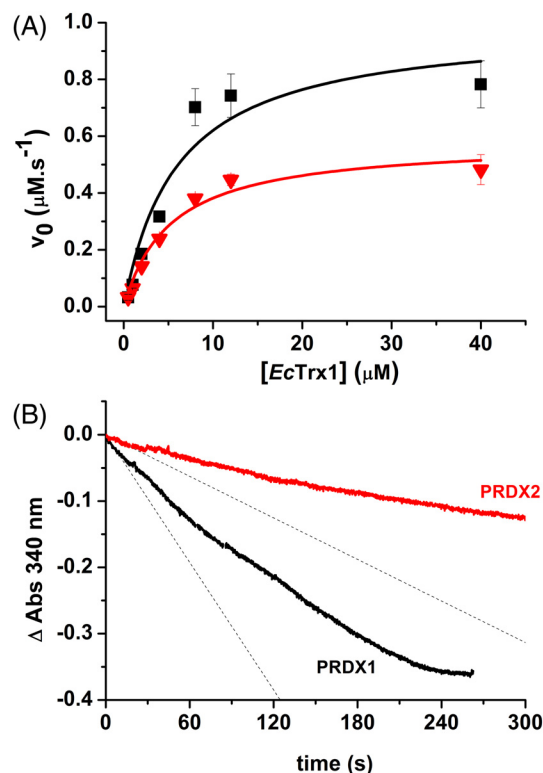
Figure 3. NADPH-linked peroxidase activity. (a) Determination of kinetic parameters (k_{cat}, K_M): reduction of H_2O_2 catalyzed by PRDX1 (black squares) or PRDX2 (red triangles) was monitored at different initial EcTrx1 concentrations with 200 μM NADPH, 1 μM EcTR, 0.5 μM PRDX1 or PRDX2 and 10 μM H_2O_2 in 50 mM phosphate buffer pH 7.4, 150 mM NaCl. NADPH oxidation was monitored at 340 nm. Experimental data was fitted to Michaelis–Menten equation (solid lines).
(b) Representative time trace of H_2O_2-dependent NADPH oxidation by the Prx/Trx/TR system at 50 μM H_2O_2. Reaction mixture contained 200 μM NADPH, 1 μM EcTR, 8 μM EcTrx1, 0.5 μM PRDX1 (black trace) or PRDX2 (red trace) in 50 mM phosphate buffer pH 7.4, 150 mM NaCl and the reaction was started by addition of H_2O_2. Dashed lines represent the initial slope of the reaction.


Figure 2. Kinetics of PRDX1 and PRDX2 oxidation by H_2O_2. (A) Time course of the intrinsic fluorescence of 0.25 μM PRDX1 (black line) or 0.25 μM PRDX2 (red line) upon oxidation with 1.25 μM or 1.5 μM H_2O_2, respectively (solid line) and 1 mM H_2O_2 (dashed line) in both cases, at pH 7.4 (traces are the average from 15 runs). (B) The slower phase was fitted to a single exponential function and the first-order rate constant (k_{obs}) plotted as a function of H_2O_2 concentration. PRDX1 (black squares) and PRDX2 (red triangles).

Differential susceptibility to hyperoxidation

The measurement of the activity at higher concentrations of H_2O_2 favors the hyperoxidation of Prx in turnover, and a slowdown of NAPDH oxidation was clearly observed, which was more pronounced for PRDX2 than for PRDX1 [Fig. 3(b) using 50 μM H_2O_2]. In addition, when reduced Prx was mixed with increasing concentrations of H_2O_2, the formation of dimers (bound by one or two disulfides) could be followed by nonreductive SDS-PAGE [Fig. 4(a)] and the presence of hyperoxidized C_P (C_P-SO_2H) detected by western blot (WB) [Fig. 4(b)]. Again, higher susceptibility to hyperoxidation was observed for PRDX2 than for PRDX1 as previously observed by Cox et al.[19] when comparing PRDX3 with cytosolic PRDX1 and PRDX2. Figure 4(a) shows the increase in monodisulfide dimers of PRDX2 with increasing H_2O_2 denoting a faster hyperoxidation (once C_P is hyperoxidized it cannot form the intermolecular disulfide) that is confirmed by western blotting [Fig. 4(b)]. In addition, at high excess of H_2O_2, hyperoxidized monomer was detected for PRDX2 and not yet for PRDX1. It is worth noting the presence of higher oligomers (tetramers) in the case of PRDX1 and not PRDX2 exposed to H_2O_2 [Fig. 4(a)] probably formed by C83 disulfides as they are reduced by β-mercaptoethanol (not shown).

Reduction of peroxynitrous acid by PRDX1

As reported before for PRDX2, PRDX1 is able to reduce peroxynitrous acid. The second-order rate constant of this reaction was determined by competition with horseradish peroxidase (HRP) as detailed in the section "Materials and Methods." First, a rate constant of $(2.0 \pm 0.2) \times 10^6$ M^{-1} s^{-1} was determined for the oxidation of HRP by peroxynitrite under our experimental conditions (Fig. 1) consistent with previously reported data.[20–22] In the presence of reduced PRDX1, the yield of peroxynitrite-dependent oxidation of HRP to Compound I was inhibited (Fig. 5) and using Equation 1, a rate constant of peroxynitrite-mediated PRDX1 oxidation was
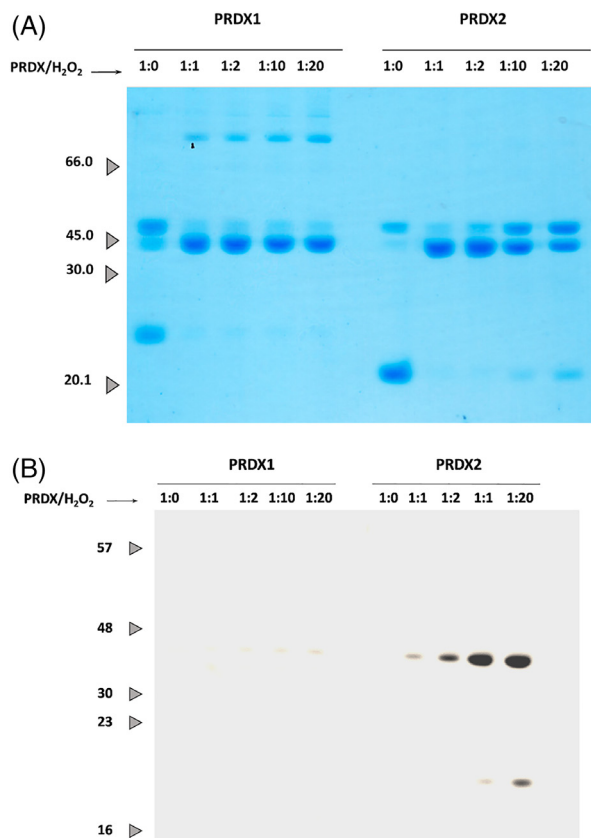
Figure 4. PRDX1 and PRDX2 differential hyperoxidation susceptibility. About 5 μM PRDX1 or PRDX2 were treated with increasing concentrations of H_2O_2. About 1 μg of protein of each sample was loaded and resolved in a 12% SDS-PAGE and analyzed by Coomassie staining (a) or WB using anti-Prx-$SO_{2/3}H$ antibody (b).

obtained, $k_{ONOOH} = (1.5 \pm 0.3) \times 10^7$ M^{-1} s^{-1} at pH 7.4 and 25 °C.

Reduction of ONOOH by PRDX1 and PRDX2 followed by intrinsic fluorescence

Upon reaction with excess of ONOOH, the fluorescence of PRDX1 shows a time course with three phases [Fig. 6(a)]. The data fit nicely to triple

Table I- *Summary of Kinetic Parameters for Human PRDX1 and PRDX2.*

	$k_{H_2O_2}^{app}$ (M^{-1} s^{-1})	k_{ONOOH}^{app} (M^{-1} s^{-1})	k_{res} (s^{-1})	K_M^{app} (μM)	k_{cat} (s^{-1})	$k_{hyp}^{H_2O_2}$ (M^{-1} s^{-1})	k_{hyp}^{ONOOH} (M^{-1} s^{-1})
PRDX1	3.8×10^7(16)	1.1×10^{7a}	9 (16)	5.5 (48)^c	4.4 (48)	1.77×10^3	2.8×10^{5b}
	1.1×10^8(17)	7.6×10^{6b}	12.9 (17) *11–12*	4	2		
PRDX2	$0.13–1 \times 10^8$(18)	1.4×10^7(18)	0.25 (16)	2.7 (48)^c	2 (48)	1.2×10^4	3.5×10^{4b}
	1.6×10^8(17)	$1.1 \times 10^{7\ b}$	2 (25)	2.4^d, 4^e (18)	0.2 (18)	1.97×10^3	
			0.64 (17)	3	1.2		
			0.2–0.3				

The values in italics were determined in the present work, see "Results" section
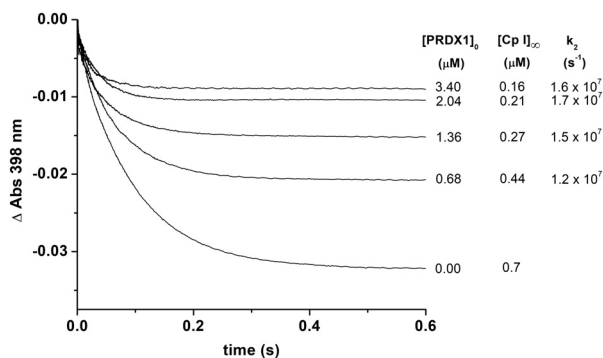[a]Competition with HRP at pH 7.4.
[b]Fluorescence time courses at pH 7.3.
[c]Rat thioredoxin.
[d]Human thioredoxin.
[e]*E. coli* thioredoxin.

Figure 5. Determination of the rate constant for the reaction of peroxynitrite with PRDX1 by competition kinetics. Time courses of HRP (5 μM) oxidation by peroxynitrite (0.7 μM) in the presence of prereduced PRDX1 (from bottom to top 0, 0.68, 1.36, 2.04, and 3.4 μM) in 100 mM sodium phosphate buffer pH 7.4 plus 0.1 mM dtpa at 25 °C. From the concentration of Compound I formed at each PRDX1 concentration, a value of k_2 was calculated using Equation 1.

exponential functions up to 13.5 μM ONOOH (Supporting Information Fig. S2). The first exponential fluorescence decay yields a rate constant that depends linearly on ONOOH concentration [Fig. 6(c)]

with a slope comparable with the oxidation rate constant obtained by HRP competitive kinetics (Fig. 5). We have assigned this rate constant to k_{ONOOH}^{app} (Table 1). The linear fit has a significant non-zero intercept (40 ± 2 s^{-1}). The rate constant from the second ascending exponential also depended linearly on ONOOH concentration [Fig. 6(d)]. In this case, the y intercept (12 ± 0.2 s^{-1}) coincided with k_{res} and, analogous to the analysis of the reaction with H$_2$O$_2$, the slope of the linear fit was assigned to the hyperoxidation reaction by ONOOH (k_{hyp}^{ONOOH}, Table 1). Finally, although the third phase could be fitted to an exponential function, the rate constant obtained had a nonlinear dependence on ONOOH concentration. This phase is coincident in time with the spontaneous decay of ONOOH via isomerization to nitrate and radical formation ($t_{1/2}$ = 2.2 s). Thus, it can be ascribed to a combination of several processes such as C83 and tryptophan oxidation (both first order in ONOOH), and oxidation/nitration of aromatic residues caused by radicals derived from ONOOH (zero order in ONOOH).

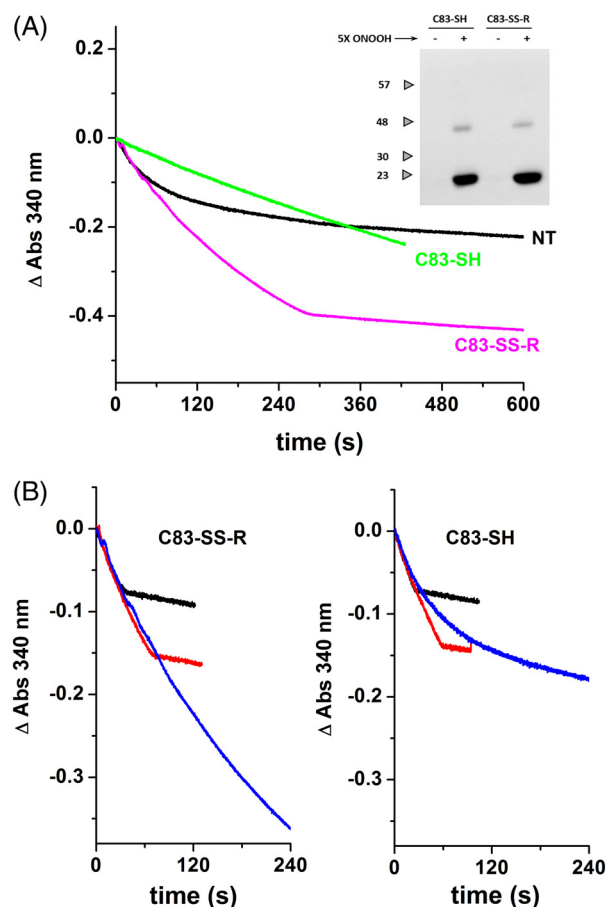The time course of PRDX2 fluorescence was somewhat simpler, as the third phase was only
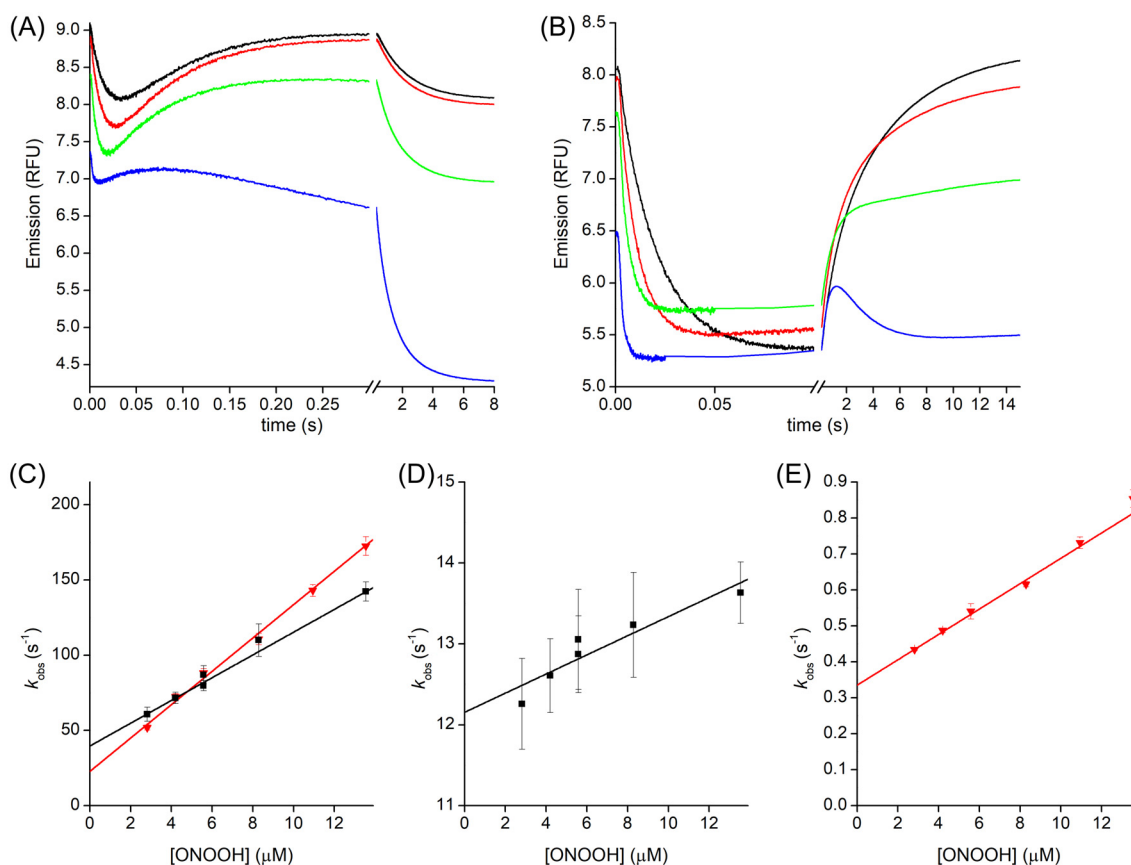
Figure 6. Kinetics of PRDX1 and PRDX2 oxidation by ONOOH. Time courses of the oxidation of PRDX1 (a) or PRDX2 (b) with excess ONOOH, from top to bottom 2.8, 8.3, 13.5 and 71 μM, and traces are averages of 15 runs. (c) Second-order plot of the rate constant of the fast exponential descending part of the time courses for PRDX1 (black squares) or PRDX2 (gray triangles). Second-order plot of the rate constant of the ascending exponential part of the time courses for PRDX1 (black squares, d) or PRDX2 (gray triangles, e). General conditions: buffer A, pH 7.3, 25 °C, λ_{ex} = 280 nm, λ_{em} > 320 nm.

apparent at very high concentrations of ONOOH [Fig. 6(b)]. The first two phases were similar to what was observed using H_2O_2 as oxidant, namely a fast decay and a much slower recovery of the fluorescence. As with PRDX1, both the descendent and the ascendent exponential phases had rate constants that depend linearly on ONOOH concentration [Fig. 6(c, e)]. The descent phase was assigned to the oxidation step of the catalytic cycle k_{ONOOH}^{app} and the ascent phase to a combination of resolution (intercept 0.34 ± 0.01 s^{-1}) and hyperoxidation (k_{hyp}^{ONOOH}, Table 1).

Nitration and hyperoxidation of PRDX1 by peroxynitrous acid

Even though peroxynitrous acid is reduced by PRDX1, other enzyme residues get modified by excess of this oxidant. As observed for PRDX2,[18,23] tyrosine nitration and dityrosine crosslinks were detected [Fig. 7(a), inset]. Unlike the case of PRDX2 whose activity was observed to increase upon nitration,[23] the treatment of disulfide PRDX1 with peroxynitrite resulted in a decrease of peroxidase activity [Fig. 7 (a)]. The presence of an extra cysteine, C83 makes the difference. Blocking both catalytic cysteines C_P-C_R (by forming the disulfide) and also C83 with methyl methanethiosulfonate before treatment with peroxynitrite, the only irreversible modification observed after peroxynitrite exposure was tyrosine nitration, but importantly, the cysteine residues could be reduced back with DTT and the activity recovered. Under these conditions, nitration of PRDX1 rendered a more active and robust peroxidase [Fig. 7(b)] in the same way as observed before with PRDX2.[23]
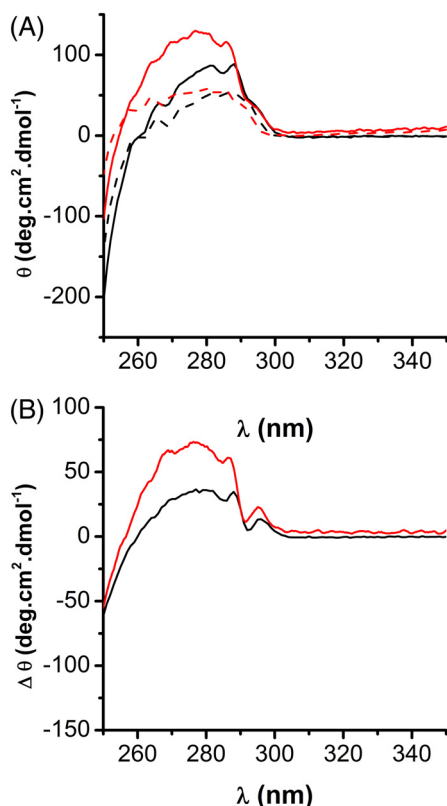
Differential near-UV circular dichroism spectra

The circular dichroism (CD) spectra in this region are influenced by the aromatic residues environment and indicative of the protein tertiary structure. The disulfide bond absorption occurs in the range of 240–290, near 260 nm, however, given that the near-UV CD bands of disulfides are generally broader than the corresponding to the aromatic side chains, it is very difficult to assess the contribution of the former to the protein spectrum. An important contribution of Phe (peak at 265 nm), Tyr and Tyr–Trp interactions (275–285 nm) and to a lesser extent Trp (shoulder at 295 nm) was observed for PRDX1, in the same way, as registered before for PRDX2[24] [Fig. 8(a)]. Upon oxidation to disulfide, there is a dramatic conformational change around these aromatic residues for PRDX2 as previously reported,[24] whereas the CD signals observed between reduced and oxidized PRDX1 were significantly smaller [Fig. 8(b)], suggesting that although similar processes take place in the active centers of PRDX1 and PRDX2, some structural differences exists between them. Far-UV CD analysis showed no differences between the two isoforms (data not shown).

Discussion

Taking advantage of the change in tryptophan fluorescence with the redox state of the enzyme, the reaction of reduced Prx with H_2O_2 was followed (Fig. 2). The oxidation of C_P-SH to C_P-SOH by H_2O_2 is extremely fast for both isoforms (Table), five orders of magnitude higher than the rate constant for most protein cysteine residues, denoting that they are highly sensitive to H_2O_2.

Once the sulfenic derivative (C_P-SOH) is formed, the conformational change and reaction with the C_R to form the disulfide is slower for PRDX2 than for PRDX1, showing a critical point of difference. Herein, we determined a first-order rate constant of disulfide

Figure 7. Peroxynitrite effect on PRDX1 depends on the redox state of C83. (a) Different samples of PRDX1 were assayed for peroxidase activity with 50 µM H_2O_2. Peroxynitrite-treated PRDX1-C83-SH, green line; C83-SS-R, magenta line; and nontreated PRDX1 (NT, black line). Inset: WB using anti-nitrotyrosine antibody (samples resolved on a 12% SDS-PAGE with β-mercaptoethanol). (b) Peroxidase activity of peroxynitrite-treated PRDX1-C83-SH (right panel) and C83-SS-R (left panel) are compared at different H_2O_2 concentration (10 µM, black line; 20 µM, red line; 50 µM, blue line).

Figure 8. Comparison of Near-UV CD spectra of PRDX1 and PRDX2. (a) About 50 μM PRDX1 (black) or PRDX2 (red) in their reduced or oxidized state (solid and dashed lines, respectively) was analyzed by CD in the near UV. (b) Reduced disulfide-oxidized differential CD spectra for PRDX1 (black line) and PRDX2 (red line) showing less differences in near-UV CD signals on PRDX1 compared to PRDX2 upon oxidation, compatible with small changes in the surroundings of aromatic residues in the former.

formation for PRDX2 of 0.25 s^{-1} at pH 7.4 and 25 °C that agrees with previous reports from our group (0.64 s^{-1} at pH 7.4, 25 °C[17]) and others (0.25 s^{-1} at pH 7.4, 22 °C[16]) and is somewhat smaller than the 2 s^{-1} first reported.[25] Importantly, the rate of disulfide formation obtained for PRDX1 is one order of magnitude higher than for PRDX2, 11 s^{-1}, and agrees with the value recently reported.[16] In addition, we recently measured similar pKa values for C$_P$-SOH (close to 7) for both enzymes, while a 1 unit difference was determined for C$_R$-SH pKas (7.4 for PRDX1 and 8.5 for PRDX2).[17] Thus, at the same pH, there is more concentration of the nucleophilic thiolate in the PRDX1 isoform that could contribute to accelerate its disulfide formation compared to PRDX2.

These differences in rates of disulfide formation are in accordance with the observed differences in hyperoxidation with excess H$_2$O$_2$ (Fig. 4) and also in turnover (Fig. 3) where PRDX2 was more readily hyperoxidized and inactivated than PRDX1. Interestingly, this higher susceptibility to hyperoxidation of PRDX2 cannot be ascribed to a higher rate of sulfinic acid formation compared to PRDX1. The determined

rate constant for the reaction of C$_P$-SOH with H$_2$O$_2$ (k_{hyp}) was similar for both isoforms, 2×10^3 M^{-1} s^{-1} under our experimental conditions [Fig. 2(b)], almost one order of magnitude lower than the rate constant previously reported for PRDX2.[25] Bolduc et al.[26] recently determined novel hyperoxidation resistance motifs in 2-Cys Prx (motif A and motif B) besides the absence of YF and GGLG (present in sensitive Prx). The presence of different structural motifs (PRDX1 presents only motif A and PRDX2 only motif B) supports the differential susceptibility to hyperoxidation that is ligated to the competing resolution process (Fig. 1). Our results indicate that the reactivity of C$_P$-SOH with H$_2$O$_2$ is the same for both isoforms, thus, the difference in hyperoxidation sensitivity is mainly laying on subtle structural differences that favor the conformational change towards the competing reaction, the oxidation to disulfide. In that sense, the near-UV CD indicates smaller differences in tertiary structure between the reduced and disulfide-oxidized form of PRDX1 than PRDX2 (Fig. 8).

Peroxynitrous acid is also a peroxide substrate for PRDX1. A second-order rate constant of $1.5 \pm 0.3 \times 10^7$ M^{-1} s^{-1} (by competition with HRP) and 1.1×10^7 M^{-1} s^{-1} by intrinsic fluorescence at pH 7.4 and 25 °C were determined (Figs. 5 and 6), similar to the previously reported value for PRDX2.[18] Thus, both PRDX1 and PRDX2 isoforms reduce H$_2$O$_2$ more efficiently than ONOOH, like all members of Prx1 subgroup, which is contrary to the expected trend based on S$_N$2 reactivity between thiolates and peroxides. The reaction is expected to be faster if it produces a less basic leaving group[27,28] and as NO$_2^-$ is significantly less basic than OH$^-$, reactions of thiolates with ONOOH are usually much faster than with H$_2$O$_2$. Therefore, both PRDX1 and PRDX2 are not only specialized in peroxide sensing and reduction but more specifically in H$_2$O$_2$, in contrast with human Prx5 that reduces peroxynitrite faster than H$_2$O$_2$. Urate hydroperoxide was also found as a substrate for both isoforms with a lower rate constant ($5-23 \times 10^5$ M^{-1} s^{-1} [16]).

We recently discussed the possibility of using the ratio of the rates of reactions 2 over 1 (k_{res}/k_{ROOH}, from Table) as a measure of the sensing ability of each Prx toward a peroxide substrate[17] as it represents the threshold concentration of substrate at which the protein switches from mostly dithiol to mostly sulfenic. The same quotient can be calculated to compare the sensing ability toward different ROOH substrates and yields that PRDX2 is more sensitive in each case, with threshold concentrations of 1.6, 23, and 110 nM for H$_2$O$_2$, ONOOH, and urate hydroperoxide, respectively. The concentrations in the case of PRDX1 are significantly higher (0.1, 1.45, and 22 μM, respectively). This differential reinforces the idea of the two Prx working as stepwise sensors, each switching in specific concentration ranges of each specific peroxide substrate.

Changes in intrinsic fluorescence also allowed us to follow the hyperoxidation of PRDX1 and PRDX2 by peroxynitrite (Fig. 6). Interestingly, the hyperoxidation with ONOOH is faster than with H_2O_2 (3.5×10^4 M^{-1} s^{-1} vs 2×10^3 M^{-1} s^{-1}) in accordance with the S_N2 expected trend and as observed before by western blotting for PRDX2.[18] The rate constant determined for PRDX1 hyperoxidation with peroxynitrite is nearly 10-fold higher than for PRDX2 (Table 1). It is unlikely that C83 oxidation contributes to the process herein interpreted as hyperoxidation, as a rate constant in the order of 10^3 M^{-1} s^{-1} is expected for a nonperoxidatic cysteine reacting with ONOOH.[29] Although k_{hyp}^{ONOOH} is higher for PRDX1 than for PRDX2, the hyperoxidation efficiency in a single turnover is related to the ratio k_{hyp}^{ONOOH} [ONOOH]/k_{res}, that is, the competition between the rates of hyperoxidation and resolution. Such ratio is higher for PRDX2 at all concentrations of ONOOH.

Disulfide-oxidized PRXD1 treated with an excess of peroxynitrite resulted in nitration of the enzyme and aggregation to oligomers [Fig. 7(a), inset] as reported before for PRDX2 isolated from erythrocytes.[18] However, the effect of peroxynitrite-dependent nitration of PRDX1 on peroxidase activity was different from what was previously observed for PRDX2 depending on the redox state of its C83 (Fig.7). This extra cysteine, even though not involved in the catalytic cycle, needs to be reduced for PRDX1 to display its full peroxidase activity. As pointed out earlier, this C83 represents a critical differential element between these isoforms.[16,30,31]

For both PRDX1 and PRDX2, the preferential peroxide substrate is H_2O_2 (over ONOOH or alkyl hydroperoxides).[32] Together they are estimated to consume most of the H_2O_2 in the cytosol from endogenous and extracellular sources.[33] They are very sensitive sensors of cytosolic H_2O_2 but once the sulfenic derivative is formed, they can take different pathways. PRDX2-C_P-SOH lasts longer and even though this increases the chance to get inactivated by hyperoxidation, it also offers the chance to condense with another cysteine residue of a redox protein (forming a mixed disulfide via its C_P). Conversely, PRDX1-C_P-SOH is more prone to react with its own C_R-SH to form the disulfide dimer and the redox signal relay depends on this disulfide oxidizing a redox protein (in this case, the mixed disulfide should involve the PRDX1-C_R). In fact, at the cellular level, different transient disulfide interactions were detected for each isoform, for example, PRDX1 with kinase ASK1[34] while PRDX2 with transcription factor STAT3.[35] The kinetics of Prx disulfide reduction, the last step in the catalytic cycle is the least studied and only thioredoxin has been assayed as a reductant so far, but other partners need to be explored. Further studies on this reduction step will shed more light on the mechanisms underlying Prx-dependent redox signaling.

Materials and methods

Chemicals

Dithiothreitol (DTT), N-ethyl maleimide (NEM), and reduced nicotinamide adenine dinucleotide phosphate (NADPH) were purchased from AppliChem GmbH (Darmstadt Germany). Hydrogen peroxide (H_2O_2), HRP, and diethylenetriaminepentaacetic acid (dtpa) were purchased from Sigma-Aldrich (St Louis, MO). 4,4′-Dithiodipyridine (DTDPy) was from Acros Organics (Fisher Scientific, Hampton, NH). Peroxynitrite was synthesized as in Reference 36. All other reagents were of analytical grade and used as received.

Recombinant proteins expression and purification

Human recombinant PRDX1 and PRDX2 were produced in *E. coli* without any affinity tag. The use of the mature protein is crucial since there is evidence that extra residues can influence 2-Cys Prx structure/activity relationship.[37,38] Recombinant PRDX1 was expressed with a pET17b plasmid and purified as previously described[6] with minor modifications. After anionic exchange chromatography, a size-exclusion chromatography was performed in a HiLoad 16/60 Superdex 200 column (GE Healthcare, Chicago, IL) equilibrated with 50 mM sodium phosphate pH 7.4, 150 mM sodium chloride, and 0.1 mM dtpa (Buffer A). Recombinant PRDX2 was expressed with a pET17b plasmid and purified as reported in Reference 38. Both, PRDX1 and PRDX2 were expressed without any extra residue in their primary structure. Expression vector pET9a (Novagen, Darmstadt, Germany) with the *E. coli* Trx1 gene (*Ec*Trx1) was expressed and purified according to Reference 39. *E. coli* thioredoxin reductase (*Ec*TR) was expressed in *E. coli* BL21(DE3) transformed with the plasmid pTrR301 and purified as reported in Reference 40. Protein purity was evaluated by SDS-PAGE.

Peroxide and protein quantification

The concentration of H_2O_2 was measured at 240 nm ($\varepsilon_{240} = 39.4$ M^{-1} cm^{-1}),[41] peroxynitrite concentration was determined at alkaline pH at 302 nm ($\varepsilon_{302} = 1670$ M^{-1} cm^{-1}),[42] HRP concentration was measured at 403 nm ($\varepsilon_{403} = 1.03 \times 10^5$ M^{-1} cm^{-1})[20] and *Ec*TR at 280 nm ($\varepsilon_{280} = 51700$ M^{-1} cm^{-1}).[43] For the rest of the proteins, concentration was measured by the absorption at 280 nm, using the corresponding ε determined with https://web.expasy.org/protparam/: ε_{280} (PRDX1)$_{SS}$ = 18,700 M^{-1} cm^{-1}, ε_{280} (PRDX1)$_{SH}$ = 18,450 M^{-1} cm^{-1}, ε_{280} (PRDX2)$_{SS}$ = 21,555 M^{-1} cm^{-1}, ε_{280} (PRDX2)$_{SH}$ = 21,430 M^{-1} cm^{-1}, ε_{280} (*Ec*Trx1) = 14,060 M^{-1} cm^{-1}.

Kinetics followed by intrinsic fluorescence

Oxidation of prereduced PRDX1 and PRDX2 by H_2O_2 was registered following the change in their intrinsic fluorescence as described in Reference 17, in an Applied Photophysics SX20 stopped-flow fluorimeter with a mixing time of <2 ms, with λ_{ex} = 280 nm, measuring the total emission above 320 nm. 0.25 μM Prx in buffer A was mixed with different concentrations of H_2O_2 (1 μM–12 mM) diluted in buffer A. At low oxidant concentration (<10 μM), the time courses were biphasic (a fast drop, followed by a slow increase in the signal) and adjustable to a double exponential function. At low oxidant concentration, the constant associated with the slower phase does not change noticeably with the concentration of H_2O_2. However, working at high H_2O_2 concentrations, the downward phase became faster than the dead time of the stopped flow, and the slow phase showed a linear dependence on H_2O_2 concentration. From the curve k_{obs} versus $[H_2O_2]$, the bimolecular rate constant of hyperoxidation, k_{hyp} (slope) and the first-order rate constant of resolution, k_{res} (y-axis intercept) for PRDX1 and PRDX2 were determined.

The kinetics of ONOOH reduction by PRDX1 and PRDX2 were performed in an SX20 stopped flow fluorimeter following the fluorescence of the proteins with λ_{ex} = 280 nm, λ_{em} > 320 nm. Reduced PRDX1 or PRDX2 (0.5 μM) in buffer A (2X), pH 7.25, were mixed with an equal volume of $ONOO^-$ (5.6–142 μM) in 1.5 mM NaOH. The pH after mixing, measured at the outlet was 7.3. The fluorescence was followed for up to 15 s and the time courses were fitted to triple (PRDX1) or double (PRDX2) exponential functions according to the number of phases observed.

NADPH-linked peroxidase activity

Peroxidase activity was measured spectrophotometrically following the NADPH consumption at 340 nm (ε_{340} = 6.22 mM^{-1} cm^{-1}) in a cuvette containing 200 μM NADPH, 1 μM EcTR, 8 μM EcTrx1 (except in Fig. 4 where 0.5–40 μM Trx is used) and 0.5 μM PRDX1 or PRDX2 in buffer A. The reaction was started adding the specified amount of H_2O_2. All spectrophotometric measurements were made with a Cary 50 spectrophotometer (Varian, Australia).

Treatment of reduced PRDX1 with excess H_2O_2 (SDS-PAGE and WB)

About 50 μL of 5 μM prereduced PRDX1 or PRDX2 were treated with 2 μL of a H_2O_2 solution so that the final concentration of peroxide corresponds to the desired excess (0–20). After 15 min, 2 mM NEM was added to the mixture to block reduced cysteines. Electrophoresis loading buffer (0.125 M Tris-HCl, 4% SDS, 20% glycerol, 0.053% bromophenol blue, pH 6.8) was added and samples were resolved in a 12% polyacrylamide gel electrophoresis with sodium dodecyl sulfate (12% SDS-PAGE). In WB experiments, the proteins resolved on the gel were transferred to PVDF membrane, blotted with rabbit polyclonal antibody against hyperoxidized Prx (Anti-Peroxiredoxin-SO3, AbFrontier, Seoul, Korea) and detection performed with fluorescent goat anti-mouse IRDye 680RD (LI-COR Biosciences, Lincoln, NE) secondary antibodies. Blots were scanned using a G:BOX Chemi XRQ (Syngene, Cambridge, UK).

Reaction rate constant with peroxynitrite determined by competence with HRP

PRDX1 capacity to reduce peroxynitrite was corroborated and characterized by competition assay with HRP as previously reported.[18,22,44] Time courses of formation of Compound I upon oxidation of 5 μM HRP by 0.7 μM peroxynitrite were recorded in the absence or in the presence of reduced PRDX1 (0.68–3.4 μM). The reaction was followed at 398 nm, the isosbestic point for HRP-compounds I and II ($\Delta\varepsilon_{398}$ = 4.2 × 10^4 M^{-1} cm^{-1} [45] in an Applied Photophysics SX20 stopped-flow spectrophotometer. HRP and PRDX1 solutions were prepared in 100 mM sodium phosphate pH 7.4 with 0.1 mM dtpa and stock peroxynitrite diluted in 10 mM NaOH. For each registered temporal course, k_2 (corresponding to the bimolecular rate constant of PRDX1 oxidation by peroxynitrite = k_{ONOOH}) was calculated using Equation 1:

$$\frac{k_{HRP}}{k_2} = \frac{\ln\left\{\frac{[HRP]_0}{[HRP]_0 - [CpI]_\infty}\right\}}{\ln\left\{\frac{[PRDX1\text{-}SH]_0}{[PRDX1\text{-}SH]_0 - [PRDX1\text{-}S_2]_\infty}\right\}} \tag{1}$$

where k_{HRP} is the rate constant of peroxynitrite-mediated HRP oxidation obtained herein (2.0 × 10^6 M^{-1} s^{-1} at pH 7.4 and 25 °C, consistent with previous report.[20,21,46] $[HRP]_0$ is the initial concentration of HRP (5 μM), $[PRDX1\text{-}SH]_0$, the initial concentration of reduced PRDX1 (0.7–3.4 μM), $[CpI]_\infty$ the concentration of Compound I at completion of reaction, $[PRDX1\text{-}S_2]_\infty$, the concentration of PRDX1 oxidized at completion of reaction, calculated as $[CpI]_\infty$ in the absence minus in the presence of the indicated concentration of PRDX1.[44]

PRDX1-controlled oxidation to disulfide

To assure the oxidation of the catalytic site but keeping C83 reduced, PRDX1 was treated with 10 mM DTT for 30 min at room temperature. Residual DTT was removed passing the mixture through a Bio-Spin column (BioRad, Hercules, CA) and protein as well as thiol concentration were immediately determined (thiol concentration was determined with DTDPy as reported in Reference 47). After reduction, three of the four thiols present in PRDX1 could be detected by

this method. As two of these thiols belong to C_P and C_R, 1 mol of H_2O_2 was added for every three moles of thiol quantified so that to yield the disulfide in the catalytic site and avoiding C83 oxidation.

Treatment of disulfide-oxidized PRDX1 with excess of peroxynitrite

Treatment of PRDX1 with peroxynitrite was performed according to the protocol reported in Reference 23 for PRDX2. Briefly, a molar excess of 5:1 peroxynitrite was added in a flux-like addition to 100 μL of 130 μM disulfide PRDX1 (i.e., oxidized in the catalytic site but with C83 as thiol) in buffer A. To protect C83 before peroxynitrite treatment, disulfide PRDX1 was treated with 1 mM MMTS for 1 hour at room temperature, and then the mixture was passed through a Bio-Spin column (BioRad) equilibrated with buffer A. Finally, peroxynitrite treatment was performed followed by protein reduction with DTT (the excess was removed by passing through a Bio-Spin column). This sample was labeled C83-SS-R. As a control, disulfide PRDX1 was treated with 10 mM NaOH instead of peroxynitrite (non-treated sample, NT).

CD spectra

Spectra of PRDX1 were acquired at 25 °C using a Chirascan Q100 Spectropolarimeter (Applied Photophysics, Leatherhead, UK). Near-UV measurements were carried out in 1 cm cells containing 50 μM PRDX1 and far-UV with 5 μM PRDX1 in 0.1 cm cells. Protein was prepared in 10 mM sodium phosphate buffer, pH 7.4. DTT was removed in the reduced samples before measurements. A scan of the buffer was subtracted from the corresponding averaged sample spectra. Data for near and far UV spectra of PRDX2 were obtained from Reference 24.

Acknowledgments

REFERENCES

1. Wood ZA, Poole LB, Karplus PA (2003) Peroxiredoxin evolution and the regulation of hydrogen peroxide signaling. Science 300:650–653.
2. Wood ZA, Schroder E, Robin Harris J, Poole LB (2003) Structure, mechanism and regulation of peroxiredoxins. Trends Biochem Sci 28:32–40.
3. Rhee SG (2016) Overview on peroxiredoxin. Mol Cells 39:1–5.
4. Sies H (2017) Hydrogen peroxide as a central redox signaling molecule in physiological oxidative stress: oxidative eustress. Redox Biol 11:613–619.
5. Fang J, Nakamura T, Cho DH, Gu Z, Lipton SA (2007) S-nitrosylation of peroxiredoxin 2 promotes oxidative stress-induced neuronal cell death in Parkinson's disease. Proc Natl Acad Sci USA 104:18742–18747.
6. Engelman R, Weisman-Shomer P, Ziv T, Xu J, Arner ES, Benhar M (2013) Multilevel regulation of 2-Cys peroxiredoxin reaction cycle by S-nitrosylation. J Biol Chem 288:11312–11324.
7. Lowther WT, Haynes AC (2011) Reduction of cysteine sulfinic acid in eukaryotic, typical 2-Cys peroxiredoxins by sulfiredoxin. Antiox Redox Signal 15:99–109.
8. Rhee SG, Kang SW, Chang TS, Jeong W, Kim K (2001) Peroxiredoxin, a novel family of peroxidases. IUBMB Life 52:35–41.
9. Nelson KJ, Knutson ST, Soito L, Klomsiri C, Poole LB, Fetrow JS (2011) Analysis of the peroxiredoxin family: using active-site structure and sequence information for global classification and residue analysis. Proteins 79: 947–964.
10. Wood ZA, Poole LB, Hantgan RR, Karplus PA (2002) Dimers to doughnuts: redox-sensitive oligomerization of 2-cysteine peroxiredoxins. Biochemistry 41:5493–5504.
11. Peskin AV, Low FM, Paton LN, Maghzal GJ, Hampton MB, Winterbourn CC (2007) The high reactivity of peroxiredoxin 2 with H(2)O(2) is not reflected in its reaction with other oxidants and thiol reagents. J Biol Chem 282:11885–11892.
12. Park JW, Piszczek G, Rhee SG, Chock PB (2011) Glutathionylation of peroxiredoxin I induces decamer to dimers dissociation with concomitant loss of chaperone activity. Biochemistry 50:3204–3210.
13. Neumann CA, Krause DS, Carman CV, Das S, Dubey DP, Abraham JL, Bronson RT, Fujiwara Y, Orkin SH, Van Etten RA (2003) Essential role for the peroxiredoxin Prdx1 in erythrocyte antioxidant defence and tumour suppression. Nature 424:561–565.
14. Lee TH, Kim SU, Yu SL, Kim SH, Park DS, Moon HB, Dho SH, Kwon KS, Kwon HJ, Han YH, Jeong S, Kang SW, Shin HS, Lee KK, Rhee SG, Yu DY (2003) Peroxiredoxin II is essential for sustaining life span of erythrocytes in mice. Blood 101:5033–5038.
15. Parsonage D, Nelson KJ, Ferrer-Sueta G, Alley S, Karplus PA, Furdui CM, Poole LB (2015) Dissecting peroxiredoxin catalysis: separating binding, peroxidation, and resolution for a bacterial AhpC. Biochemistry 54: 1567–1575.
16. Carvalho LAC, Truzzi DR, Fallani TS, Alves SV, Toledo JC Jr, Augusto O, Netto LES, Meotti FC (2017) Urate hydroperoxide oxidizes human peroxiredoxin 1 and peroxiredoxin 2. J Biol Chem 292:8705–8715.
17. Portillo-Ledesma S, Randall LM, Parsonage D, Dalla Rizza J, Karplus PA, Poole LB, Denicola A, Ferrer-Sueta G (2018) Differential kinetics of two-cysteine peroxiredoxin disulfide formation reveal a novel model for peroxide sensing. Biochemistry 57: 3416–3424.
18. Manta B, Hugo M, Ortiz C, Ferrer-Sueta G, Trujillo M, Denicola A (2009) The peroxidase and peroxynitrite reductase activity of human erythrocyte peroxiredoxin 2. Arch Biochem Biophys 484:146–154.
19. Cox AG, Pearson AG, Pullar JM, Jonsson TJ, Lowther WT, Winterbourn CC, Hampton MB (2009) Mitochondrial peroxiredoxin 3 is more resilient to hyperoxidation than cytoplasmic peroxiredoxins. Biochem J 421:51–58.
20. Floris R, Piersma SR, Yang G, Jones P, Wever R (1993) Interaction of myeloperoxidase with peroxynitrite. A

comparison with lactoperoxidase, horseradish peroxidase and catalase. Eur J Biochem 215:767–775.

21. Ogusucu R, Rettori D, Munhoz DC, Netto LE, Augusto O (2007) Reactions of yeast thioredoxin peroxidases I and II with hydrogen peroxide and peroxynitrite: rate constants by competitive kinetics. Free Rad Biol Med 42:326–334.

22. Reyes AM, Vazquez DS, Zeida A, Hugo M, Pineyro MD, De Armas MI, Estrin D, Radi R, Santos J, Trujillo M (2016) PrxQ B from Mycobacterium tuberculosis is a monomeric, thioredoxin-dependent and highly efficient fatty acid hydroperoxide reductase. Free Rad Biol Med 101:249–260.

23. Randall LM, Manta B, Hugo M, Gil M, Batthyany C, Trujillo M, Poole LB, Denicola A (2014) Nitration transforms a sensitive peroxiredoxin 2 into a more active and robust peroxidase. J Biol Chem 289:15536–15543.

24. Randall L, Manta B, Nelson KJ, Santos J, Poole LB, Denicola A (2016) Structural changes upon peroxynitrite-mediated nitration of peroxiredoxin 2; nitrated Prx2 resembles its disulfide-oxidized form. Arch Biochem Biophys 590:101–108.

25. Peskin AV, Dickerhof N, Poynton RA, Paton LN, Pace PE, Hampton MB, Winterbourn CC (2013) Hyperoxidation of peroxiredoxins 2 and 3: rate constants for the reactions of the sulfenic acid of the peroxidatic cysteine. J Biol Chem 288:14170–14177.

26. Bolduc JA, Nelson KJ, Haynes AC, Lee J, Reisz JA, Graff AH, Clodfelter JE, Parsonage D, Poole LB, Furdui CM, Lowther WT (2018) Novel hyperoxidation resistance motifs in 2-Cys peroxiredoxins. J Biol Chem 293:11901–11912.

27. Trindade DF, Cerchiaro G, Augusto O (2006) A role for peroxymonocarbonate in the stimulation of biothiol peroxidation by the bicarbonate/carbon dioxide pair. Chem Res Toxicol 19:1475–1482.

28. Ferrer-Sueta G, Manta B, Botti H, Radi R, Trujillo M, Denicola A (2011) Factors affecting protein thiol reactivity and specificity in peroxide reduction. Chem Res Toxicol 24:434–450.

29. Trujillo M, Radi R (2002) Peroxynitrite reaction with the reduced and the oxidized forms of lipoic acid: new insights into the reaction of peroxynitrite with thiols. Arch Biochem Biophys 397:91–98.

30. Lee W, Choi KS, Riddell J, Ip C, Ghosh D, Park JH, Park YM (2007) Human peroxiredoxin 1 and 2 are not duplicate proteins: the unique presence of CYS83 in Prx1 underscores the structural and functional differences between Prx1 and Prx2. J Biol Chem 282:22011–22022.

31. Chae HZ, Oubrahim H, Park JW, Rhee SG, Chock PB (2012) Protein glutathionylation in the regulation of peroxiredoxins: a family of thiol-specific peroxidases that function as antioxidants, molecular chaperones, and signal modulators. Antiox Redox Signal 16:506–523.

32. Randall LM, Ferrer-Sueta G, Denicola A (2013) Peroxiredoxins as preferential targets in H2O2-induced signaling. Methods Enzymol 527:41–63.

33. Benfeitas R, Selvaggio G, Antunes F, Coelho PM, Salvador A (2014) Hydrogen peroxide metabolism and sensing in human erythrocytes: a validated kinetic model and reappraisal of the role of peroxiredoxin II. Free Rad Biol Med 74:35–49.

34. Jarvis RM, Hughes SM, Ledgerwood EC (2012) Peroxiredoxin 1 functions as a signal peroxidase to receive, transduce, and transmit peroxide signals in mammalian cells. Free Rad Biol Med 53:1522–1530.

35. Sobotta MC, Liou W, Stocker S, Talwar D, Oehler M, Ruppert T, Scharf AN, Dick TP (2015) Peroxiredoxin-2 and STAT3 form a redox relay for H2O2 signaling. Nat Chem Biol 11:64–70.

36. Romero N, Radi R, Linares E, Augusto O, Detweiler CD, Mason RP, Denicola A (2003) Reaction of human hemoglobin with peroxynitrite. Isomerization to nitrate and secondary formation of protein radicals. J Biol Chem 278:44049–44057.

37. Cao Z, Bhella D, Lindsay JG (2007) Reconstitution of the mitochondrial PrxIII antioxidant defence pathway: general properties and factors affecting PrxIII activity and oligomeric state. J Mol Biol 372:1022–1033.

38. Haynes AC, Qian J, Reisz JA, Furdui CM, Lowther WT (2013) Molecular basis for the resistance of human mitochondrial 2-Cys peroxiredoxin 3 to hyperoxidation. J Biol Chem 288:29714–29723.

39. Santos J, Marino-Buslje C, Kleinman C, Ermacora MR, Delfino JM (2007) Consolidation of the thioredoxin fold by peptide recognition: interaction between E. coli thioredoxin fragments 1-93 and 94-108. Biochemistry 46:5148–5159.

40. Mulrooney SB (1997) Application of a single-plasmid vector for mutagenesis and high-level expression of thioredoxin reductase and its use to examine flavin cofactor incorporation. Prot Express Purif 9:372–378.

41. Nelson DP, Kiesow LA (1972) Enthalpy of decomposition of hydrogen peroxide by catalase at 25 degrees C (with molar extinction coefficients of H 2 O 2 solutions in the UV). Analyt Biochem 49:474–478.

42. Radi R, Beckman JS, Bush KM, Freeman BA (1991) Peroxynitrite oxidation of sulfhydryls. The cytotoxic potential of superoxide and nitric oxide. J Biol Chem 266:4244–4250.

43. Wang PF, Veine DM, Ahn SH, Williams CH Jr (1996) A stable mixed disulfide between thioredoxin reductase and its substrate, thioredoxin: preparation and characterization. Biochemistry 35:4812–4819.

44. Trujillo M, Ferrer-Sueta G, Radi R (2008) Kinetic studies on peroxynitrite reduction by peroxiredoxins. Methods Enzymol 441:173–196.

45. Hayashi Y, Yamazaki I (1979) The oxidation-reduction potentials of compound I/compound II and compound II/ferric couples of horseradish peroxidases A2 and C. J Biol Chem 254:9101–9106.

46. Staudacher V, Trujillo M, Diederichs T, Dick TP, Radi R, Morgan B, Deponte M (2018) Redox-sensitive GFP fusions for monitoring the catalytic mechanism and inactivation of peroxiredoxins in living cells. Redox Biol 14:549–556.

47. Grassetti DR, Murray JF Jr (1967) Determination of sulfhydryl groups with 2,2′- or 4,4′-dithiodipyridine. Arch Biochem Biophys 119:41–49.

48. Chae HZ, Chung SJ, Rhee SG (1994) Thioredoxin-dependent peroxide reductase from yeast. J Biol Chem 269:27670–27678.

Dalla Rizza, J. et al "Differential parameters between cytosolic 2-Cys peroxiredoxins, PRDX1 and PRDX2"

Figure S1. Determination of second-order rate constant for the reaction of HRP with peroxynitrite at pH 7.4 and 25 °C.

Peroxynitrite (1 µM) was rapidly mixed in the stopped-flow spectrophotometer with the indicated concentrations of HRP (2.5 - 13 µM) and compound I formation was followed at 398 nm. Experimental data was fitted to single exponential curves and observed rate constants of peroxynitrite decay was plotted against HRP concentration to determine the rate constant of peroxynitrite-mediated HRP oxidation at pH 7.4 and 25 °C. From the slope, $k_2 = (2.0 \pm 0.2) \times 10^6$ $M^{-1}s^{-1}$
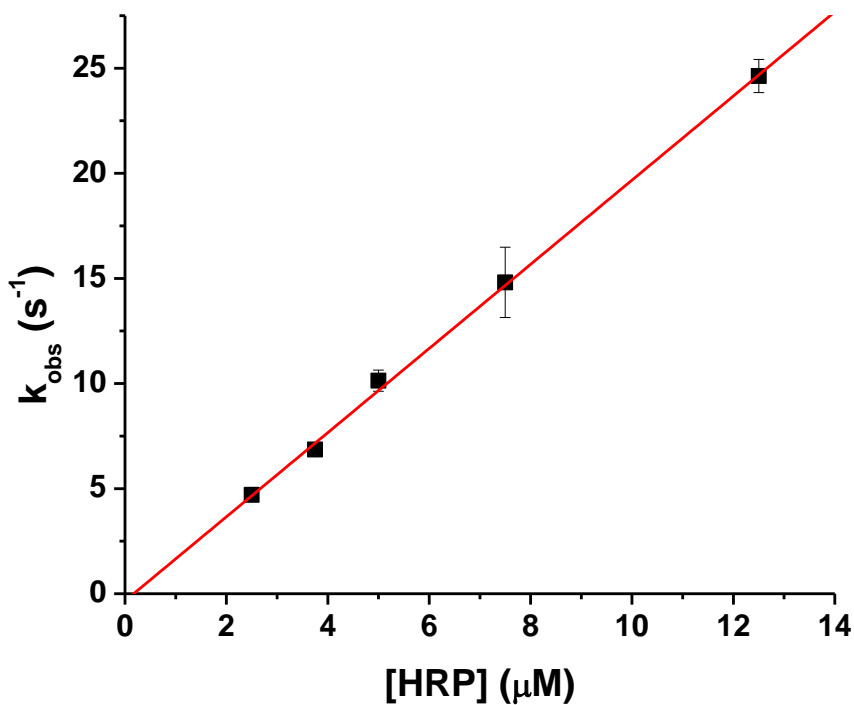
Figure S2. Time course and data fitting of PRDX1 oxidation by ONOOH. PRDX1 (0.25 µM) was reacted with 14 µM ONOOH (green line). The time course of the fluorescence (t > 2 ms) was fitted to a triple exponential function (black line). The residual shows the goodness of the fit.